Numerical Modelling of Multi-dimensional Steady Ideal Gas and Fluid Flows

Vom Fachbereich Maschinenbau
an der Technischen Universität Darmstadt
zur
Erlangung des Grades eines Doktor-Ingenieurs (Dr.-Ing.)
genehmigte

D i s s e r t a t i o n

vorgelegt von
Dipl.-Math. Nina Yurievna Shokina

aus Novosibirsk

Berichterstatter: Prof. Dr. rer. nat. M. Schäfer

Mitberichterstatter: Prof. Dr. rer. nat. K. G. Roesner

Tag der Einreichung: 23. Mai 2000

Tag der mündlichen Prüfung: 7. Februar 2001

Darmstadt 2000
D 17

Abstract

The thesis is devoted to the numerical modelling of two- and three-dimensional ideal fluid flows in channels of complicated geometries on the basis of the adaptive grid method.

Iterative finite difference methods for the numerical modelling of ideal gas and fluid flows are developed using new dependent variables. For two-dimensional flows these variables are stream function and vorticity function, for three-dimensional flows these variables are: vector potential and vorticity vector.

The set of equations for the stream function and vorticity, for which the appropriate boundary conditions are taken into account, are solved together with the energy equation and the relations of the marching method for the pressure calculation by a finite difference approximation on a curvilinear grid. Also the equations for the covariant components of vector potential, the boundary conditions for these components, and the equations for the contravariant components of the vorticity vector are constructed on curvilinear grids.

For the construction of curvilinear grids - adapted either to the singularities of the solution or to the complicated geometry of domains - the equidistribution method is developed. The governing equations of the equidistribution method are solved using a finite difference approximation. The equations for the construction of curvilinear adaptive grids are obtained for two- and three-dimensional domains, for surfaces and curves in two- and three-dimensional spaces.

The developed algorithms for calculating ideal gas flows are modified for the numerical solution of problems on steady ideal fluid flows with gravitational surface waves within the framework of the shallow water theory. For river channels of complicated configuration in the presence of islands the first approximation of this method is applied.

For the realization of the developed algorithms the effective complexes of computer codes are created. The investigation of the problems on the fluid flows through channels and rivers of complicated form is carried out.

Die Dissertation behandelt die numerische Modellierung zwei- und dreidimensionaler Strömungen idealer Fluide in Kanälen mit kompizierter Geometrie auf der Grundlage eines adaptiven Gittergenerierungsverfahrens. Iterative finite Differenzenverfahren werden unter Einführung neuer Variabler für die numerische Modellierung von Strömungen idealer Gase und Flüssigkeiten entwickelt. Für zweidimensionale Strömungen sind es die Variablen Stromfunktion und Rotation, für dreidimensionale Strömungen: Vektorpotential und Rotation.

Das Gleichungssystem für die Stromfunktion und die Rotation wird unter Berücksichtigung der geeigneten Randbedingungen zusammen mit der Energiegleichung und den Gleichungen für die Berechnung des Drucks mit Hilfe eines finiten Differenzenverfahrens auf einem krummlinigen Gitter gelöst. Auch die Gleichungen für die kovarianten Komponenten des Vektorpotentials, die Randbedingungen für diese Komponenten und die Gleichungen für die kontravarianten Komponenten der Rotation werden auf dem krummlingen Gitter behandelt.

Zur Konstruktion des krummlinigen Gitters - den Singularitäten der Lösung oder der komplizierten Geometrie des Gebietes angepaßt - wird die "equidistribution method" entwickelt. Die Grundgleichungen für die "equidistribution method" werden mittels eines finiten Differenzenverfahrens gelöst. Die Gleichungen für die Konstruktion krummliniger adaptiver Gitter werden für zwei- und dreidimensionale Gebiete, für Flächen und Kurven im zwei- und dreidimensionalen Raum abgeleitet.

Die entwickelten Lösungsalgorithmen zur Berechnung idealer Gasströmungen werden für die numerische Lösung von stationären Strömungsproblemen idealer Fluide unter Einschluß von Schwerewellen in Rahmen der Flachwassertheorie modifiziert. Diese Methode wird auch für die Berechnung von Strömungen in Flüssen mit komplizierter Berandung beim Vorhandensein von Inseln angewandt.

Für die Realisierung der entwickelten Algorithmen werden effektive komplexe Rechenprogramme entwickelt. Es werden Untersuchungen von Strömungsproblemen durch Kanäle und Flußläufe mit komplizierter Geometrie durchgeführt.

Contents

Notations

f_{Cor} — dimensionless value of Coriolis parameter
f_{Ch} — dimensionless value of Chezy coefficient
g — free fall acceleration
g_{11}, g_{12}, g_{13}, g_{22}, g_{23}, g_{33} — components of metric tensor
h — step of one-dimensional grid (in Chapter 4) or function describing
     bottom (in Chapters 11-12)
h_0 — characteristic depth
h_1, h_2 — steps of two-dimensional grid
h_1, h_2, h_3 — steps of three-dimensional grid
k — Coriolis parameter
$\mathbf{n}$ — external normal
p — pressure
$\mathbf{q}$ — coordinate vector in curvilinear system of coordinates
q^1, q^2, q^3 — curvilinear coordinates
t — time
$\mathbf{u}$ — velocity vector
w — control function
$\mathbf{x}$ — coordinate vector in Cartesian system of coordinates
x^1, x^2, x^3 — Cartesian coordinates
x, y, z — Cartesian coordinates

C — Chezy coefficient
H — total energy (in Chapters 2-6) or total depth (in Chapters 11-12)
J — Jacobian
$K(P)$ — area of dependence for node P
$K_n(P)$ — neighbourhood of the n-th level of node P
N — number of nodes of one-dimensional grid
N_1, N_2 — numbers of nodes of two-dimensional grid
N_1, N_2, N_3 — numbers of nodes of three-dimensional grid
Q — computational domain
$\bar{Q}$ — computational domain with its boundary
$\bar{Q}_h$ — total set of grid nodes in computational domain
Q_h — total set of internal grid nodes in computational domain
Q_h^0 — total set of internal grid nodes with half-integer indices in compu-
     tational domain
$\bar{Q}_h^0$ — total set of grid nodes with half-integer indices in computational
     domain

R^2 — two-dimensional space
R^3 — three-dimensional space
S — measure of mesh (length, square, volume)

γ — boundary of computational domain
γ_0 — impermeable part of boundary of computational domain
γ_0^{is} — image of contour of island in computational domain
γ_1 — inlet to computational domain
γ_2 — outlet from computational domain
γ_h — total set of boundary grid nodes in computational domain
$\gamma_{1,h}^0$ — total set of boundary grid nodes with half-integer indices in computational domain
δ_ω — relaxation parameter for vorticity function
δ_ρ — relaxation parameter for density
$\delta^{\alpha\beta}$ — Kronecker's symbols
ε_ψ — accuracy for calculation of stream function
ε_ω — accuracy for calculation of vorticity function
η — elevation of fluid surface above non-perturbed level
κ — adiabatic exponent
ν — viscosity
ρ — density
$\vec{\tau}$ — tangential unit vector
τ — iterative parameter
τ_ψ — iterative parameter for stream function
$\vec{\psi}$ — vector potential
ψ — stream function
ψ^{is} — value of stream function on contour of island
$\vec{\omega}$ — vorticity vector
ω — vorticity function

Γ — boundary of physical domain
Γ_0 — impermeable part of boundary of physical domain
Γ_0^{is} — boundary of island
Γ_1 — inlet to physical domain
Γ_2 — outlet from physical domain
$\Gamma_{\alpha\beta}^\gamma$ — Christoffel's symbols
$\Sigma(P)$ — pattern in node P
$\Sigma'(P)$ — neighbourhood of the node P
Ω — physical domain
$\bar{\Omega}$ — physical domain with its boundary
$\bar{\Omega}_h$ — total set of grid nodes in physical domain

$\mathcal{H}$ — Hilbert space

List of Figures

List of Tables

Chapter 1

Introduction

Nowadays the numerical modelling of steady fluid flows in channels and ducts is based mostly on the viscous fluid model. The algorithms, based on the Navier-Stokes equations, use finite difference method, finite element method, final volume method, boundary element method, spectral method and other methods. The reviews on these algorithms are presented in [5], [10]–[12], [24, 44, 82, 83, 109, 110, 117, 126].

The ideal fluid model has been rather seldom used for modelling of steady flows in channels, because the calculations on the basis of this model fail to take into account the influence of viscous effects. However, if some relations between the sizes of the channel and velocities of the fluid are fulfilled, then some characteristics of the flow are quite satisfactorily described by the model of inviscid fluid. The calculation results on the basis of the Euler equations can be used as the initial approximation for the iterative methods of solving the stationary Navier-Stokes equations. In addition, for developing the software packages it is necessary [14, 50, 62, 63, 81, 83, 84, 112, 162] to take into account not only the realisations of complicated models which adequately reflect the real phenomena, but also the realisations of simpler models which help one to obtain the preliminary representation of the flow and to investigate some integrated characteristics. Therefore, the series of models is necessary for a more comprehensive investigation of the phenomenon and for finding out which sides of the phenomenon can be described by simpler models, and when it is necessary to use complicated models. Thus, the development of reliable and effective algorithms on the basis of the ideal fluid model for calculating the flows in channels is an important issue.

The problem of the modelling of steady fluid flows within the framework of the ideal fluid model is rather complicated, despite the simpler form of the equations of this model then the Navier-Stokes equations. The difficulties are connected with the mixed type of the system of the Euler equations. For a stationary case this system is of elliptic-hyperbolic type [107], therefore the methods [95, 96, 119, 162] for solving pure elliptic or pure hyperbolic equations are inapplicable here. The solution of an evolutionary system for establishing the steady state which is obtained by adding the derivatives with respect to time is not effective either, because of the lack of dissipation mechanisms [38, 39]. Thus, the iterative methods based on the solution of the stationary equations are used more widely.

The numerical modelling of two-dimensional ideal fluid flows has been developed, for example, in [164, 165] where Cartesian coordinates and rectangular grids are used. In [53, 106] the required dependent variables are taken as new independent variables.

The method [100] can be applied only to the flows with small modifications of a stream direction. The iterative methods [41, 53] are applicable only when the external forces are potential. The technique of [26] is realized only for domains which are composed of rectangles. The passage to the stream function ψ and the vorticity ω of the fluid is used for calculating two-dimensional ideal fluid flows (see, for example, [41, 42, 164, 165]). This passage is one of the basic approaches to modelling of viscous fluid flows. For domains of complicated geometry all these methods require the additional modification, in particular, in the case of an arbitrary curvilinear grid.

In [151], finite element method is used for calculating three-dimensional steady ideal incompressible fluid flows in channels. Vortical flows in channels are investigated numerically by finite difference method [1, 18, 19]. In the latter article the external forces are assumed potential.

The list of the articles devoted to the modelling of flows in channels on the basis of the Navier-Stokes equations is more extensive than for the ideal fluid model.

It is possible to single out the following three classes among finite difference methods for three-dimensional Navier-Stokes equations: 1) the methods based on the approximations of the equations for original variables: the velocity $\mathbf{u}$ and the pressure p; 2) the methods based on the approximations of the equations for new variables: the vector potential $\vec{\psi}$ and the vorticity vector $\vec{\omega}$; 3) the methods where the velocity $\mathbf{u}$ and the vorticity vector $\vec{\omega}$ are taken as dependent variables.

In the majority of the articles devoted to numerical modelling of three-dimensional incompressible fluid flows the velocity and the pressure are taken as dependent variables. The difficulty of using this approach for calculating the steady problems is connected with the continuity equation. In the known algorithms this equation is fulfilled only approximately. For example, in articles [139, 141] the continuity equation is assumed to be not fully satisfied and the schemes are considered which lead to the formation of the source terms in this equation while the order of these terms should be higher, than the order of approximation of the equations. In [47], in order to satisfy the continuity equation it is suggested that the Neumann problem for the Poisson equation should be solved with respect to the corrections to the components of the velocity on each step of the iterative process. There are also other approaches to satisfying the continuity equation [5, 12, 44], in particular, the approach based on using the artificial compressibility method for solving the stationary problems for the establishing the steady state [51]. In [31, 40, 105] $\mathbf{u} - \vec{\omega}$ formulation is used and the velocity vector field is calculated by solving the Poisson equations for each component of the velocity. In [45], unlike in the articles mentioned above, the components of the velocity are calculated on each iterative step by solving the continuity equation and the relations which yield the connection between the velocity and the vorticity. The relevant references are given in the book [44].

The first impressive results for two-dimensional case of the modelling of incompressible fluid flows within the framework of the Navier-Stokes equations are obtained for $\psi - \omega$ formulation (for two-dimensional flows ψ is the stream function, ω is the vorticity function). Nowadays this approach is very popular. The attempts of generalizing this approach to three-dimensional case have encountered the difficulties which are connected with the statement of boundary conditions for three-dimensional analogue of the stream function, i.e. for the vector potential $\vec{\psi}$. That is one of the reasons of rare usage of $\vec{\psi} - \vec{\omega}$ formulations for numerical modelling of three-dimensional flows. However, the passage to dependent variables $\vec{\psi}, \vec{\omega}$ has the series of advantages over the classical $\mathbf{u} - p$ approach.

2

In particular, the continuity equation at the differential level is fulfilled automatically for $\vec{\psi}-\vec{\omega}$ formulation. At the difference level it is fulfilled when the appropriate approximation of the components of the velocity and the staggered grids are used. In addition, for solving the stationary problems there is no necessity of calculating the pressure on the intermediate iterations. The pressure is eliminated from the computational process and it can be restored after the convergence of iterations for $\vec{\psi}$ and $\vec{\omega}$. Usually the Poisson equation obtained from the motion equations and supplemented by the inhomogeneous boundary Neumann conditions is used for calculating the pressure. It is necessary to achieve the coordinated approximation of the right-hand side of the Poisson equation and the boundary conditions for the solvability of this problem. It is rather difficult to achieve this coordinated approximation at the difference level even for the uniform rectangular grids (see, for example, [20, 117]).

The algorithms based on $\vec{\psi}-\vec{\omega}$ formulation are developed, for example, in [153, 160]. Among the first articles of this direction there is the research of convective flows [9]. This approach is used for the convection problems in the rectangular three-dimensional cavity in [108]. The boundary conditions for the vector potential in the flow problems are considered for simply connected domains in [11, 55, 99, 160] and for multiply connected domains in [116, 161]. The similar statements are used for the research of flows in ducts, for example, in [163]. In the problems with impermeable walls the boundary conditions for the vector potential are considered in [9, 94]. For the first time the boundary conditions for the vector potential for the flows in cavities with impermeable walls are obtained to the best of our knowledge in [55]. However, they have appeared unsuitable for numerical realisation in the flow problems. Therefore, the articles have appeared where the simpler methods of constructing the boundary conditions are suggested which are suitable for the flow problems. Thus, in [8, 56, 116] the scalar potential is introduced additionally to the vector potential and it is shown that the inhomogeneous boundary conditions can be retained only for the scalar potential, and the boundary conditions become homogeneous for the vector potential. Afterwards this approach is developed in article [114], which is devoted to the modelling of stationary three-dimensional incompressible fluid flow around the cube using rectangular non-uniform grids condensed in the neighbourhood of the cube. In the vertexes of the cube the original formulas for the components of the normal to the boundary of the cube and special approximating formulas for the normal derivative of the scalar potential are applied.

The algorithms where the scalar potential is used along with the vectorial potential have also some disadvantages despite the simpler form of the boundary conditions. These disadvantages are indicated, for example, in [117, 160]. The most noticeable of these drawbacks is the larger number of unknown variables and the necessity to solve more equations. Thus, using $\mathbf{u}-p$ formulation we have to solve three equations for the components of the velocity, one Poisson equation for the pressure with inhomogeneous boundary conditions for the normal derivative of the pressure and the additional equation for the corrections which ensures the fulfilling of the continuity equation [16, 47]. Using the vector potential and the scalar potential it is necessary to solve three equations of hyperbolic type for the components of the vorticity vector, three Poisson equations for the components of the vector potential and the Laplace equation for the scalar potential.

With the increase in the potency of computer facilities this disadvantage ceases to be essential and now it is possible not to take it into consideration any longer. The other disadvantage which is more significant is connected with the continuity equation. Using

the scalar potential, as well as for $\mathbf{u} - p$ formulations, the continuity equation in the difference form is not fulfilled precisely [160]. However, for the algorithms based on $\vec{\psi} - \vec{\omega}$ formulation the continuity equation in the difference form is fulfilled precisely using the staggered grids, and it is fulfilled independently of how accurately the vector potential has been calculated. In addition, the scalar potential can have the ruptures in the angular points of the boundary. This disadvantage stimulated the appearance of articles [153, 160] where instead of the scalar potential the solenoidal vector is introduced with the generally nonzero vorticity which satisfies the boundary conditions at entering and outgoing parts of the boundary.

In the present thesis the algorithms for calculating steady ideal fluid flows are based on $\vec{\psi} - \vec{\omega}$ formulations. The direct transposition of algorithms for calculating viscous fluid flows based on $\vec{\psi} - \vec{\omega}$ formulations to a case of ideal fluid flow is impossible for several reasons. Firstly, these two models differ by the statement of the boundary conditions. For the ideal fluid only one condition for the velocity, i.e. the impermeability condition, is put on the rigid walls. It is written as the equality of the normal component of the velocity to zero. In the problems on viscous fluid flows the condition on the velocity is usually imposed in the form of the no-slip condition on the impermeable boundary. Secondly, the systems of equations of these models are of various types. For example, in a case of two-dimensional steady viscous incompressible fluid flows the passage to new dependent variables ψ, ω gives two equations of elliptic type with respect to ψ and ω. And it is necessary to set ψ and to calculate ω over the entire boundary of the domain. In a case of ideal fluid flow the equation for the stream function is also of elliptic type, but for the vorticity the equation is of hyperbolic type of the first order. Therefore, for the numerical solution the values of the vorticity are required not over the entire boundary, but only at the inlets where the trajectories enter the flow domain.

Finally, in all the mentioned articles where $\vec{\psi} - \vec{\omega}$ formulations are used for describing three-dimensional flows the iterative algorithms or the algorithms of the method of establishing the steady state are oriented to the application of rectangular uniform grids (see, for example, review [11]). There are practically no articles of this kind for curvilinear three-dimensional grids. Two-dimensional curvilinear grids constructed by the algebraic method together with $\psi - \omega$ approach are used, for example, in [127] for the modelling of two-dimensional ideal fluid flow through the channels with curvilinear boundaries. This technique lays in the basis of [67, 156] devoted to the modelling of axially symmetric steady ideal compressible fluid flows on curvilinear grids. Here the grids are adapted to the geometry of channels and they are constructed by solving the differential equations for the node coordinates [68, 124].

The present thesis has the following purposes.

1. The development and the substantiation of the iterative finite difference methods for the numerical solution of two-dimensional and three-dimensional stationary problems on ideal fluid flows through the channels of complicated geometry in $\psi - \omega$ formulations using adaptive grids.

2. The development and the substantiation of the algorithms of the equidistribution method for constructing adaptive grids on flat and space curves, in flat domains, on surfaces and in three-dimensional domains.

3. The development of the iterative finite difference method for the calculation of steady fluid flows with the surface waves within the framework of two-dimensional shallow water model using adaptive grids.

4. The realisation of the developed algorithms as the complexes of computer codes for the numerical solution of the problems.

The thesis consists of Introduction (Chapter 1), 11 chapters describing contents and results of researches, Conclusion (Chapter 13) and References. The basic results of the thesis are published in [70]–[74], [128]–[137].

Chapters 2 - 6 are devoted to the development of the iterative finite difference method for the numerical solution of two-dimensional stationary problems on ideal fluid flows through the channels of complicated geometry using new dependent variables: the stream function ψ and the vorticity function ω on adaptive grids.

In Chapter 2 the initial mathematical statement of the problem on subsonic steady flows of perfect gas in channels is given. The vector of the mass expenditure $\rho\mathbf{u}$ and the total energy H are given at the inlet Γ_1 of the simply connected domain Ω. The impermeability conditions are given on the rigid walls and the normal component $\rho\mathbf{u} \cdot \mathbf{n}$ of the vector of the mass stream is given at the outlet Γ_2. The mathematical statement of the problem on steady ideal incompressible fluid flow is also presented. For incompressible fluid the density ρ is constant and the total energy is not given at the inlet. The mathematical aspects of the statement correctness of the stationary problems on incompressible fluid flows are considered in [2]–[4], [7, 52, 113, 152].

For the numerical solution of the problem new dependent variables, i.e. the stream function ψ and the vorticity function ω, are introduced. The equation for the stream function is of elliptic type at $\rho > 0$, as well as for two-dimensional Navier-Stokes equations for the incompressible fluid. If we consider the equation for the vorticity function at the given velocity vector and density then this equation will be of a hyperbolic type of the first order with respect to ω. Thus, it has the different type from that for the stationary Navier-Stokes equations where the equation for the vorticity is of elliptic type, as well as the equation for the stream function.

In Chapter 3 with the help of one-to-one non-degenerate mapping

$$x^\alpha = x^\alpha(q^1, q^2), \quad \alpha = 1, 2, \tag{1.1}$$

of the unit square Q in the plane of coordinates $q^1 O q^2$ onto the physical domain Ω the equations for ψ, ω and H are written in new independent variables q^α. Thus, the domain of solution Q which is named "computational domain" becomes simpler, but now the equations have a more complicated form. The Jacobian of the transformation and the components of the metric tensor enter into the coefficients of these equations along with the required functions.

The obtained equations are approximated on a curvilinear grid. The equidistribution method is developed for constructing a grid. The essence of the method is explained in hapter 4. The equidistribution principle for two-dimensional case consists in the requirement of the constancy of the product of mesh square and the value of the given control function w at the centre of the mesh. The differential equations for constructing two-dimensional adaptive grids (ED2-equations) are obtained on the basis of the equidistribution principle.

The equivalence of the equidistribution principle and the differential equations of the equidistribution method is proved. It is shown that in two-dimensional case ED2-equations follow from the equidistribution principle under the additional assumption about the orthogonality of the mapping (1.1). The inverse statement is also correct

about the realisation of the equidistribution principle for the solutions of ED2-equations which satisfy the conditions of non-degeneracy and orthogonality of the mapping.

The coordinates of any quasi-orthogonal adaptive grid are shown to satisfy the difference equations of the equidistribution method if the components of the metric tensor and the Jacobian are calculated at the centres of the meshes.

The equations for the arrangement of the nodes on the boundary of two-dimensional domain using the same control function w as inside domain are obtained.

In the articles of other authors [29, 34, 35, 60, 138] the equidistribution principle is used separately in each coordinate direction for constructing two-dimensional grids. Therefore, one-dimensional equidistribution method [13] is actually applied to constructing a multi-dimensional grid. Only in [22] two-dimensional equidistribution principle is used implicitly for constructing two-dimensional grid. The reviews of other methods for constructing grids are given in [48, 79], [88]–[92], [150].

Chapter 5 is devoted to the development of the iterative finite difference method for the numerical solution of two-dimensional stationary problems on ideal fluid flows through the channels of complicated geometry using adaptive grids. The finite difference equations for the grid stream function, the vorticity and the total energy are obtained by the integro-interpolational method by the approximation of the integrated relations which are the integrated analogues of the differential equations. The staggered grids are used for approximation: the grid functions ψ, ρ and the pressure p are defined in the integer nodes of a grid, the components of the metric tensor and the Jacobian of the mapping (1.1), the vorticity function and the total energy are calculated at the centres of the meshes. Using the staggered grids we retain some properties of the solutions of the differential equations, in particular, the continuity equation on a curvilinear grid is fulfilled on each step of the iterative process within the round-off errors.

Approximating the integrated relation for the stream function the integrals along the sides of the integration contour are calculated using the trapezoid formula. Thus, the nine-point difference equation is obtained which approximates the differential equation for the stream function with the second order with respect to the space variables q^1 and q^2 for smooth solutions and sufficiently smooth coefficients. In the particular case of the Poisson equation and the square grid the obtained approximation changes over to the scheme of the "oblique cross" which is mentioned in the book [120].

It is proved that the difference operator which is appropriate to the obtained finite difference equation is self-adjoint and positively definite. The proof is carried out assuming the uniform ellipticity of the differential equation for the stream function.

It is shown that on grid functions which assign the correspondence between the nodes of the physical domain and the computational domain the obtained difference equation is satisfied identically when the right-hand side is equal to zero. Thus, the difference scheme for the stream function retains the property of the differential equation for this function.

Approximating the integrated relation for the vorticity function in the interior nodes the integrals along the sides of the contour of integration are calculated according to the signs of the contravariant components of the velocity. The vorticity function is taken either from the centre of the mesh enveloped by the contour or from the centre of an adjacent mesh. This approximation leads to the scheme with the differences directed against the stream. The pattern of this difference equation can consist of one, three or four nodes, i.e. it is variable. It is shown that in the case when no closed streamlines are present and no stationary points of gas exist it is possible to calculate the value of ω in

any node by the values of ω at the inlet of the domain.

For this purpose the definitions of the difference analogues of the absence of closed streamlines and stationary points of gas are introduced. The condition of the absence of stationary points of gas means that even on one side of a mesh the appropriate contravariant component of the velocity differs from zero. For obtaining the difference analogue of the condition of the absence of closed streamlines the concepts of "the pattern of the difference equation" for the vorticity, "the neighbourhood of the node", "the neighbourhood of the n-th level", "the area of dependence for the node" are introduced. The theorem about the necessary and sufficient conditions for the absence of closed streamlines is proved.

The following direct (non-iterative) method is suggested for obtaining the solution of the system of difference equations for the vorticity. Let it be necessary to calculate ω in some node P. If there are nodes in its neighbourhood where the values of ω have not yet been calculated, then we pass from the node P to any of these nodes and we begin to investigate its neighbourhood. As a result of such passage upstream from node to node we come either to the node where the values of ω in the nodes of its neighbourhood have been calculated or to the inlet of the domain where the values of the vorticity are known from the boundary conditions. Further the values of ω in all nodes of the area of dependence are calculated in the inverse order, i.e. downstream, and then ω is calculated in the node P. This method has common features with the implicit method of running calculation which is frequently used for solving non-stationary one-dimensional problems of gas dynamics [118]. The method for the solution of the difference equations for the vorticity function is the generalization of the method [77], which is using the rectangular grids, for the curvilinear grids.

The difference equations for calculating H differ from the equations for the vorticity only by its homogeneity and they are solved by the same direct method.

As it was told above, the values of the vorticity at the inlet are assumed to be known. However, there are no such values in $\psi - \omega$ formulation. The values of the stream function and its normal derivative are given at the inlet. Thus, there is the problem of calculating the values of the vorticity at the inlet of the domain. This problem is completely similar to the problem of calculating the vorticity on the boundary for the Navier-Stokes equations. The difference is that it is required to calculate the values of the vorticity over the entire boundary for the Navier-Stokes equations, and in our case it is required only at the inlet of the domain. On the rigid walls and the outlet of the boundary the values of the vorticity are not required either for the differential equations or for the constructed difference scheme.

Various methods for obtaining the values of the vorticity function on the boundary for calculating viscous fluid flows are presented in [5, 110, 117]. In [110] the table of calculation results of flow in the cavity on the rectangular grid is shown. It demonstrates the influence of various methods of approximation of the boundary condition for the vorticity on the exactitude of numerical solution. The exhaustive review and comparison of articles devoted to local and global methods of calculating the vorticity on the boundary of two-dimensional domain are presented in [36]. The boundary condition for the vorticity of the first order of the exactitude is offered for the first time in [148]. In article [57] the strict substantiation of the convergence of some difference schemes for calculating two-dimensional and three-dimensional flows is presented. For these schemes the vorticity function on the boundary is calculated by the formulas like the Thom formula. The approximate conditions of the second and third orders are considered in [85]. The

approximating formulas for the vorticity with the weight parameters are constructed in [145, 168, 169]. The relaxation procedures [144, 146] are applied in order to prevent a divergence of iterative processes using the approximate formulas for calculating the vorticity on the boundary.

In [33, 58, 59, 87, 103, 122] the immediate calculation of the vorticity on the boundary is not performed. Instead, the given conditions for normal and tangential components of the velocity vector are used. They are written as the conditions for the stream function and its normal derivative to the boundary. On the intermediate iterations the velocity of fluid on the rigid boundary is not equal to the given value, but when the iterations converge the no-slip condition is fulfilled. The strict substantiation of the convergence of such algorithm is given in [58]. In [25, 111] the values of the vorticity function are calculated not on the boundary, but in the interior nodes of a grid which are adjacent to the boundary. Papers [154, 155], [157]–[159] devoted to the problem of calculating the vorticity on the boundary solving the Navier-Stokes equations in the stream function - vorticity formulation are also worth mentioning.

In the present thesis the approximation of the boundary values of the vorticity is based on the relation which connects the vorticity function with the covariant components of the velocity. In the difference formula for the vorticity the covariant components of the velocity on the boundary are known and they do not vary during the global iterative process. The values of the covariant components of the velocity in the interior nodes adjacent to the boundary are calculated using the values of other grid functions taken from the previous iteration. The relaxation procedure is also used for calculating the boundary values of the vorticity.

The pressure is defined on the basis of approximation of the expression which follows from the motion equations written in the Gromeka-Lamb form in curvilinear coordinates. The method of coordinated approximation is used for calculating the pressure. It means that the approximation of the integrands is similar to the approximation applied to obtaining the difference equation for the vorticity function. It is proved that for such approach the pressure does not depend on the path of integration. The links of this path pass along the sides of curvilinear meshes. Such a method is considered in [76] for the case of rectangular grids.

For viscous incompressible fluid flows the Poisson equation is usually used for calculating the pressure. This equation is obtained from the motion equations and is supplemented by the inhomogeneous Neumann boundary conditions. It is necessary to achieve the coordinated approximation of the right-hand side of the Poisson equation and the boundary conditions for the solvability of such a problem. It is rather difficult to attain this coordinated approximation at the difference level even on the uniform rectangular grids. This problem is considered in [20, 117]. Therefore, the so-called marching method of calculating the pressure is offered and for the first time it is substantiated in [115]. The generalization of this method in curvilinear coordinates is the method of coordinated approximation applied in the present thesis for calculating the pressure in ideal compressible fluid flow.

The chapter is conlcluded with the description of the global iterative process of solving the difference problem on gas flow. The process consists of three stages. At the first stage the problem on the potential ideal incompressible fluid flow is solved. This solution is the initial approximation for calculating the vortical ideal incompressible fluid flow which is the initial approximation for solving the problem on the vortical gas flow.

It is proved that the given process has the important property of the preservation of constant flow on an arbitrary curvilinear grid.

In Chapter 6 the results of testing the developed algorithm on the problems with the known exact solutions [6] are described. The essentially vortical incompressible plane fluid flow in the channel with the stream bending by an angle of 270^0 is investigated. The problem on the plane vortical non-isoenergetic gas flow is solved for the curvilinear channel. The Mach numbers varied from 0.25 at the inlet up to 0.62 at the outlet, thus the flow is only subsonic.

The serviceability of the presented algorithm is shown on these examples. The influence of various scheme parameters and grid parameters on the exactitude of numerical solution and convergence speed of the iterative process is investigated.

Chapters 7 - 10 are devoted to the development of the iterative finite difference method for the numerical solution of three-dimensional stationary problems on ideal fluid flows through the channels of complicated geometry using new dependent variables: the vector potential ψ and the vorticity vector ω on adaptive grids.

In Chapter 7 the initial mathematical statement of the problem on steady ideal incompressible fluid flow in channels is given. The velocity vector $\mathbf{u}$ is given at the inlet Γ_1 of the simply connected domain Ω. The impermeability conditions are given on the rigid walls and the normal component $\mathbf{u} \cdot \mathbf{n}$ of the velocity vector is given at the outlet Γ_2.

The mathematical aspects of the statement correctness of the stationary problems on three-dimensional incompressible fluid flows which are similar to the described problem are considered in [7, 49, 65, 101].

As it has already been mentioned, in the present thesis $\vec{\psi}$ - $\vec{\omega}$ formulation of the problem is used. Therefore, we need not to solve the continuity equation, as it will be fulfilled automatically. And, secondly, there is no pressure as an unknown function.

In all articles by other authors where $\vec{\psi} - \vec{\omega}$ formulation is used for viscous fluid flows the vector potential is assumed to be solenoidal. It leads to the simplifying of the equation for the vector potential, but it also results in the algorithm complexity, because of the requirement of realisation of this condition in each node of a grid. The realisation of this condition in curvilinear coordinates is problematic, thus, we do not require this condition to be fulfilled in the present thesis.

With the help of one-to-one non-degenerate mapping

$$x^\alpha = x^\alpha(q^1, q^2, q^3), \quad \alpha = 1, 2, 3, \tag{1.2}$$

of the unit cube Q in the space of coordinates q^1, q^2, q^3 onto the physical domain Ω the equations for $\vec{\psi}, \vec{\omega}$ are written in new independent variables q^α.

The obtained equations are approximated on a curvilinear grid. For constructing a grid three-dimensional equidistribution method is developed.

In Chapter 8 the equidistribution principle is formulated and the equations of the equidistribution method for constructing three-dimensional adaptive grids are obtained.

Here the equidistribution principle consists in the requirement of the constancy of the product of mesh volume and the value of the given control function w at the centre of the mesh. The relation between the volume of three-dimensional mesh and the numerical value of the Jacobian of the mapping (1.2) at the centre of the mesh is obtained. On the basis of this connection the equidistribution principle in the difference form is written using the Jacobian of the mapping. The differential analogue of the principle is used for obtaining the differential equations of the equidistribution method (ED3-equations).

9

The equivalence of the equidistribution principle and the differential equations of the equidistribution method is proved.

For the solution of the system of nonlinear difference equations which is obtained by the approximation of the differential ED3-equations the method of stabilizing corrections is used [96] .

The conditions are formulated which make possible the construction of a grid on lateral surfaces bounding the physical domain by the equidistribution method using the same control function as inside the domain.

The differential equations and the difference equations for constructing the grids on surfaces are obtained. According to the equidistribution principle the product of the area of each mesh of the two-dimensional grid covering the curvilinear face and the value of the control function at the centre of the mesh must be a constant value for this face.

The similar approach where a grid on lateral surfaces of three-dimensional domain is constructed on the basis of the equations for interior nodes is used, for example, in [143]. Here the well known equations from [48, 150] are used as the basis.

The differential equations and the difference equations for constructing the grids on space curves bounding the faces of the physical domain are obtained. The equidistribution principle means that the lengths of the segments between two adjacent nodes of the grid are inversely proportional to the values of the control function at the centres of these segments.

The conditions are formulated which make it possible to construct grid on a curve by the equidistribution method using the same control function as inside the domain.

For a flat curve with the natural parametrization the equation for constructing a grid on a space curve changes over to the equation for constructing a grid on a plane curve. For a straight segment it changes over to the equation for constructing a grid on a straight segment which is considered in Chapter 4.

For constructing three-dimensional grids in articles by other authors (see, for example, [17]), as well as in articles devoted to constructing two-dimensional grids, one-dimensional equidistribution principle is used separately in each coordinate direction. In the present thesis on the basis of the uniform methodology multi-dimensional equidistribution principle is formulated and the equations of the equidistribution method are obtained for grids covering the varieties in two-dimensional and three-dimensional spaces: a domain in R^2, a curve in R^2, a domain in R^3, a surface in R^3, a curve in R^3.

In Chapter 9 the iterative finite difference method is developed for the numerical solution of three-dimensional stationary problems on ideal incompressible fluid flows through the channels of complicated geometry using new dependent variables: the vector potential $\vec{\psi}$ and the vorticity vector $\vec{\omega}$ on adaptive grids. Using the staggered grids we retain some properties of the solution of the differential equations, in particular, the difference continuity equation on a curvilinear grid is fulfilled on each step of the iterative process within the round-off errors.

The finite difference equations for the components of grid function $\vec{\psi}$ are obtained by the integro-interpolational method by approximating the integrated relations which are the integrated analogues of the differential equations. Approximating the integrated relations in the interior nodes the integrals over the faces of the surface of integration (i.e. over the faces of a parallelepiped) are calculated using the three-dimensional analogue of the trapezoid formula. The obtained 27-point difference equation is the three-dimensional analogue of the "oblique cross" scheme [120].

These equations are written in all interior nodes. The boundary values for the covariant components of the vector potential are given not on all faces of the computational domain. In particular, for the first component ψ_1 the boundary values are not given on the left boundary $q^1 = 0$ and the right boundary $q^1 = 1$. Therefore, the additional difference equations are added obtained also by the integro-interpolational method making use of the smaller parallelepipeds as the surfaces of integration.

Thus, the 18-point difference equation for ψ_1 is obtained in the nodes of the left and right faces. Contrary to the articles of other authors, here the vector potential is not assumed to be solenoidal for calculating the boundary values.

The difference equations for the second and third covariant components of the vector potential are obtained similarly. The additional equations for the second component are written in the nodes of the anterior and back faces, and for the third component – in the nodes of the lower and upper faces of the computational domain Q.

The numerical realisation of the boundary conditions for the vector potential is considered using the problem on the incompressible fluid flow in the curved duct by way of example. For obtaining these conditions it is assumed that the fluid enters the domain by the direction of interior normal to the inlet.

Using the given values of the normal component of the velocity vector at the inlet and the outlet and the impermeability conditions on the rigid walls we obtain the formulas for the covariant components of the vector potential which are tangential to the faces. Thus, two components of $\vec{\psi}$ are known on each face. These components do not vary during the iterative process. The transversal component is calculated on each step of the global iterative process using the above-described difference formulas.

This process for calculating the boundary values of $\vec{\psi}$ is used earlier in [11] for the case of Cartesian coordinates and uniform rectangular grids. We managed to generalize it to the case of curvilinear grids.

As it was mentioned earlier, the vorticity function is calculated by the direct (non-iterative) method in the two-dimensional case, and the signs of the components of the velocity could be alternating. We did not manage to generalize this method to the three-dimensional case, therefore here it is assumed that the sign of one of the components of the velocity is fixed.

In particular, for the channel which is used in test calculations the second contravariant component of the velocity is positive everywhere in domain. The first and third components can be of alternating signs. From the physical point of view it means that the primary direction of the fluid flow is the direction along the axis of the channel with possible rotation of the fluid partiles around this axis. The mathematical implication is that this condition leads to the hyperbolicity of the system of equations with respect to the components of the vorticity vector. There are well known effective methods of solving hyperbolic systems [48]. By analogy with t-hyperbolic systems it is possible to name this system "q^2-hyperbolic" and it is possible to use the well known methods for solving hyperbolic systems of equations. In the present thesis the implicit two-dimensional scheme "predictor - corrector" by S.K. Godunov [48] is used. The scheme is realized by the scalar sweeps in each of two coordinate directions. For its realisation it is necessary to know all three components of the vorticity vector at the inlet of the domain.

The formulas for calculating the boundary values of the components of the vorticity vector at the inlet are obtained similarly to the two-dimensional case using the given values of the velocity at the inlet and the values of the vector potential which have already been

calculated from the previous iteration in the grid nodes adjacent to the boundary.

The boundary conditions for the components of the vorticity vector of three-dimensional viscous flow are considered earlier in the articles [94, 160] and books [5, 11, 44].

At the end of the chapter the global iterative process of solving the difference problem on three-dimensional steady ideal incompressible fluid flow in channels is described. The process consists of two stages: at the first stage the problem on the potential ideal incompressible fluid flow is solved. This solution is the initial approximation for calculating the vortical ideal incompressible fluid flow.

In Chapter 10 the calculation results of the series of three-dimensional problems are presented. The first series of calculations is carried out for the domain of simple form, i.e. for the parallelepiped with the faces parallel to the coordinate planes of Cartesian system of coordinates. The flow pattern is investigated for various boundary conditions for the velocity vector at the inlet and the outlet. The numerical results are compared either to the exact solutions or, when the flow is independent of the third coordinate (i.e. there is actually a two-dimensional flow), with the solutions obtained with the help of the two-dimensional algorithm developed in Chapters 2 - 6. These simple examples demonstrate the serviceability of the presented algorithm. The influence of various scheme parameters on the convergence speed of the iterative process is investigated.

The other series of calculations is performed for the duct with the square cross-section and with the stream bending by an angle of $180°$. The calculations are also carried out for the various boundary conditions for the velocity vector at the inlet and the outlet. As it has been shown by the results of other authors [8, 16, 18, 19, 21, 23, 32, 46, 47, 54, 61, 93, 97, 140, 147, 160, 163, 166], if there is a shift stream at the inlet, then the secondary flows appear in the curved part of a duct. These secondary flows are imposed on the primary flow which is given by the velocity vector at the inlet. The results of the present thesis are qualitatively coinciding with the conclusions of [18, 19] about the appearance of the rotary motion of the ideal fluid partiles around the axis of the curved channel.

In Chapters 11 - 12 the algorithms for calculating ideal gas flows described in Chapters 2 - 6 are applied to the numerical solution of the problems on stationary fluid flows with the surface gravitational waves in the river channels of complicated configuration within the framework of the plane shallow water model of the first approximation.

In Chapter 11 the mathematical statement of the problem on steady fluid flow with the surface gravitational waves is presented in initial variables: the velocity vector $\mathbf{u}$ and the elevation $\eta(\mathbf{x})$ of the fluid surface above the non-perturbed level.

It is known [107] that the system of equations of the shallow water coincides with the system of equations of gas dynamics for perfect gas with the adiabatic exponent equal to two. Therefore, the developed algorithm for calculating ideal gas flows using new dependent variables ψ and ω on curvilinear grids can be applied to the numerical solution of the problem on fluid flows with the surface gravitational waves within the framework of the plane shallow water model of the first approximation. Here we would like to mention the book [80] where the possibility of using $\psi - \omega$ formulation for calculating oceanic flows is emphasized.

The global iterative process of solving the difference problem on steady fluid flow with the surface waves is solved in three stages. At the first stage the problem on the potential flow "under the cover" is solved ($\eta(\mathbf{x}) \equiv 0, \ \omega(\mathbf{x}) \equiv 0$). This solution is the initial approximation for calculating the vortical flow "under the cover" ($\eta(\mathbf{x}) \equiv 0$) which is the initial approximation for solving the problem on the vortical fluid flow with free

surface.

The approximation of the equation for ψ in these problems is completely similar to the approximation for the problems on the ideal gas flows.

The closed streamlines can appear here, therefore the equation for the vorticity is approximated by the other scheme, i.e. by the scheme with central differences. The obtained system of equations is solved by the implicit method of establishing the steady state with splitting of the operator on the upper time level and the realisation by the sweep method.

Since the value $H^2/2$ is the analogue of the pressure, then the method of coordinated approximation is also used for its calculation.

The numerical results of modelling of the fluid flow with the surface waves on the given part of the river-bed are presented. The geometry and parameters are taken from the article [15]. The series of calculations for various geometries of the bottom and for various flow velocities at the inlet is presented.

In Chapter 12 the iterative algorithm on adaptive grids for calculating steady flows in the rivers with islands is developed on the basis of the plane shallow water model using new dependent variables – the stream function ψ and the vorticity function ω.

Similar to Chapter 11 the plane shallow water model of the first approximation is used for describing ideal incompressible fluid flows with free surface. The equations of this model are the same as in Chapter 11. The domain of solution Ω is multiply connected, because there are islands in the river-bed. Therefore, the differences of the algorithm for multiply connected domains from the algorithm described in Chapter 11 for simply connected domains are emphasized here.

The modification of the equidistribution method for constructing curvilinear grids in doubly connected domains is presented.

The algorithm for calculating the value of the stream function on the contour of the island is described for all stages of the iterative process. Calculating the potential flow the value of ψ on the contour of the island is defined in the following way. Some calculations of the flow in the simply connected domain are performed with the decreasing depth of the shoal in that place where the island should be. The limiting value of the stream function is defined when the depth of the shoal becomes close to zero. This approximate value of ψ is taken as the value of ψ on the contour of the island for calculating the potential flow.

Calculating the vortical flow the value of ψ on the contour of the island is obtained from the independence condition of the total depth of the contour of integration in the method of coordinated approximation. The similar approach for the definition of values of the stream function on the interior contours of multiply connected domains is used in algorithms for calculating viscous fluid flows, for example, in [86, 142].

Some results of numerical modelling are presented for the flow around the island in the river-bed with the contour of coastal line which is taken from the article [15].

In Chapter 13 the basic results of researches are summarised.

The proofs of all lemmas and theorems are provided in Appendix.

The following tools were used: Microsoft Fortran, Microsoft Paint, WATCOM Fortran, Graphic Workshop Professional, Tecplot.

Chapter 2

Mathematical models of two-dimensional steady ideal gas and fluid flows in Cartesian coordinates

2.1 Mathematical model of two-dimensional steady ideal gas flow in Cartesian coordinates

Let Ω be a simply connected domain in the plane of Cartesian coordinates $x^1 O x^2$. The mathematical statement of the problem on steady flow of ideal gas through the domain Ω consists in obtaining the velocity vector $\mathbf{u}$, the pressure p, the density ρ, and the total energy H, satisfying the continuity equation, the motion equation and the energy equation in Ω:

$$\nabla \cdot \rho \mathbf{u} = 0, \tag{2.1}$$

$$(\rho \mathbf{u} \cdot \nabla)\mathbf{u} + \nabla p = \mathbf{f}, \qquad \mathbf{x} = (x^1, x^2) \in \Omega, \tag{2.2}$$

$$\nabla \cdot \rho \mathbf{u} H = 0, \tag{2.3}$$

and the boundary conditions on the boundary $\Gamma = \partial \Omega$:

$$\rho \mathbf{u} \Big|_{\mathbf{x} \in \Gamma_1} = \vec{\nu}_1(\mathbf{x}), \quad \mathbf{u} \cdot \mathbf{n} \Big|_{\mathbf{x} \in \Gamma_0} = 0, \quad \rho \mathbf{u} \cdot \mathbf{n} \Big|_{\mathbf{x} \in \Gamma_2} = \nu_2(\mathbf{x}), \tag{2.4}$$

$$H \Big|_{\mathbf{x} \in \Gamma_1} = H_1(\mathbf{x}), \tag{2.5}$$

where $\mathbf{u} = (u_1, u_2)$, $u_\alpha (\alpha = 1, 2)$ are the components of the velocity vector along the axes Ox^α. $\mathbf{f}$ is the vector of external forces, $\mathbf{f} = (f_1, f_2)$. $\nabla = \left(\frac{\partial}{\partial x^1}, \frac{\partial}{\partial x^2} \right)$, $\mathbf{n}$ is the external normal to Γ. $\Gamma = \Gamma_1 \cup \Gamma_0 \cup \Gamma_2$, Γ_1 is the inlet to Ω $(\vec{\nu}_1 \cdot \mathbf{n} < 0)$, Γ_0 is the impermeable part of the boundary, Γ_2 is the outlet from Ω $(\nu_2 > 0)$, $\Gamma_1 \cap \Gamma_2 = \emptyset$ (see Fig.2.1).

The following equality is fulfilled for the total energy of the perfect gas:

$$H = \frac{\kappa p}{\rho(\kappa - 1)} + \frac{V^2}{2}, \tag{2.6}$$
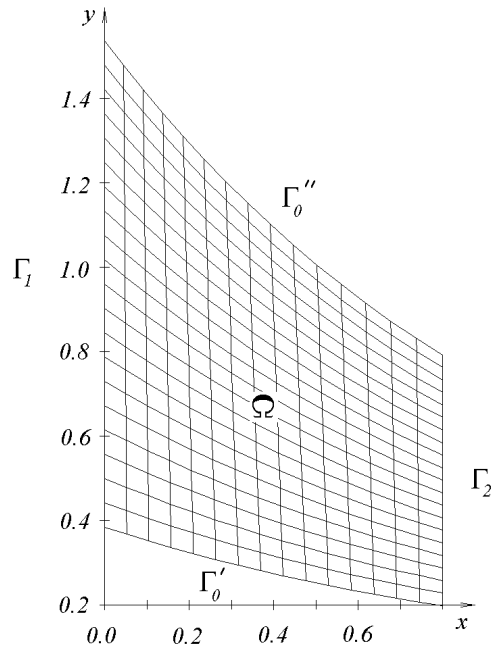
Figure 2.1: The initial ("uniform") grid in the physical domain Ω
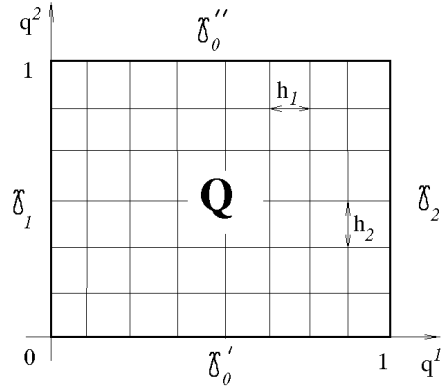
Figure 2.2: The uniform grid in the computational domain Q

where κ is the adiabatic exponent, $V = |\mathbf{u}|$.

In addition to (2.4)–(2.5), the pressure is given at the certain point $M_0 \in \bar{\Omega}$:

$$p(M_0) = p_0. \tag{2.7}$$

Let us introduce the function $\nu(s)$:

$$\nu(s) = \begin{cases} \vec{\nu}_1(\mathbf{x}) \cdot \mathbf{n}(\mathbf{x}), & \mathbf{x}(s) \in \Gamma_1, \\ 0, & \mathbf{x}(s) \in \Gamma_0, \\ \nu_2(\mathbf{x}), & \mathbf{x}(s) \in \Gamma_2, \end{cases} \tag{2.8}$$

where s is the length of the boundary counted from a certain fixed point, $\mathbf{x} = \mathbf{x}(s)$ is the parametric equation of the boundary Γ.

By applying the Green's formula to the equation (2.1) we obtain the necessary condi-

16

tion of the solvability for the problem described above:

$$\int_0^S \nu(s)ds = 0, \tag{2.9}$$

where S is the length of the boundary Γ.

For the numerical solution of the problem new dependent variables, i.e. the stream function ψ and the vorticity function ω, are introduced:

$$\rho u_1 = \frac{\partial \psi}{\partial x^2}, \quad \rho u_2 = -\frac{\partial \psi}{\partial x^1}, \quad \omega = \mathrm{rot}\ \mathbf{u} \equiv -\frac{\partial u_1}{\partial x^2} + \frac{\partial u_2}{\partial x^1}. \tag{2.10}$$

Therefore we obtain the following equations for ψ and ω:

$$\mathrm{div}\ \left(\frac{1}{\rho}\ \nabla \psi\right) = -\omega, \tag{2.11}$$

$$\nabla \cdot \rho \mathbf{u} \omega = -\mathrm{rot}\ \left(\rho \nabla \frac{V^2}{2}\right) + \mathrm{rot}\mathbf{f}. \tag{2.12}$$

The boundary values of ψ are uniquely defined from the conditions (2.4) (with the accuracy up to the additive constant ψ_0):

$$\psi(s) = \psi_0 + \int_0^s \nu(\xi)d\xi. \tag{2.13}$$

Under the same conditions the normal derivative of ψ at the inlet Γ_1 is obtained:

$$\frac{\partial \psi}{\partial \mathbf{n}}\ \Big|_{x \in \Gamma_1} = \vec{\nu}_1 \cdot \vec{\tau}, \tag{2.14}$$

where $\vec{\tau}$ is the unit vector in the tangential direction to Γ_1.

If the equation (2.12) is considered with the given velocity vector $\mathbf{u}$ and density ρ, then this equation is the first-order linear equation with respect to ω. According to the theory of equations with non-negative characteristic form [104], for such linear equation the boundary conditions must be given on those parts of the boundary Γ where $\mathbf{u} \cdot \mathbf{n} < 0$, i.e. at the inlet Γ_1. The conditions (2.4) do not allow us to calculate the value $\omega\ \Big|_{\Gamma_1}$, but for the numerical calculation of the problem these boundary conditions can be obtained by means of conditions (2.13), (2.14).

2.2 Mathematical model of two-dimensional steady ideal fluid flow in Cartesian coordinates

The mathematical statement of the problem on steady flow of ideal fluid through the domain Ω consists in obtaining the velocity vector $\mathbf{u}$ and the pressure p satisfying the equations of continuity and motion in Ω (see Fig.2.3):

$$\nabla \cdot \mathbf{u} = 0, \tag{2.15}$$

17
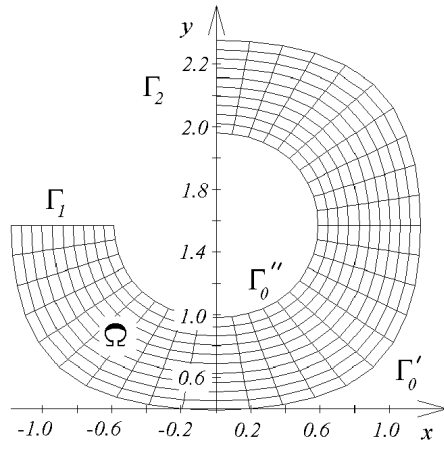
Figure 2.3: The initial ("uniform") grid in the physical domain Ω
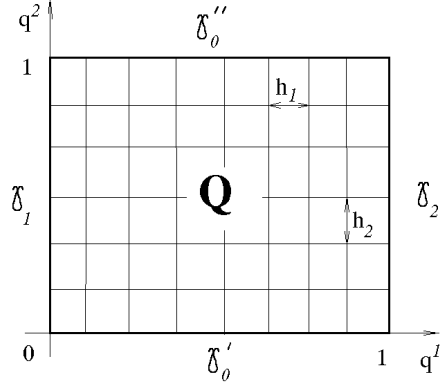
Figure 2.4: The uniform grid in the computational domain Q

$$(\mathbf{u} \cdot \nabla)\mathbf{u} + \nabla p = \mathbf{f}, \quad \mathbf{x} = (x^1, x^2) \in \Omega \tag{2.16}$$

and the boundary conditions on the boundary $\Gamma = \partial\Omega$:

$$\mathbf{u}\Big|_{\mathbf{x}\in\Gamma_1} = \vec{\nu}_1(\mathbf{x}), \quad \mathbf{u}\cdot\mathbf{n}\Big|_{\mathbf{x}\in\Gamma_0} = 0, \quad \mathbf{u}\cdot\mathbf{n}\Big|_{\mathbf{x}\in\Gamma_2} = \nu_2(\mathbf{x}), \tag{2.17}$$

The density of the fluid is assumed to be 1.

The correctness of the problems on non-stationary or steady ideal fluid flows through the given domains is considered in [2]–[4], [7, 52, 64, 66, 69, 113, 152, 167] and other papers. It is known that for the solution to be unique the pressure must also be given at the certain point $M_0 \in \bar{\Omega}$ in addition to the conditions (2.17):

$$p(M_0) = p_0. \tag{2.18}$$

In order to eliminate the pressure from the basic equations new dependent variables, i.e. the stream function ψ and the vorticity function ω, are introduced:

$$u_1 = \frac{\partial\psi}{\partial x^2}, \quad u_2 = -\frac{\partial\psi}{\partial x^1}, \quad \omega = \mathrm{rot}\,\mathbf{u} \equiv -\frac{\partial u_1}{\partial x^2} + \frac{\partial u_2}{\partial x^1}. \tag{2.19}$$

Then we obtain the following equations for ψ and ω:

$$\Delta\psi = -\omega, \tag{2.20}$$

18

$$\mathbf{u} \cdot \nabla \omega = \mathrm{rot}\mathbf{f}. \tag{2.21}$$

The boundary values of ψ and the normal derivative of ψ at the inlet are uniquely determined from the conditions (2.17) using formulas (2.13), (2.14).

Chapter 3

Mathematical models of two-dimensional steady ideal gas and fluid flows in curvilinear coordinates

3.1 Mathematical model of two-dimensional steady ideal gas flow in curvilinear coordinates

Let

$$x^\alpha = x^\alpha(q^1, q^2), \quad \alpha = 1, 2, \tag{3.1}$$

be a one-to-one non-degenerate mapping of the square Q in the plane of coordinates $q^1 O q^2$ onto the domain Ω. For simplicity, let us assume that the inlet and the outlet are the connected parts of the boundary. Γ_1 is the image under the mapping (3.1) of the left side γ_1 of the square Q, Γ_2 is the image of the right side γ_2. The impermeable part Γ_0 consists of two intervals Γ_0' and Γ_0'' which are the images of the lower side γ_0' and the upper side γ_0'' of Q respectively. The domain Ω and its prototype Q are shown in Fig.2.1 and Fig.2.2.

The equations (2.11), (2.12) and (2.3) have the following form in new independent variables q^α:

$$\frac{\partial}{\partial q^1}\left(k_{11}\frac{\partial\psi}{\partial q^1} + k_{12}\frac{\partial\psi}{\partial q^2}\right) + \frac{\partial}{\partial q^2}\left(k_{21}\frac{\partial\psi}{\partial q^1} + k_{22}\frac{\partial\psi}{\partial q^2}\right) = -J\omega, \tag{3.2}$$

$$\frac{\partial}{\partial q^1}(\rho J v^1 \omega) + \frac{\partial}{\partial q^2}(\rho J v^2 \omega) =$$

$$= -\frac{\partial}{\partial q^1}\left(\rho\frac{\partial}{\partial q^2}\left(\frac{u^2}{2}\right)\right) + \frac{\partial}{\partial q^2}\left(\rho\frac{\partial}{\partial q^1}\left(\frac{u^2}{2}\right)\right) - \frac{\partial f_1}{\partial q^2} + \frac{\partial f_2}{\partial q^1}, \tag{3.3}$$

$$\frac{\partial}{\partial q^1}(\rho J v^1 H) + \frac{\partial}{\partial q^2}(\rho J v^2 H) = 0, \tag{3.4}$$

where

$$k_{11} = \frac{g_{22}}{\rho J}, \quad k_{12} = k_{21} = -\frac{g_{12}}{\rho J}, \quad k_{22} = \frac{g_{11}}{\rho J},$$

21

$g_{\alpha\beta}$ $(\alpha, \beta = 1, 2)$ are the covariant components of the metric tensor:

$$g_{11} = x_{q^1}^2 + y_{q^1}^2, \quad g_{12} = x_{q^1} x_{q^2} + y_{q^1} y_{q^2}, \quad g_{22} = x_{q^2}^2 + y_{q^2}^2,$$

$x = x^1$, $y = x^2$, J is the Jacobian of the mapping (3.1):

$$J = x_{q^1} y_{q^2} - x_{q^2} y_{q^1}.$$

f_α are the covariant components of the vector $\mathbf{f}$. The contravariant velocity components v^α are connected with ψ by the following relations:

$$v^1 = \frac{1}{\rho J} \frac{\partial \psi}{\partial q^2}, \quad v^2 = -\frac{1}{\rho J} \frac{\partial \psi}{\partial q^1}. \tag{3.5}$$

The transformation (3.1) is non-degenerate, therefore $J \neq 0$. Further we assume that the Jacobian is positive everywhere in Ω: $J > 0$.

In calculating the pressure the motion equations in the Gromeka-Lamb form written in curvilinear coordinates are used:

$$-\rho J v^2 \omega + \rho \frac{\partial}{\partial q^1} \frac{u^2}{2} + \frac{\partial p}{\partial q^1} = f_1,$$

$$\rho J v^1 \omega + \rho \frac{\partial}{\partial q^2} \frac{u^2}{2} + \frac{\partial p}{\partial q^2} = f_2. \tag{3.6}$$

If we introduce the covariant components of the velocity v_α:

$$v_\alpha = g_{\alpha 1} v^1 + g_{\alpha 2} v^2, \quad \alpha = 1, 2, \tag{3.7}$$

then the equation (3.2) can be written in a different form:

$$\omega = \frac{1}{J} \left(-\frac{\partial v_1}{\partial q^2} + \frac{\partial v_2}{\partial q^1} \right). \tag{3.8}$$

This relation is used for obtaining the numerical values of ω at the inlet Γ_1.

The boundary conditions for ψ have the following form in new coordinates:

$$\psi \Big|_{\mathbf{q} \in \gamma} = \bar{\psi}(\mathbf{q}), \tag{3.9}$$

$$k_{11} \frac{\partial \psi}{\partial q^1} + k_{12} \frac{\partial \psi}{\partial q^2} = -x_{q^2} \nu_{1,1} - y_{q^2} \nu_{1,2}, \quad \mathbf{q} = (0, q^2), \tag{3.10}$$

where $\bar{\psi}(\mathbf{q})$ is the function from the right-hand side of the equation (2.13), $\nu_{1,\alpha}$ $(\alpha = 1, 2)$ are Cartesian components of the vector $\vec{\nu}_1$.

As it has been noted above, with the given functions $\mathbf{u}$ and ρ the equation (2.12) can be considered hyperbolic. The characteristics of this equation enter the domain Ω through the inlet Γ_1, leave the domain Ω through Γ_2 and do not cross the impermeable part Γ_0.

Is the same true for the equation (3.3)? I.e., if the functions ρ, J, v^α and the right-hand side are given and the equation is considered as the linearized equation with respect to ω, will then the part γ_1 be the inlet to Q $(v^1 > 0)$, γ_2 – the outlet from Q $(v^1 > 0)$ and γ_0 – the impermeable part of Q $(v^2 = 0)$? The answer to this question is given by the following lemma.

Lemma 3.1. *The contravariant components of the velocity satisfy the following relations on the boundary $\gamma = \partial Q$:*

$$v^1 \Big|_{\gamma_1} > 0, \quad v^1 \Big|_{\gamma_2} > 0, \quad v^2 \Big|_{\gamma_0' \cup \gamma_0''} = 0. \tag{3.11}$$

This result will be essentially used later for constructing the difference scheme for the vorticity in the nodes near the boundary.

3.2 Mathematical model of two-dimensional steady ideal fluid flow in curvilinear coordinates

For incompressible fluid the equations have the same form as the equations for gas in new independent variables with the only difference that it is necessary to put $\rho = 1$:

$$\frac{\partial}{\partial q^1} \left(k_{11} \frac{\partial \psi}{\partial q^1} + k_{12} \frac{\partial \psi}{\partial q^2} \right) + \frac{\partial}{\partial q^2} \left(k_{21} \frac{\partial \psi}{\partial q^1} + k_{22} \frac{\partial \psi}{\partial q^2} \right) = -J\omega, \tag{3.12}$$

$$\frac{\partial}{\partial q^1} J v^1 \omega + \frac{\partial}{\partial q^2} J v^2 \omega = 0, \tag{3.13}$$

where

$$k_{11} = \frac{g_{22}}{J}, \quad k_{12} = k_{21} = -\frac{g_{12}}{J}, \quad k_{22} = \frac{g_{11}}{J}.$$

The domain Ω and its prototype Q are shown in Fig.2.3 and Fig.2.4.

Chapter 4

Method for grid generation in two-dimensional domains

4.1   One-dimensional equidistribution method

At the beginning of this chapter the equidistribution principle will be formulated and the equation of the equidistribution method for constructing one-dimensional non-uniform grids on the given segment will be obtained. This will be done either for the transformations of continuous argument or for the discrete transformations. The information given here is commonly known (see, for example, [13, 34, 35]), but it would be difficult to present the further results without this introduction. The accent is made on the equivalence of the principle and the equations of the equidistribution method either at differential or at difference levels.

Further in Section 4.2 and in Chapter 8 the attempts will be made to follow the realisation of this equivalence constructing two-dimensional and three-dimensional grids.

In [13] the equidistribution method for constructing one-dimensional adaptive grids covering the segment $[0; \ L]$ is described. The essence of the equidistribution method consists in achieving the constancy of the product of mesh length and the value of the control function w at the centre of the mesh.

Let x_j be the coordinates of grid nodes, $j = 1, \ldots, N$,

$$x_1 = 0, \ x_N = L. \tag{4.1}$$

The length of the mesh $[x_j; \ x_{j+1}]$ is denoted by $S_{j+1/2}$, therefore the equidistribution principle has the following form:

$$w(x_{j+1/2})S_{j+1/2} = \tilde{C}_h = \text{const}, \quad j = 1, \ldots, N - 1. \tag{4.2}$$

Thus, the lengths of meshes are small where the control function w has large values and, on the contrary, they are large in that part of $\Omega = (0; \ L)$ where the function w has small values.

Hereinafter we assume that the control function satisfies the restrictions:

$$1 \le w(x) \le W, \quad W = \text{const} < \infty, \quad x \in \bar{\Omega}. \tag{4.3}$$

The equidistribution principle (4.2) is the difference analogue of the following differential equation:

$$w(x)\frac{dx}{dq}(q) = C, \quad C = \text{const}, \quad q \in Q = (0; \ 1), \tag{4.4}$$

where

$$x = x(q), \quad q \in \bar{Q}, \tag{4.5}$$

$$x(0) = 0, \quad x(1) = L, \tag{4.6}$$

is the required one-to-one mapping of $\bar{Q}$ onto $\bar{\Omega}$.

The equation (4.4) is named "the equidistribution principle in differential form". The equation (4.4) can be written in a different equivalent form:

$$\frac{dq}{dx} = \frac{w}{C}. \tag{4.7}$$

From the above, after the integration over Ω and using (4.6), the formula is obtained for calculating the constant C:

$$C = \int_0^L w(x)dx, \tag{4.8}$$

and after the integration over the interval $[x_j; x_{j+1}]$ the following relation is obtained:

$$Ch = \int_{x_j}^{x_{j+1}} w(x)dx, \quad j = 1, ..., N - 1.$$

Here $x_j = x(q_j)$, q_j is the coordinate of the node with the number j of the uniform grid with the step size h covering the unit segment Q, $q_j = (j - 1)h$, $h = 1/(N - 1)$.

The latter equation shows that the function $w(x)$ is uniformly distributed over all meshes $[x_j, x_{j+1}]$ of the constructed grid and the lengths of the meshes satisfy the following inequalities:

$$\frac{hL}{W} \leq x_{j+1} - x_j \leq hLW, \quad j = 1, ..., N - 1. \tag{4.9}$$

It must be noted that the equation (4.4) is nonlinear, therefore the numerical solution must be based on the iterative process. The process can be constructed, for example, on the basis of the following corollary from the equation (4.4):

$$x(q) = C \int_0^q \frac{dq}{w(x(q))}, \tag{4.10}$$

where

$$C = L \left/ \int_0^1 \frac{dq}{w(x(q))} \right. . \tag{4.11}$$

Using the quadrature formula of rectangles the following expression for the node coordinates can be obtained:

$$x_k^{n+1} = C_h^n \sum_{j=1}^{k-1} \frac{h}{w(x_{j+1/2}^n)}, \quad k = 2, ..., N - 1, \tag{4.12}$$

26

where n is the iteration number,

$$C_h^n = L \bigg/ \sum_{j=1}^{N-1} \frac{h}{w(x_{j+1/2}^n)}. \tag{4.13}$$

However, as it has been observed by many authors (see, for example, [28]) the disadvantage of the iterative process (4.12) is that the lengths of meshes oscillate, i.e. long and short meshes alternate. This situation occurs for a rapidly changing control function w.

Therefore, for the calculation of the coordinates the approximation of the corollary of the equation (4.4) is used obtained by the differentiation of (4.4):

$$\frac{d}{dq}\left(w(x)\frac{dx}{dq}\right)(q) = 0, \quad q \in Q. \tag{4.14}$$

This equation is named "the equation of the equidistribution method in differential form" or "ED1-equation". Its difference analogue:

$$\frac{1}{h}\left[w(x_{j+1/2})\frac{x_{j+1}-x_j}{h} - w(x_{j-1/2})\frac{x_j-x_{j-1}}{h}\right] = 0, \quad j = 2, \ldots, N-1, \tag{4.15}$$

is named "ED1-equation in difference form".

Further, instead of (4.2) and (4.4) we shall use the relations into which the Jacobian of the mapping (4.5) will enter. Let us denote the Jacobian by J, $J(q) = \frac{dx}{dq}(q)$. Then the equidistribution principle (4.4) has the following form:

$$w(x(q))J(q) = C, \quad C = \text{const}, \quad q \in Q. \tag{4.16}$$

If the Jacobian J at the centre of the mesh is approximated by the central difference:

$$J_{j+1/2} = \frac{x_{j+1}-x_j}{h}, \tag{4.17}$$

then the difference analogue (4.2) of the equidistribution principle follow from (4.16), and it can be written as follows:

$$w(x_{j+1/2})J_{j+1/2} = \frac{\tilde{C}_h}{h} \equiv C_h = \text{const}, \quad j = 1, \ldots, N-1. \tag{4.18}$$

In a one-dimensional case the equidistribution principle and ED1-equation are equivalent in the sense that if the mapping (4.5) satisfies the equidistribution principle (4.16), then the function $x = x(q)$ is also the solution of ED1-equation (4.14) and, on the contrary, any solution of ED1-equation (4.14) satisfies the equidistribution principle (4.16).

If the approximation (4.17) is used, then the equivalence is also valid at the difference level: if the node coordinates of the grid satisfy the equidistribution principle (4.18), then the grid function x_j is the solution of the difference ED1-equations (4.15) and, on the contrary, the solution of these equations gives the grid which satisfies the equidistribution principle (4.18).

The method of constructing adaptive grids on the basis of the equation (4.14) is named "ED1-method for rectilinear segments".

The solution of the problem (4.15)–(4.1) can be found, for example, with the help of the following iterative process:

$$\frac{x_j^{n+1}-x_j^n}{\tau} = \frac{1}{h}\left[w(x_{j+1/2}^n)\frac{x_{j+1}^{n+1}-x_j^{n+1}}{h} - w(x_{j-1/2}^n)\frac{x_j^{n+1}-x_{j-1}^{n+1}}{h}\right], \tag{4.19}$$
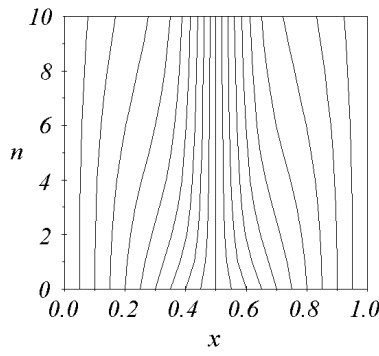
Figure 4.1: The convergence of the iterative process (4.19) for $\tau = 0.001$

where $\tau > 0$ is the iterative parameter, $j = 2, ..., N - 1$. The uniform grid with the step $\Delta x = L/(N - 1)$ can be taken as the initial approximation x_j^0.

When the iterative process converges the node coordinates of the constructed grid satisfy the following equations:

$$w(x_{j+1/2})\frac{x_{j+1} - x_j}{h} = C_h = \text{const}, \quad j = 1, ..., N - 1, \tag{4.20}$$

which are the difference analogues of (4.4). Here

$$C_h = \sum_{j=1}^{N-1} w(x_{j+1/2})(x_{j+1} - x_j) = L \left/ \sum_{j=1}^{N-1} \frac{h}{w(x_{j+1/2})} \right. . \tag{4.21}$$

The difference equations (4.19) with the boundary conditions (4.1) are solved by the sweep method which is well stipulated for an arbitrary value of the iterative parameter τ, because of the restriction (4.3). As calculations have shown, the convergence of the iterative process is slowed down for small values of τ. When these values are too large the process converges non-monotonically. The optimum value τ_{opt} exists giving the monotonic convergence with the fastest rate of convergence for the iterative process (4.19).

This is illustrated in Figures 4.1, 4.2 and 4.3 where the process of the iteration convergence for the grid using the following control function is shown:

$$w(x) = 1 + \alpha \exp(-a(x - 1/2)^2).$$

The experimental values of the parameters are $L = 1, \alpha = 10, a = 50$.

The choice of the control function w influences significantly the grid. The different ways of selection of w are discussed in [5, 30, 98, 149, 150].

The main requirement consists in a higher solution accuracy on the constructed non-uniform grid in comparison with the accuracy of the numerical solution on the uniform grid with the same number of nodes. For this purpose it is proposed to construct a grid ensuring the minimum approximation error [30].

Let us consider the simple example where the derivative of the function $u = x^3$, $x \in [0, L]$, $L > 1$, is approximated by the finite-difference expression $\frac{u_{j+1} - u_j}{x_{j+1} - x_j}$ on uniform and non-uniform grids. These grids are constructed using the following control functions:

$$w_1(x) = 1,$$

$$w_2(x) = 1 + \alpha|u_{xx}|,$$

28
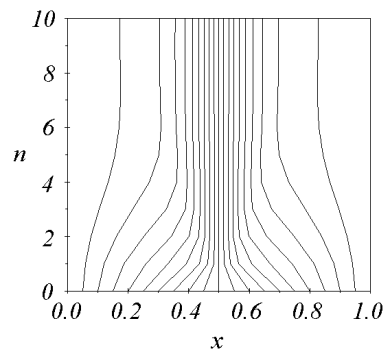
Figure 4.2: The convergence of the iterative process (4.19) for $\tau = 0.01$
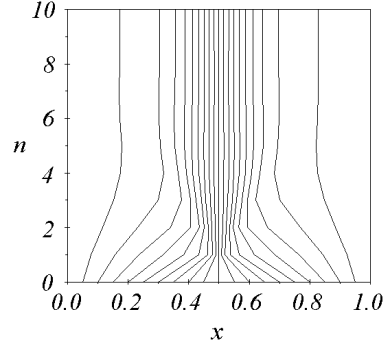
Figure 4.3: The convergence of the iterative process (4.19) for $\tau = 0.1$

$$w_3(x) = 1 + \alpha |u_x|,$$

$$w_4(x) = 1 + \alpha |u|.$$

The error of the derivative calculation is obtained using the following formula:

$$\delta = \max_j |u_x(x_j) - \frac{u_{j+1} - u_j}{x_{j+1} - x_j}|.$$

The analytical expression for the solution $x = x(q)$ of the problem (4.4)–(4.6) can be obtained for each of control functions mentioned above. If the error is investigated for large values of α and small step size h, then we obtain the following estimations of ψ:

$$\delta_1 \sim 3L^2 h,$$

$$\delta_2 \sim \frac{3}{2} L^2 h,$$

$$\delta_3 \sim L^2 h^{\frac{2}{3}},$$

$$\delta_4 \sim L^2 h^{\frac{1}{2}}.$$

It is clear that using the second control function the error of the derivative calculation is reduced two times. The errors of calculations on the grids constructed on the basis of w_3 and w_4 are larger than for the uniform grid.

29

This example shows that the unsuccessful choice of a control function can lead to the deterioration in the accuracy of the calculation. The similar investigation of the possibility of reducing the calculation accuracy under the excessive condensation of a grid can be found in [125].

In Section 4.2 and in Chapter 8 the equidistribution principle will be given in a multi-dimensional case, the equations of the equidistribution method will be obtained and some sufficient conditions will be defined for the principle and the equations of the equidistribution method to be equivalent in the sense mentioned above.

4.2   Two-dimensional equidistribution method

In two-dimensional case the analogue of the length of one-dimensional mesh is the square of the mesh of two-dimensional grid with the nodes $\mathbf{x}_j$ covering the domain Ω with the boundary Γ. Here $\mathbf{x} = (x^1, x^2)$, $j = (j_1, j_2)$ is multi-index, $j_\alpha = 1, \ldots, N_\alpha$, $\alpha = 1, 2$. The square of quadrangular mesh with vertexes $\mathbf{x}_{j_1,j_2}$, $\mathbf{x}_{j_1+1,j_2}$, $\mathbf{x}_{j_1+1,j_2+1}$, $\mathbf{x}_{j_1,j_2+1}$ is denoted by $S_{j+1/2}$. Then the equidistribution principle, that is the analogue of (4.2), has the following form:

$$w(\mathbf{x}_{j+1/2})S_{j+1/2} = \tilde{C}_h, \quad j_\alpha = 1, \ldots, N_\alpha - 1, \tag{4.22}$$

where $w(\mathbf{x}_{j+1/2})$ is the value of the given control function at the centre of the mesh. The coordinates of this centre are defined as the arithmetical average of the appropriate coordinates of four vertexes of the mesh.

We denote the total set of the grid nodes by $\bar{\Omega}_h$. Let us assume that the set $\bar{\Omega}_h$ is the image of the uniform rectangular grid $\bar{Q}_h$ covering the square $\bar{Q} = [0; 1] \times [0; 1]$ under the one-to-one mapping

$$x^\alpha = x^\alpha(q^1, q^2), \quad \alpha = 1, 2, \tag{4.23}$$

of the plane $q^1 O q^2$ onto the plane of Cartesian coordinates $x^1 O x^2$. The domain Ω and its prototype Q are shown in Fig.2.3 and Fig.2.4. The mapping (4.23) is unknown, and the differential equations for the definition of this mapping will be obtained.

Let us take the identity which is satisfied by an arbitrary smooth mapping (4.23):

$$\frac{\partial}{\partial q^1}\left(\frac{g_{22}}{J}\frac{\partial x^\alpha}{\partial q^1} - \frac{g_{12}}{J}\frac{\partial x^\alpha}{\partial q^2}\right) + \frac{\partial}{\partial q^2}\left(-\frac{g_{12}}{J}\frac{\partial x^\alpha}{\partial q^1} + \frac{g_{11}}{J}\frac{\partial x^\alpha}{\partial q^2}\right) = 0, \quad \alpha = 1, 2. \tag{4.24}$$

This identity represents the Laplace equation with respect to unknown functions x^α written in new coordinates q^α. The covariant components of the metric tensor of the required transformation (4.23) are denoted by $g_{\alpha\beta}$.

In order to narrow the set of functions satisfying the identity (4.24), we introduce the additional restrictions on these functions. Firstly, we assume that the system of coordinates defined by the required mapping (4.23) is orthogonal. It can be written in the following form:

$$g_{12} = 0. \tag{4.25}$$

And, secondly, it is assumed that the mapping (4.23) satisfies the equidistribution principle in differential form that is similar to the principle (4.16) in one-dimensional case:

$$w(\mathbf{x}(\mathbf{q}))J(\mathbf{q}) = C, \quad C = \text{const}, \quad \mathbf{q} = (q^1, q^2) \in Q, \tag{4.26}$$

where J is the Jacobian of the mapping (4.23). Using these conditions in the identity (4.24) we obtain two-dimensional equations of the equidistribution method or ED2-equations in differential form:

$$\frac{\partial}{\partial q^1}\left(wg_{22}\frac{\partial x^\alpha}{\partial q^1}\right) + \frac{\partial}{\partial q^2}\left(wg_{11}\frac{\partial x^\alpha}{\partial q^2}\right) = 0, \qquad \alpha = 1, 2. \tag{4.27}$$

Thus, in two-dimensional case ED2-equations follow from the equidistribution principle (4.26) under the additional assumption of the orthogonality of the mapping (4.23). It can be shown that the converse statement about the realisation of the equidistribution principle is correct for some solutions of the equations (4.27).

Lemma 4.1. *If the mapping (4.23) assigned by the solutions of the equations (4.27) is non-degenerate and orthogonal, then the equidistribution principle (4.26) is fulfilled for it.*

The obtained ED2-equations (4.27) differ from the equations that are used by other authors for constructing multi-dimensional grids on the basis of the idea of equidistribution. For example, in [37, 78, 102] the Thompson system of equations of [150] is taken as the basis:

$$g_{22}\left(x^\alpha_{q^1 q^1} + P_1 x^\alpha_{q^1}\right) + g_{11}\left(x^\alpha_{q^2 q^2} + P_2 x^\alpha_{q^2}\right) - 2g_{12}x^\alpha_{q^1 q^2} = 0. \tag{4.28}$$

The one-dimensional analogue of this system is written in the following form:

$$\frac{d^2 x}{dq^2} + P\frac{dx}{dq} = 0.$$

This equation is compared with ED1-equation (4.14) written in the form:

$$w\frac{d^2 x}{dq^2} + \frac{dw}{dq}\frac{dx}{dq} = 0,$$

and the conclusion is made that the function P should be chosen as follows:

$$P = \frac{1}{w}\frac{dw}{dq}.$$

Therefore, for the equation (4.28) it is natural to choose the functions P_α in the form:

$$P_\alpha = \frac{1}{w}\frac{dw}{dq^\alpha}.$$

Thus, we obtain the following equations:

$$g_{22}\frac{\partial}{\partial q^1}\left(w\frac{\partial x^\alpha}{\partial q^1}\right) + g_{11}\frac{\partial}{\partial q^2}\left(w\frac{\partial x^\alpha}{\partial q^2}\right) - 2g_{12}w\frac{\partial^2 x^\alpha}{\partial q^1 \partial q^2} = 0, \quad \alpha = 1, 2. \tag{4.29}$$

It is obvious, that the equations (4.29) are non-conservative in comparison with our equations (4.27).

Let us show how we should approximate the equation (4.27) if we want the node coordinates of the curvilinear grid satisfying the equidistribution principle to satisfy the difference equations.

Let us assume that $\bar{Q}$ is covered by the uniform rectangular grid with the number of nodes N_α and the step size h_α in the direction of the axes Oq^α, $h_\alpha = 1/(N_\alpha - 1)$, $\alpha = 1, 2$. Let $\mathbf{q}_j = (q^1_{j_1}, q^2_{j_2})$, $j = (j_1, j_2)$, $j_\alpha = 1, \ldots, N_\alpha$, $q^\alpha_{j_\alpha} = (j_\alpha - 1)h_\alpha$.

We introduce two basis operators of the difference derivatives:

$$(D_{q^1}\varphi)(\mathbf{q}) = \frac{\varphi(q^1 + h_1/2, q^2) - \varphi(q^1 - h_1/2, q^2)}{h_1}, \tag{4.30}$$

$$(D_{q^2}\varphi)(\mathbf{q}) = \frac{\varphi(q^1, q^2 + h_2/2) - \varphi(q^1, q^2 - h_2/2)}{h_2}, \tag{4.31}$$

On using these derivatives for writing the difference operators it is necessary to take into account the defintion areas of the grid functions. In some cases the grid functions refer not to the nodes of the grid with the integer indices, but, for example, to the centers of the meshes (the nodes with the half-integer indexes) or to the centers of the sides of the meshes (the nodes with one integer index and one half-integer index).

Thus, the result of applying the operators D_{q^α} depends on the nodes where the grid function φ is defined. In addition, this result obviously depends upon the point where it is necessary to calculate the derivative. If the function φ is defined in the integer nodes $\mathbf{q}_j = (q^1_{j_1}, q^2_{j_2})$, then it is assumed that

$$(D_{q^1}\varphi)_{j_1+1/2, j_2} = \frac{\varphi_{j_1+1, j_2} - \varphi_{j_1, j_2}}{h_1},$$

$$(D_{q^1}\varphi)_{j_1, j_2} = \frac{(D_{q^1}\varphi)_{j_1-1/2, j_2} + (D_{q^1}\varphi)_{j_1+1/2, j_2}}{2},$$

$$(D_{q^1}\varphi)_{j_1, j_2+1/2} = \frac{(D_{q^1}\varphi)_{j_1, j_2} + (D_{q^1}\varphi)_{j_1, j_2+1}}{2},$$

$$(D_{q^1}\varphi)_{j_1+1/2, j_2+1/2} = \frac{(D_{q^1}\varphi)_{j_1+1/2, j_2} + (D_{q^1}\varphi)_{j_1+1/2, j_2+1}}{2}.$$

The formula (4.30) for grid functions which are defined at the centers of the meshes $\mathbf{q}_{j+1/2} = (q^1_{j_1+1/2}, q^2_{j_2+1/2})$, $q^\alpha_{j_\alpha+1/2} = q^\alpha_{j_\alpha} + h_\alpha/2$, $\alpha = 1, 2$, has the following form:

$$(D_{q^1}\varphi)_{j_1, j_2+1/2} = \frac{\varphi_{j_1+1/2, j_2+1/2} - \varphi_{j_1-1/2, j_2+1/2}}{h_1},$$

$$(D_{q^1}\varphi)_{j_1, j_2} = \frac{(D_{q^1}\varphi)_{j_1, j_2-1/2} + (D_{q^1}\varphi)_{j_1, j_2+1/2}}{2},$$

$$(D_{q^1}\varphi)_{j_1+1/2, j_2+1/2} = \frac{(D_{q^1}\varphi)_{j_1, j_2+1/2} + (D_{q^1}\varphi)_{j_1+1, j_2+1/2}}{2},$$

$$(D_{q^1}\varphi)_{j_1+1/2, j_2} = \frac{(D_{q^1}\varphi)_{j_1, j_2} + (D_{q^1}\varphi)_{j_1+1, j_2}}{2}.$$
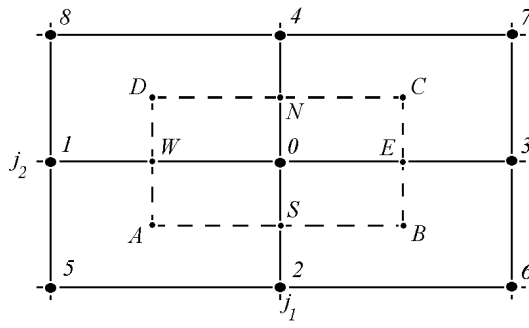
Figure 4.4: The pattern of the difference equations and the integration contour in the internal node $\mathbf{q}_j \in Q_h$

If the grid function φ is defined at the centers of the horizontal sides of the meshes $\mathbf{q}_{j_1+1/2, j_2} = (q^1_{j_1+1/2}, q^2_{j_2})$, then the following expressions are taken as the difference derivative (4.30):

$$(D_{q^1}\varphi)_{j_1,j_2} = \frac{\varphi_{j_1+1/2,j_2} - \varphi_{j_1-1/2,j_2}}{h_1},$$

$$(D_{q^1}\varphi)_{j_1+1/2,j_2} = \frac{(D_{q^1}\varphi)_{j_1,j_2} + (D_{q^1}\varphi)_{j_1+1,j_2}}{2},$$

$$(D_{q^1}\varphi)_{j_1,j_2+1/2} = \frac{(D_{q^1}\varphi)_{j_1,j_2} + (D_{q^1}\varphi)_{j_1,j_2+1}}{2},$$

$$(D_{q^1}\varphi)_{j_1+1/2,j_2+1/2} = \frac{(D_{q^1}\varphi)_{j_1+1/2,j_2} + (D_{q^1}\varphi)_{j_1+1/2,j_2+1}}{2}.$$

Similarly, using the average values of φ, if it is necessary, the difference derivative $D_{q^1}\varphi$ is calculated for grid functions defined at the centers of the vertical sides of the meshes $\mathbf{q}_{j_1,j_2+1/2} = (q^1_{j_1}, q^2_{j_2+1/2})$. The derivative $D_{q^2}\varphi$ is calculated in a similar way.

The difference equations for the node coordinates are obtained by the integro-interpolational method. The equations (4.27) are substituted by the following integrated relations:

$$\oint_{\mathcal{C}} wg_{22}\frac{\partial x^\alpha}{\partial q^1}dq^2 - wg_{11}\frac{\partial x^\alpha}{\partial q^2}dq^1 = 0, \quad \alpha = 1, 2, \tag{4.32}$$

where $\mathcal{C}$ is the contour of the rectangle. The sides of this rectangle are parallel to the axes Oq^α and divide the distances from the considered interior node $\mathbf{q}_j$ to the nodes, adjacent to it, in two equal parts.

Fig.4.4 shows the nine-point pattern of the difference equations and the integration contour (denoted by the dashed line) in the internal node $\mathbf{q}_j \in Q_h$.

The integrals along the sides of this contour are approximated by the trapezoid formula, assuming that the grid functions x^α are defined in the integer nodes $\mathbf{q}_j$, and the function w – at the centers of the meshes. The components of the metric tensor $g_{\alpha\beta}$ and

the Jacobian are also defined at the centers of the meshes and are calculated using the following formulas:

$$(g_{11})_{j+1/2} = (D_{q^1}x^1 D_{q^1}x^1 + D_{q^1}x^2 D_{q^1}x^2)_{j+1/2}, \tag{4.33}$$

$$(g_{12})_{j+1/2} = (D_{q^1}x^1 D_{q^2}x^1 + D_{q^1}x^2 D_{q^2}x^2)_{j+1/2}, \tag{4.34}$$

$$(g_{22})_{j+1/2} = (D_{q^2}x^1 D_{q^2}x^1 + D_{q^2}x^2 D_{q^2}x^2)_{j+1/2}, \tag{4.35}$$

$$J_{j+1/2} = \left(D_{q^1}x^1 D_{q^2}x^2 - D_{q^2}x^1 D_{q^1}x^2\right)_{j+1/2}. \tag{4.36}$$

Since the resulting expressions are rather awkward, the approximation formula only for the side BC of the integration contour $ABCD$ at $\alpha = 1$ is presented here:

$$\int\limits_{(BC)} wg_{22}\frac{\partial x}{\partial q^1}dq^2 \approx \frac{h_2}{2}\left[wg_{22}(C)\frac{x(7) + x(3) - x(4) - x(0)}{2h_1}+\right.$$

$$\left.+wg_{22}(B)\frac{x(3) + x(6) - x(0) - x(2)}{2h_1}\right] \equiv \frac{h_2}{2}\left[wg_{22}D_{q_1}x(C) + wg_{22}D_{q_1}x(B)\right]. \tag{4.37}$$

Thus, we obtain the following difference ED2-equations:

$$(D_{q^1}(wg_{22}D_{q^1}x^\alpha) + D_{q^2}(wg_{11}D_{q^2}x^\alpha))_j = 0. \tag{4.38}$$

It is necessary to take into account that the grid complexes $wg_{\beta\beta}D_{q^{3-\beta}}x^\alpha$, $\alpha, \beta = 1, 2$, are defined at the centers of the meshes also.

If the Jacobian of the mapping is calculated using the formula (4.36), then

$$S_{j+1/2} = J_{j+1/2}h_1h_2. \tag{4.39}$$

Thus, the equidistribution principle in difference form (4.22) can be written in the form similar to (4.18):

$$w(\mathbf{x}_{j+1/2})J_{j+1/2} = \frac{\tilde{C}_h}{h_1h_2} \equiv C_h = \text{const}, \quad j_\alpha = 1, \ldots, N_\alpha - 1. \tag{4.40}$$

A grid with convex meshes is named "quasi-orthogonal" if the centerlines of each quadrangular mesh are perpendicular. Taking into account the approximation (4.34) the condition of quasi-orthogonality can be written in the form of the condition (4.25):

$$(g_{12})_{j+1/2} = 0. \tag{4.41}$$

A grid with convex meshes is named "adaptive" if for each mesh the equidistribution principle in difference form (4.40) is fulfilled.

As it has been noted above, for orthogonal two-dimensional mappings (4.23) the equidistribution principle in differential form (4.26) and ED2-equations (4.27) are equivalent. At the difference level it is possible to prove that the grid functions defining the curvilinear grid which satisfies the equidistribution principle in difference form (4.40) are the solutions of the difference ED2-equations (4.38).

Lemma 4.2. *The coordinates of the nodes of any quasi-orthogonal adaptive grid with convex meshes satisfy the equations (4.38).*

The method of constructing adaptive grids on the basis of the equations (4.27) is named "ED2-method for plane domains".

The difference equations (4.38) are nonlinear. They represent the nine-point formula. The matrix of the coefficients of these equations is symmetric and has the diagonal predominance. In practice, on constructing a grid simpler difference equations are used. They are obtained on the basis of the quadrature formula of rectangles. Thus, instead of (4.37), the following approximation is applied:

$$\int_{(BC)} wg_{22}\frac{\partial x}{\partial q^1}dq^2 \approx h_2 \cdot wg_{22}(E)\frac{x(3) - x(0)}{h_1}, \tag{4.42}$$

where

$$wg_{22}(E) = \frac{wg_{22}(C) + wg_{22}(B)}{2}.$$

The approximation of the integrals yields two systems of the difference equations for the determination of coordinates x^α. For solving the obtained systems it is possible to use an iterative process where on each step the coefficients $wg_{\beta\beta}$ of the difference equations are calculated from the previous iteration. Then for the approximation (4.42) the difference equations can be considered as the five-point formula:

$$\sum_{k=0}^{4} \alpha_k \varphi(k) = 0, \quad \mathbf{q}_j \in Q_h, \tag{4.43}$$

where $\varphi(k) = x^\alpha(k)$ and the coefficients α_k are calculated as follows:

$$\alpha_1 = \frac{h_2}{h_1}k_{11}(W), \quad \alpha_3 = \frac{h_2}{h_1}k_{11}(E), \quad \alpha_2 = \frac{h_1}{h_2}k_{22}(S),$$

$$\alpha_4 = \frac{h_1}{h_2}k_{22}(N), \quad \alpha_0 = -(\alpha_1 + \alpha_2 + \alpha_3 + \alpha_4), \tag{4.44}$$

where $k_{11} = wg_{22}, \ k_{22} = wg_{11}$.

On considering the matrix $\mathcal{A}$ of the coefficients α_k of the difference equations (4.43) we can conclude that it is symmetric and has the diagonal predominance.

As in [22], the obtained systems of difference equations supplemented with the boundary conditions are solved by the method of alternating directions:

$$\frac{\bar{\varphi}_j - \varphi_j^n}{\tau/2} = \Lambda_1\bar{\varphi}_j + \Lambda_2\varphi_j^n,$$

$$\frac{\varphi_j^{n+1} - \bar{\varphi}_j}{\tau/2} = \Lambda_1\bar{\varphi}_j + \Lambda_2\varphi_j^{n+1}, \quad \mathbf{q}_j \in Q_h, \tag{4.45}$$

where $\varphi = x^\alpha, \ \alpha = 1, 2,$

$$\Lambda_1\varphi = \frac{1}{h_1}\left[k_{11}(E)\frac{\varphi(3) - \varphi(0)}{h_1} - k_{11}(W)\frac{\varphi(0) - \varphi(1)}{h_1}\right],$$

$$\Lambda_2 \varphi = \frac{1}{h_2} \left[k_{22}(N) \frac{\varphi(4) - \varphi(0)}{h_2} - k_{22}(S) \frac{\varphi(0) - \varphi(2)}{h_2} \right]. \tag{4.46}$$

Here the coefficients $k_{\beta\gamma}$ of the operators Λ_α are calculated using the node coordinates from the n-th iteration.

For constructing a grid the boundary conditions are necessary. If the positions of the nodes on the boundary are given, then the difference problem of Dirichlet type is solved for the equations (4.45). As the calculations have shown, the result can be unsatisfactory because of the strong skewness of the grid (non-orthogonality of coordinate lines) near the boundary. It happens because the positions of the nodes are defined by the difference equations (4.45) and the control function w inside the domain. And the nodes are placed under the different conditions on the boundary. Thus, this arrangement can appear to be unsuccessful.

The other type of boundary conditions is obtained from the requirement of the orthogonality of an appropriate set of coordinate lines to the boundary. However, this kind of definition for the node coordinates on the boundary leads sometimes to the shrinkage of nodes to the angles of domain Ω during the iterative process. Such undesirable effect is observed when the boundary of domain Ω has the angles larger than 90^0.

Therefore, we use the following method for calculating the nodes on the boundary: two-dimensional equidistribution method is used inside the domain and one-dimensional equidistribution method is used on the boundary. For the definitiness let us take the lower side $q^2 = 0$ of quadrate Q in Fig.2.1b and the part of the boundary $\partial\Omega$ corresponding to it under the mapping (4.23). Let the considered segment of the boundary be given in the parametric representation:

$$x^\alpha = f^\alpha(q), \quad 0 \le q \le 1, \quad \alpha = 1, 2. \tag{4.47}$$

Let this segment has the length L. If the arc length of the boundary is denoted by $s = s(q)$, then the following equality for $s(q)$ is fulfilled:

$$s(q) = \int_0^q \sqrt{\left(\frac{\partial f^1}{\partial q}\right)^2 + \left(\frac{\partial f^2}{\partial q}\right)^2} \, dq. \tag{4.48}$$

For the nodes on the boundary to be condensed in accordance with the control function w, it is assumed that the analogue of the equality (4.14) is satisfied for the arc length on the considered segment of the boundary:

$$\frac{d}{dq^1}\left(w \frac{ds}{dq^1}\right) = 0, \quad 0 \le q^1 \le 1, \tag{4.49}$$

where $w(s) = w(s(q^1)) = w(f^1(q(q^1)), f^2(q(q^1)))$. The parameters q^1 and q are connected by the relation (4.48) where the value $s(q^1)$ should be used in the left-hand side. Thus, the equation for constructing a grid on the plane curve is the following:

$$\frac{d}{dq^1}\left(w \sqrt{\left(\frac{\partial f^1}{\partial q^1}\right)^2 + \left(\frac{\partial f^2}{\partial q^1}\right)^2} \frac{dq}{dq^1}\right) = 0. \tag{4.50}$$

The equation (4.50) is named "EDC2-equation". It is supplemented by the boundary conditions of the type of (4.6):

$$s(0) = 0, \quad s(1) = L.$$
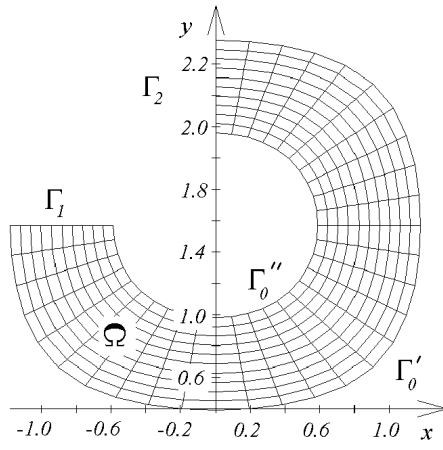
Figure 4.5: The initial approximation ("uniform grid")

The obtained problem is solved by the iterative method. The grid with the nodes uniformly distributed over the arc length is taken as the initial approximation.

The method of constructing adaptive grids on the basis of the equation (4.50) is named "EDC2-method for plane curves".

Further, in Chapter 8, it will be shown, that the considered method of distributing the nodes on the boundary of two-dimensional domain is the particular case of the equidistribution method for constructing grids on space curves. And the conditions, under which the same control function w can be used for placing the nodes either inside the domain or on its boundary, will be indicated.

4.3 Test case of the channel with the stream bending by an angle of 270^0

In Section 6.1 the results of calculations of the fluid flow in the channel with the stream bending by an angle of 270^0 are presented. Let us consider the grid generation for the domain from this test problem which is shown in Fig.2.3. The example of the grid which can be taken as the initial approximation for the iterative process (4.45) is shown in Fig.4.5. Its boundary consists of two rectilinear parts Γ_1 and Γ_2:

$$\Gamma_1 = \left\{ (x, y) \ \Big| \ -\frac{3\pi}{8} \le x \le -\frac{3\pi}{16}, \ y = \frac{\pi}{2} \right\},$$

$$\Gamma_2 = \left\{ (x, y) \ \Big| \ x = 0, \ \frac{11\pi}{16} \le y \le \frac{7\pi}{8} \right\},$$

and the curvilinear parts Γ_0' and Γ_0'' are given parametrically by the equation (4.47), where

$$f^1(q) = x_0 \cos \pi \left(\frac{3}{2}q - 1 \right),$$

$$f^2(q) = \arcsin \left(\frac{\cos x_0}{\cos f^1(q)} \right), \tag{4.51}$$
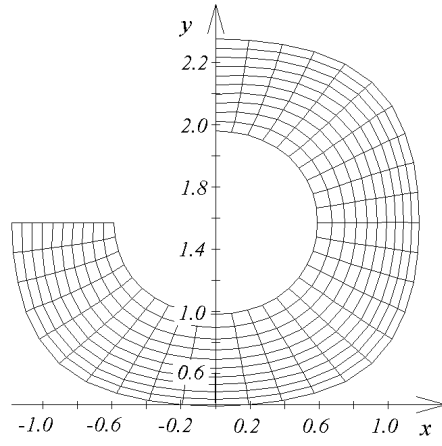
Figure 4.6: The grid with the uniform initial approximation after 30 iterations, $w = 1$

$x_0 = \frac{3\pi}{8}$ for Γ_0' and $x_0 = \frac{3\pi}{16}$ for Γ_0''.

The example of the grid which can be taken as the initial approximation for the iterative process (4.45) is shown in Fig.4.5.

Firstly, the nodes are placed either uniformly or with the condensation over the arc length along the boundaries Γ_0' and Γ_0'' depending on the control function. Then the nodes $\mathbf{x}_{j_1,1}$ and $\mathbf{x}_{j_1,N_2}$ with the same numbers j_1 are connected with the straight segments and these segments are divided into $N_2 - 1$ equal parts.

Fig.4.6 shows the grid obtained after 30 iterations with $w \equiv 1$. It can be seen that the grid is quasi-uniform inside the domain and it is very close to orthogonal. The condensation of coordinate lines is observed near the part Γ_0' of the boundary. This grid is the analogue of the uniform grid in one-dimensional case.

The grid constructed using the following control function:

$$w(x, y) = 1 + \alpha|\omega(x, y)| \tag{4.52}$$

is considered where $\alpha = 2$, $\omega(x, y) = 2 \cos x \sin y$. The choice of the control function is made in this way because of the numerical solution of the test problem on incompressible ideal fluid flow in the domain Ω on the curvilinear grid. The function ω is the vorticity function.

The given problem has the following exact solution:

$$u(x, y) = \cos x \cos y,$$

$$v(x, y) = \sin x \sin y,$$

where $u(x, y)$, $v(x, y)$ are the components of the velocity vector $\mathbf{u} = (u, v)$. The calculations have shown that the accuracy of the numerical solution for $\alpha = 2$ is enhanced in comparison with the solution on the grid presented in Fig.4.6 ($\alpha = 0$).

Fig.4.7 shows the grid obtained also after 30 iterations, but for $w = 1 + \alpha|\mathbf{u}(x, y)|^2$, $\alpha = 2$. The accuracy of the solution of the given problem is decreased on this grid.

The other advantage of the considered method for constructing adaptive grids is the high stability of the iterative process with respect to the choice of initial approximation. Fig.4.8 shows the other initial approximation. It is carried out in the following way. The

38
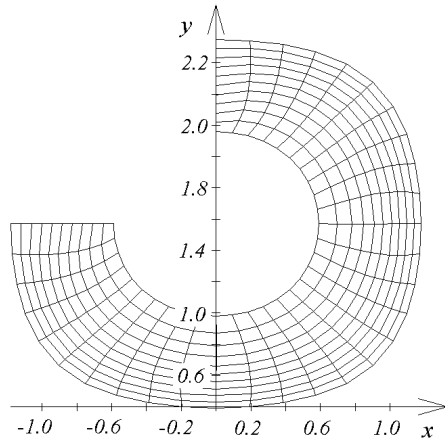
Figure 4.7: The grid with the uniform initial approximation after 30 iterations, $w = 1 + \alpha|\mathbf{u}(x,y)|^2$
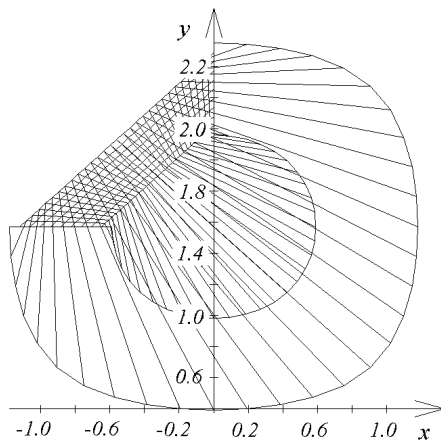
Figure 4.8: The "bad" initial approximation
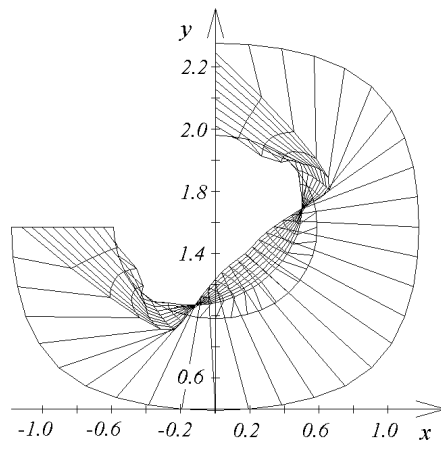
Figure 4.9: The grid with the "bad" initial approximation after 30 iterations, $w = 1 + \alpha|\omega(x,y)|$

nodes are placed uniformly along Γ_1 and Γ_2, after that the appropriate nodes x_{1,j_2} and x_{N_1,j_2}, $j_2 = 2, ..., N_2 - 1$, are connected with the straight segments, and these segments are divided into $N_2 - 1$ equal parts.

On comparing Fig.4.5 and Fig.4.8 it can be seen that the initial grid shown in Fig.4.8 is very bad, because it significantly differs from the final grid and its nodes are placed outside the domain Ω. Nevertheless, the iterative process converges for this bad initial approximation as well (see Fig.4.9), though it converges considerably slower than for the initial grid presented in Fig.4.5. During the further iterations the grid is obtained, similar to the grid constructed on the basis of the "good" initial approximation.

4.4   Test case of the part of the river-bed

Now let us illustrate the possibilities of two-dimensional equidistribution method by the example of the domain which is used in Chapter 11 for the modelling of the flow on the part of the river-bed.

The example of the grid which can be taken as the initial approximations for the iterative process (4.45) is shown in Fig.4.10. It is constructed as the initial approximation for the previous test case.

The grid obtained after 100 iterations with the control function $w \equiv 1$ is shown in Fig.4.11.

The grid constructed with the following control function depending on the width of the channel $B(x^1)$ in the direction perpendicular to the axes of the channel is shown in Fig.4.12:

$$w(x^1, x^2) = 1 + \alpha/B(x^1). \tag{4.53}$$

It is clear that there is the condensation of the grid in the places where the river-bed narrows.

The experiments with modification of the iterative parameter τ in (4.45) in the range $1.7 - 1.9$ have showed that the grid is practically independent of the value of τ.
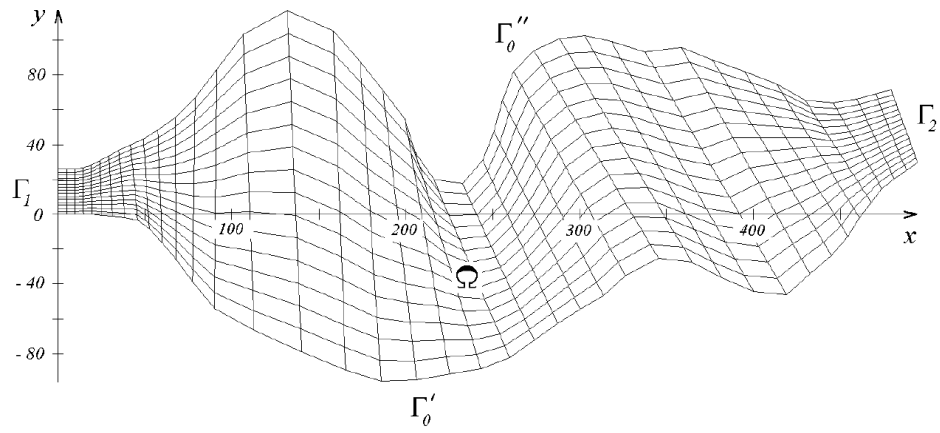
Figure 4.10: The initial approximation, $N_1 = 41$, $N_2 = 16$
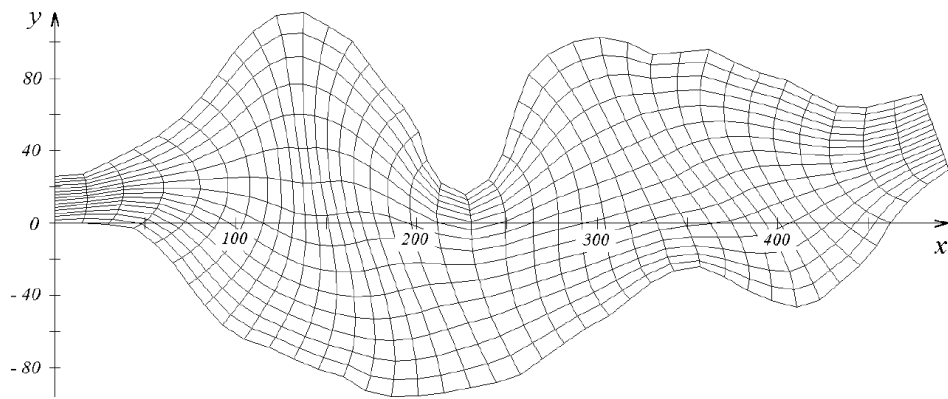
Figure 4.11: The grid after 100 iterations, $N_1 = 41$, $N_2 = 16$, $w \equiv 1$
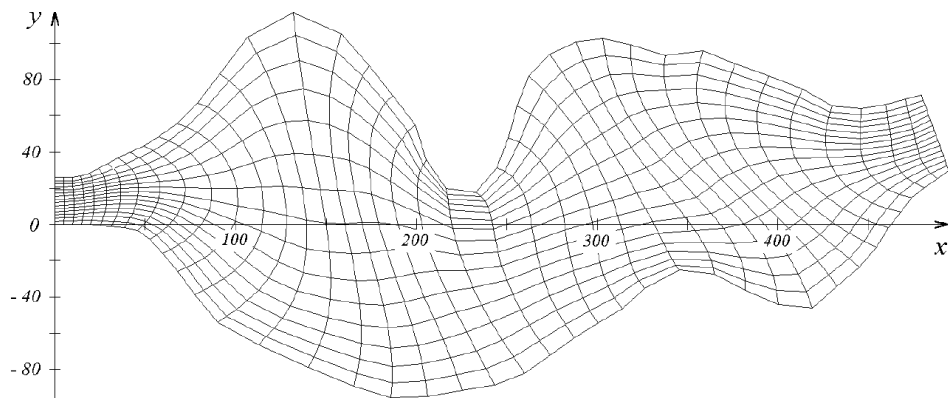
Figure 4.12: The grid after 100 iterations, $N_1 = 41$, $N_2 = 16$, $\alpha = 1000$

41
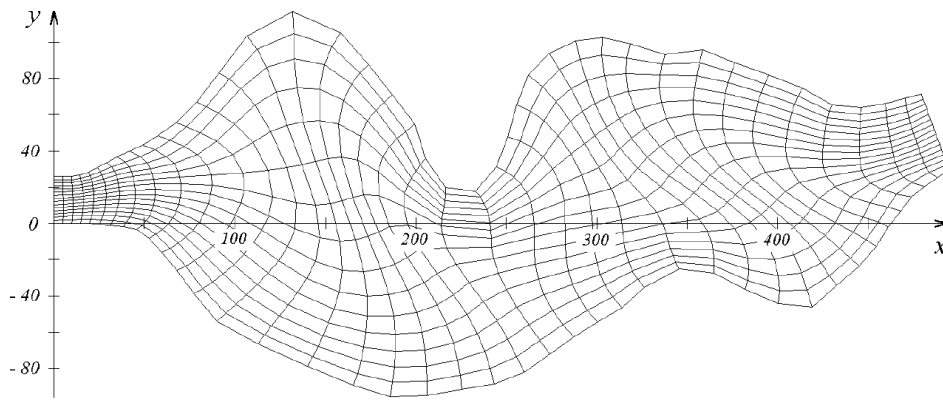
Figure 4.13: The grid after 1000 iterations, $N_1 = 41$, $N_2 = 16$, $\alpha = 1000$
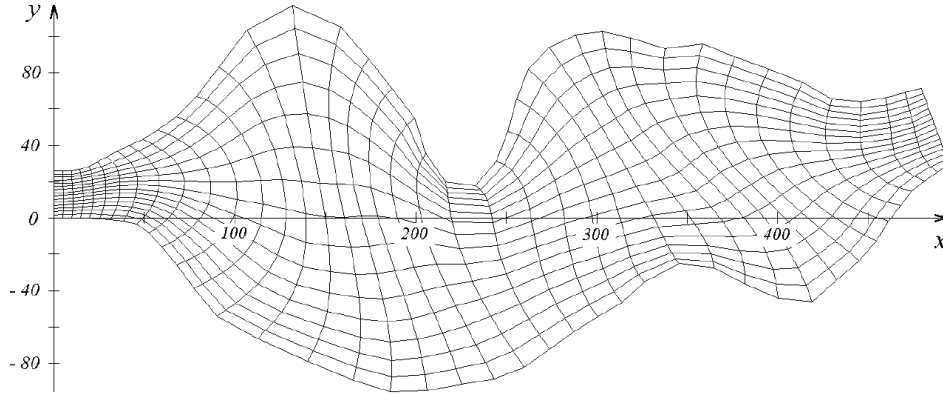
Figure 4.14: The grid after 1000 iterations, $N_1 = 61$, $N_2 = 23$, $\alpha = 1000$

Further, experiments are carried out with the larger number of iterations. These experiments show that the coordinate lines of the grid become smoother with the increase in the number of nodes. The example of such a grid is shown in Fig.4.13.

Usually the finer grids are used in calculations. As an example, the grid with 1.5 times larger number of nodes, compared with the previous grids, is shown in Fig.4.14. This grid is constructed using the control function (4.53) also.

4.5   General conclusions

The examples of grid generation only for two domains are considered in this chapter. The calculations of fluid and gas flows were performed for many other domains where the equidistribution method for grid generation was used. The experience of work with this method has shown that the method is very economic. It is suitable for grid generation in domains with the complicated geometry and it allows to obtain the results of high accuracy for gas and fluid flows.

42

Chapter 5

Finite-difference scheme and iterative process

5.1 Difference equation for the stream function

Let us introduce some notations. The total set of internal nodes of the grid is denoted by Q_h, $\gamma_h = \bar{Q}_h \backslash Q_h$ is the set of boundary nodes. We shall also use the grid Q_h^0 consisting of the points $\mathbf{q}_{j+1/2} = (q_{j_1}^1 + h_1/2,\ q_{j_2}^2 + h_2/2)$ which are the mesh centers of the grid $\bar{Q}_h$. Let $\gamma_{1,h}^0$ be the total set of nodes which are distributed on γ_1 with the coordinates $(0,\ q_{j_2}^2 + h_2/2)$, $\quad \bar{Q}_h^0 = Q_h^0 \cup \gamma_{1,h}^0$.

The examples of each type of nodes are shown in Fig.5.1. The nodes of Q_h are denoted by squares, the nodes of γ_h – by rhombuses, the nodes of Q_h^0 – by circles and the nodes of $\gamma_{1,h}^0$ – by crosses.

For the problem on gas flow the difference equations for the grid functions ψ, ω, H are obtained by the integro-interpolational method by approximation of the integrated relations which are the integrated analogues of the differential equations (3.2)–(3.4):

$$\oint_{\mathcal{C}} \left(k_{11}\frac{\partial \psi}{\partial q^1} + k_{12}\frac{\partial \psi}{\partial q^2} \right) dq^2 - \left(k_{21}\frac{\partial \psi}{\partial q^1} + k_{22}\frac{\partial \psi}{\partial q^2} \right) dq^1 = -\int_{D_\mathcal{C}} \int J\omega dq^1 dq^2, \qquad (5.1)$$

$$\oint_{\mathcal{C}} \rho J v^1 \omega dq^2 - \rho J v^2 \omega dq^1 = -\oint_{\mathcal{C}} \left(\rho\frac{\partial}{\partial q^2}\frac{V^2}{2} - f_2 \right) dq^2 + \left(\rho\frac{\partial}{\partial q^1}\frac{V^2}{2} - f_1 \right) dq^1, \quad (5.2)$$

$$\oint_{\mathcal{C}} \rho J v^1 H dq^2 - \rho J v^2 H dq^1 = 0, \qquad (5.3)$$

where $D_\mathcal{C}$ is the rectangle with the contour $\mathcal{C}$ denoted by the dashed line in Fig.5.2 for ψ and in Fig.5.3 for ω and H.

On approximating the relation (5.1) the function ψ is assumed to be defined in the integer nodes of a grid, the coefficients $k_{\alpha\beta}$, the Jacobian J and the vorticity function ω are calculated at the mesh centers of a grid, i.e. at the points of the grid Q_h^0.

The integrals along the sides of the rectangle $ABCD$ (see Fig.5.2) are calculated using the trapezoid formula. Then in the interior node $\mathbf{q}_{j_1,j_2}$ the following difference equation is obtained:

$$\Lambda\psi_{j_1,j_2} \equiv (D_{q^1}F^1 + D_{q^2}F^2) = (J\omega)_{j_1,j_2}. \qquad (5.4)$$
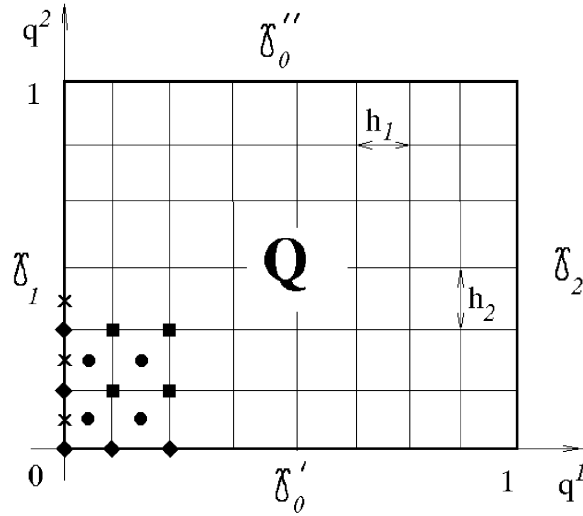
Figure 5.1: The examples of each type of the nodes in the computational domain Q: the nodes of Q_h are denoted by squares, the nodes of γ_h – by rhombuses, the nodes of Q_h^0 – by circles, the nodes of $\gamma_{1,h}^0$ – by crosses
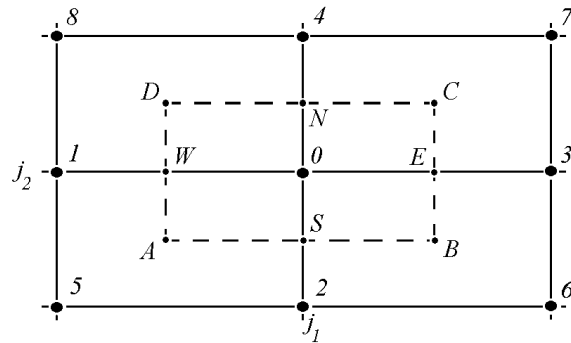
Figure 5.2: The pattern of the difference equation for ψ

Here the right-hand side is supposed to be equal to the arithmetical average of the values of $J\omega$ at the centers of adjacent meshes:

$$F^1(\mathbf{q}_{j_1+1/2,j_2+1/2}) = (k_{11}D_{q^1}\psi + k_{12}D_{q^2}\psi)(\mathbf{q}_{j_1+1/2,j_2+1/2}),$$

$$F^2(\mathbf{q}_{j_1+1/2,j_2+1/2}) = (k_{12}D_{q^1}\psi + k_{22}D_{q^2}\psi)(\mathbf{q}_{j_1+1/2,j_2+1/2}).$$

The operators D_{q^α} were defined earlier by the formulas (4.30)–(4.31).

It is easy to verify that the difference equation (5.4) approximates the differential equation (3.2) with the second order of accuracy on h_1 and h_2 for the smooth solutions and the smooth coefficients. The obtained nine-point difference equation can be written as follows:

$$\sum_{i=0}^{8} \alpha_i \psi_i = h_1 h_2 J\omega(0), \tag{5.5}$$

where the coefficients α_i are the following:

$$\alpha_1 = \beta_1 + \beta_4, \quad \alpha_2 = -\beta_1 - \beta_2, \quad \alpha_3 = \beta_2 + \beta_3, \quad \alpha_4 = -\beta_3 - \beta_4,$$

$$\alpha_0 = -\alpha_5 - \alpha_6 - \alpha_7 - \alpha_8,$$

$$\beta_1 = \frac{h_2}{4h_1}k_{11}(A) - \frac{h_1}{4h_2}k_{22}(A), \quad \beta_2 = \frac{h_2}{4h_1}k_{11}(B) - \frac{h_1}{4h_2}k_{22}(B),$$

$$\beta_3 = \frac{h_2}{4h_1}k_{11}(C) - \frac{h_1}{4h_2}k_{22}(C), \quad \beta_4 = \frac{h_2}{4h_1}k_{11}(D) - \frac{h_1}{4h_2}k_{22}(D),$$

$$\alpha_5 = \frac{h_2}{4h_1}k_{11}(A) + \frac{h_1}{4h_2}k_{22}(A) + \frac{1}{2}k_{12}(A),$$

$$\alpha_6 = \frac{h_2}{4h_1}k_{11}(B) + \frac{h_1}{4h_2}k_{22}(B) - \frac{1}{2}k_{12}(B),$$

$$\alpha_7 = \frac{h_2}{4h_1}k_{11}(C) + \frac{h_1}{4h_2}k_{22}(C) + \frac{1}{2}k_{12}(C),$$

$$\alpha_8 = \frac{h_2}{4h_1}k_{11}(D) + \frac{h_1}{4h_2}k_{22}(D) - \frac{1}{2}k_{12}(D).$$

The obtained system of equations with respect to ψ_j is solved by the method of successive over relaxation (the SOR-method). The values of ψ_j on the boundary are defined on the basis of the given Dirichlet condition (3.9).
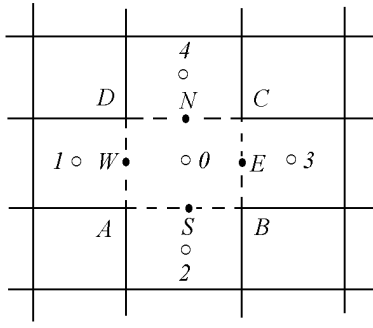
Figure 5.3: The pattern of the difference equations for ω and H

5.2 Difference equations for the vorticity function and the total energy

Now the approximation of the equations for the vorticity and the total energy is considered. It is assumed, that the grid functions ω and H are defined at the centers of the meshes of a grid covering the computational domain Q. As it has been mentioned above, the rectangular contour shown in Fig.5.3 is taken as the contour of integration of the relation (5.2).

Depending on the quadrature formula we obtain different schemes for the vorticity. Let us consider now the approximation which leads to one of the simple schemes, i.e. to the upwind scheme. On approximating (5.2) we obtain the following equation:

$$\Lambda_1\omega(\mathbf{q}_{j+1/2}) + \Lambda_2\omega(\mathbf{q}_{j+1/2}) = d_{j+1/2}, \quad \mathbf{q}_{j+1/2} \in Q_h^0, \tag{5.6}$$

where

$$\Lambda_1\omega(\mathbf{q}_{j+1/2}) = \frac{1}{h_1}\{\rho J v^1\omega(E) - \rho J v^1\omega(W)\},$$

$$\Lambda_2\omega(\mathbf{q}_{j+1/2}) = \frac{1}{h_2}\{\rho J v^2\omega(N) - \rho J v^2\omega(S)\}.$$

The values of ω on the mesh sides are calculated according to the signs of the contravariant components of the velocity. Therefore, ω is taken either from the centre of a mesh enveloped by the contour $\mathcal{C}$ or from the centre of an adjacent mesh. The difference analogues of the relations (3.5) are used for calculating the values of $\rho J v^\alpha$. For example, for the approximation of the integral in left-hand side of (5.2) along the side BC we assume the following:

$$\omega(E) = \begin{cases} \omega_0, & \text{if } v^1(E) \geq 0, \\ \omega_3, & \text{if } v^1(E) < 0, \end{cases}$$

$$\rho J v^1(E) = \frac{\psi(C) - \psi(B)}{h_2}.$$

In calculating the contravariant component of the velocity $v^1(E)$ the second of these formulas is used, therefore the sign of v^1 coincides with the sign of the complex $\rho J v^1$,

because $\rho > 0$ and $J > 0$. The right-hand side of the relation (5.2) is approximated as follows:

$$d_{j+1/2} = h_1(f_1)_{j_1+1/2,j_2} - \frac{\rho_{j_1,j_2} + \rho_{j_1+1,j_2}}{2} \left(\left(\frac{V^2}{2} \right)_{j_1+1,j_2} - \left(\frac{V^2}{2} \right)_{j_1,j_2} \right) +$$

$$+ h_2(f_2)_{j_1+1,j_2+1/2} - \frac{\rho_{j_1+1,j_2} + \rho_{j_1+1,j_2+1}}{2} \left(\left(\frac{V^2}{2} \right)_{j_1+1,j_2+1} - \left(\frac{V^2}{2} \right)_{j_1+1,j_2} \right) -$$

$$- h_1(f_1)_{j_1+1/2,j_2+1} + \frac{\rho_{j_1,j_2+1} + \rho_{j_1+1,j_2+1}}{2} \left(\left(\frac{V^2}{2} \right)_{j_1+1,j_2+1} - \left(\frac{V^2}{2} \right)_{j_1,j_2+1} \right) - \quad (5.7)$$

$$- h_2(f_2)_{j_1,j_2+1/2} + \frac{\rho_{j_1,j_2} + \rho_{j_1,j_2+1}}{2} \left(\left(\frac{V^2}{2} \right)_{j_1,j_2+1} - \left(\frac{V^2}{2} \right)_{j_1,j_2} \right).$$

The difference equation (5.6) approximates the differential equation (3.3) with the first order for smooth solutions and smooth coefficients. The pattern of this difference equation can consist of one, three or four nodes, i.e. it is variable. It is possible to show that when no closed streamlines are present and no stationary points of gas exist, then it is possible to calculate a value of ω in any node by the values at the inlet of the domain. For this purpose, it is possible to use the non-iterative method – the generalized method of running calculation which is described in details below.

Thus, the values of ω at the inlet of the domain are necessary for calculating the vorticity, i.e. the values in the nodes of $\gamma_{1,h}^0$ are necessary. There are no such values in the initial statement of the problem. Therefore, some algorithm is necessary for obtaining ω at the inlet of the domain using the given boundary conditions and the values of grid functions in the nodes adjacent to the boundary. These values are taken from the previous iteration or from the previous time step, depending on what process of calculating (the iterative method or the method of establishing the steady state) is used for solving the complete set of difference equations.

The vorticity at the inlet γ_1 is calculated on the basis of the formula (3.8).

The integro-interpolational method is applied to obtaining the difference expressions. The different integration contours are taken for various types of nodes at the inlet. The patterns of three types of nodes are shown in Figures 5.4, 5.5 and 5.6.

Thus, for the case a) we obtain the following approximation:

$$\frac{h_1}{2} v_1(B) + \frac{h_2}{2} \left(v_2(B) + v_2(C) \right) - \frac{h_1}{2} v_1(C) - h_2 v_2(0) = (J\omega)(0) \frac{h_1 h_2}{2}; \quad (5.8)$$

for the case b):

$$\frac{h_1}{2} v_1(0) + \frac{h_2}{2} v_2(C) - \frac{h_1}{2} v_1(C) - \frac{h_2}{2} v_2(0) = (J\omega)(0) \frac{h_1 h_2}{4}; \quad (5.9)$$

and for the case c):

$$\frac{h_1}{2} v_1(B) + \frac{h_2}{2} v_2(B) - \frac{h_1}{2} v_1(0) - \frac{h_2}{2} v_2(0) = (J\omega)(0) \frac{h_1 h_2}{4}. \quad (5.10)$$
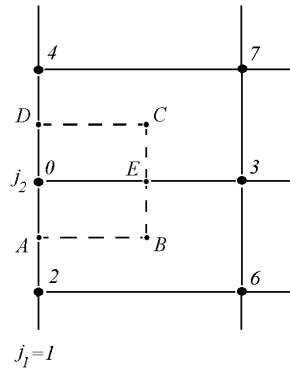
Figure 5.4: The pattern of the difference equation for calculating the vorticity at the inlet
$j_1 = 1, \quad 1 < j_2 < N_2$
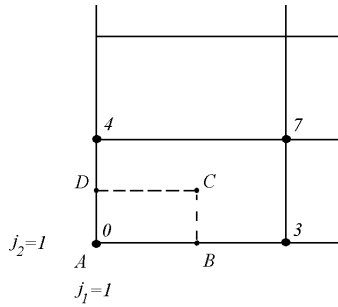
Figure 5.5: The pattern of the difference equation for calculating the vorticity at the inlet
$j_1 = 1, \quad j_2 = 1$
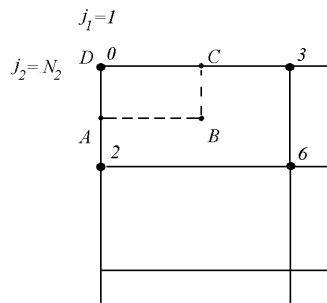
Figure 5.6: The pattern of the difference equation for calculating the vorticity at the inlet
$j_1 = 1, \quad j_2 = N_2$

The covariant components of the velocity at the centers of the meshes are approximated on the basis of the formulas which follow from the expressions (3.7) and (3.5):

$$v_\alpha = \frac{g_{\alpha 1}}{\rho J}\frac{\partial \psi}{\partial q^2} - \frac{g_{\alpha 2}}{\rho J}\frac{\partial \psi}{\partial q^1}, \quad \alpha = 1,2.$$

In the integer nodes (the boundary nodes denoted by the number "0" in Fig.5.3) they are approximated on the basis of the formulas:

$$v_\alpha = x_{q^\alpha} u_1 + y_{q^\alpha} u_2, \quad \alpha = 1,2,$$

which connect Cartesian and covariant components of the velocity. It is necessary to use the appropriate components of the vector $\vec{\nu}_1$ from the boundary condition (2.4) instead of u_α in these formulas. For the component v_2 this formula coincides with the formula for the normal derivative of ψ at the inlet Γ_1, i.e. with the formula (2.14) (or with (3.10), if the condition is written in coordinates q^α). The Jacobian in the integer node in the right-hand side is calculated with the help of central or one-sided differences depending on the type of a node.

Below, analyzing the difference scheme it will be shown that the approximation (5.8)–(5.10) retains the series of properties of the solutions of the initial system of the differential equations.

The boundary conditions for the vorticity are investigated in the series of other articles [25, 85, 122, 145, 146, 148]. Let us show that the boundary condition for the vorticity (5.8) written in Cartesian coordinates is the modification of the known Thom formula [148]. For the problem:

$$\frac{\partial \omega}{\partial t} + (\mathbf{u} \cdot \nabla)\omega = \nu \Delta \omega,$$

$$\Delta \psi = -\omega, \tag{5.11}$$

$$u_1 = \frac{\partial \psi}{\partial y}, \quad u_2 = -\frac{\partial \psi}{\partial x},$$

with the following boundary conditions:

$$\psi = 0, \quad \frac{\partial \psi}{\partial \mathbf{n}} = 0,$$

the Thom formula for the case a) has the following form (we use the notations of Fig.5.3):

$$\omega(0) = -\frac{2}{h_1^2}\psi(3). \tag{5.12}$$

The condition (5.8) for the problem (5.11) in Cartesian coordinates has the form:

$$\omega(0) = \frac{2}{h_1 h_2}\left[\frac{h_1}{2}\frac{\partial \psi}{\partial y}(B) + \frac{h_2}{2}\left(-\frac{\partial \psi}{\partial x}(B) - \frac{\partial \psi}{\partial x}(C)\right) - \frac{h_1}{2}\frac{\partial \psi}{\partial y}(C) + h_2\frac{\partial \psi}{\partial x}(0)\right] \approx$$

$$\approx \frac{2}{h_1 h_2}\left[\frac{h_1}{2}\cdot\frac{1}{2}\left(\frac{\psi(3) - \psi(6)}{h_2} + \frac{\psi(0) - \psi(2)}{h_2}\right) - \right.$$

49

$$-\frac{h_2}{2}\cdot\frac{1}{2}\left(\frac{\psi(3)-\psi(0)}{h_1}+\frac{\psi(6)-\psi(2)}{h_1}\right)-$$

$$-\frac{h_2}{2}\cdot\frac{1}{2}\left(\frac{\psi(7)-\psi(4)}{h_1}+\frac{\psi(3)-\psi(0)}{h_1}\right)-$$

$$-\frac{h_1}{2}\cdot\frac{1}{2}\left(\frac{\psi(7)-\psi(3)}{h_2}+\frac{\psi(4)-\psi(0)}{h_2}\right)+h_2\frac{\partial\psi}{\partial x}(0)\Bigg].$$

From the boundary conditions of the problem it follows that $\psi(0)=\psi(2)=\psi(4)=0$, $\frac{\partial\psi}{\partial x}(0)=\frac{\partial\psi}{\partial \mathbf{n}}(0)=0$. Therefore,

$$\omega(0)=\frac{2}{h_1h_2}\left[\frac{h_1}{4h_2}(2\psi(3)-\psi(6)-\psi(7))+\frac{h_2}{4h_1}(2\psi(3)+\psi(6)+\psi(7))\right]=$$

$$=-\frac{2}{h_1h_2}\cdot\frac{h_1}{4h_2}h_2^2\cdot\frac{\psi(7)-2\psi(3)+\psi(6)}{h_2^2}-$$

$$-\frac{2}{h_1h_2}\cdot\frac{h_2}{4h_1}\cdot 4\cdot\frac{1}{2}\left(\frac{\psi(6)+\psi(3)}{2}+\frac{\psi(3)+\psi(7)}{2}\right)=$$

$$=-\frac{1}{2}\cdot\frac{\psi(7)-2\psi(3)+\psi(6)}{h_2^2}-\frac{2}{h_1^2}\cdot\frac{1}{2}\left(\frac{\psi(6)+\psi(3)}{2}+\frac{\psi(3)+\psi(7)}{2}\right).$$

Thus,

$$\omega(0)=-\frac{1}{2}D_{q^2}^2\psi(3)-\frac{2}{h_1^2}\tilde\psi(3),\tag{5.13}$$

where $\tilde\psi(3)$ is the average value of ψ calculated using the formula in the last item.

On comparing (5.12) and (5.13) we see that the formula (5.13) is the modification of the Thom formula (5.12).

The relations (5.2) and (5.3) differ only by their right-hand sides, therefore, the difference equations for calculating H differ from the equations for the vorticity only by their homogeneity:

$$\sum_{k=0}^{4}\beta_k H_k=0,\tag{5.14}$$

where

$$\beta_1=\begin{cases}-\psi(D)+\psi(A), & \psi(D)>\psi(A),\\ 0, & \psi(D)\le\psi(A),\end{cases}$$

$$\beta_2=\begin{cases}\psi(B)-\psi(A), & \psi(A)>\psi(B),\\ 0, & \psi(A)\le\psi(B),\end{cases}$$

$$\beta_3 = \begin{cases} \psi(C) - \psi(B), & \psi(C) < \psi(B), \\ 0, & \psi(C) \geq \psi(B), \end{cases}$$

$$\beta_4 = \begin{cases} \psi(D) - \psi(C), & \psi(C) > \psi(D), \\ 0, & \psi(C) \leq \psi(D), \end{cases}$$

$$\beta_0 = -(\beta_1 + \beta_2 + \beta_3 + \beta_4),$$

here (see Lemma 5.3)

$$\beta_k \leq 0, \quad k = 1, 2, 3, 4; \quad \beta_0 \geq 0.$$

5.3 Difference equation for the pressure

The pressure is defined on the basis of the approximation of the following expression which follows from the equations (3.6):

$$p(\mathbf{q}_j) = p_0 + \int\limits_{\gamma(\mathbf{q}_0, \mathbf{q}_j)} \left(f_1 + \rho J v^2 \omega - \rho \frac{\partial}{\partial q^1} \frac{u^2}{2} \right) dq^1 +$$

$$+ \left(f_2 - \rho J v^1 \omega - \rho \frac{\partial}{\partial q^2} \frac{u^2}{2} \right) dq^2. \tag{5.15}$$

Let us assume that the grid function p is defined in the integer nodes. Therefore, we take a polygonal line whose links are parallel to the axes Oq^α and pass along the sides of the meshes as a curve γ, connecting the point $\mathbf{q}_j$, where it is required to define the pressure, with the point $\mathbf{q}_0$, where the pressure is given initially in (2.7).

On comparing (5.15) and (5.2) we see that the integrands in these integrated relations are identical. Therefore, if the integrals in (5.15) are approximated using the formulas (5.7) which are applied for obtaining the difference equation for the vorticity, then the pressure does not depend on the path of integration γ. Thus, for calculating the pressure the method of coordinated approximation is used. For the case of rectangular grids it is considered in [76]. For viscous incompressible fluid flows it is known as the marching method for calculating the pressure [115]. Firstly, the values of the pressure are defined in the nodes at the inlet and then the values of p are obtained in the other nodes of the grid using the following formulas:

$$p_{1,j_2+1} = p_{1,j_2} + h_2 \frac{(f_2)_{1,j_2} + (f_2)_{1,j_2+1}}{2} -$$

$$- (\psi_{1,j_2+1} - \psi_{1,j_2}) \omega_{1,j_2+1/2} - \frac{\rho_{1,j_2} + \rho_{1,j_2+1}}{2} \left(\left(\frac{u^2}{2} \right)_{1,j_2+1} - \left(\frac{u^2}{2} \right)_{1,j_2} \right),$$

$$j_2 = 1, ..., N_2 - 1,$$

$$p_{j_1+1,j_2} = p_{j_1+1,j_2} + h_1 \frac{(f_1)_{j_1,j_2} + (f_1)_{j_1+1,j_2}}{2} - \tag{5.16}$$

$$- (\psi_{j_1+1,j_2} - \psi_{j_1,j_2})\,\widetilde{\omega} - \frac{\rho_{j_1,j_2} + \rho_{j_1+1,j_2}}{2}\left(\left(\frac{u^2}{2}\right)_{j_1+1,j_2} - \left(\frac{u^2}{2}\right)_{j_1,j_2}\right),$$

$$\widetilde{\omega} = \begin{cases} \omega_{j_1+1/2,j_2-1/2}, & \text{if } v^2_{j_1+1/2,j_2} \geq 0, \\ \omega_{j_1+1/2,j_2+1/2}, & \text{if } v^2_{j_1+1/2,j_2} < 0, \end{cases}$$

$$j_1 = 1, ..., N_1 - 1, \quad j_2 = 1, ..., N_2.$$

The density is calculated on the basis of (2.6) and the re-interpolation of the total energy into the integer nodes is performed.

5.4 Some features of the difference scheme for the stream function

Let us present some results of investigation of the difference scheme (5.4) for ψ. Some notations from the book [119] are used further.

Let $\overset{\circ}{\psi}$ be the function defined only in the interior nodes, and ψ be the function defined in all nodes. $\psi = \overset{\circ}{\psi}$ in the interior nodes and $\psi = 0$ on the boundary.

We denote the space of the functions $\overset{\circ}{\psi}$ by $\mathcal{H}$. Let us introduce the operator $A : \mathcal{H} \to \mathcal{H}$ by the formula $A\,\overset{\circ}{\psi} = -\Lambda\psi$. This operator is self-adjoint and positively definite in the Hilbert space $\mathcal{H}$ with the following scalar product:

$$(\overset{\circ}{\psi}, \overset{\circ}{\varphi}) = \sum_{j_1=2}^{N_1-1} \sum_{j_2=2}^{N_2-1} \overset{\circ}{\psi}_{j_1,j_2}\,\overset{\circ}{\varphi}_{j_1,j_2}\, h_1 h_2, \quad \overset{\circ}{\psi}, \overset{\circ}{\varphi} \in \mathcal{H}.$$

Lemma 5.1. *The difference operator A is self-adjoint.*

We prove the positive definiteness of the operator A assuming the uniform ellipticity of the equation (3.2) (see Appendix for the details):

$$\sum_{\alpha,\beta=1}^{2} k_{\alpha\beta}\zeta_\alpha\zeta_\beta \geq c_1(\zeta_1^2 + \zeta_2^2), \tag{5.17}$$

where ζ_1, ζ_2 are the arbitrary numbers, $c_1 = \text{const} > 0$.

Lemma 5.2. *The difference operator A is positively definite in the Hilbert space $\mathcal{H}$ and the following estimation is fulfilled:*

$$(A\,\overset{\circ}{\varphi}, \overset{\circ}{\varphi}) \geq C(\overset{\circ}{\varphi}, \overset{\circ}{\varphi}),$$

where

$$C = c_1 \frac{\pi^2}{(\max\{h_1, h_2\})^2}[h_1^2 + h_2^2 - 2\pi^2 h_1^2 h_2^2].$$

5.5 Some features of the difference scheme for the vorticity function

The difference equation (5.6) can be written in the following form:

$$\sum_{k=0}^{4} \beta_k \omega_k = d_0, \tag{5.18}$$

where

$$\beta_1 = \begin{cases} -h_2 \rho J v^1(W), & v^1(W) > 0, \\ 0, & v^1(W) \leq 0, \end{cases}$$

$$\beta_2 = \begin{cases} -h_1 \rho J v^2(S), & v^2(S) > 0, \\ 0, & v^2(S) \leq 0, \end{cases}$$

$$\beta_3 = \begin{cases} h_2 \rho J v^1(E), & v^1(E) < 0, \\ 0, & v^1(E) \geq 0, \end{cases} \tag{5.19}$$

$$\beta_4 = \begin{cases} h_1 \rho J v^2(N), & v^2(N) < 0, \\ 0, & v^2(N) \geq 0, \end{cases}$$

$$\beta_0 = -(\beta_1 + \beta_2 + \beta_3 + \beta_4).$$

Lemma 5.3. *The coefficients of the difference equation (5.18) satisfy the following relations:*

$$\beta_k \leq 0, \quad k = 1, 2, 3, 4; \quad \beta_0 \geq 0; \quad \sum_{k=0}^{4} \beta_k = 0. \tag{5.20}$$

Thus, the scheme (5.6) is formally the five-point formula, though for some nodes $\mathbf{q}_{j+1/2} \in Q_h^0$ its pattern consists of a smaller number of nodes. For example, if $v^1 > 0$ and $v^2 > 0$ in some subdomain, then the coefficients β_3 and β_4 become equal to zero, and the scheme is actually the three-point formula in this subdomain.

For the scheme (5.6) no boundary values of ω are required, except the values of ω at the inlet γ_1. Let us show, for example, that the values of ω on γ_0' do not enter into the difference equations. Let us consider the node $\mathbf{q}_{j+1/2}$ near the boundary. For this node the side AB of the integration contour (see Fig.5.3) lays on γ_0'. Therefore, $v^2(S) = 0$ because of Lemma 3.1, and, consequently, the coefficient $\beta_2 = 0$ for $\omega(S)$. Similarly, it can be shown that the boundary conditions of ω on γ_0'' and γ_2 are not necessary.

Now let us assume that the mesh with the centre $\mathbf{q}_{j+1/2}$ is adjacent to γ_1 (to the pre-image of the inlet). Due to Lemma 3.1 $v^1(W) > 0$ and, therefore, the boundary value $\omega(W)$ is necessary in this case. This value is obtained on the basis of the difference equations (5.8)–(5.10) by averaging the values ω_j calculated in the integer boundary nodes.

For solving the system of equations (5.18) some iterative method can be used [121]. At the same time, it is necessary to remember that this iterative process is applied on

each step of the global iterative process for obtaining the grid functions $\psi_j, \ \omega_{j+1/2},$ $H_{j+1/2}, \ p_{j+1/2}, \ \rho_j$, and it can require significant computer time. In the present thesis the resource-sparing direct method is suggested for solving the system (5.18). This method can be applied when some conditions are fulfilled for the velocity vector. These conditions are not too burdensome and they are fulfilled for the comparatively wide range of considered problems. The requirements imposed on the flow velocity can be formulated in the following way: no stagnation zone exists in the domain Ω (i.e. for all $\mathbf{x} \in \Omega$ the condition $|\mathbf{u}(\mathbf{x})| \geq \varepsilon$ must be fulfilled, where ε is some positive number) and no closed streamlines in Ω are allowed.

Let us now formulate the difference analogues of these requirements which are sufficient for the application of the direct method for solving the equation (5.18). These analogues are based on the following lemma:

Lemma 5.4. *Let* $\mathbf{q}_{j+1/2} \in Q_h^0$. *Then the following statements for the coefficients of the equation (5.18) are equivalent (the notations of Fig.5.3 are used):*
1. $\beta_0 = 0$;
2. $\beta_1 = \beta_2 = \beta_3 = \beta_4 = 0$;
3. $v^1(W) = v^1(E) = v^2(N) = v^2(S) = 0$;
4. $\psi(A) = \psi(B) = \psi(C) = \psi(D)$.

Therefore, if even on one side of an elementary mesh the respective (normal) contravariant velocity component differs from zero, then the coefficient $\beta_0 \neq 0$, and at least one of the coefficients $\beta_k \neq 0$ $(k = 1, 2, 3, 4)$. Thus, the condition of the absence of stationary points in fluid have the form of the following inequality on the difference level:

$$\beta_0 > 0. \tag{5.21}$$

Stating the difference analogue of the condition of the absence of closed streamlines we need the concept of "the area of dependence for the equation (5.18)" and the concept of "the pattern of this equation" [165].

Definition: The set of the nodes where the coefficients β_k $(k = 0, 1, ..., 4)$ differ from zero is named "the pattern $\Sigma(P)$ of the equation (5.18) in the node $P = \mathbf{q}_{j+1/2}$"

The condition (5.21) guarantees that the pattern of any node $P \in Q_h^0$ is not empty. If this condition is fulfilled, then the pattern consists of at least two nodes. The maximum number of nodes in the pattern is equal to five.

Definition: The total set of the nodes of the pattern $\Sigma(P)$ which do not coincide with P is named "the neighbourhood $\Sigma'(P)$ of the node P".

As it has already been noted above, the condition (5.21) guarantees that at least for one k the coefficient $\beta_k \neq 0$ $(k = 1, 2, 3, 4)$. Therefore, when (5.21) is realized the neighbourhood of any node P is not empty. The nodes entering into the neighbourhood are denoted by Q_k.

The neighbourhood $\Sigma'(P)$ of the node P is also named "the neighbourhood of the first level of the node P" and denoted by $K_1(P)$, i.e. $K_1(P) = \Sigma'(P)$. On considering the neighbourhoods of all nodes Q_k entering in $K_1(P)$ we obtain the neighbourhood of the

second level of the node P:

$$K_2(P) = \bigcup_{Q_k \in K_1(P)} \Sigma'(Q_k).$$

If the neighbourhood $K_n(P)$ of the n-th level of the node P is already constructed, then the following set of nodes:

$$K_{n+1}(P) = \bigcup_{Q_k \in K_n(P)} \Sigma'(Q_k)$$

is taken as "the neighbourhood of the $(n+1)$-th level".

It may turn out that some neighbourhood $K_n(P)$ will include the node Q_k located at the inlet γ_1. We consider that the value $\omega(Q_k)$ in this node is known, therefore for such nodes no neighbourhoods of higher levels are constructed, i.e. it is assumed that

$$\Sigma'(Q_k) = \emptyset, \quad Q_k \in \gamma_{1,h}^0.$$

Passing from the neighbourhood of one level to the neighbourhood of a higher level we can have two possibilities: either at some n_0 the neighbourhood of the n_0-th level is completely located at the inlet, $K_{n_0}(P) \subseteq \gamma_{1,h}^0$, or for all n $K_n(P)$ also contains other nodes of the grid Q_h^0, i.e. $K_n(P) \not\subseteq \gamma_{1,h}^0$. In the first case it is assumed that $K(P) = \bigcup_{i=1}^{n_0} K_i(P)$, and in the second case it is assumed that $K(P) = \bigcup_{i=1}^{\infty} K_i(P)$.

Definition: The set of the nodes $K(P)$ is named "the area of dependence for the node P".

Theorem 5.1. *If* $Q \in K_1(P)$, *then* $P \notin K_1(Q)$. *If* $Q_2 \in K(Q_1)$, $Q_3 \in K(Q_2)$, *then* $Q_3 \in K(Q_1)$.

Making use of this theorem the following statement can be proved.

Theorem 5.2. *For the realisation of the condition*

$$P \notin K(P) \tag{5.22}$$

in the arbitrary node $P \in Q_h^0$ *it is necessary and sufficient that some neighbourhood of the node* P *should be completely located at the inlet (in other words, some number* n_0 *should exist, such that* $K_{n_0} \subseteq \gamma_{1,h}^0$ *).*

The solution ω of the differential equation (2.12) is constant on each streamline. If a streamline is started at the inlet Γ_1, then the value of ω on this streamline is equal to the boundary value of the vorticity at the point where the trajectory enters the domain Ω. If there are no closed streamlines in Ω, then the values of ω are determined uniquely in terms of the values $\omega \big|_{\Gamma_1}$. When there are closed streamlines in Ω the value of ω on such streamlines can not be obtained only in terms of the boundary values. The similar situation arises when the condition (5.22) is violated: if $P \in K(P)$, then the value $\omega(P)$ can not be obtained only in terms of the values of ω in the nodes of $\gamma_{1,h}^0$. Therefore, the condition (5.22) can be interpreted in some sense as the difference analogue for the absence of closed streamlines.

It is shown in [77] that if the conditions (5.21) and (5.22) are satisfied for all nodes $P \in Q_h^0$, then the solution of the equation (5.18) exists and it is unique.

The following direct (non-iterative) method is suggested for obtaining the solution of the equation (5.18). Let ω be already calculated in some nodes and let it be necessary to calculate ω in the node P. If the values of ω have already been calculated in all nodes $Q_k \in \Sigma'(P)$, then, by (5.21), $\omega(P)$ can be found from the equation (5.18). If there is one or more nodes Q_k in the neighbourhood $\Sigma'(P)$ where the values of ω have not been yet calculated, then we pass from the node P to any of these nodes investigating its neighbourhood. As a result of such passage from node to node we shall come (by the virtue of Theorem 5.2) to the node $\bar{P}_0$ where the values of ω in the nodes of its neighbourhood either have been calculated or are known from the boundary conditions. Therefore, $\omega(\bar{P}_0)$ can be obtained from the equation (5.18). In the same way the values of ω are calculated in all nodes of the area of dependence $K(P)$ and then in the node P itself.

5.6   Iterative process

In this section the iterative process for solving the difference problem on the gas flow is described.

First of all, the incompressible fluid flow is considered, i.e. it is assumed that $\rho_j \equiv 1$ in all formulas.

As the initial approximation for the iterative process of calculating the incompressible fluid flow, the solution of the problem on the potential flow is chosen: $\omega^0 \equiv 0$. Thus, the homogeneous equation (5.4) is solved.

Further, the calculation of the vortical ideal incompressible fluid flow is carried out.

Let ψ_j^n, $\omega_{j+1/2}^n$ be the n-th iterative approximation. The process of obtaining the $(n+1)$-th approximation is divided into the following steps.

1. The equation (5.4) is solved by the SOR-method where the values ω^n in the right-hand side are taken from the n-th iteration. The condition of the termination of iterations has the following form:

$$||\psi_j^{n+1} - \psi_j^n||_{L_1} < \varepsilon_\psi. \tag{5.23}$$

2. The values of $\bar{\omega}$ in the nodes of $\gamma_{1,h}^0$ are calculated using the formulas (5.8)–(5.10). For obtaining the values $v_2(B)$ and $v_2(C)$ the values of the stream function from the $(n+1)$-th iteration are used. The immediate application of the indicated formulas to the calculation of $\omega\big|_{\gamma_1}$ leads to the divergence of the iterative process. Therefore, $\bar{\omega}$ with the weight δ_ω is taken as $\omega^{n+1}\big|_{\gamma_1}$:

$$\omega^{n+1}(\mathbf{q}) = \delta_\omega \bar{\omega}(\mathbf{q}) + (1 - \delta_\omega)\omega^n(\mathbf{q}), \quad \mathbf{q} \in \gamma_{1,h}^0, \tag{5.24}$$

where $\delta_\omega > 0$ is the relaxation parameter selected experimentally.

3. The equation (5.18) is solved by the above-described direct method in order to obtain the values $\omega^{n+1}(\mathbf{q}_{j+1/2})$, $\mathbf{q}_{j+1/2} \in Q_h^0$. Here the values $\psi^{n+1}(\mathbf{q}_j)$, $\mathbf{q}_j \in \bar{Q}_h$ are used for calculating the coefficients β_k.

4. The following condition for the termination of iterations is checked:

$$||\omega_{j+1/2}^{n+1} - \omega_{j+1/2}^n||_{L_1} < \varepsilon_\omega. \tag{5.25}$$

The solution of the problem on the incompressible fluid flow is the initial approximation for the calculation of the gas flow. Let ψ_j^n, $\omega_{j+1/2}^n$, $H_{j+1/2}^n$, p_j^n, ρ_j^n be the n-th iterative approximation.

The process of obtaining the $(n+1)$-th approximation includes three stages of calculating the incompressible fluid flow and the following additional stages which are stipulated by the necessity of calculating the density, the pressure and the total energy.

5. The total energy $H_{j+1/2}^{n+1}$ is calculated by the generalized method of running calculation.

6. The values p_j^{n+1} are obtained by the method of coordinated approximation.

7. The density ρ_j^{n+1} is calculated. The preliminary values of $\bar{\rho}_j$ are obtained on the basis of formulas (2.6), and the values interpolated on $\bar{\rho}_j$ and ρ_j^n are taken as the final values:

$$\rho_j^{n+1} = \delta_\rho \bar{\rho}_j + (1 - \delta_\rho)\rho_j^{n+1}, \tag{5.26}$$

where the parameter $\delta_\rho > 0$ increases linearly from 0 up to 1 during the iterative process.

The iterations for the gas proceed up to the convergence of the density values.

Finally, let us show that the described iterative process using the approximations indicated above does not deviate the constant flow from the equilibrium. If the parameters of the constant flow are taken as the initial approximation, then the flow stays the same during the iterations despite the application of curvilinear grids. Considering this property we leave out the questions connected with approximate calculations: here it is supposed that all calculations are carried out precisely.

Let the numerical solution have the following form on the n-th iteration:

$$u_1^n \equiv u_0 = \text{const}, \quad u_2^n \equiv 0, \quad \rho^n \equiv \rho_0 = \text{const}, \quad p^n \equiv p_0 = \text{const},$$

$$H^n = \frac{\kappa p_0}{\rho_0(\kappa - 1)} + \frac{u_0^2}{2} = H_0 = \text{const}.$$

Therefore,

$$\psi_{j_1,j_2}^n = u_0 \rho_0 y_{j_1,j_2}, \quad \omega_{j_1+1/2,j_2+1/2}^n \equiv 0.$$

The following statement is fulfilled.

Lemma 5.5. *For $\omega \equiv 0$ the functions $x = x(q^1, q^2)$, $y = y(q^1, q^2)$ satisfy the difference equation (5.4).*

Therefore, $\psi_{j_1,j_2}^{n+1} = \psi_{j_1,j_2}^n = u_0 \rho_0 y_{j_1,j_2}$.

According to the described procedure of calculations, the values of ω are obtained. Using the formulas (5.8)–(5.10) it is easy to obtain that $\omega^{n+1}\big|_{\gamma_1} = 0$.

As there are no closed streamlines and stagnation points ($\mathbf{u} \neq 0$) in the flow domain, the values $\omega_{j_1+1/2,j_2+1/2}^{n+1}$ are defined using the boundary values of the vorticity at the inlet. As the boundary values of the vorticity have zero values, therefore $\omega_{j_1+1/2,j_2+1/2}^{n+1} \equiv 0$. Similarly, we obtain that $H_{j_1+1/2,j_2+1/2}^{n+1} \equiv H_0$.

Let us show that the pressure on the $(n+1)$-th iteration remains constant also: $p^{n+1} \equiv p_0$. This conclusion follows from the formulas (5.16) if calculating $u^2 = u_1^2 + u_2^2$ we use the following formulas for obtaining Cartesian components of $\mathbf{u}$:

$$
u_\alpha = \frac{\partial x^\alpha}{\partial q^1} \frac{1}{\rho J} \frac{\partial \psi}{\partial q^2} - \frac{\partial x^\alpha}{\partial q^2} \frac{1}{\rho J} \frac{\partial \psi}{\partial q^1}, \quad \alpha = 1, 2.
$$

Here the derivatives of the variables x^α and ψ with respect to q^1 and q^2 are approximated by central differences in interior nodes and by one-sided differences of the second order in the boundary nodes. For example, we get the following expression in the interior node j_1, j_2:

$$
(u_\alpha)_{j_1,j_2} = \frac{x^\alpha_{j_1+1,j_2} - x^\alpha_{j_1-1,j_2}}{2h_1} \frac{1}{\rho J} \frac{\psi_{j_1,j_2+1} - \psi_{j_1,j_2-1}}{2h_2} -
$$

$$
- \frac{x^\alpha_{j_1,j_2+1} - x^\alpha_{j_1,j_2-1}}{2h_1} \frac{1}{\rho J} \frac{\psi_{j_1+1,j_2} - \psi_{j_1-1,j_2}}{2h_2}.
$$

The density $\rho^{n+1}_{j_1,j_2}$ is obtained from the difference analogue of (2.6). According to the proved equalities we have: $p^{n+1} \equiv p_0$, $H^{n+1} \equiv H_0$, $u^2 = u_0^2$, therefore $\rho^{n+1} \equiv \rho_0$.

Thus, it is shown that the constructed iterative process does not deviate the constant flow from the equilibrium using curvilinear grids.

5.7   Global process of the solution of the problem

In conclusion of this chapter let us explain how the complete algorithm works. It includes the algorithm of constructing the grid and the algorithm of calculating the problems on gas and fluid flows on this grid.

In test calculations carried out for debugging the complexes of computer codes the exact solutions of the problems are known. Therefore, the information about the exact solution is used for selecting the control function w for constructing a grid. In these calculations the grid is constructed before solving the problem.

In the practical problems the exact solution is not known, therefore we proceed in the following way. At the beginning $w \equiv 1$ is taken as the control function and the quasi-uniform grid adapted only to the geometry of the boundaries of two-dimensional domain is constructed. The preliminary solution is calculated on this grid. Then using the obtained information the grid is constructed adaptive not only to the geometry of the domain, but also to the singularities of the solution. And, finally, the numerical solution is obtained on this grid.

Chapter 6

Results of the calculations of two-dimensional steady ideal gas and fluid flows

6.1 Results of the calculations of the fluid flow in the channel with the stream bending by an angle of 270^0

Now we shall present the results of the numerical solution of the problem on ideal fluid flow with the known exact solution.

The flow domain is described in Section 4.3 and is shown in Fig.6.1.

The exact solution of the problem (2.15)–(2.17) is written in the following form for the given domain Ω:

$$u_{1,\text{exact}} = u_1(x, y) = \cos x \cdot \cos y,$$

$$u_{2,\text{exact}} = u_2(x, y) = \sin x \cdot \sin y,$$

$$p_{\text{exact}} = p(x, y) = p_0 - \frac{1}{4}(\cos 2x - \cos 2y),$$

$$\vec{\nu}_1(x, y) = (0, \sin x), \quad \nu_2(x, y) = -\cos y.$$

Let us show that the necessary solvability condition (2.9) is fulfilled. The function $\nu(s)$ is written as follows:

$$\nu(s) = \begin{cases} \sin x, & \mathbf{x}(s) \in \Gamma_1, \\ 0, & \mathbf{x}(s) \in \Gamma_0, \\ -\cos y, & \mathbf{x}(s) \in \Gamma_2. \end{cases}$$

Therefore,

$$\int_0^S \nu(s)ds = \cos x \Big|_{-\frac{3}{8}\pi}^{-\frac{3}{16}\pi} + 0 + \sin y \Big|_{\frac{11}{16}\pi}^{\frac{7}{8}\pi} + 0 = 0.$$
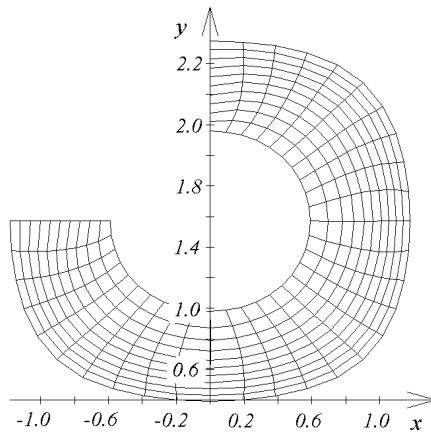
Figure 6.1: The flow domain for the problem on the fluid flow in the channel with the stream bending by an angle of 270^0

Thus, the necessary solvability condition of the stated problem is fulfilled.
From (2.19) it follows that

$$\psi_{\text{exact}} = \psi(x, y) = \cos x \cdot \sin y,$$

$$\omega_{\text{exact}} = \omega(x, y) = 2 \cos x \cdot \sin y.$$

The grid is constructed using the algorithm described in Chapter 4. The grid is adapted to the solution making use of a control function w.

Table 6.1 shows the results of testing the algorithms for calculating the stream function and the vorticity function using three different grids. In the first case the equation (5.4) is solved with ω_{exact} in the right-hand side. In the second case the equation (5.18) is solved with $d = 0$ and with the coefficients β_k calculated using ψ_{exact}.

Table 6.1: The accuracy of solution of the equations for ψ and ω.

Grid $N_1 \times N_2$	$\|\psi_h - \psi_{\text{exact}}\|_{L_1}$	$\|\omega_h - \omega_{\text{exact}}\|_{L_1}$
16×6	0.206_{-2}	0.157_{-1}
31×11	0.637_{-3}	0.738_{-2}
61×21	0.157_{-3}	0.356_{-2}

It is clear that the numerical values ψ_h converge to the exact solution with the second order and the numerical values ω_h converge to the exact solution with the first order. Each grid is constructed using the control function $w = 1 + \alpha|\omega_{\text{exact}}|$, $\alpha = 4$.

The influence of the relaxation parameter τ_ψ in the SOR-method on the behaviour of convergence of the iterative process for ψ using the nine-point scheme (5.5) is identical to the influence of the parameter for the usual five-point scheme. Fig.6.2 shows the behaviour of the norm of the difference $\|\psi_h - \psi_{exact}\|_{L_1}$ during the iterative process for various values of τ_ψ.

It is clear that the convergence is slow and monotone for small values of τ_ψ. There exists an optimum value of τ_ψ that leads to the fastest and monotone convergence of

60
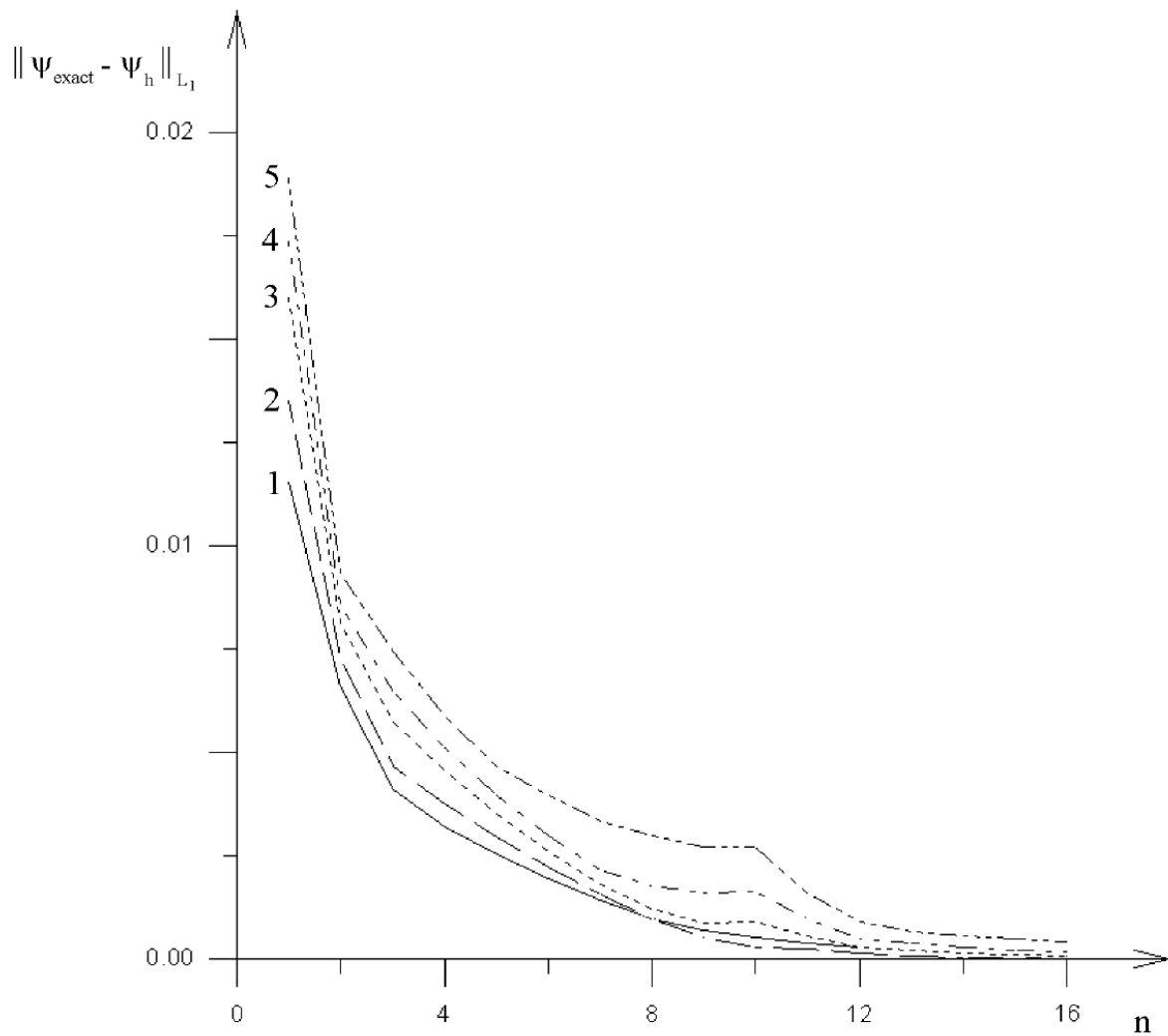
Figure 6.2: The influence of the relaxation parameter τ_ψ on the convergence of the iterative process for the stream function. $N_1 = 31$, $N_2 = 11$. $\tau_\psi = 1.5(1)$; $\tau_\psi = 1.6(2)$; $\tau_\psi = 1.7(3)$; $\tau_\psi = 1.75(4)$; $\tau_\psi = 1.8(5)$

the process. When τ_ψ becomes closer to the value 3, the convergence of the process looses the property of monotonicity. The grid is constructed using the control function $w = 1 + \alpha|\omega_{\mathrm{exact}}|$, $\alpha = 4$.

The next feature of the algorithm for calculating the stream function is the increasing of the optimum value of the relaxation parameter with the refinement of the grid (see Table 6.2).

Table 6.2: The dependence of the optimum value of the relaxation parameter $\tau_{\psi,\ opt}$ on the grid size.

Grid $N_1 \times N_2$	$\tau_{\psi,\ opt}$
16×6	1.5
31×11	1.6
61×21	1.75

It is identical to the feature of the SOR-method used for solving the difference equation appearing when applying the standard five-point cross-scheme for the approximation of the Laplace equation. The calculations for various grids are carried out, each grid is constructed using the control function $w = 1 + \alpha|\omega_{\mathrm{exact}}|$, $\alpha = 4$. The parameter τ_ψ is given the values 1.5, 1.6, 1.7, 1.75, 1.8.

Table 6.3 illustrates the influence of the relaxation parameter δ_ω on the total number of iterations n_{last} in the global iterative process $\psi - \omega$.

Table 6.3: The dependence of the total number of iterations on the parameter δ_ω. $N_1 = 31$, $N_2 = 11$, $\varepsilon_\omega = 0.1_{-4}$.

δ_ω	0.5	1	5	10	13	14	14.2	14.4	14.9	15	16	17
n_{last}	336	185	44	22	17	16	15	15	15	15	19	22

It can be seen that the successful choice of the parameter δ_ω can lead to the essential decrease in the number of iterations. For excessive values of δ_ω the process diverges. The grid is constructed using the control function $w = 1 + \alpha|\omega_{\mathrm{exact}}|$, $\alpha = 4$.

On refining the grid the optimum value of the parameter δ_ω varies. It depends on many factors, but if the calculations are carried out using the same control function w and with the same accuracy of convergence ε_ω, then $\delta_{\omega,opt}$ is increased with refining the grid. Table 6.4 shows the results for three grids. The grids are constructed making use of the control function $w = 1 + \alpha|\omega_{\mathrm{exact}}|$, $\alpha = 4$. The accuracy of the convergence is $\varepsilon_\omega = 0.1_{-4}$.

Table 6.5 shows the influence of the grid on the solution accuracy. It can be seen that it is possible to increase the accuracy of the calculations with the same number of nodes by using the successfully constructed grid. It is achieved by the choice of the appropriate control function w.

The calculations are carried out on the grids of the size 31×11 constructed using four different control functions. The parameter α is given the values between 1 and 10. The calculations have shown that the greatest accuracy of the calculated velocity components

Table 6.4: The dependence of the optimum value of the parameter $\delta_{\omega,opt}$ on the grid size.

Grid $N_1 \times N_2$	$\delta_{\omega,opt}$
16×6	11.2
31×11	14.4
61×21	20.1

Table 6.5: The dependence of the calculation accuracy of the velocity vector components on the choice of the control function. $N_1 = 31$, $N_2 = 11$, $\delta_\omega = 14.4$, $\alpha = 4$.

w	1	$1 + \alpha|\mathbf{u}_{\text{exact}}|^2$	$1 + \alpha|\omega_{\text{exact}}|$	$1 + \alpha\omega_{\text{exact}}^2$
$\|u_{1,h} - u_{1,\text{exact}}\|_{L_1}$	0.676_{-2}	0.120_{-1}	0.545_{-2}	0.661_{-2}
$\|u_{2,h} - u_{2,\text{exact}}\|_{L_1}$	0.656_{-2}	0.116_{-2}	0.537_{-2}	0.668_{-2}

is obtained using the control function $w = 1 + \alpha|\omega_{\text{exact}}|$, $\alpha = 4$. Table 6.5 presents the results for other control functions with the same value of the parameter $\alpha = 4$ for comparison.

6.2 Results of the calculations of the gas flow in the curvilinear channel

The algorithm for the calculation of ideal gas flow is tested on the problem with the known exact solution from the book [6]. In this book the solution is written in the implicit form, therefore here we present all explicit formulas. The exact solution is defined by the function $F(x)$ which is the solution of the following ordinary differential equation:

$$\frac{dF}{dx} = -\frac{F^2 \left(1 - \beta\frac{\kappa}{\kappa-1}F^{\kappa-1}\right)}{\beta\frac{\kappa(\kappa+1)}{2(\kappa-1)}F^{\kappa-1} - 1}, \tag{6.1}$$

where κ is the adiabatic exponent, β is some constant which is defined below.

The equation (6.1) is supplemented by the boundary condition:

$$F(x_0) = F_0. \tag{6.2}$$

According to [6] the solutions can be either subsonic or supersonic depending on the choice of F_0.

Using the obtained values of F the streamlines are calculated by the following formula:

$$y = b \cdot A^{-1/2},$$

where b is an arbitrary constant.

The exact solution is defined by the formulas:

$$u_{1,\text{exact}} = y^\alpha \frac{A^{\frac{\alpha+1}{2}}}{F}, \quad u_{2,\text{exact}} = -y^{\alpha+1} A^{\frac{\alpha+1}{2}}, \tag{6.3}$$

$$\rho = \frac{c_1}{y^{2\alpha}} F A^{-\alpha}, \quad p = c_2 F^\kappa, \quad H = y^{2\alpha} A^\alpha \left(c_3 + \frac{y^2}{2} A \right),$$

where $A(x) = 2c_3 F^2 \left(1 - \beta \frac{\kappa}{\kappa-1} F^{\kappa-1} \right)$, α is an arbitrary constant, $c_j > 0$ ($j = 1, 2, 3$), β is the constant calculated using c_j as follows:

$$\beta = \frac{c_2}{c_1 c_3}.$$

In the present thesis the algorithm of obtaining the exact solution is the following. Firstly, the function F is numerically calculated by the Runge-Kutta method of the 4-th order on the interval $[x_0, x_1]$. Then the streamlines are calculated using the obtained values of F. Two values b_1 and b_2 give two streamlines $y = y(x)$ and $y = y(x)$ which bound the test domain.

The following values of parameters are taken for obtaining the function F and for defining two streamlines:

$$\kappa = 1.4, \ \beta = 0.3, \ F_0 = 0.86, \ x_0 = 0, \ x_1 = 0.8, \ b_1 = 0.05, \ b_2 = 0.2.$$

In order to obtain the exact solution the following values of parameters are taken:

$$\alpha = 0, \ c_1 = 1, \ c_2 = 0.3, \ c_3 = 1.$$

The domain of the flow for the given values of parameters is shown in Fig.6.3. The grid is constructed and the exact solution is calculated by the formulas (6.3) on this grid. The Mach numbers varied from 0.25 at the inlet up to 0.62 at the outlet, thus the flow is subsonic only.

Table 6.6 shows the results of testing the algorithm for numerical solving the problem on gas flow.

Table 6.6: The solution accuracy of the gas flow problem.

Grid $N_1 \times N_2$	$\|u_{1,h} - u_{1,\text{exact}}\|_{L_1}$	$\|u_{2,h} - u_{2,\text{exact}}\|_{L_1}$
8×11	0.418_{-3}	0.571_{-3}
15×21	0.100_{-3}	0.134_{-3}
29×41	0.313_{-4}	0.365_{-4}

The numerical values of the components of the velocity converge to the exact solution with the second order. Fig.6.3. shows the velocity vector field of the gas flow.
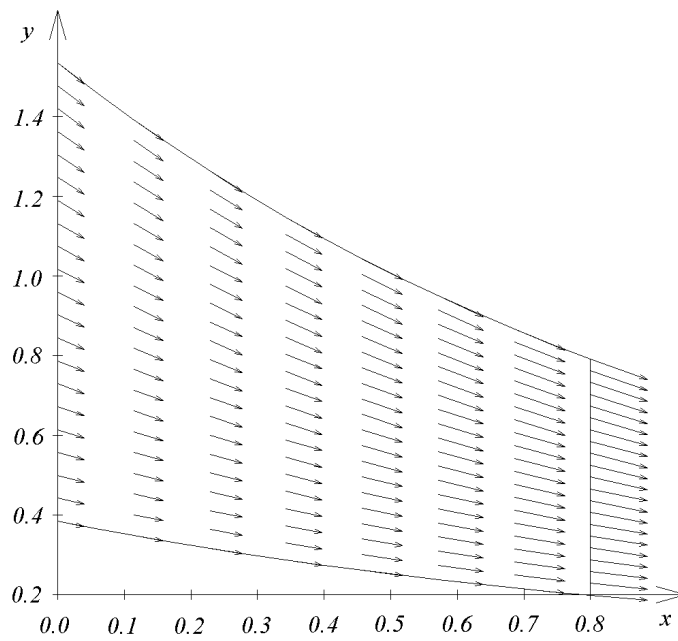
Figure 6.3: The velocity vector field of the gas flow

Chapter 7

Mathematical models of three-dimensional steady ideal fluid flows

7.1 Mathematical model of three-dimensional steady ideal fluid flow in Cartesian coordinates

Let Ω be a simply connected domain in the space of Cartesian coordinates x^1, x^2, x^3. The mathematical statement of the problem on steady ideal fluid flow through the domain Ω consists in obtaining the velocity vector $\mathbf{u}$ and the pressure p, satisfying the continuity equation and the motion equation in Ω:

$$\operatorname{div} \mathbf{u} = \mathbf{0}, \tag{7.1}$$

$$(\mathbf{u} \cdot \nabla) \cdot \mathbf{u} + \nabla p = 0, \qquad \mathbf{x} = (x^1, x^2, x^3) \in \Omega, \tag{7.2}$$

and the boundary conditions on the boundary $\Gamma = \partial\Omega$:

$$\mathbf{u}\Big|_{\mathbf{x}\in\Gamma_1} = \vec{\nu}_1(\mathbf{x}), \quad \mathbf{u}\cdot\mathbf{n}\Big|_{\mathbf{x}\in\Gamma_0} = 0, \quad \mathbf{u}\cdot\mathbf{n}\Big|_{\mathbf{x}\in\Gamma_2} = \nu_2(\mathbf{x}), \tag{7.3}$$

where $\mathbf{u} = (u_1, u_2, u_3)$, $u_\alpha(\alpha = 1, 2, 3)$ are the components of the velocity vector along the axes Ox^α, $\nabla = \left(\frac{\partial}{\partial x^1}, \frac{\partial}{\partial x^2}, \frac{\partial}{\partial x^3}\right)$, $\mathbf{n}$ is the external normal to Γ, $\Gamma = \Gamma_1 \cup \Gamma_0 \cup \Gamma_2$, Γ_1 is the inlet to Ω $(\vec{\nu}_1 \cdot \mathbf{n} < 0)$, Γ_0 is the impermeable part of the boundary, Γ_2 is the outlet from Ω $(\nu_2 > 0)$, $\Gamma_1 \cap \Gamma_2 = \emptyset$.

Let us introduce the function $\nu(\mathbf{x})$:

$$\nu(\mathbf{x}) = \begin{cases} \vec{\nu}_1(\mathbf{x}) \cdot \mathbf{n}(\mathbf{x}), & \mathbf{x} \in \Gamma_1, \\ 0, & \mathbf{x} \in \Gamma_0, \\ \nu_2(\mathbf{x}), & \mathbf{x} \in \Gamma_2. \end{cases} \tag{7.4}$$

Then the necessary solvability condition for the problem described above has the following form:

$$\int_{\Gamma_1} \nu(\mathbf{x}) d\Gamma_1 = -\int_{\Gamma_2} \nu(\mathbf{x}) d\Gamma_2. \tag{7.5}$$

This condition expresses the law of the mass balance.

For the solution uniqueness the pressure must also be specified at the certain point $M_0 \in \bar{\Omega}$ in addition to the conditions (7.3):

$$p(M_0) = p_0. \tag{7.6}$$

Solving the Euler equations (7.1)–(7.2) there are difficulties connected, firstly, with the satisfaction of the continuity equation and, secondly, with the absence of reliable and effective algorithm for calculating the pressure from the equation (7.2). In order to overcome these difficulties we use new formulation of the problem which, firstly, does not require solving the continuity equation, because it is fulfilled automatically, and, secondly, where there is no pressure as an unknown function.

Using the following formula of vector analysis [170]:

$$(\mathbf{u} \cdot \nabla) \cdot \mathbf{u} = \nabla \frac{|\mathbf{u}|^2}{2} - \mathbf{u} \times \text{rot } \mathbf{u}, \tag{7.7}$$

it is possible to write the motion equation (7.2) in the Gromeka-Lamb form:

$$-\mathbf{u} \times \text{rot } \mathbf{u} + \nabla(\frac{|\mathbf{u}|^2}{2} + p) = 0. \tag{7.8}$$

Applying the operator rot to the both parts of this equation and using the formula:

$$\text{rot } (\nabla \varphi) = 0, \tag{7.9}$$

we obtain the following corollary of the system (7.1)–(7.2):

$$\text{div } \mathbf{u} = \mathbf{0}, \tag{7.10}$$

$$\text{rot } (\mathbf{u} \times \vec{\omega}) = 0, \tag{7.11}$$

$$\text{rot } \mathbf{u} = \vec{\omega}, \tag{7.12}$$

where $\vec{\omega} = (\omega_1, \omega_2, \omega_3)$ is the vorticity vector. Thus, there is no pressure as an unknown function in this system. Let us specify the algorithm for calculating p which works after the iterative process of the solution of the equations (7.10)–(7.12).

We write the equation (7.8) as follows:

$$\nabla p = \mathbf{r}, \tag{7.13}$$

and we assume that

$$p(M) = p_0 + \int_{\gamma(M_0, M)} r_1 dx^1 + r_2 dx^2 + r_3 dx^3, \tag{7.14}$$

where

$$\mathbf{r} = (r_1, r_2, r_3) = \mathbf{u} \times \text{ rot } \mathbf{u} - \nabla \frac{|\mathbf{u}|^2}{2}, \tag{7.15}$$

p_0 is the value of the pressure at the point M_0 from the condition (7.6), $\gamma(M_0, M)$ is an arbitrary smooth curve connecting the points M_0 and $M \in \bar{\Omega}$.

On using the formula (7.14) a question arises: whether the pressure will depend on the path of integration γ or not. The realisation of the following equality:

$$\oint_C r_\alpha dx^\alpha = 0 \tag{7.16}$$

(the summation on the index α is made here, $\alpha = 1, 2, 3$) for any closed curve C is sufficient [43] for the value $p(M)$ to be independent of the choice of a curve $\gamma(M_0, M)$.

Let us check the equality (7.16). Under the Stokes theorem [123] we have the following:

$$\oint_C r_\alpha dx^\alpha = \int_{S_C} \text{rot } \mathbf{r} \cdot \mathbf{n} \, dS, \tag{7.17}$$

where S_C is the surface with the edge C in three-dimensional space. If we use the relations (7.9) and (7.11), then we obtain the following expression:

$$\text{rot } \mathbf{r} = \text{rot } \left(\mathbf{u} \times \text{rot } \mathbf{u} - \nabla \frac{|\mathbf{u}|^2}{2} \right) = \text{rot } (\mathbf{u} \times \text{rot } \mathbf{u}) = 0,$$

therefore, the validity of the equality (7.16) is proved.

The system (7.1)–(7.2) consists of four scalar equations with respect to four dependent variables u_1, u_2, u_3, p, and the system (7.10)–(7.12) consists of seven scalar equations with respect to six dependent variables. These variables are three components of the velocity vector $\mathbf{u}$: u_1, u_2, u_3 and three components of the vorticity vector $\vec{\omega}$: ω_1, ω_2, ω_3. Therefore, the system (7.10)–(7.12) is overdetermined. It is necessary for its solvability that the equations (7.10)–(7.12) were not independent. For the considered system this requirement is fulfilled, because by virtue of the first equation and the formula of vector analysis:

$$\text{div } (\text{rot } \mathbf{u}) = 0, \tag{7.18}$$

it follows from the third equation that

$$\text{div } \vec{\omega} = 0. \tag{7.19}$$

It is the necessary solvability condition of the system of equations (7.10)–(7.12).

For the numerical solution of the problem (7.1)–(7.3) new dependent variables, i.e. the vector potential $\vec{\psi} = (\psi_1, \psi_2, \psi_3)$ and the vorticity vector $\vec{\omega} = (\omega_1, \omega_2, \omega_3)$, are introduced:

$$\vec{\omega} = \text{rot } \mathbf{u}, \tag{7.20}$$

$$\mathbf{u} = \text{rot } \vec{\psi}. \tag{7.21}$$

Therefore, we obtain the new system of equations:

$$\Delta\vec{\psi} = -\vec{\omega} + \nabla(\text{div } \vec{\psi}), \tag{7.22}$$

$$\text{rot } (\text{rot } \vec{\psi} \times \vec{\omega}) = 0. \tag{7.23}$$

The boundary conditions are obtained from (7.3) using (7.5) and the definition (7.21). We shall discuss the boundary conditions for the equations (7.22)–(7.23) later when the statement of the concrete problem on three-dimensional fluid flow will be given.

69

If the solution $\vec{\psi}$, $\vec{\omega}$ of this system is found, then the vector function $\vec{\omega}$ and the velocity vector $\mathbf{u}$, which is defined in terms of $\vec{\psi}$ by the formula (7.21), are the solution of the system (7.10)–(7.12). It can easily be shown using the formula (7.18) and the following formula of vector analysis [170]:

$$\operatorname{rot}(\operatorname{rot}\vec{\psi}) = -\Delta\vec{\psi} + \nabla(\operatorname{div}\vec{\psi}). \tag{7.24}$$

The inverse statement is also correct. If $\mathbf{u}$, $\vec{\omega}$ are the solution of the system (7.10)–(7.12) and the vector function $\vec{\psi}$ is introduced so that the equality (7.21) is fulfilled, then the vector functions $\vec{\psi}$, $\vec{\omega}$ are the solution of the system (7.22)–(7.23). Therefore, the systems of equations (7.10)–(7.12) and (7.22)–(7.23) are equivalent.

Thus, using $\vec{\psi} - \vec{\omega}$ formulation the continuity equation (7.1) is fulfilled automatically.

In articles, where $\vec{\psi} - \vec{\omega}$ formulation is used, the following additional condition is added to the equations (7.22)–(7.23):

$$\operatorname{div}\vec{\psi} = 0. \tag{7.25}$$

For example, in [94] the solenoidal vector potential is used. It simplifies the equation (7.22), but it also results in the algorithm complexity, because of the requirement of realisation of the condition (7.25) in each node of a grid. The realisation of this condition in curvilinear coordinates is problematic, therefore we do not require this condition to be fulfilled in the present thesis and we use the equation for $\vec{\psi}$ in the form (7.22).

Thus, the initial system of equations (7.1)–(7.2) is replaced by the equivalent system of equations (7.22)–(7.23), (7.14) which is approximated in curvilinear coordinates by the finite difference scheme.

7.2 Mathematical model of three-dimensional steady ideal fluid flow in curvilinear coordinates

Let

$$x^\alpha = x^\alpha(q^1, q^2, q^3), \quad \alpha = 1, 2, 3, \tag{7.26}$$

be a one-to-one non-degenerate mapping of the unit cube Q in the space of coordinates q^1, q^2, q^3 onto the domain Ω. The equations (7.22)–(7.23) have the following form in new curvilinear coordinates q^α:

$$\frac{\partial}{\partial q^\alpha}\left(Jg^{\alpha\gamma}\frac{\partial\psi_\beta}{\partial q^\gamma}\right) = -J\omega_\beta + \frac{\partial}{\partial q^\alpha}\left(Jg^{\alpha\gamma}\frac{\partial\psi_\gamma}{\partial q^\beta}\right) + v_\alpha\varepsilon^{\alpha\mu\gamma}\frac{\partial g_{\beta\gamma}}{\partial q^\mu}, \quad \beta = 1, 2, 3, \tag{7.27}$$

$$\frac{\partial}{\partial q^\alpha}J\left(v^\alpha\omega^\beta - v^\beta\omega^\alpha\right) = 0, \quad \beta = 1, 2, 3, \tag{7.28}$$

where ψ_β, ω_β are the covariant components of the vector functions $\vec{\psi}$, $\vec{\omega}$. The summation is made on repeating indexes α and γ from 1 to 3. $g^{\alpha\gamma}$ are the elements of the inverse matrix for the matrix of the components of the metric tensor of the transformation (7.26), v_α are the covariant components of the velocity, v^α are the contravariant components of

70

the velocity. The following formulas connect covariant and contravariant components of the vectors:

$$v^1 = \frac{1}{J}\left(\frac{\partial \psi_3}{\partial q^2} - \frac{\partial \psi_2}{\partial q^3}\right),$$

$$v^2 = \frac{1}{J}\left(\frac{\partial \psi_1}{\partial q^3} - \frac{\partial \psi_3}{\partial q^1}\right),$$ (7.29)

$$v^3 = \frac{1}{J}\left(\frac{\partial \psi_2}{\partial q^1} - \frac{\partial \psi_1}{\partial q^2}\right),$$

$$v_\alpha = g_{\alpha\gamma}v^\alpha, \quad w_\alpha = g_{\alpha\gamma}w^\alpha,$$ (7.30)

$$\varepsilon^{\alpha\mu\gamma} = \begin{cases} 1, & \alpha\mu\gamma \quad is\ the\ even\ permutation\ of\ numbers \quad \alpha,\mu,\gamma, \\ -1, & \alpha\mu\gamma \quad is\ the\ odd\ permutation\ of\ numbers \quad \alpha,\mu,\gamma. \end{cases}$$

The solvability condition (7.19) have the following form for the system of equations (7.27)–(7.28):

$$\frac{\partial}{\partial q^\alpha}(Jw^\alpha) = 0.$$ (7.31)

The Gromeka-Lamb equations can be written in curvilinear coordinates in the form (7.13):

$$\frac{\partial p}{\partial q^\beta} = r_\beta, \quad \beta = 1, 2, 3,$$ (7.32)

where

$$r_1 = Jv^2\omega^3 - Jv^3\omega^2 - \frac{\partial}{\partial q^1}\frac{|\mathbf{u}|^2}{2},$$

$$r_2 = -Jv^1\omega^3 + Jv^3\omega^1 - \frac{\partial}{\partial q^2}\frac{|\mathbf{u}|^2}{2},$$

$$r_3 = Jv^1\omega^2 - Jv^2\omega^1 - \frac{\partial}{\partial q^3}\frac{|\mathbf{u}|^2}{2}.$$

These equations are used for calculating the pressure by the formula similar to (7.14):

$$p(M) = p_0 + \int_{\gamma(M_0,M)} r_1 dq^1 + r_2 dq^2 + r_3 dq^3.$$ (7.33)

Unlike (7.14), now M is the point in the computational domain Q, M_0 is the pre-image of the appropriate point from (7.6) under the mapping (7.26). $\gamma(M_0, M)$ is an arbitrary curve connecting the points M and M_0 in the computational domain Q.

The realisation of the equality:

$$\oint_{S_C} r_1 dq^1 + r_2 dq^2 + r_3 dq^3 = 0 \tag{7.34}$$

for an arbitrary closed curve C which is located in Q is necessary and sufficient for the pressure calculated by the formula (7.33) to be independent of the choice of a curve γ.

According to the Stokes theorem [123], this equality is equivalent to the following expression:

$$\oint_{S_C} \left(-\frac{\partial r_1}{\partial q^2} + \frac{\partial r_2}{\partial q^1} \right) dq^1 dq^2 + \left(-\frac{\partial r_2}{\partial q^3} + \frac{\partial r_3}{\partial q^2} \right) dq^2 dq^3 + \left(-\frac{\partial r_1}{\partial q^3} + \frac{\partial r_3}{\partial q^1} \right) dq^1 dq^3 = 0.$$

$$\tag{7.35}$$

Each of the brackets in the intergrand is equal to zero by virtue of the equation (7.28). Thus, the equality (7.34) is fulfilled.

Chapter 8

Method of grid generation in three-dimensional domains

8.1   Three-dimensional equidistribution method

Let us consider the principle and the equations of the equidistribution method for constructing a grid inside the three-dimensional simply connected domain Ω with the motionless boundary Γ. Let

$$x^\alpha = x^\alpha(q^1, q^2, q^3), \qquad \alpha = 1, 2, 3, \tag{8.1}$$

be a one-to-one non-degenerate sufficiently smooth mapping of the unit cube Q onto the domain Ω. Ω is named "the physical domain" and Q – "the computational domain" (see Fig.8.1).

For an arbitrary mapping of this kind the identity which is similar to (4.24) and which follows from the Laplace equation written in new coordinates q^β is fulfilled:

$$\frac{\partial}{\partial q^\gamma}\left(Jg^{\gamma\beta}\frac{\partial x^\alpha}{\partial q^\beta}\right) = 0, \qquad \alpha, \beta, \gamma = 1, 2, 3. \tag{8.2}$$
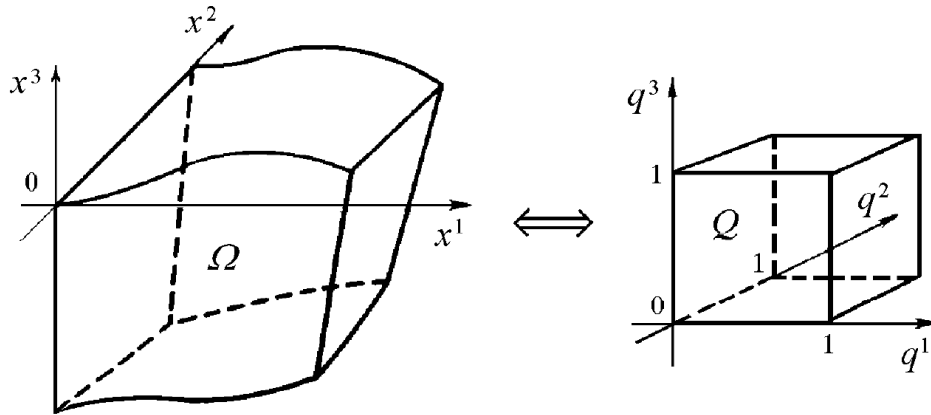
Figure 8.1: The physical domain Ω and the computational domain Q

Unlike (4.24), here we use the contravariant components $g^{\gamma\beta}$ of the metric tensor:

$$g^{\gamma\beta} = \sum_{\alpha=0}^{3} \frac{\partial q^{\gamma}}{\partial x^{\alpha}} \frac{\partial q^{\beta}}{\partial x^{\alpha}}. \qquad \beta, \gamma = 1, 2, 3.$$

We use the tensor rule of summation on the repeating upper and lower indices γ and β. This rule will be used everywhere further if the opposite will not be said.

For the orthogonal mapping (8.1) the following conditions are fulfilled:

$$g_{12} = 0, \qquad g_{13} = 0, \qquad g_{23} = 0. \tag{8.3}$$

Therefore, the identities (8.2) have the form of the following equations without the mixed derivatives of the functions x^{α}:

$$\frac{\partial}{\partial q^1}\left(\frac{g_{22}g_{33}}{J}\frac{\partial x^{\alpha}}{\partial q^1}\right) + \frac{\partial}{\partial q^2}\left(\frac{g_{11}g_{33}}{J}\frac{\partial x^{\alpha}}{\partial q^2}\right) + \frac{\partial}{\partial q^3}\left(\frac{g_{11}g_{22}}{J}\frac{\partial x^{\alpha}}{\partial q^3}\right) = 0, \quad \alpha = 1, 2, 3. \tag{8.4}$$

If we require the mapping (8.1) to satisfy the equidistribution principle in differential form:

$$w(\mathbf{x}(\mathbf{q}))J(\mathbf{q}) = C, \quad C = \text{const}, \quad \mathbf{q} = (q^1, q^2, q^3) \in Q, \tag{8.5}$$

where J is the Jacobian of the mapping (8.1), $\mathbf{x} = (x^1, x^2, x^3)$, then the functions $x^{\alpha} = x^{\alpha}(q^1, q^2, q^3)$ are the solutions of the following three-dimensional equations of the equidistribution method in differential form ("ED3-equations"):

$$\frac{\partial}{\partial q^1}\left(wg_{22}g_{33}\frac{\partial x^{\alpha}}{\partial q^1}\right) + \frac{\partial}{\partial q^2}\left(wg_{11}g_{33}\frac{\partial x^{\alpha}}{\partial q^2}\right) + \frac{\partial}{\partial q^3}\left(wg_{11}g_{22}\frac{\partial x^{\alpha}}{\partial q^3}\right) = 0, \quad \alpha = 1, 2, 3.$$

$$\tag{8.6}$$

As in two-dimensional case, the following statement which is opposite to the above formulated statement is fulfilled.

Lemma 8.1. *If the mapping (8.1) given by the solutions of the equations (8.6) is non-degenerate and orthogonal, then it is also adaptive in the sense of the realisation of the equality (8.5).*

Let us cover the unit cube Q by the rectangular uniform grid with the number of nodes N_{α} in the direction of the axes Oq^{α}. The nodes of the grid are denoted by $\mathbf{q}_j = (q_{j1}^1, q_{j2}^2, q_{j3}^3)$, j is the multi-index, $j = (j_1, j_2, j_3)$, $j_{\alpha} = 1, ..., N_{\alpha}$, $q_{j_{\alpha}}^{\alpha} = (j_{\alpha} - 1)h_{\alpha}$, $h_{\alpha} = 1/(N_{\alpha} - 1)$, $\alpha = 1, 2, 3$. The total set of the nodes $\mathbf{q}_j$ is denoted by $\bar{Q}_h$, the total set of interior nodes – by Q_h and the total set of boundary nodes – by γ_h. Thus, $\bar{Q}_h = Q_h \cup \gamma_h$.

Together with the grid $\bar{Q}_h$ the grids with the nodes which are moved on the distance of a half step in one, two or in three coordinate directions are also used. These nodes are named "the nodes with the half-integer indices" or "the half-integer nodes". In the computational domain Q the coordinates of the half-integer nodes which are the middles of the edges are calculated by the following formulas:

$$\mathbf{q}_{j_1+1/2, j_2, j_3} = (q_{j_1+1/2}^1, q_{j_2}^2, q_{j_3}^3),$$

$$\mathbf{q}_{j_1,j_2+1/2,j_3} = (q_{j_1}^1,\ q_{j_2+1/2}^2,\ q_{j_3}^3),$$

$$\mathbf{q}_{j_1,j_2,j_3+1/2} = (q_{j_1}^1,\ q_{j_2}^2,\ q_{j_3+1/2}^3),$$

where $q_{j_\alpha+1/2}^\alpha = q_{j_\alpha}^\alpha + h_\alpha/2$.

For the nodes coinciding with the centres of the faces we assume:

$$\mathbf{q}_{j_1+1/2,j_2+1/2,j_3} = (q_{j_1+1/2}^1,\ q_{j_2+1/2}^2,\ q_{j_3}^3),$$

$$\mathbf{q}_{j_1,j_2+1/2,j_3+1/2} = (q_{j_1}^1,\ q_{j_2+1/2}^2,\ q_{j_3+1/2}^3),$$

$$\mathbf{q}_{j_1+1/2,j_2,j_3+1/2} = (q_{j_1+1/2}^1,\ q_{j_2}^2,\ q_{j_3+1/2}^3).$$

The centre of the mesh has the following coordinates:

$$\mathbf{q}_{j+1/2} \equiv \mathbf{q}_{j_1+1/2,j_2+1/2,j_3+1/2} = (q_{j_1+1/2}^1,\ q_{j_2+1/2}^2,\ q_{j_3+1/2}^3).$$

Let us introduce the following basis difference operators:

$$(D_{q_1}\varphi)(\mathbf{q}) = \frac{\varphi(q^1 + h_1/2, q^2, q^3) - \varphi(q^1 - h_1/2, q^2, q^3)}{h_1}, \tag{8.7}$$

$$(D_{q_2}\varphi)(\mathbf{q}) = \frac{\varphi(q^1, q^2 + h_2/2, q^3) - \varphi(q^1, q^2 - h_2/2, q^3)}{h_2}, \tag{8.8}$$

$$(D_{q_3}\varphi)(\mathbf{q}) = \frac{\varphi(q^1, q^2, q^3 + h_3/2) - \varphi(q^1, q^2, q^3 - h_3/2)}{h_3}. \tag{8.9}$$

For the calculation of the differences (8.7)–(8.9), as well as for the calculation of the differences (4.30)–(4.31) in two-dimensional case, it is necessary to take into account the definition area of the grid function φ and to use the averaging if it is necessary. For example, for calculating the differences of the functions x^α defined in the integer nodes $\mathbf{q}_j$ we assume

$$(D_{q^1}x^\alpha)_{j+1/2} = \frac{x_{j_1+1,j_2+1/2,j_3+1/2}^\alpha - x_{j_1,j_2+1/2,j_3+1/2}^\alpha}{h_1}, \tag{8.10}$$

where $x_{j_1,j_2+1/2,j_3+1/2}^\alpha$ are the coordinates of the centre of the face with the number j_1.

Let us explain what we name "the centre of the face". The mesh (see Fig.8.2) of the curvilinear grid covering the physical domain Ω is the hexahedron with non-planar, generally speaking, faces.

Despite the fact that the face is a nonlinear quadrangle, the segments connecting the middles of the opposite sides of the face are located in one plane. These segments are are named "the centrelines of the faces". They are intersected at some point which we name "the centre of the face". For example, for the face j_1 the centre is the point $\mathbf{x}_{j_1,j_2+1/2,j_3+1/2}$. Each coordinate of this point is equal to the arithmetical average of the appropriate coordinates of the four vertexes of this face.

We name the segments connecting the centres of the opposite faces "the centrelines of the mesh". It is easy to show that the centrelines of the convex mesh are intersected at one point. This point we name "the centre of the mesh" and denote by $\mathbf{x}_{j+1/2}$.
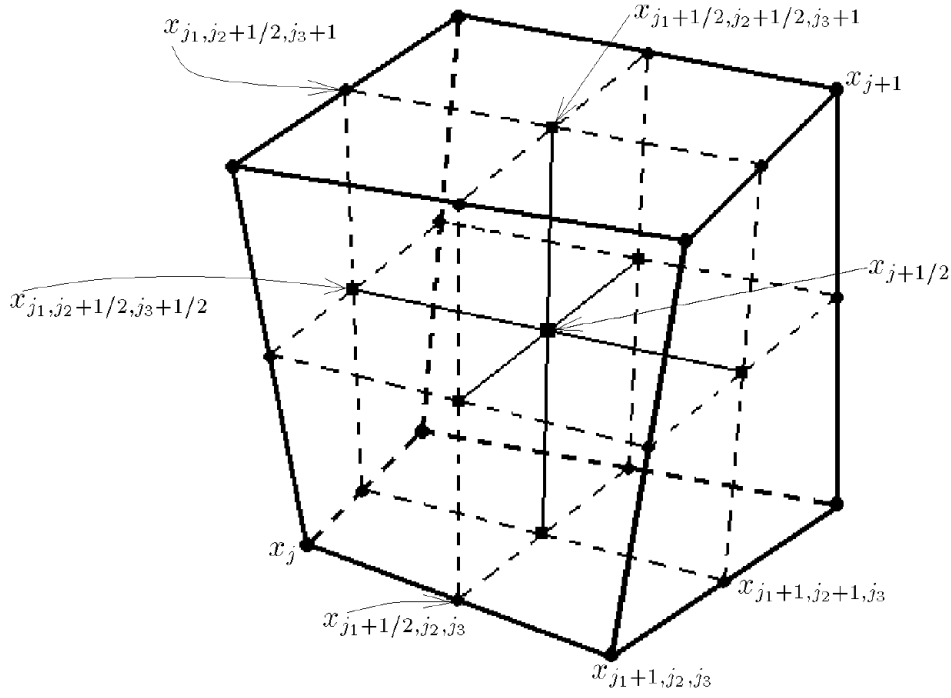
Figure 8.2: The mesh of the curvilinear three-dimensional grid, the centrelines of the mesh, the centrelines of the faces, the centres of the faces and the centre of the mesh

The volume of the mesh is calculated by the following formula:

$$S_{j+1/2} = (\mathbf{x}_{j_1+1,j_2+1/2,j_3+1/2} - \mathbf{x}_{j_1,j_2+1/2,j_3+1/2}) \cdot \tag{8.11}$$

$$\cdot \left[\left(\mathbf{x}_{j_1+1/2,j_2+1,j_3+1/2} - \mathbf{x}_{j_1+1/2,j_2,j_3+1/2} \right) \left(\mathbf{x}_{j_1+1/2,j_2+1/2,j_3+1} - \mathbf{x}_{j_1+1/2,j_2+1/2,j_3} \right) \right].$$

If we use the basis operators (8.7)–(8.9) for calculating the Jacobian J of the mapping (8.1), then the obtained equality is similar to (4.39):

$$S_{j+1/2} = J_{j+1/2} h_1 h_2 h_3. \tag{8.12}$$

Therefore, the requirement of the constancy of the product of the volumes of the meshes and the control function w is the analogue of (8.5) at the difference level:

$$w(\mathbf{x}_{j+1/2}) S_{j+1/2} = \tilde{C}_h, \quad j_\alpha = 1, \ldots, N_\alpha - 1, \quad \alpha = 1, 2, 3. \tag{8.13}$$

This equality we name "the three-dimensional equidistribution principle in difference form". It is obvious that by virtue of (8.12) this principle can be written in the following form:

$$w(\mathbf{x}_{j+1/2}) J_{j+1/2} = \frac{\tilde{C}_h}{h_1 h_2 h_3} \equiv C_h = \text{const}, \quad j_\alpha = 1, \ldots, N_\alpha - 1. \tag{8.14}$$

The difference equations for the node coordinates are obtained by the integro-interpolational method. For this purpose, the equations (8.6) are substituted by the integrated relations:

$$\oint_S w g_{22} g_{33} \frac{\partial x^\alpha}{\partial q^1} dq^2 dq^3 - w g_{11} g_{33} \frac{\partial x^\alpha}{\partial q^2} dq^1 dq^3 + w g_{11} g_{22} \frac{\partial x^\alpha}{\partial q^3} dq^1 dq^2 = 0, \quad \alpha = 1, 2, 3,$$

76

Figure 8.3: The pattern of the difference equations for the calculation of the node coordinates and the integration surface in the internal node $\mathbf{q}_j \in Q_h$

$$\tag{8.15}$$

where $\mathcal{S}$ is the surface of the parallelepiped. The faces of this parallelepiped are parallel to the axes Oq^α and divide the distances from the considered interior node $\mathbf{q}_j$ to the nodes adjacent to it into two equal parts. Fig.8.3 shows the 27-point pattern of the difference equations and the integration surface (denoted by the dashed line) in the internal node $\mathbf{q}_j \in Q_h$.

The integrals over the faces of the surface $\mathcal{S}$ are approximated by the trapezoidal formula assuming that the grid functions x^α are defined in the integer nodes $\mathbf{q}_j$, the components of the metric tensor $g_{\gamma\beta}$ and the control function w are defined at the centres of the meshes $\mathbf{q}_{j+1/2}$.

Since the resulting expressions are rather awkward, the approximating formula only for the face $BCGF$ of the integration surface $ABCDEFGH$ for $\alpha = 1$ is presented here. The derivative $\frac{\partial x}{\partial q^1}$ in the nodes B, C, G, F is calculated using the formula (8.10):

$$\oint\limits_{(BCGF)} w g_{22} g_{33} \frac{\partial x}{\partial q^1} dq^2 dq^3 \approx \tag{8.16}$$

$$\approx \frac{1}{4} \cdot h_2 h_3 \cdot \left[w g_{22} g_{33}(B) \frac{1}{h_1} \left(\frac{x_{20} + x_{12} + x_3 + x_6}{4} - \frac{x_{15} + x_{10} + x_0 + x_2}{4} \right) + \right.$$

$$+ w g_{22} g_{33}(C) \frac{1}{h_1} \left(\frac{x_{12} + x_{21} + x_7 + x_3}{4} - \frac{x_{10} + x_{16} + x_4 + x_0}{4} \right) +$$

77

$$+wg_{22}g_{33}(G)\frac{1}{h_1}\left(\frac{x_3 + x_7 + x_{25} + x_{13}}{4} - \frac{x_0 + x_4 + x_{17} + x_9}{4}\right) +$$

$$+wg_{22}g_{33}(F)\frac{1}{h_1}\left(\frac{x_6 + x_3 + x_{13} + x_{24}}{4} - \frac{x_2 + x_0 + x_9 + x_{18}}{4}\right)\Bigg] =$$

$$= \frac{h_2 h_3}{4}\left[wg_{22}g_{33}(B)D_{q^1}x(B) + wg_{22}g_{33}(C)D_{q^1}x(C)+\right.$$

$$\left.+wg_{22}g_{33}(G)D_{q^1}x(G) + wg_{22}g_{33}(F)D_{q^1}x(F)\right].$$

Thus, we obtain the following difference equations:

$$(\Lambda_1 x^\alpha + \Lambda_2 x^\alpha + \Lambda_3 x^\alpha)_j = 0, \quad \alpha = 1, 2, 3, \quad \mathbf{q}_j \in Q_h, \tag{8.17}$$

where

$$(\Lambda_1 x^\alpha)_j = D_{q^1}\left(wg_{22}g_{33}D_{q^1}x^\alpha\right)_j,$$

$$(\Lambda_2 x^\alpha)_j = D_{q^2}\left(wg_{11}g_{33}D_{q^2}x^\alpha\right)_j,$$

$$(\Lambda_3 x^\alpha)_j = D_{q^3}\left(wg_{11}g_{22}D_{q^3}x^\alpha\right)_j.$$

The equations (8.17) are named "the equations of the equidistribution method" or "ED3-equations in difference form".

The difference equations (8.17) are nonlinear and 27-point formula. The matrix of the coefficients of these equations is symmetric and has the diagonal predominance. In practice the simpler difference equations are used for constructing a grid. They are obtained on the basis of the quadrature formula of rectangles. Thus, instead of (8.16), the following approximation is applied:

$$\oint_{(BCGF)} wg_{22}g_{33}\frac{\partial x}{\partial q^1}dq^2 dq^3 \approx \tag{8.18}$$

$$\approx h_2 h_3 \frac{1}{4}\left[wg_{22}g_{33}(B) + wg_{22}g_{33}(C) + wg_{22}g_{33}(G) + wg_{22}g_{33}(F)\right]\frac{x_3 - x_0}{h_1}.$$

As a result of the approximation of the integrals we obtain three difference equations for calculating the coordinates x^α. Fig.8.4 shows the pattern of these equations.

For solving the obtained equations it is possible to use the iterative process where at each step the coefficients $wg_{\beta\beta}$ of the difference equations are calculated from the previous iteration. Then for the approximation (8.18) the difference equation can be considered as the 7-point formula:

$$\sum_{k=0}^{6} \alpha_k \varphi(k) = 0, \quad \mathbf{q}_j \in Q_h, \tag{8.19}$$

78
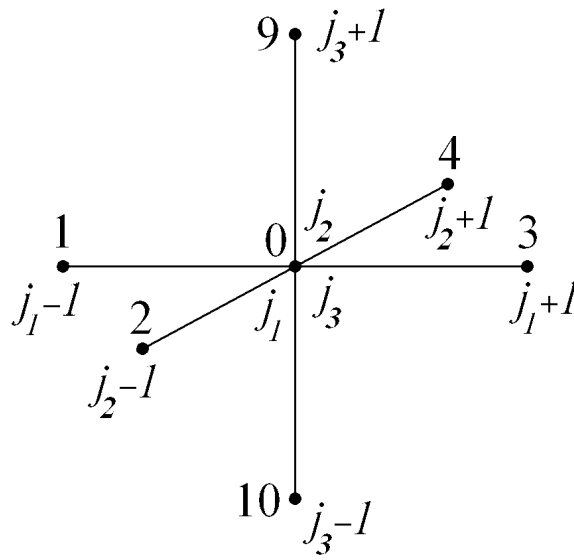
Figure 8.4: The pattern of the difference equations for the calculation of the node coordinates x^α in the internal node $\mathbf{q}_j \in Q_h$

where $\varphi(k) = x^\alpha(k)$, $k = 1, 2, 3, 4$, $\varphi(5) = x^\alpha(9)$, $\varphi(6) = x^\alpha(10)$ and the coefficients α_k are calculated as follows:

$$\alpha_3 = \frac{h_2 h_3}{h_1} \left[w g_{22} g_{33}(B) + w g_{22} g_{33}(C) + w g_{22} g_{33}(G) + w g_{22} g_{33}(F) \right],$$

$$\alpha_1 = \frac{h_2 h_3}{h_1} \left[w g_{22} g_{33}(A) + w g_{22} g_{33}(D) + w g_{22} g_{33}(H) + w g_{22} g_{33}(F) \right],$$

$$\alpha_4 = \frac{h_1 h_3}{h_2} \left[w g_{11} g_{33}(D) + w g_{11} g_{33}(C) + w g_{11} g_{33}(G) + w g_{11} g_{33}(H) \right],$$

$$\alpha_2 = \frac{h_1 h_3}{h_2} \left[w g_{11} g_{33}(A) + w g_{11} g_{33}(B) + w g_{11} g_{33}(F) + w g_{11} g_{33}(E) \right],$$

$$\alpha_5 = \frac{h_1 h_2}{h_3} \left[w g_{11} g_{22}(E) + w g_{11} g_{22}(F) + w g_{11} g_{22}(G) + w g_{11} g_{22}(H) \right],$$

$$\alpha_6 = \frac{h_1 h_2}{h_3} \left[w g_{11} g_{22}(A) + w g_{11} g_{22}(B) + w g_{11} g_{22}(C) + w g_{11} g_{22}(D) \right],$$

$$\alpha_0 = -(\alpha_1 + \alpha_2 + \alpha_3 + \alpha_4 + \alpha_5 + \alpha_6). \tag{8.20}$$

On considering the matrix $\mathcal{A}$ of the coefficients α_k of the difference equation (8.19) we see that it is symmetric and has the diagonal predominance.

For the solution of the system (8.17) the method of stabilizing corrections is used:

$$\frac{\varphi^{n+1/3} - \varphi^n}{\tau} = \Lambda_1 \varphi^{n+1/3} + \Lambda_2 \varphi^n + \Lambda_3 \varphi^n, \tag{8.21}$$

$$\frac{\varphi^{n+2/3} - \varphi^{n+1/3}}{\tau} = \Lambda_2(\varphi^{n+2/3} - \varphi^n), \tag{8.22}$$

$$\frac{\varphi^{n+1} - \varphi^{n+2/3}}{\tau} = \Lambda_3(\varphi^{n+1} - \varphi^n), \tag{8.23}$$

where $\varphi = x^\alpha$, n is the iteration number, τ is the iterative parameter which is chosen experimentally. Λ_α are the three-point difference operators, for example:

$$(\Lambda_1 x^\alpha)_j = \frac{1}{h_1 h_2 h_3} \left[\alpha_3 (\varphi_3 - \varphi_0) - \alpha_1 (\varphi_0 - \varphi_1) \right].$$

Each of the steps (8.21)–(8.23) is realized by the scalar sweep method. It is assumed that the coordinates of the nodes on the boundary $\Gamma = \partial\Omega$ are already known.

The method of constructing adaptive grids on the basis of the equations (8.6) is named "ED3-method for three-dimensional domains".

8.2 Grid generation on space surfaces

Let us obtain the equations of the equidistribution method for constructing the grids on the lateral surfaces bounding the physical domain Ω. We assume that the domain Ω is the hexahedron. Each face of this hexahedron is the surface on which one of the faces of the cube Q is mapped by means of the mapping (8.1).

If we follow the uniform methodology of grid generation inside the domain and on its boundary, then it is necessary to construct the grid on the lateral surfaces also on the basis of the equidistribution principle.

According to the principle, the product of the area of each mesh of two-dimensional grid covering the curvilinear face and the value of the control function w at the centre of this mesh must be the constant value for this face. Proceeding from this principle it is possible to write the equations. The finite-difference analogues of these equations will be used for calculating the coordinates of the grid nodes on the surface. The procedure of obtaining such equations is presented below. It is based on the projection of three-dimensional equations (8.6) on the boundary surfaces under some additional assumptions about the behaviour of the mapping (8.1) near the boundaries.

We shall explain the algorithm making use of the example of obtaining the equations for the part Γ_{bot} of the boundary surface Γ. Γ_{bot} is the image of the lower boundary $q^3 = 0$ of the cube Q. It is assumed that this part of the boundary is given parametrically:

$$x^\alpha = f^\alpha(p^1, p^2), \qquad 0 \le p^\beta \le 1, \quad \alpha = 1, 2, 3, \quad \beta = 1, 2. \tag{8.24}$$

The following assumptions are made concerning the mapping (8.1):
- the coordinate lines of the mapping are orthogonal on Γ_{bot};
- the curvature of coordinate lines of the third set is equal to zero at the points of their intersection with Γ_{bot};
- the coordinate surfaces $q^3 = $ const are "parallel" to the surface Γ_{bot} in some neighbourhood of this surface.

The second assumption was used earlier in [143] for obtaining the equations for the surface grid from the equations [150] for the interior nodes.

We use the following mathematical form of these assumptions:

$$g_{12} = g_{13} = g_{23} = 0, \qquad \mathbf{q} = (q^1, q^2, 0), \tag{8.25}$$

$$\frac{\partial \mathbf{r}_3}{\partial q^3} = \frac{1}{2g_{33}} \frac{\partial g_{33}}{\partial q^3} \mathbf{r}_3, \qquad \mathbf{q} = (q^1, q^2, 0), \tag{8.26}$$

$$g_{33} = \text{const}, \qquad \mathbf{q} = (q^1, q^2, 0). \tag{8.27}$$

The vector tangential to the coordinate line q_α is denoted by $\mathbf{r}_\alpha$, i.e. $\mathbf{r}_\alpha = \partial \mathbf{r}/\partial q^\alpha$, where $\mathbf{r}$ is the position vector of the point.

Lemma 8.2. *If the conditions (8.25)–(8.27) are satisfied and the equation (8.6) is fulfilled in Ω up to the boundary Γ_{bot}, then*

$$wJ(q^1, q^2, 0) = \text{const}, \qquad 0 < q^\alpha < 1, \quad \alpha = 1, 2. \tag{8.28}$$

The equality (8.28) means that the mapping (8.1) satisfies the equidistribution principle in differential form on the boundary surface Γ_{bot}.

Obtaining the equations for calculating the node coordinates on the surface we consider the values $\partial(wJ)/\partial q^\alpha = 0$ as the solution of the following homogeneous system:

$$\frac{\partial p^\alpha}{\partial q^2} \frac{\partial wJ}{\partial q^1} - \frac{\partial p^\alpha}{\partial q^1} \frac{\partial wJ}{\partial q^2} = 0, \qquad \alpha = 1, 2. \tag{8.29}$$

The determinant of this system $\tilde{J} = p^1_{q^1} p^2_{q^2} - p^1_{q^2} p^2_{q^1}$ is not equal to zero. Let $\tilde{g}_{\alpha\beta}$ be the covariant components of the metric tensor of one-to-one non-degenerate mapping

$$p^\beta = p^\beta(q^1, q^2), \quad \beta = 1, 2, \tag{8.30}$$

with the Jacobian $\tilde{J} > 0$, i.e.

$$\tilde{g}_{\alpha\beta} = \frac{\partial p^1}{\partial q^\alpha} \frac{\partial p^1}{\partial q^\beta} + \frac{\partial p^2}{\partial q^\alpha} \frac{\partial p^2}{\partial q^\beta}, \qquad \alpha, \beta = 1, 2. \tag{8.31}$$

Then the following formulas are fulfilled for the mapping (8.30):

$$\tilde{J} \tilde{g}^{\beta 1} \frac{\partial p^\alpha}{\partial q^1} + \tilde{J} \tilde{g}^{\beta 2} \frac{\partial p^\alpha}{\partial q^2} = (-1)^{\alpha+\beta} \frac{\partial p^{3-\alpha}}{\partial q^{3-\beta}}, \qquad \alpha, \beta = 1, 2, \tag{8.32}$$

where

$$\tilde{g}^{11} = \frac{\tilde{g}_{22}}{\tilde{J}^2}, \quad \tilde{g}^{22} = \frac{\tilde{g}_{11}}{\tilde{J}^2}, \quad \tilde{g}^{12} = -\frac{\tilde{g}_{12}}{\tilde{J}^2}. \tag{8.33}$$

By rewriting the equations (8.29) in the divergent form:

$$\frac{\partial}{\partial q^1} \left(wJ \frac{\partial p^\alpha}{\partial q^2} \right) - \frac{\partial}{\partial q^2} \left(wJ \frac{\partial p^\alpha}{\partial q^1} \right) = 0$$

81

and using the identities (8.32) at the additional assumption about the orthogonality of the system of coordinates (8.30) we obtain the following equations for the functions $p^\alpha(q^1, q^2)$, $\alpha = 1, 2$ ("EDS-equations"):

$$\frac{\partial}{\partial q^1}\left(w\sqrt{g_{11}g_{22}}\frac{\tilde{g}_{22}}{\tilde{J}}\frac{\partial p^\alpha}{\partial q^1}\right) + \frac{\partial}{\partial q^2}\left(w\sqrt{g_{11}g_{22}}\frac{\tilde{g}_{11}}{\tilde{J}}\frac{\partial p^\alpha}{\partial q^2}\right) = 0, \quad \alpha = 1, 2. \tag{8.34}$$

The condition (8.27) is also used for obtaining these equations.

For the numerical solution of EDS-equations the covariant components $\hat{g}_{\alpha\beta}$ of the metric tensor of the surface Γ_{bot} are used instead of the components $g_{\alpha\beta}$. The covariant components $\hat{g}_{\alpha\beta}$ are connected with the values $g_{\alpha\beta}$ by the following relations:

$$g_{\alpha\beta} = \hat{g}_{\gamma\varepsilon}\frac{\partial p^\gamma}{\partial q^\alpha}\frac{\partial p^\varepsilon}{\partial q^\beta}, \qquad \alpha, \beta, \gamma, \varepsilon = 1, 2, \tag{8.35}$$

where

$$\hat{g}_{\alpha\beta} = \frac{\partial x^\gamma}{\partial p^\alpha}\frac{\partial x^\gamma}{\partial p^\beta}\delta_{\gamma\gamma}, \qquad \alpha, \beta = 1, 2, \tag{8.36}$$

(the summation on the index $\gamma = 1, 2, 3$ is made here).

The finite-difference equations for the calculation of the node coordinates $\mathbf{x}_{j_1,j_2,1}$ are obtained by the approximation of the equations (8.34) on the nine-point pattern with the help of the integro-interpolational method. These difference equations are similar to (4.38):

$$\left(D_{q^1}(\tilde{w}\tilde{g}_{22}D_{q^1}p^\alpha) + D_{q^2}(\tilde{w}\tilde{g}_{11}D_{q^2}p^\alpha)\right)_{j_1,j_2,1} = 0, \quad \alpha = 1, 2, \tag{8.37}$$

where the grid function $\tilde{w} = w\sqrt{g_{11}g_{22}}/\tilde{J}$ refers to the centres of the meshes. These systems of nonlinear difference equations are solved by the longitudinal-transversal sweep method.

If the surface Γ_{bot} is plane, for example, it is located in the plane $x^3 = x_0^3$, and we take Cartesian coordinates x^α ($\alpha = 1, 2$) as the parameters p^β, then $\hat{g}_{\alpha\beta} = \delta_{\alpha\beta}$, $g_{\alpha\beta} = \tilde{g}_{\alpha\beta}$, $J = \tilde{J}$, and the equations (8.34) change over to the equations (4.38) of ED2-method for constructing the grids in plane domains.

The method of constructing adaptive grids on the basis of the equations (8.34) is named "EDS-method for surfaces".

8.3 Grid generation on space curves

Now we will obtain the equations of the equidistribution method for calculating the node coordinates on the space curve which is one of the edges of the curvilinear hexahedron Ω. For the definiteness let this edge (further it is denoted by L) belong to two surfaces which are the images under the mapping (8.1) of the faces $q^3 = 0$ and $q^2 = 0$ of the unit cube Q.

We proceed from the general principle of the equidistribution method. Therefore, we construct the grid on the considered edge so that the lengths of the segments between two adjacent nodes of the grid are inversely proportional to the values of the control function at the centres of these segments.

It is desirable to use the same control function w for the best fitting of the node position inside the domain and on the curve L. However, in this case w is responsible for the degree of the concentration of the nodes according the different features. Inside the domain the values of w govern the volumes of the meshes, and on L they govern the length of one of the edges of the hexahedral mesh.

Generally, the usage of the same control function can lead to some undesirable effects. For example, the volumes of the meshes situated near the boundary will decrease when moving along L, and the lengths of the edges of these meshes located on L will increase. In order to avoid any undesirable consequences it is necessary to impose the additional restrictions on the mapping (8.1).

Let the functions x^α, which define the mapping (8.1), be the solutions of ED3-equations (8.6). Let us formulate the additional assumptions about the behaviour of the functions x^α in the neighbourhood of the curve L. Realizing these assumptions the functions x^α satisfy the equidistribution principle on L:

$$\sqrt{g_{11}}w = \text{const}, \qquad \mathbf{q} = (q^1, 0, 0). \tag{8.38}$$

L is the line of intersection of two lateral faces of the domain Ω and the equations of EDS-method on these faces are obtained using the conditions of the type of (8.25)–(8.27). Therefore, the same conditions can be used for obtaining the equations for the grid on L. Actually only the part of the conditions written for each of two faces is sufficient here. The following restrictions on the mapping (8.1) are used:

$$g_{\alpha\beta} = 0, \quad \alpha \neq \beta, \qquad \mathbf{x} \in L, \tag{8.39}$$

$$\frac{\partial \mathbf{r}_3}{\partial q^3} = \Gamma_{33}^3 \mathbf{r}_3, \quad \frac{\partial \mathbf{r}_2}{\partial q^2} = \Gamma_{22}^2 \mathbf{r}_2, \qquad \mathbf{x} \in L, \tag{8.40}$$

$$\frac{\partial g_{\alpha\alpha}}{\partial q^\beta} = 0, \quad \alpha = 2, 3, \quad \beta = 1, 2, 3, \quad \beta \neq \alpha, \qquad \mathbf{x} \in L, \tag{8.41}$$

where $\Gamma_{\alpha\beta}^\gamma$ are the Christoffel's symbols.

These restrictions mean the following:

- the coordinate lines of the mapping are orthogonal on L;

- the curvature of coordinate lines of the second and third sets is equal to zero at the points of their intersection with L;

- the coordinate surfaces $q^2 = \text{const}$ and $q^3 = \text{const}$ are "parallel" to the curve L in some neighbourhood of this curve.

Lemma 8.3. *If the conditions (8.39)–(8.41) are satisfied and the equation (8.6) is fulfilled in Ω up to the boundary edge L, then the equality (8.38) is fulfilled on L.*

L is the intersection of two surfaces $q^2 = 0$ and $q^3 = 0$, therefore it is possible to assume that their parametric equations (8.24) coincide on L and these equations have the following form at the points of L:

$$x^\alpha = f^\alpha(p), \qquad 0 \leq p \leq 1, \quad \alpha = 1, 2, 3. \tag{8.42}$$

This parametric equation of the curve L is used in the equation of the equidistribution method ("EDC3-equation"):

$$\frac{\partial}{\partial q^1}\left(w\sqrt{\left(\frac{\partial f^1}{\partial p}\right)^2 + \left(\frac{\partial f^2}{\partial p}\right)^2 + \left(\frac{\partial f^3}{\partial p}\right)^2}\,\frac{\partial p}{\partial q^1}\right) = 0, \tag{8.43}$$

which is obtained by the differentiation of the equality (8.38) with respect to the variable q^1. For the plane curve with the natural parameterization EDC3-equation changes over to EDC2-equation (4.50). If L is the straight segment, then ED1-equation (4.14) follows from (8.43).

We use the three-point difference equation for the approximation of (8.43):

$$D_{q^1}(\widetilde{w}D_{q^1}p)_{j_1} = 0, \quad j_1 = 2, \ldots, N_1 - 1, \tag{8.44}$$

where

$$\widetilde{w} = w(f^1(p), f^2(p), f^3(p))\sqrt{(D_p f^1)^2 + (D_p f^2)^2 + (D_p f^3)^2}.$$

The grid function $\widetilde{w}$ is defined in the half-integer nodes $p_{j_1+1/2}$ of the non-uniform grid p_{j_1}. The function $p(q)$ is defined in the integer nodes of the uniform grid $q^1_{j_1}$.

The nonlinear equation (8.44) is solved by the iterative method. The linear function is taken as the initial approximation for the function $p = p(q^1)$. In order to calculate the value of p on the $(\nu + 1)$-th iteration the values $\widetilde{w}_{j_1+1/2}$ from the ν-th iteration are used. If the iterative process converges, then the following equality is fulfilled for the limiting values of the node coordinates on L:

$$w_{j_1+1/2,1,1}|\mathbf{x}_{j_1+1,1,1} - \mathbf{x}_{j_1,1,1}| = \text{const}, \quad j_1 = 1, \ldots, N_1 - 1. \tag{8.45}$$

The parametric equation of the boundary is used only for constructing the grid. Realizing the calculations on the constructed curvilinear grid it is considered that the boundary, in particular L, is defined by the nodes of the grid, i.e. it is the polygonal line with the vertices in the nodes of the grid. For such a description of the boundary the equality (8.45) means cp that the product of the arc length of the boundary between the adjacent nodes and the control function w is constant, i.e. the grid satisfies the equidistribution principle on the curvilinear edge.

The method of constructing adaptive grids on the basis of the equation (8.43) is named "EDC3-method for space curves".

8.4 Algorithm of grid generation in three-dimensional domain

The main ideas of the chapter are formulated in the present section.

The grid in three-dimensional domain, i.e. in the curvilinear hexahedron, is constructed as follows. Firstly, the node coordinates on the edges of the hexahedron, i.e. on the space curves, are calculated with the help of EDC3-method. These coordinates are the boundary values for constructing the grid on the faces of the domain, i.e. on the space surfaces. The grid on the faces is constructed with the help of EDS-method and

Figure 8.5: The grid after 100 iterations with the control function $w = 1$

Figure 8.6: The grid after 100 iterations with the control function $w = 1 + 10(z + 1)$

the coordinates of its nodes are the boundary values for constructing the grid inside the domain with the help of ED3-method.

The grids in the plane domains are constructed with the help of ED2-method which is the special case of EDS-method. The grid on the boundaries of two-dimensional domains, i.e. on the plane curves, is constructed with the help of EDC2-method which is the special case of EDC3-method.

The grids on the straight segments are constructed with the help of ED1-method which is also the special case of EDC3-method.

8.5 Examples of grids

The examples of three-dimensional grids constructed with the help of the equidistribution method are presented in the following figures.

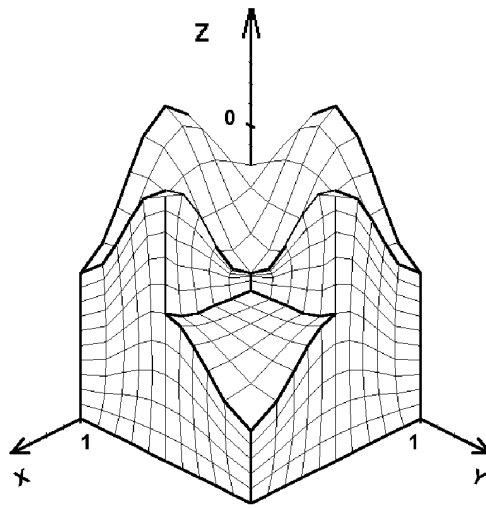Figures 8.5 and 8.7 show the grids which are constructed with the help of the control

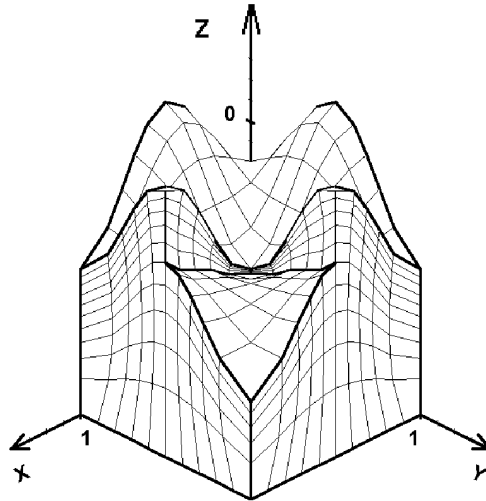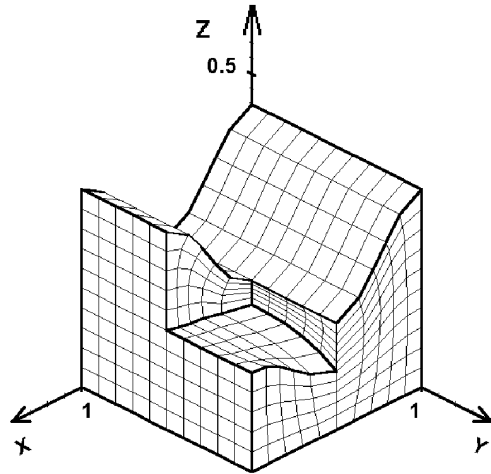Figure 8.7: The grid after 100 iterations with the control function $w = 1$
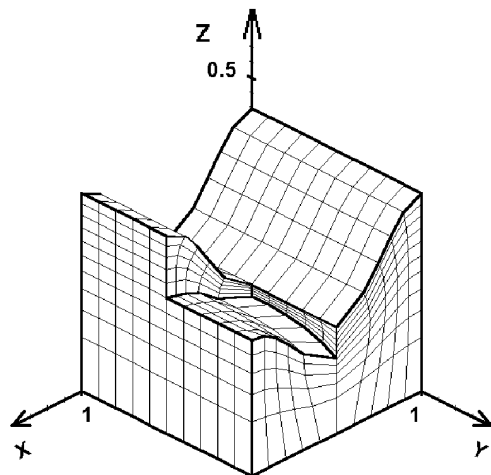
Figure 8.8: The grid after 100 iterations with the control function $w = 1 + 10(z + 1)$
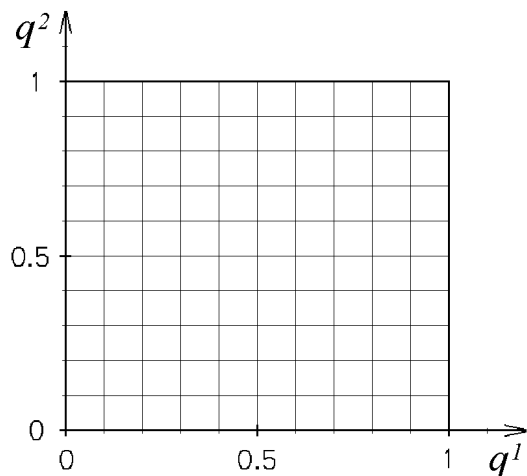
Figure 8.9: The stages of grid generation for the face $x = 0$ of the domain shown in Fig.8.6: the grid in the computational domaian
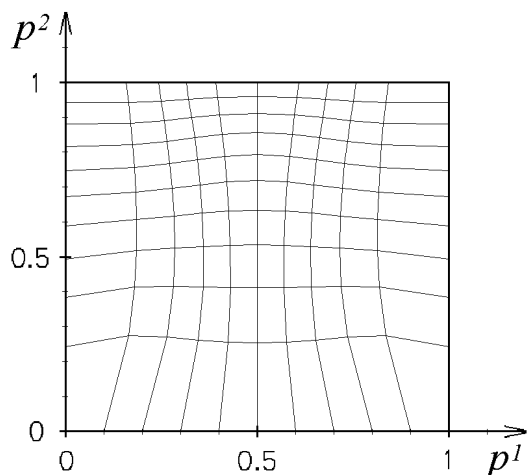
Figure 8.10: The stages of grid generation for the face $x = 0$ of the domain shown in Fig.8.6: the grid in the plane of the parameters

function $w = 1$.

Figures 8.6 and 8.8 show the grids which are constructed with the help of the control function $w = 1 + 10(z + 1)$. These control function leads to the condensation of the grid lines near the upper boundary of the domain.

The excisions are specially made in order to see the behaviour of grid lines inside the domains.

Figures 8.9, 8.10 and 8.11 present the stages of grid generation for the face $x = 0$ of the domain which is shown in Fig.8.6. The uniform grid in the computational domain is presented in Fig.8.9. The curvilinear grid in the plane of the parameters is shown in Fig.8.10. And Fig.8.11 presents the grid on the face $x = 0$ in the physical domain.

Figure 8.11: The stages of grid generation for the face $x = 0$ of the domain shown in Fig.8.6: the grid in the physical domain

Chapter 9

Finite-difference scheme and iterative process

9.1 Difference equations for the components of the vector potential

The grid functions are defined in the following nodes of the staggered grid (see Fig.9.1). The contravariant components of the velocity v^α are defined in the centres of the faces $q^\alpha = \mathrm{const}$, the components of the vector potential ψ^1, ψ^2 and ψ^3 are defined in the integer nodes $\mathbf{q}_j$, $j = (j_1, j_2, j_3)$ is the multi-index. The components of the vorticity vector ω^α are defined at the centres of the faces $q^2 = \mathrm{const}$. The components of the metric tensor $g^{\alpha\gamma}$, $g_{\alpha\gamma}$, $\alpha, \gamma = 1, 2, 3$, and the Jacobian – in the half-integer nodes $\mathbf{q}_{j_1+1/2, j_2+1/2, j_3+1/2}$. It is assumed that the covariant components of the vectors are defined at the same nodes as the contravariant components.
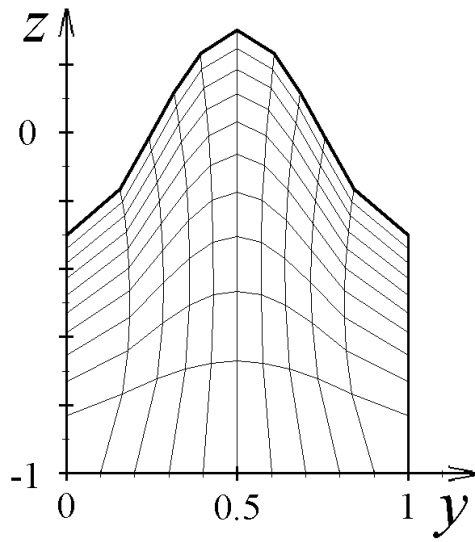
The difference equations for the components of $\vec{\psi}$ are obtained with the help of the integro-interpolational method by the approximation of the integrated relations which are the integrated analogues of the differential equations (7.27). For example, the integrated relation for the first component of the vector function $\vec{\psi}$ has the following form:

$$
\oint_{\mathcal{C}} Jg^{1\gamma}\frac{\partial \psi_1}{\partial q^\gamma}dq^2 dq^3 - Jg^{2\gamma}\frac{\partial \psi_1}{\partial q^\gamma}dq^1 dq^3 + Jg^{3\gamma}\frac{\partial \psi_1}{\partial q^\gamma}dq^1 dq^2 =
$$

$$
= \int\int_{D_{\mathcal{C}}}\int \left(-J\omega_1 + v_\alpha \varepsilon^{\alpha\mu\gamma}\frac{\partial g_{1\gamma}}{\partial q^\mu}\right)dq^1 dq^2 dq^3 + \tag{9.1}
$$

$$
+ \oint_{\mathcal{C}} Jg^{1\gamma}\frac{\partial \psi_\gamma}{\partial q^1}dq^2 dq^3 - Jg^{2\gamma}\frac{\partial \psi_\gamma}{\partial q^1}dq^1 dq^3 + Jg^{3\gamma}\frac{\partial \psi_\gamma}{\partial q^1}dq^1 dq^2.
$$

Obtaining the difference equations the surface of the parallelepiped $D_{\mathcal{C}}$ is taken as $\mathcal{C}$. The faces of this parallelepiped are perpendicular to the coordinate axes Oq^α and they are placed at the distance $h_\alpha/2$ from the considered node (see Fig.9.2).

We apply the three-dimensional analogue of the trapezoid formula to calculating the integrals in (9.1). For this analogue the integrand is substituted by the average value of
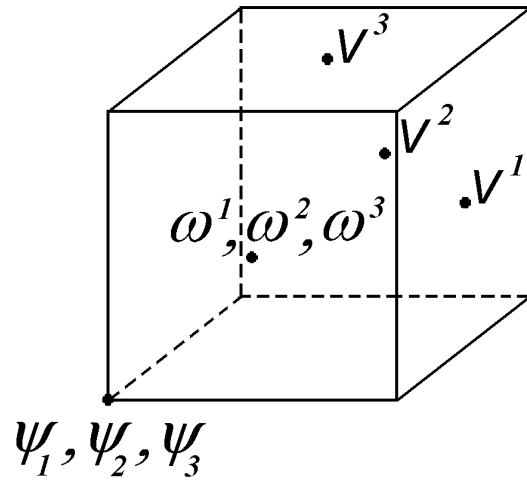
Figure 9.1: The grid nodes where the components of the velocity vector, the components of the vorticity vector and the components of the vector potential are defined
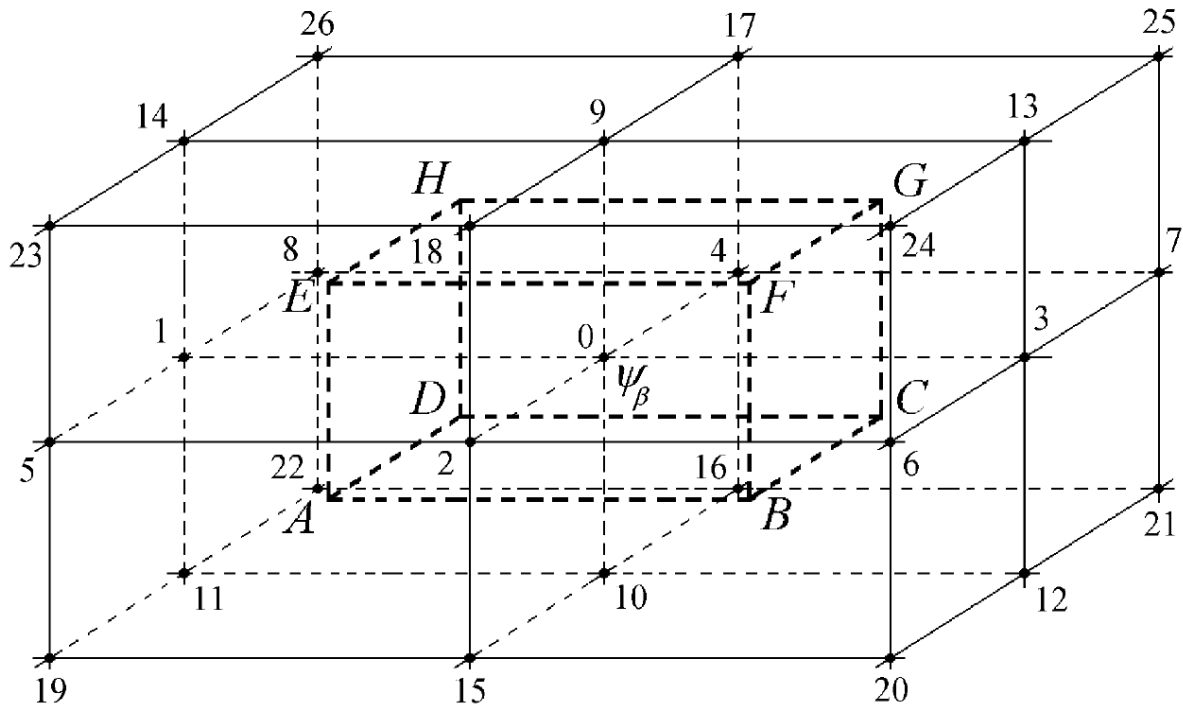
Figure 9.2: The surface of integration and the pattern of the difference equations for the components of the vector potential

the function in four vertexes of the rectangle. For example, on the left face $q^1 = q^1_{j_1-1/2}$ with the vertexes A, D, H, E this formula leads to the following approximation of the integral:

$$\int\int_{q^1=q^1_{j_1-1/2}} \Psi dq^2 dq^3 \sim \frac{h_2 h_3}{4}\left(\Psi_{j_1-1/2,j_2-1/2,j_3-1/2} + \Psi_{j_1-1/2,j_2+1/2,j_3-1/2}+\right.$$

$$\left.+\Psi_{j_1-1/2,j_2-1/2,j_3+1/2} + \Psi_{j_1-1/2,j_2+1/2,j_3+1/2}\right), \tag{9.2}$$

where

$$\Psi_{j_1-1/2,j_2\pm1/2,j_3\pm1/2} = \left(k_{11}D_{q^1}\psi_1 + k_{12}D_{q^2}\psi_1 + k_{13}D_{q^3}\psi_1\right)_{j_1-1/2,j_2\pm1/2,j_3\pm1/2}, \tag{9.3}$$

$$k_{\alpha\gamma} = Jg^{\alpha\gamma}, \tag{9.4}$$

D_{q^α} are the basis operators of the difference derivatives (8.7)–(8.9).

Using the formulas of the type (9.2) for each face of the rectangular parallelepiped D_C we obtain the 27-point difference equation for ψ_1:

$$\left(\sum_{k=0}^{26}\alpha_k\,(\psi_1)_k\right)_j = P_j, \tag{9.5}$$

P_j is the approximation of the right-hand side of the equation (9.1) in the node $\mathbf{q}_j$. The pattern of this equation is shown in Fig.9.2.

In the iterative process the right-hand side is obtained using the values which are calculated from the previous iteration. Therefore, the right-hand side does not contribute to the coefficients α_k which are calculated as follows:

$$\alpha_1 = \beta^1_A + \beta^1_D + \beta^1_E + \beta^1_H, \qquad \alpha_2 = \beta^2_A + \beta^2_B + \beta^2_E + \beta^2_F,$$

$$\alpha_3 = \beta^1_B + \beta^1_C + \beta^1_F + \beta^1_G, \qquad \alpha_4 = \beta^2_C + \beta^2_D + \beta^2_G + \beta^2_H,$$

$$\alpha_5 = -\beta^3_A - \beta^3_E, \qquad \alpha_6 = -\beta^3_B - \beta^3_F,$$

$$\alpha_7 = -\beta^3_C - \beta^3_G, \qquad \alpha_8 = -\beta^3_D - \beta^3_H,$$

$$\alpha_9 = \beta^3_E + \beta^3_F + \beta^3_G + \beta^3_H, \qquad \alpha_{10} = \beta^3_A + \beta^3_B + \beta^3_C + \beta^3_D,$$

$$\alpha_{11} = -\beta^2_A - \beta^2_D, \qquad \alpha_{12} = -\beta^2_B - \beta^2_C, \tag{9.6}$$

$$\alpha_{13} = -\beta^2_G - \beta^2_F, \qquad \alpha_{14} = -\beta^2_E - \beta^2_H,$$

$$\alpha_{15} = -\beta^1_A - \beta^1_B, \qquad \alpha_{16} = -\beta^1_C - \beta^1_D,$$

$$\alpha_{17} = -\beta^1_G - \beta^1_H, \qquad \alpha_{18} = -\beta^1_E - \beta^1_F,$$

91

$$\alpha_{19} = \beta_A, \qquad \alpha_{20} = \beta_B, \qquad \alpha_{21} = \beta_C, \qquad \alpha_{22} = \beta_D,$$

$$\alpha_{23} = \beta_E, \qquad \alpha_{24} = \beta_F, \qquad \alpha_{25} = \beta_G, \qquad \alpha_{26} = \beta_H,$$

$$\alpha_0 = -\sum_{k=1}^{26} \alpha_k,$$

where

$$\beta^\alpha = \frac{h_1 h_2 h_3}{16}\left(\frac{k_{\alpha\alpha}}{h_\alpha^2} - \sum_{m\neq\alpha,n\neq\alpha}^{1\div 3}\frac{(\sigma k)_{m,n}}{h_m h_n}\right), \qquad \alpha = 1,2,3,$$

$$\beta = \frac{h_1 h_2 h_3}{16}\sum_{m,n=1}^{3}\frac{(\sigma k)_{m,n}}{h_m h_n},$$

$$\sigma_{m,n} = sign(\sigma_m \sigma_n),$$

σ_α are determined by the shifts of the indices of the node $\mathbf{q}$ where β^α and β are calculated with respect to the node $\mathbf{q}_{j_1,j_2,j_3}$ which has the number "0" in the pattern. For example, for the node $\mathbf{q}_{j_1+1/2,j_2-1/2,j_3-1/2}$ coinciding with the point B in Fig.9.2 we have the following:

$$\sigma_1 = 1/2, \quad \sigma_2 = -1/2, \quad \sigma_3 = -1/2, \quad \sigma_{11} = \sigma_{22} = \sigma_{33} = 1,$$

$$\sigma_{12} = \sigma_{21} = -1, \quad \sigma_{13} = \sigma_{31} = -1, \quad \sigma_{23} = \sigma_{32} = 1.$$

The equation (9.5) with respect to $(\psi_1)_j$ is written in all interior nodes $\mathbf{q}_j$ ($j_\alpha = 2,\ldots,N_\alpha - 1$, $\alpha = 1,2,3$) of the cube Q. There are $N_0 = (N_1 - 2)\times(N_2 - 2)\times(N_3 - 2)$ equations, but the values of ψ_1 are unknown in the interior nodes and, as it will be shown below describing the boundary conditions, they are unknown in the nodes of the left and right boundaries of the domain Q. Therefore, the values of ψ_1 are unknown in $N_0 + 2\times(N_2 - 2)\times(N_3 - 2)$ nodes. Thus, it is necessary to write the additional difference equations for ψ_1 in the nodes of the faces $q^1 = 0$, $q^1 = 1$. The process of obtaining these difference equations is given below.

The difference equations for the second and third covariant components of the vector potential are obtained similarly. It is necessary to write the additional equations for the second component in the nodes of the front face $q^2 = 0$ and the back face $q^2 = 1$, and for the third component – in nodes of the lower face $q^3 = 0$ and the upper face $q^3 = 1$ of the domain Q.

9.2 Boundary conditions for the vector potential

The numerical realisation of the boundary conditions for the vector potential is considered for the problem on incompressible fluid flow in the curved duct of rectangular cross-section (see Fig.9.3).

The boundary Γ of the flow domain Ω consists of the inlet $\Gamma_1 = \{(x^1, 0, x^3) \mid 0 \leq x^1 \leq L_1, \ 0 \leq x^3 \leq L_3\}$; the outlet $\Gamma_2 = \{(x^1, 0, x^3) \mid L_1' \leq x^1 \leq L_1' + L_1, \ 0 \leq x^3 \leq L_3\}$ which
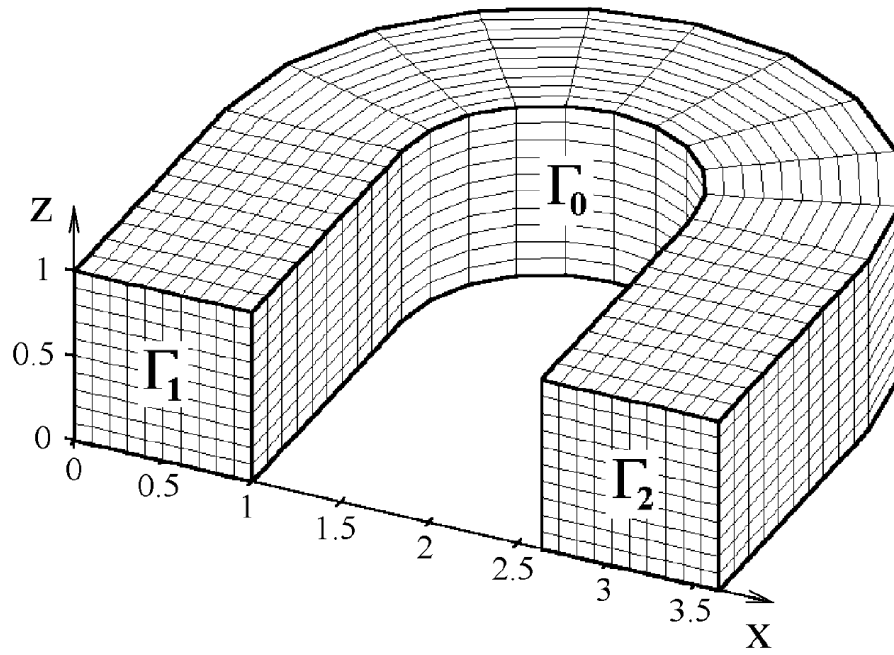
Figure 9.3: The duct with the stream bending by an angle of $180°$

are located in the plane $x^1 O x^3$, and the impermeable wall Γ_0 consisting of four parts: Γ_0^{top}, Γ_0^{bot}, Γ_0^{left}, Γ_0^{right}.

The walls Γ_0^{left} and Γ_0^{right} are the cylindrical surfaces. The forming lines of these surfaces are parallel to the axis $O x^3$. The directing lines consist of the straight segments which are parallel to the axis $O x^2$ for $0 \leq x^2 \leq L_2$ and of the arcs of the semicircles with the radii R^{left} and R^{right} respectively. $2 R^{left} = L_1' + L_1$, $2 R^{right} = L_1' - L_1$. It is assumed that the parts Γ_0^{bot} and Γ_0^{top} lie in the horizontal planes $x^3 = 0$ and $x^3 = L_3$ respectively.

Further for the sake of simplicity we shall use the following notations: $x^1 = x$, $x^2 = y$, $x^3 = z$.

We assume that the domain Ω is the image of the unit cube Q. Thus, the inlet Γ_1 is the image of the face $q^2 = 0$, the outlet Γ_2 is the image of the face $q^2 = 1$, and the impermeable parts of the boundary Γ_0^{left}, Γ_0^{right} Γ_0^{bot} and Γ_0^{top} are the images of the faces $q^1 = 0$, $q^1 = 1$, $q^3 = 0$ and $q^3 = 1$ respectively.

We assume that the fluid enters the domain Ω by the direction of the interior normal to the inlet Γ_1:

$$\vec{\nu}_1(\mathbf{x}) = (0, \ \nu_1(\mathbf{x}), \ 0), \quad \nu_1 \geq 0, \quad \mathbf{x} \in \Gamma_1. \tag{9.7}$$

Therefore, it follows from the assumption (9.7) that

$$v^2 = \frac{\partial q^2}{\partial y} \nu_1. \tag{9.8}$$

Thus, using the expressions (7.29) we obtain the following relation for the covariant components of the vector potential at the pre-image γ_1 of the inlet Γ_1:

$$\frac{\partial \psi_1}{\partial q^3} - \frac{\partial \psi_3}{\partial q^1} = \frac{\partial q^2}{\partial y} \nu_1. \tag{9.9}$$

For the definition of components ψ_1 and ψ_3 which are tangential to γ_1 we use the equality (9.9). We select the functions ψ_1 and ψ_3 so that this equality is satisfied. For example, it is possible to put

$$\psi_1(\mathbf{q}) \equiv 0, \quad \psi_3(\mathbf{q}) = -\int_0^{q^1} \frac{\partial q^2}{\partial y}\nu_1(\xi, 0, q^3)d\xi, \quad \mathbf{q} \in \gamma_1. \tag{9.10}$$

Let us consider the other parts of the boundary. The impermeability condition is written as $v^1 = 0$ at Γ_0^{left}, therefore the following equality must be fulfilled on it:

$$\frac{\partial \psi_3}{\partial q^2} - \frac{\partial \psi_2}{\partial q^3} = 0. \tag{9.11}$$

Thus, we assume that

$$\psi_2(\mathbf{q}) \equiv 0, \quad \psi_3(\mathbf{q}) \equiv 0, \quad \mathbf{q} \in \gamma_0^{left}. \tag{9.12}$$

Taking into account the formula (7.29) the impermeability condition $v^3 = 0$ at Γ_0^{bot} has the following form :

$$\frac{\partial \psi_2}{\partial q^1} - \frac{\partial \psi_1}{\partial q^2} = 0. \tag{9.13}$$

Using it we can assume the following:

$$\psi_1(\mathbf{q}) \equiv 0, \quad \psi_2(\mathbf{q}) \equiv 0, \quad \mathbf{q} \in \gamma_0^{bot}. \tag{9.14}$$

We obtain the following relations for two other impermeable faces:

$$\psi_2(\mathbf{q}) = \int_0^{q^3} F(\xi)d\xi, \quad \mathbf{q} \in \gamma_0^{right},$$

$$\psi_3(\mathbf{q}) = q^2 F(q^3) - \int_0^1 \frac{\partial q^2}{\partial y}\nu_1(\xi, 0, q^3)d\xi, \quad \mathbf{q} \in \gamma_0^{right}, \tag{9.15}$$

$$\psi_1(\mathbf{q}) \equiv 0, \quad \psi_2(\mathbf{q}) \equiv 0, \quad \mathbf{q} \in \gamma_0^{top}, \tag{9.16}$$

where

$$F(q^3) = \int_0^1 \frac{\partial q^2}{\partial y}\nu_1(\xi, 0, q^3)d\xi - \int_0^1 \frac{\partial q^2}{\partial y}\nu_2(\xi, 1, q^3)d\xi. \tag{9.17}$$

At the outlet Γ_2 the following connection between the tangential components of the vector potential is obtained from the boundary condition (7.3) and the formula (7.29):

$$\frac{\partial \psi_1}{\partial q^3} - \frac{\partial \psi_3}{\partial q^1} = \frac{\partial q^2}{\partial y}\nu_2, \quad \mathbf{q} \in \gamma_2. \tag{9.18}$$

Therefore, it is possible to put:

$$\psi_1(\mathbf{q}) \equiv 0, \quad \psi_3(\mathbf{q}) = -\int_0^{q^1} \frac{\partial q^2}{\partial y}\nu_2(\xi, 1, q^3)d\xi, \quad \mathbf{q} \in \gamma_2. \tag{9.19}$$

94

It is possible to write the solvability condition (7.5) in the following form:

$$\int_0^1 F(q^3)dq^3 = 0. \tag{9.20}$$

From here the continuity of the function $\psi_2(\mathbf{q})$ at the points $\mathbf{q} \in \gamma_0^{top} \cap \gamma_0^{right}$, and the continuity of function $\psi_3(\mathbf{q})$ at the points $\mathbf{q} \in \gamma_0^{right} \cap \gamma_2$ follow.

As it is mentioned above, it is necessary to the write the additional difference equations in the nodes of the faces. Let us consider the first component ψ_1 of the vector potential. The values of ψ_1 on the faces γ_1, γ_2, γ_0^{bot}, γ_0^{top} are given by the formulas (9.10), (9.19), (9.14), (9.16). And the values of ψ_1 on the faces γ_0^{left}, γ_0^{right} are unknown. Therefore, it is necessary to write the additional difference equations for ψ_1 in the nodes of these faces, i.e. in the nodes $\mathbf{q}_{j_1,j_2,j_3}$, where $j_1 = 1$ or $j_1 = N1$, $j_2 = 2, \ldots, N_2 - 1$, $j_3 = 2, \ldots, N_3 - 1$.

First of all, let us consider the simple case when $q^\alpha = x^\alpha$ ($\alpha = 1, 2, 3$) and the grid is rectangular and uniform. Then the equation (7.27) has the following form for ψ_1:

$$\frac{\partial^2 \psi_1}{\partial x^2} + \frac{\partial^2 \psi_1}{\partial y^2} + \frac{\partial^2 \psi_1}{\partial z^2} = -J\omega_1 + \frac{\partial}{\partial x}\left(\frac{\partial \psi_1}{\partial x}\right) + \frac{\partial}{\partial y}\left(\frac{\partial \psi_2}{\partial x}\right) + \frac{\partial}{\partial z}\left(\frac{\partial \psi_3}{\partial x}\right). \tag{9.21}$$

This equation can be written as follows:

$$\Delta \psi_1 = -J\omega_1 + \frac{\partial}{\partial x}\left(\operatorname{div} \vec{\psi}\right). \tag{9.22}$$

Usually on using $\vec{\psi}$ - $\vec{\omega}$ formulation it is assumed that

$$\operatorname{div} \vec{\psi} = 0. \tag{9.23}$$

Then the boundary condition on γ_0^{left} is obtained with the help of this additional assumption. Therefore, the condition has the following form:

$$\frac{\partial \psi_1}{\partial x}\Big|_{\mathbf{x} \in \gamma_0^{left}} = -\left(\frac{\partial \psi_2}{\partial y} + \frac{\partial \psi_3}{\partial z}\right)\Big|_{\mathbf{x} \in \gamma_0^{left}} \tag{9.24}$$

Using the given values ψ_2 and ψ_3 at γ_0^{left} it is possible to find the tangential derivatives of ψ_2 and ψ_3 with respect to y and z. Thus, it is possible to define the normal derivative $\frac{\partial \psi_1}{\partial x}$. This approach is used, for example, in the book [11].

In the present thesis the condition (9.23) is not used. We use the approximation of the equation (9.22) on the basis of the integrated relation (9.1). This relation has the following form for the case of Cartesian coordinates, the equation (9.22), and the integration surface which is shown in Fig.9.4:

$$\oint_{BCGF} \frac{\partial \psi_1}{\partial x}dydz - \oint_{ADHE} \frac{\partial \psi_1}{\partial x}dydz + \oint_{DCGH} \frac{\partial \psi_1}{\partial y}dxdz -$$

$$- \oint_{ABFE} \frac{\partial \psi_1}{\partial y}dxdz + \oint_{EFGH} \frac{\partial \psi_1}{\partial z}dxdy - \oint_{ABCD} \frac{\partial \psi_1}{\partial z}dxdy = \tag{9.25}$$

$$= -\int\int\int_{D_c} J\omega_1 dxdydz + \oint_{BCGF} \left(\frac{\partial \psi_1}{\partial x} + \frac{\partial \psi_2}{\partial y} + \frac{\partial \psi_3}{\partial z}\right)dydz -$$
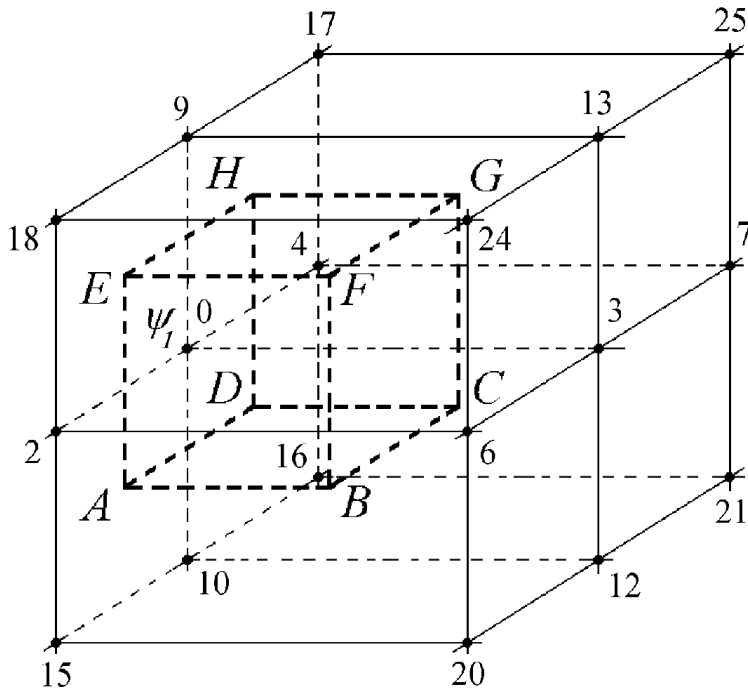
Figure 9.4: The surface of integration and the pattern of the difference equations for the first component of the vector potential on the left face

$$- \oint\limits_{ADHE} \left(\frac{\partial \psi_1}{\partial x} + \frac{\partial \psi_2}{\partial y} + \frac{\partial \psi_3}{\partial z} \right) dy dz.$$

In this relation it is possible to write the integral over $ADHE$ as follows:

$$\oint\limits_{ADHE} \left(\frac{\partial \psi_1}{\partial x} + \frac{\partial \psi_2}{\partial y} + \frac{\partial \psi_3}{\partial z} \right) dy dz = \oint\limits_{ADHE} \frac{\partial \psi_1}{\partial x} dy dz + \oint\limits_{ADHE} \left(\frac{\partial \psi_2}{\partial y} + \frac{\partial \psi_3}{\partial z} \right) dy dz.$$

$$(9.26)$$

Hence it is clear that the second item in the left-hand side of the equation (9.25) and the first item in the right part of the relation (9.26) are mutually cancelled. Thus, only the derivatives of the known components ψ_2 and ψ_3 are calculated on the face $ADHE$.

Actually, we obtained the boundary condition (9.24) without using the assumption (9.23). And it is possible to apply this approach in the case of curvilinear coordinates.

We wrote the equation (9.21) in the form (9.22), and now we write the equation (7.27) as follows:

$$\frac{\partial}{\partial q^1} \left(Jg^{1\gamma} \frac{\partial \psi_1}{\partial q^\gamma} \right) + \frac{\partial}{\partial q^2} \left(Jg^{2\gamma} \frac{\partial \psi_1}{\partial q^\gamma} \right) + \frac{\partial}{\partial q^3} \left(Jg^{3\gamma} \frac{\partial \psi_1}{\partial q^\gamma} \right) =$$

$$= -J\omega_1 + \frac{\partial}{\partial q^1} \left(Jg^{11} \frac{\partial \psi_1}{\partial q^1} + Jg^{12} \frac{\partial \psi_1}{\partial q^2} + Jg^{13} \frac{\partial \psi_1}{\partial q^3} \right) + \tag{9.27}$$

$$+\frac{\partial}{\partial q^1}\left(Jg^{12}\frac{\partial\psi_2}{\partial q^1}+Jg^{13}\frac{\partial\psi_3}{\partial q^1}\right)+\frac{\partial}{\partial q^2}\left(Jg^{22}\frac{\partial\psi_2}{\partial q^1}+Jg^{23}\frac{\partial\psi_3}{\partial q^1}\right)+$$

$$+\frac{\partial}{\partial q^3}\left(Jg^{32}\frac{\partial\psi_2}{\partial q^1}+Jg^{33}\frac{\partial\psi_3}{\partial q^1}\right)+\frac{\partial\psi_1}{\partial q^1}\left[\frac{\partial}{\partial q^2}\left(Jg^{12}\right)+\frac{\partial}{\partial q^3}\left(Jg^{13}\right)\right]-$$

$$-\frac{\partial\psi_1}{\partial q^2}\frac{\partial}{\partial q^1}\left(Jg^{12}\right)-\frac{\partial\psi_1}{\partial q^3}\frac{\partial}{\partial q^1}\left(Jg^{13}\right)+v_\alpha\varepsilon^{\alpha\mu\gamma}\frac{\partial g_{1\gamma}}{\partial q^\mu}.$$

Let us write the integrated relation for (9.27):

$$\oint_{BCGF}\left(Jg^{11}\frac{\partial\psi_1}{\partial q^1}+Jg^{12}\frac{\partial\psi_1}{\partial q^2}+Jg^{13}\frac{\partial\psi_1}{\partial q^3}\right)dq^2dq^3-$$

$$-\oint_{ADHE}\left(Jg^{11}\frac{\partial\psi_1}{\partial q^1}+Jg^{12}\frac{\partial\psi_1}{\partial q^2}+Jg^{13}\frac{\partial\psi_1}{\partial q^3}\right)dq^2dq^3+$$

$$\oint_{DCGH}\left(Jg^{21}\frac{\partial\psi_1}{\partial q^1}+Jg^{22}\frac{\partial\psi_1}{\partial q^2}+Jg^{23}\frac{\partial\psi_1}{\partial q^3}\right)dq^1dq^3-$$

$$-\oint_{ABFE}\left(Jg^{21}\frac{\partial\psi_1}{\partial q^1}+Jg^{22}\frac{\partial\psi_1}{\partial q^2}+Jg^{23}\frac{\partial\psi_1}{\partial q^3}\right)dq^1dq^3+$$

$$\oint_{EFGH}\left(Jg^{31}\frac{\partial\psi_1}{\partial q^1}+Jg^{32}\frac{\partial\psi_1}{\partial q^2}+Jg^{33}\frac{\partial\psi_1}{\partial q^3}\right)dq^1dq^2-$$

$$-\oint_{ABCD}\left(Jg^{31}\frac{\partial\psi_1}{\partial q^1}+Jg^{32}\frac{\partial\psi_1}{\partial q^2}+Jg^{33}\frac{\partial\psi_1}{\partial q^3}\right)dq^1dq^2=$$

$$=-\int\int_{D_c}\int J\omega_1 dq^1dq^2dq^3+ \tag{9.28}$$

$$+\oint_{BCGF}\left(Jg^{11}\frac{\partial\psi_1}{\partial q^1}+Jg^{12}\frac{\partial\psi_1}{\partial q^2}+Jg^{13}\frac{\partial\psi_1}{\partial q^3}\right)dq^2dq^3-$$

$$-\oint_{ADHE}\left(Jg^{11}\frac{\partial\psi_1}{\partial q^1}+Jg^{12}\frac{\partial\psi_1}{\partial q^2}+Jg^{13}\frac{\partial\psi_1}{\partial q^3}\right)dq^2dq^3+$$

$$+\oint_{BCGF}\left(Jg^{12}\frac{\partial\psi_2}{\partial q^1}+Jg^{13}\frac{\partial\psi_3}{\partial q^1}\right)dq^2dq^3-$$

$$-\oint_{ADHE} \left(Jg^{12}\frac{\partial\psi_2}{\partial q^1} + Jg^{13}\frac{\partial\psi_3}{\partial q^1}\right) dq^2 dq^3 +$$

$$+\oint_{DCGH} \left(Jg^{22}\frac{\partial\psi_2}{\partial q^1} + Jg^{23}\frac{\partial\psi_3}{\partial q^1}\right) dq^1 dq^3 -$$

$$-\oint_{ABFE} \left(Jg^{22}\frac{\partial\psi_2}{\partial q^1} + Jg^{23}\frac{\partial\psi_3}{\partial q^1}\right) dq^1 dq^3 +$$

$$+\oint_{EFGH} \left(Jg^{32}\frac{\partial\psi_2}{\partial q^1} + Jg^{33}\frac{\partial\psi_3}{\partial q^1}\right) dq^1 dq^2 -$$

$$-\oint_{ABCD} \left(Jg^{32}\frac{\partial\psi_2}{\partial q^1} + Jg^{33}\frac{\partial\psi_3}{\partial q^1}\right) dq^1 dq^2 +$$

$$+\int\int_{D_C}\int \left[\frac{\partial\psi_1}{\partial q^1}\left(\frac{\partial}{\partial q^2}(Jg^{12}) + \frac{\partial}{\partial q^3}(Jg^{13})\right) - \right.$$

$$\left. -\frac{\partial\psi_1}{\partial q^2}\frac{\partial}{\partial q^1}(Jg^{12}) - \frac{\partial\psi_1}{\partial q^3}\frac{\partial}{\partial q^1}(Jg^{13}) + v_\alpha\varepsilon^{\alpha\mu\gamma}\frac{\partial g_{1\gamma}}{\partial q^\mu}\right] dq^1 dq^2 dq^3.$$

It is clear that the second item in the left-hand side is reduced with the third item in the right-hand side. Therefore, only the known components ψ_2 and ψ_3 are used on the face $ADHE$. On carrying out the approximation on the faces $DCGH$, $ABFE$, $EFGH$, $ABCD$ the integrands are calculated in the interior nodes B, C, G, F. For example,

$$\oint_{DCGH} \Psi dq^1 dq^3 \sim \frac{h_1 h_3}{4}(\Psi_C + \Psi_G), \tag{9.29}$$

where

$$\Psi_{C,G} = (k_{21}D_{q^1}\psi_1 + k_{22}D_{q^2}\psi_1 + k_{23}D_{q^3}\psi_1)_{C,G}.$$

The integral over the face $BCGF$ is approximated in the same way as for the equations in the interior nodes.

Thus, we obtain the 18-point difference equations for the nodes $\mathbf{q}_{1,j_2,j_3}$, $j_2 = 2, \ldots, N_2 - 1$, $j_3 = 2, \ldots, N_3 - 1$:

$$\left(\sum_k \alpha_k (\psi_1)_k\right)_j = P_j^{left}, \tag{9.30}$$

where P_j^{left} is the approximation of the right-hand side of the equation (9.28) taking into account the reductions of some items.

The coefficients α_k have the following form:

$$\alpha_1 = 0, \qquad\qquad \alpha_2 = \beta_B^2 + \beta_F^2,$$

$$\alpha_3 = \beta_B^1 + \beta_C^1 + \beta_F^1 + \beta_G^1, \qquad \alpha_4 = \beta_C^2 + \beta_G^2,$$

$$\alpha_5 = 0, \qquad\qquad \alpha_6 = -\beta_B^3 - \beta_F^3,$$

$$\alpha_7 = -\beta_C^3 - \beta_G^3, \qquad\qquad \alpha_8 = 0,$$

$$\alpha_9 = \beta_F^3 + \beta_G^3, \qquad\qquad \alpha_{10} = \beta_B^3 + \beta_C^3,$$

$$\alpha_{11} = 0, \qquad\qquad \alpha_{12} = -\beta_B^2 - \beta_C^2, \qquad\qquad (9.31)$$

$$\alpha_{13} = -\beta_G^2 - \beta_F^2, \qquad\qquad \alpha_{14} = 0,$$

$$\alpha_{15} = \beta_B^1, \qquad\qquad \alpha_{16} = -\beta_C^1,$$

$$\alpha_{17} = -\beta_G^1, \qquad\qquad \alpha_{18} = \beta_F^1,$$

$$\alpha_{19} = 0, \quad \alpha_{20} = \beta_B, \qquad \alpha_{21} = \beta_C, \quad \alpha_{22} = 0,$$

$$\alpha_{23} = 0, \quad \alpha_{24} = \beta_F, \qquad \alpha_{25} = \beta_G, \quad \alpha_{26} = 0,$$

$$\alpha_0 = -\sum_{k=1}^{26} \alpha_k,$$

where β^α and β are described above.

If we put β^α and β equal to zero at the points A, D, H, E, then the coefficients of the equation (9.30) are obtained from the coefficients of the equation (9.5).

The similar connection takes place between the coefficients of the equation (9.5) and the coefficients of the difference equations for the nodes of the right face $q^1 = 1$ of the domain Q. In this case $\beta^\alpha = 0$ and $\beta = 0$ at the points B, C, G, F.

The additional difference equations for ψ_2 in the nodes of the front and back faces, and the additional difference equations for ψ_3 in the nodes of the lower and upper faces are obtained in the same way as the difference equations for ψ_1 in the nodes of the left and right faces.

The obtained systems of difference equations for the components of the vector potential ψ_α are solved by the method of successive over relaxation.

9.3 Difference equations for the components of the vorticity vector

Now we shall describe the algorithm of calculating the vorticity vector. We assume that the following condition is fulfilled everywhere in the domain Ω:

$$v^2 > 0, \tag{9.32}$$

and the components v^1, v^3 can be alternating. From the physical point of view it means that the primary direction of fluid flow is the direction along the axis of the channel with possible rotation of the fluid partiles around this axis. The mathematical implication is that the condition (9.32) leads, as it will be shown below, to the hyperbolicity of the system of equations with respect to the components of the vorticity vector. There are well known effective methods for solving the hyperbolic systems [48].

In Chapter 3 in solving two-dimensional problem on gas flow the equation for the vorticity function (3.3) is of hyperbolic type. Therefore, the reliable and effective generalized method of running calculation is used for its solution. In three-dimensional problem it is hard to define the type of the equations for the components of the vorticity vector written in the form (7.28). Therefore, we write them in a different form:

$$\frac{\partial}{\partial q^\alpha}\left(Jv^\alpha\omega^\beta\right) = J\omega^\alpha\frac{\partial v^\beta}{\partial q^\alpha} \equiv f^\beta, \quad \beta = 1, 2, 3. \tag{9.33}$$

Here the condition (7.31) is used. These equations have the following vector form:

$$\frac{\partial}{\partial q^2}\left(Jv^2\vec{\omega}\right) + \frac{\partial}{\partial q^1}\left(Jv^1\vec{\omega}\right) + \frac{\partial}{\partial q^3}\left(Jv^3\vec{\omega}\right) = \mathbf{f}. \tag{9.34}$$

We have written the derivative with respect to q^2 as the first term in the given equation in order to emphasize that q^2 plays the role of the time-like variable.

The continuity equation has the following form in curvilinear coordinates:

$$\frac{\partial}{\partial q^1}\left(Jv^1\right) + \frac{\partial}{\partial q^2}\left(Jv^2\right) + \frac{\partial}{\partial q^3}\left(Jv^3\right) = 0. \tag{9.35}$$

On using it, the equation (9.34) can be written in non-divergent form:

$$Jv^2\frac{\partial\vec{\omega}}{\partial q^2} + Jv^1\frac{\partial\vec{\omega}}{\partial q^1} + Jv^3\frac{\partial\vec{\omega}}{\partial q^3} = \mathbf{f}. \tag{9.36}$$

If the right-hand side $\mathbf{f}$ is considered as the known function of q^1, q^2, q^3, then when the condition (9.32) is fulfilled the obtained vector equation represents the system of three scalar equations of hyperbolic type with respect to the components of the vector $\vec{\omega}$. We use the implicit method "predictor-corrector" by S.K. Godunov [48] for its solution.

At the first step "predictor" the implicit splitting scheme is used for approximation of the equation (9.36). With the help of this scheme the auxiliary value $\vec{\omega}^*$ is calculated on the faces $q^1 = q^1_{j_1}$ and $q^3 = q^3_{j_3}$. Let us present the derivation of the splitting scheme for the face $q^1 = q^1_{j_1}$. The following equation is approximated on this face:

$$Jv^2\frac{\partial\vec{\omega}}{\partial q^2} + Jv^1\frac{\partial\vec{\omega}}{\partial q^1} = \mathbf{f}. \tag{9.37}$$

Taking into account the definition area of the grid vector function $\vec{\omega}$ we obtain the following form of the scheme:

$$\left(Jv^2\right)_{j_1,j_2,j_3+1/2} \cdot \frac{\vec{\omega}^*_{j_1,j_2+1/2,j_3+1/2} - \frac{1}{2}\left(\vec{\omega}_{j_1+1/2,j_2,j_3+1/2} + \vec{\omega}_{j_1-1/2,j_2,j_3+1/2}\right)}{h_2^*} +$$

$$+ \left(Jv^1\right)_{j_1,j_2,j_3+1/2} \cdot \frac{\vec{\omega}^*_{j_1+1/2,j_2+1/2,j_3+1/2} - \vec{\omega}^*_{j_1-1/2,j_2+1/2,j_3+1/2}}{h_1} = \mathbf{f}_{j_1,j_2,j_3+1/2}, \qquad (9.38)$$

where $h_2^* = \frac{h_2}{2}\left(1 + \theta\right))$, $\theta \geq 0$. $\vec{\omega}^*_{j_1+1/2,j_2+1/2,j_3+1/2}$ is the auxiliary value defined by the following implicit formula:

$$\left(Jv^2\right)_{j_1+1/2,j_2,j_3+1/2} \cdot \frac{\vec{\omega}^*_{j_1+1/2,j_2+1/2,j_3+1/2} - \vec{\omega}_{j_1+1/2,j_2,j_3+1/2}}{h_2^*} +$$

$$+ \left(Jv^1\right)_{j_1+1/2,j_2,j_3+1/2} \cdot \frac{\vec{\omega}^*_{j_1+1,j_2+1/2,j_3+1/2} - \vec{\omega}^*_{j_1,j_2+1/2,j_3+1/2}}{h_1} = \mathbf{f}_{j_1,j_2,j_3+1/2}. \qquad (9.39)$$

Substituting the values $\vec{\omega}^*_{j_1+1/2,j_2+1/2,j_3+1/2}$ and $\vec{\omega}^*_{j_1-1/2,j_2+1/2,j_3+1/2}$ which are calculated with the help of (9.39) into the formula (9.38) we obtain the splitting scheme for the face $q^1 = q^1_{j_1}$:

$$\left(Jv^2\right)_{j_1,j_2,j_3+1/2} \cdot \frac{\vec{\omega}^*_{j_1,j_2+1/2,j_3+1/2} - \frac{1}{2}\left(\vec{\omega}_{j_1+1/2,j_2,j_3+1/2} + \vec{\omega}_{j_1-1/2,j_2,j_3+1/2}\right)}{h_2^*} +$$

$$+ \left(Jv^1\right)_{j_1,j_2,j_3+1/2} \cdot \frac{\vec{\omega}_{j_1+1/2,j_2,j_3+1/2} - \vec{\omega}_{j_1-1/2,j_2,j_3+1/2}}{h_1} -$$

$$- \frac{h_2^*}{h_1}\left(Jv^1\right)_{j_1,j_2,j_3+1/2} \cdot \left[\left(\frac{v^1}{v^2}\right)_{j_1+1/2,j_2,j_3+1/2} \cdot \frac{\vec{\omega}^*_{j_1+1,j_2+1/2,j_3+1/2} - \vec{\omega}^*_{j_1,j_2+1/2,j_3+1/2}}{h_1} -\right.$$

$$\left. - \left(\frac{v^1}{v^2}\right)_{j_1-1/2,j_2,j_3+1/2} \cdot \frac{\vec{\omega}^*_{j_1,j_2+1/2,j_3+1/2} - \vec{\omega}^*_{j_1-1,j_2+1/2,j_3+1/2}}{h_1}\right]$$

$$= \mathbf{f}_{j_1,j_2,j_3+1/2}, \qquad (9.40)$$

$$j_1 = 2, ..., N_1 - 1; \ \ j_2 = 1, ..., N_2 - 1; \ \ j_3 = 1, ..., N_3 - 1.$$

On the face $q^3 = q^3_{j_3}$ the value $\vec{\omega}^*$ is calculated on the basis of similar splitting scheme obtained by approximation of the following equation:

$$Jv^2\frac{\partial\vec{\omega}}{\partial q^2} + Jv^3\frac{\partial\vec{\omega}}{\partial q^3} = \mathbf{f}. \qquad (9.41)$$

This scheme has the form:

$$\left(Jv^2\right)_{j_1+1/2,j_2,j_3} \cdot \frac{\vec{\omega}^*_{j_1+1/2,j_2+1/2,j_3} - \frac{1}{2}\left(\vec{\omega}_{j_1+1/2,j_2,j_3+1/2} + \vec{\omega}_{j_1+1/2,j_2,j_3-1/2}\right)}{h_2^*} +$$

$$+ \left(Jv^3\right)_{j_1+1/2,j_2,j_3} \cdot \frac{\vec{\omega}_{j_1+1/2,j_2,j_3+1/2} - \vec{\omega}_{j_1+1/2,j_2,j_3-1/2}}{h_3} -$$

$$-\frac{h_2^*}{h_3}\left(Jv^3\right)_{j_1+1/2,j_2,j_3} \cdot \left[\left(\frac{v^3}{v^2}\right)_{j_1+1/2,j_2,j_3+1/2} \cdot \frac{\vec{\omega}^*_{j_1+1/2,j_2+1/2,j_3+1} - \vec{\omega}^*_{j_1+1/2,j_2+1/2,j_3}}{h_3} -\right.$$

$$\left. - \left(\frac{v^3}{v^2}\right)_{j_1+1/2,j_2,j_3-1/2} \cdot \frac{\vec{\omega}^*_{j_1+1/2,j_2+1/2,j_3} - \vec{\omega}^*_{j_1+1/2,j_2+1/2,j_3-1}}{h_3}\right]$$

$$= \mathbf{f}_{j_1+1/2,j_2,j_3}, \qquad (9.42)$$

$$j_1 = 1, ..., N_1 - 1; \; j_2 = 1, ..., N_2 - 1; \; j_3 = 2, ..., N_3 - 1.$$

Therefore, the auxiliary value $\vec{\omega}^*$ is calculated on the faces $q^1 = q^1_{j_1}$ and $q^3 = q^3_{j_3}$ at the step "predictor". After that the value of the vorticity vector $\vec{\omega}$ is calculated at the next level on q^2 at the step "corrector". The following explicit approximation of the equation (9.34) is used for this purpose:

$$\frac{\left(Jv^2\vec{\omega}\right)_{j_1+1/2,j_2+1,j_3+1/2} - \left(Jv^2\vec{\omega}\right)_{j_1+1/2,j_2,j_3+1/2}}{h_2} +$$

$$+\frac{\left(Jv^1\vec{\omega}^*\right)_{j_1+1,j_2+1/2,j_3+1/2} - \left(Jv^1\vec{\omega}^*\right)_{j_1,j_2+1/2,j_3+1/2}}{h_1} + \qquad (9.43)$$

$$+\frac{\left(Jv^3\vec{\omega}^*\right)_{j_1+1/2,j_2+1/2,j_3+1} - \left(Jv^3\vec{\omega}^*\right)_{j_1+1/2,j_2+1/2,j_3}}{h_3} = \mathbf{f}_{j_1+1/2,j_2+1/2,j_3+1/2},$$

$$j_1 = 1, ..., N_1 - 1; \; j_2 = 1, ..., N_2 - 1; \; j_3 = 1, ..., N_3 - 1.$$

Let us describe the order of solving the obtained difference equations (9.40), (9.42), (9.43). The equations (9.40), (9.42) are the three-point formulas and it is possible to use the sweep method for their solution. For the equation (9.40) the sweep is carried out in q^1-direction at fixed $j_3 = 1, ..., N_3 - 1$. For the equation (9.42) the sweep is carried out in q^3-direction at fixed $j_1 = 1..., N_1 - 1$. For the realisation of the sweeps it is necessary to supplement the equations (9.40), (9.42) by the equations for the boundary nodes on the impermeable walls.

Let us show how the difference equations are constructed, for example, for the face $q^1 = 0$. We apply the splitting method to the equation for the vorticity vector in divergent form (9.34). Thus, we approximate the following equation in the boundary node:

$$\frac{\partial}{\partial q^2}\left(Jv^2\vec{\omega}\right) + \frac{\partial}{\partial q^1}\left(Jv^1\vec{\omega}\right) = \mathbf{f}. \qquad (9.44)$$

Taking into account the impermeability condition $v^1 = 0$ on the face $q^1 = 0$ we obtain the following implicit approximation of this equation:

$$\frac{1}{h_2^*} \left\{ \frac{1}{2} \left[\left(Jv^2\vec{\omega}^* \right)_{j_1+1,j_2+1/2,j_3+1/2} + \left(Jv^2\vec{\omega}^* \right)_{j_1,j_2+1/2,j_3+1/2} \right] - \right.$$

$$\left. - \left(Jv^2\vec{\omega} \right)_{j_1+1/2,j_2,j_3+1/2} \right\} + \frac{1}{h_1} \left(Jv^1\vec{\omega}^* \right)_{j_1+1,j_2+1/2,j_3+1/2} = \mathbf{f}_{j_1+1/2,j_2,j_3+1/2}, \quad (9.45)$$

$$j_1 = 1; \ j_2 = 1, ..., N_2 - 1; \ j_3 = 1, ..., N_3 - 1.$$

Writing the similar equation at $j_1 = N_1$ we close the system of equations (9.40) and, therefore, we can apply the sweep method.

Similarly, using the impermeability condition $v^3 = 0$ on the faces $q^3 = 0$, $q^3 = 1$ we obtain the boundary conditions for applying the sweep method in q^3-direction.

The application of the sweep method is correct because the obtained difference equations have the property of diagonal predominance.

The boundary values of $\vec{\omega}^*$ on the impermeable walls are used only at the step "predictor" for the realisation of the sweeps. It follows from the formula (9.43) that the boundary values of $\vec{\omega}^*$ are not required at the step "corrector" by virtue of the impermeability condition.

9.4   Boundary conditions for the vorticity vector at the inlet

The vorticity vector is calculated by the marching method, i.e. from one level in q^2-direction to another level. Therefore, the boundary values for the components of the vorticity vector are required at the inlet for the beginning of calculation. Thus, using the given algorithm for solving three-dimensional problem, as for solving two-dimensional problem, we need to calculate the vorticity vector at the inlet of the domain. There are no boundary values for the vorticity vector in the initial statement of the problem. We calculate them using the boundary conditions (7.3) and the obtained values of the vector potential inside the domain. The following formulas are used for calculating $\vec{\omega}$ on γ_1:

$$\left(J\omega^1 \right)_{j_1+1/2,j_2,j_3+1/2} = \frac{(v_3)_{j_1+1/2,j_2+1/2,j_3+1/2} - (v_3)_{j_1+1/2,j_2,j_3+1/2}}{h_2/2} -$$

$$- \frac{(v_2)_{j_1+1/2,j_2,j_3+1} - (v_2)_{j_1+1/2,j_2,j_3}}{h_3},$$

$$\left(J\omega^2 \right)_{j_1+1/2,j_2,j_3+1/2} = \frac{(v_1)_{j_1+1/2,j_2,j_3+1} - (v_1)_{j_1+1/2,j_2,j_3}}{h_3} - \quad (9.46)$$

$$- \frac{(v_3)_{j_1+1,j_2,j_3+1/2} - (v_3)_{j_1,j_2,j_3+1/2}}{h_1},$$

$$\left(J\omega^3\right)_{j_1+1/2,j_2,j_3+1/2} = \frac{(v_2)_{j_1+1,j_2,j_3+1/2} - (v_2)_{j_1,j_2,j_3+1/2}}{h_1} -$$

$$-\frac{(v_1)_{j_1+1/2,j_2+1/2,j_3+1/2} - (v_1)_{j_1+1/2,j_2,j_3+1/2}}{h_2/2}.$$

$$j_1 = 1, ..., N_1 - 1; \quad j_2 = 1; \quad j_3 = 1, ..., N_3 - 1.$$

These formulas include the values of the covariant components of the velocity at the inlet and at the centres of the mesh adjacent to the inlet. The values at the centres of the mesh $(v_\alpha)_{j_1+1/2,j_2+1/2,j_3+1/2}$, $\alpha = 1, 3$, are calculated using the contravariant components of the velocity by the formulas (7.30). The contravariant components of the velocity are obtained with the help of the finite difference analogues of the formulas (7.29) using the components of the vector potential:

$$\left(Jv^1\right)_{j_1,j_2+1/2,j_3+1/2} = (D_{q^2}\psi_3 - D_{q^3}\psi_2)_{j_1,j_2+1/2,j_3+1/2},$$

$$\left(Jv^2\right)_{j_1+1/2,j_2,j_3+1/2} = (D_{q^3}\psi_1 - D_{q^1}\psi_3)_{j_1+1/2,j_2,j_3+1/2}, \tag{9.47}$$

$$\left(Jv^3\right)_{j_1+1/2,j_2+1/2,j_3} = (D_{q^1}\psi_2 - D_{q^2}\psi_1)_{j_1+1/2,j_2+1/2,j_3},$$

where D_{q^α} are the basis difference operators (8.7)–(8.9).

In addition, the formulas (9.46) include the covariant components of the velocity at the inlet. They are calculated using the boundary conditions (7.3):

$$v_\alpha = \frac{\partial x^1}{\partial q^\alpha}u_1 + \frac{\partial x^2}{\partial q^\alpha}u_2 + \frac{\partial x^3}{\partial q^\alpha}u_3. \tag{9.48}$$

In particular, for the problem on the flow in the duct described above these formulas have the following form:

$$v_1 = 0, \qquad v_2 = \frac{\partial x^2}{\partial q^\alpha}v_1, \qquad v_3 = 0. \tag{9.49}$$

It follows from the formulas (9.46) that the component ω^2 of the vorticity vector does not depend on the interior values of the vector potential $\vec{\psi}$. Therefore, the value of ω^2 is completely defined by the given boundary conditions (7.3). This component does not vary from the iteration to iteration. In particular, under the conditions (9.7) we obtain $\omega^2 \equiv 0$. The component ω^1 and ω^3 tangential to the inlet vary during the iterative process because they depend on the interior values of $\vec{\psi}$.

In the case of Cartesian coordinates, the rectangular uniform grid, and $u_3 = 0$ (i.e. in the case of two-dimensional flow) the conditions (9.46) change over to the analogue of the known Thom formula [148].

9.5 Iterative process

Let us describe the global iterative process for solving three-dimensional problem on the ideal incompressible fluid flow. As in the two-dimensional case the process begins by the calculation of the potential fluid flow at $\vec{\omega} \equiv 0$. For this purpose the difference equations of the type (9.5) for ψ_1, ψ_2, ψ_3 are solved. The boundary values for the tangential covariant components of $\vec{\psi}$ are given before the beginning of the iterative process. These values do not vary during the iterations. The normal covariant components of $\vec{\psi}$ are calculated on each iteration. The procedure of calculation is described in Section 9.2.

The iterations are carried out for all three components of $\vec{\psi}$ at once. The following condition for the termination of the iteratitions is used:

$$||\psi_\alpha^{n+1} - \psi_\alpha^n||_{L_1} < \varepsilon_\psi, \quad \alpha = 1, 2, 3, \tag{9.50}$$

where n is the number of iteration, $\varepsilon_\psi > 0$ is the given exactitude of calculations.

The obtained solution of the problem on the potential ideal incompressible fluid flow is the initial approximation for the solution of the problem on the vortical fluid flow.

Let $\vec{\psi}^n$, $\vec{\omega}^n$ be the n-th iterative approximation. The process of obtaining the $(n+1)$-th approximation is divided into the following three steps.

1. The equations of the type (9.5) for ψ_1, ψ_2, ψ_3 are solved by the SOR-method where the values $\vec{\omega}^n$, $\vec{\psi}^n$ in the right-hand side are taken from the n-th iteration.

2. The values of the components of the vorticity vector at the inlet of the domain are calculated using the formulas (9.46). The obtained values of $\vec{\psi}^{n+1}$ are used for the definition of the covariant components of the velocity at the centres of the meshes adjacent to the boundary. The boundary conditions (7.3) are used for calculating the covariant components of the velocity at the inlet.

Similarly to the iterative process for the two-dimensional problem considered in Section 5.6 the relaxation procedure (5.24) is used.

3. The values $\vec{\omega}^{n+1}$ are calculated using the marching method inside the domain and also at the outlet γ_2. The right-hand side $\mathbf{f}$ in the equations (9.40), 9.42), (9.43) is taken from the n-th iteration.

The iterative process proceeds up to the realisation of the given condition of the termination of iterations:

$$||\omega_\alpha^{n+1} - \omega_\alpha^n||_{L_1} < \varepsilon_\omega, \quad \alpha = 1, 2, 3. \tag{9.51}$$

The finite difference analogue of the continuity equation (9.35) is fulfilled on each step of this iterative process within the round-off errors:

$$\left(D_{q^1}\left(Jv^1 \right) + D_{q^2}\left(Jv^2 \right) + D_{q^3}\left(Jv^3 \right) \right)_{j_1+1/2, j_2+1/2, j_3+1/2} = 0,$$

$$j_\alpha = 1, ..., N_\alpha - 1, \quad \alpha = 1, 2, 3. \tag{9.52}$$

Chapter 10

Results of the calculations of three-dimensional steady ideal fluid flows

10.1 Results of the calculations of the flow in the parallelepiped

In this chapter the calculation results of the series of three-dimensional problems are presented.

The first series of calculations is carried out for the domain of a simple form, i.e. for a parallelepiped with the faces parallel to the coordinate planes of Cartesian system of coordinates. The rectangular uniform grids are used.

In the case of the uniform fluid inflow (the function $\nu_1(\mathbf{x})$ from (9.7) is set equal to a constant) the flow is potential. The iterative process is converged after one iteration because the initial approximation already satisfies the difference equations.

In the second test the following functions $\nu_1(\mathbf{x})$ and $\nu_2(\mathbf{x})$ from (7.3) are taken:

$$\nu_1(\mathbf{x}) = \alpha + \beta z, \quad \nu_2(\mathbf{x}) = \nu_1(\mathbf{x}), \tag{10.1}$$

where α and β are some constants.

The problem with such boundary conditions has the following exact solution:

$$u_1 = 0, \quad u_2 = \alpha + \beta z, \quad u_3 = 0,$$

$$\psi_1 = 0, \quad \psi_2 = 0, \quad \psi_3 = -x \cdot \nu_1, \tag{10.2}$$

$$\omega_1 = -\beta, \quad \omega_2 = 0, \quad \omega_3 = 0.$$

This solution satisfies the equations (7.1), (7.22), (7.23). In this case the flow is vortical, therefore, some iterations are necessary.

The calculations show that the convergence speed of the iterative process is essentially influenced by the value of the parameter δ_ω in the relaxation procedure of calculating the boundary values of $\vec{\omega}$ at the inlet Γ_1.
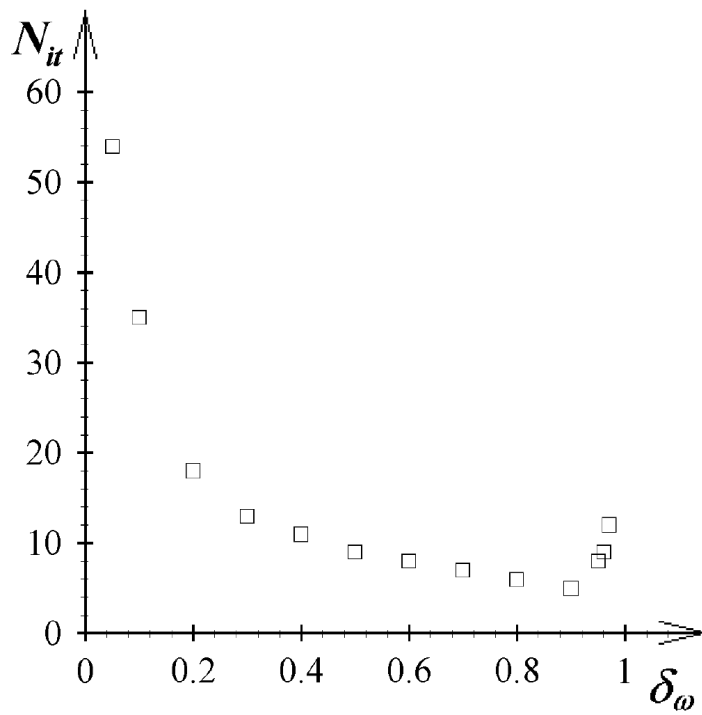
Figure 10.1: The dependence of the total number N_{it} of iterations in the global iterative process on the relaxation parameter δ_ω

Fig.10.1 shows the dependence of the total number of iterations N_{it} in the global iterative process on the relaxation parameter δ_ω at $\alpha = 0.75$, $\beta = 0.5$ for the parallelepiped of the size $1 \times \frac{100}{38} \times 1$. The number of the grid nodes is $11 \times 31 \times 11$.

The convergence of the global iterative process is decelerated for very small values of δ_ω. There exists the limiting value of δ_ω, for this value the iterative process unconverges. In our case this value is equal to 0.98.

The dependence of the optimum value of δ_ω on the degree of skewness of the velocity profile at the inlet, i.e. on the values of the coefficients α and β, is investigated.

The calculations for two other velocity profiles are done: for the values $\alpha = 0.25$, $\beta = 1.5$, and $\alpha = 0.995$, $\beta = 0.01$. It is possible to conclude that with the increase in β the optimum value of δ_ω decreases.

In the third problem the vortical flow in parallelepiped is calculated, but on the contrary to (10.1) the constant value for the normal component of the velocity vector is given at the outlet: $\nu_2 = 1$.

For such boundary conditions the velocity vector is parallel to the plane yOz, i.e. the flow is actually two-dimensional. Thus, it is possible to compare the calculations of the vortical fluid flow using three-dimensional algorithm and the two-dimensional algorithm described in Chapters 2 - 6.

Fig.10.2 shows the velocity vector field of three-dimensional flow in the cut $j_1 = 6$ in x-direction. The modification of the boundary condition for ν_2 in comparison with (10.1) leads only to the local modification of the flow in small neighbourhood upstream from the outlet Γ_2.

Figures 10.3 and 10.4 shows the graphs of the second Cartesian component u_2 of the velocity vector in two cuts perpendicular to the y-axis. In the same figures the dashed
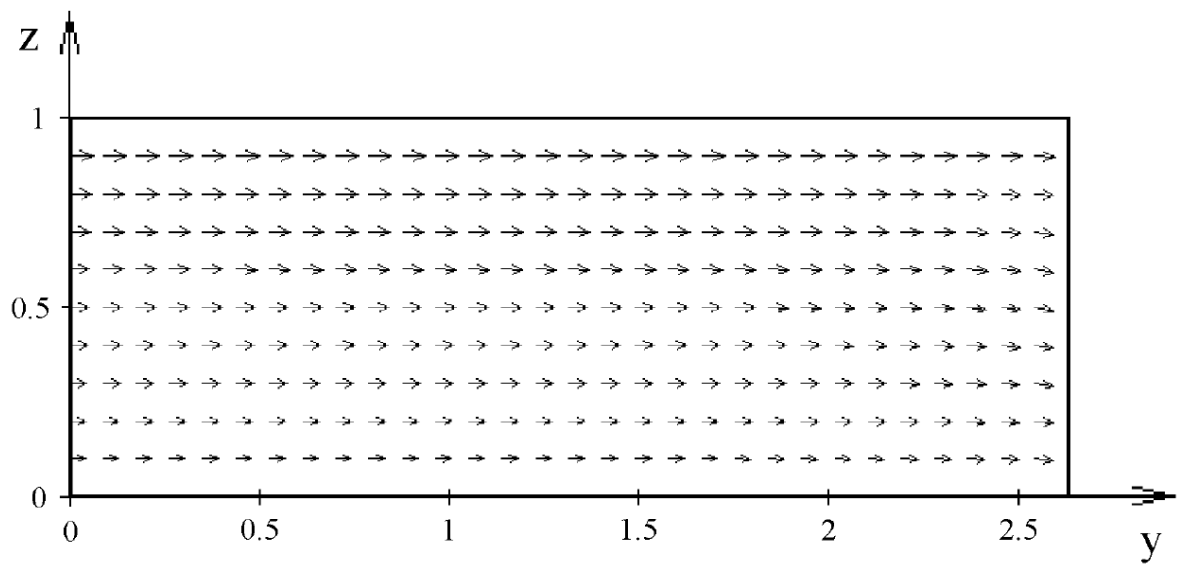
Figure 10.2: The velocity vector field of three-dimensional flow in the cut $j_1 = 6$ in x-direction

lines show the results obtained by calculating two-dimensional flow. It is clear that the results of the calculations using different algorithms almost coincide.

10.2 Results of the calculations of the flow in the duct with the stream bending by an angle of $180°$

The other series of calculations is done for the duct with square cross-section and the stream bending by an angle of $180°$. The duct is decribed in Section 9.2. The following parameter values are taken: $L_1 = 1$, $L_3 = 1$, $L'_1 = \frac{62}{38}$, $L_2 = \frac{69}{38}$.

The adaptive grid is shown in Fig.10.5. As it has been shown by other authors ([54]), secondary flows appear near the impermeable boundary. Thus, it is necessary to condense the grid near the impermeable boundary of the duct. For this purpose in the present calculations the control function $w = 1 + \alpha_0[(x - x_0)^2 + (y - y_0)^2 + (z - z_0)^2]$ is used, where $\alpha_0 > 0$, x_0, y_0, z_0 are the coordinates of the cross point of the axial line of the duct with the plane which goes through the point (x, y, z) perpendicularly to this line.

At first, the calculations with the uniform expenditure at the inlet and the outlet, i.e. for $\nu_1 = 1$, $\nu_2 = 1$, are done. This flow is actually potential and two-dimensional. The flow picture is identical in the planes $z = $ const. This flow picture is shown in Fig.10.6.

Figures 10.7, 10.8, 10.9, 10.10 and 10.11 show the projections of the velocity vector on the cross-sections of the duct in the beginning of the turn ($j_2 = 11$, $j_2 = 12$), in the cut near the plane of symmetry of the duct ($j_2 = 15$), and at the end of the curvilinear part of the duct ($j_2 = 19$, $j_2 = 20$). For the best visualization the vector lengths are enlarged 10 times in comparison with Fig.10.6.

In Figures 10.7, 10.8, 10.9, 10.10 and 10.11 $q^1 = 0$ corresponds to the exterior wall, and $q^1 = 1$ corresponds to the interior wall of the duct. It is visible that in the beginning
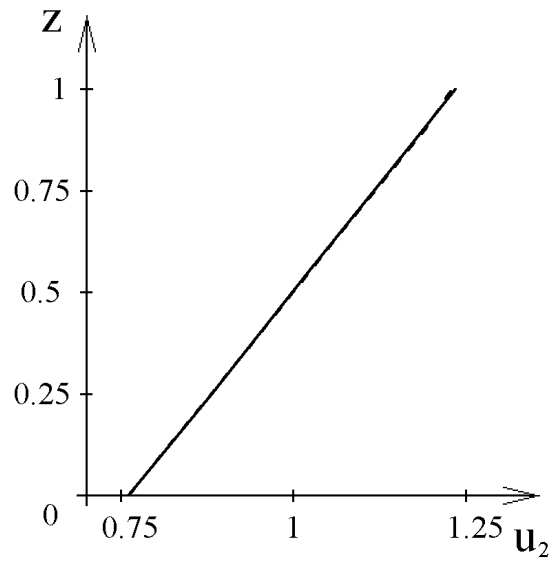
109

Figure 10.3: The graphs of the second Cartesian component u_2 of the velocity vector in the cut $j_2 = 20$ in y-direction
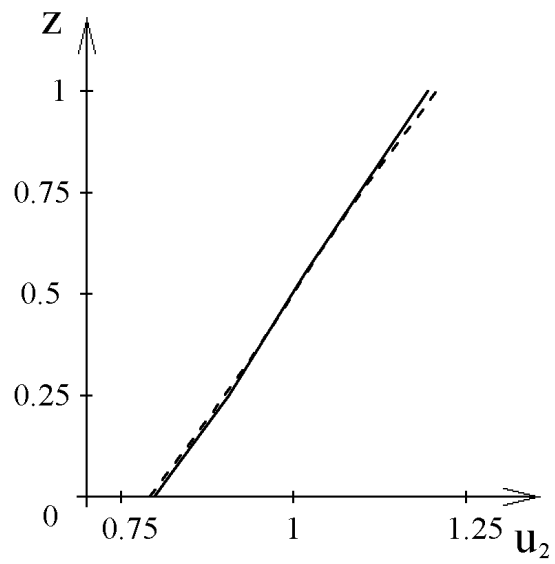

Figure 10.4: The graphs of the second Cartesian component u_2 of the velocity vector in the cut $j_2 = 25$ in y-direction
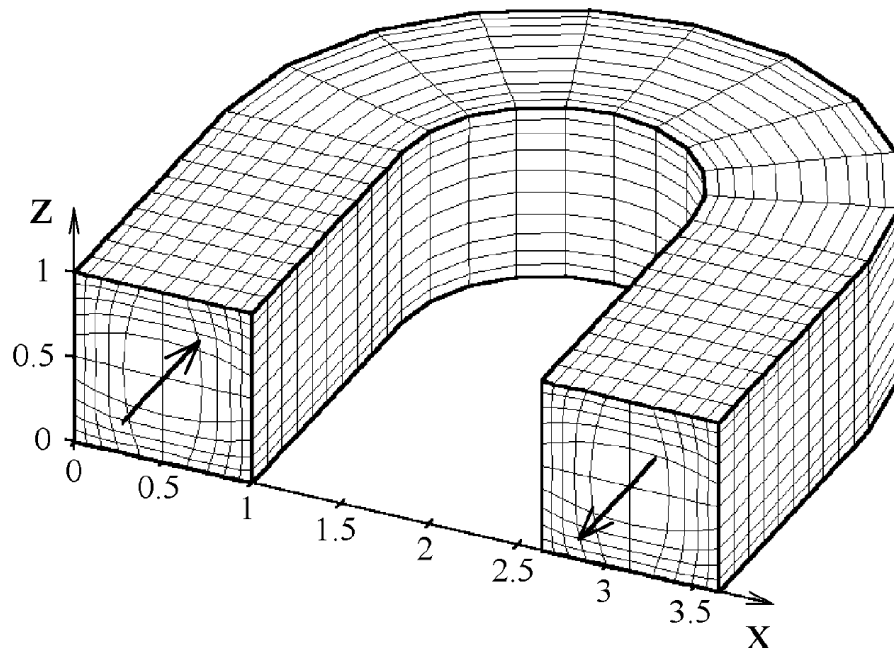
Figure 10.5: The duct with the stream bending by an angle of $180°$ and the curvilinear grid at $\alpha_0 = 10$

of the bending part the projection of the velocity vector is directed to the interior wall of the duct, and at the end of this part – to the exterior wall of the duct.

The particles of the fluid are moving parallel to the upper and lower walls of the duct. Near the plane of symmetry the projection of the velocity vector on the cross-section is practically equal to zero, the velocity vector is perpendicular to this cut. Therefore, the randomness of the motion is caused only by the calculation error.

For $\alpha = 0.9$, $\beta = 0.2$ the picture of flow is essentially different. Figures 10.12, 10.13, 10.14, 10.15, and 10.16 show the projections of the velocity vector on the plane of cuts a, b, c, d, e, which are presented in Fig.10.6.

It is clear that the shift stream at the inlet leads to the appearance of the secondary flow with the alternating component u_3 of the velocity vector. In the previous test u_3 is practically equal to zero. Thus, the flow is of screw type now.

The obtained results are qualitatively coordinated with the conclusions of [18, 19] about the motion of the fluid particles in the neighbourhood of the upper wall in the direction of the exterior wall and in the neighbourhood of the lower wall – in the direction of the interior wall.

Figures 10.17, 10.18, 10.19, 10.20 and 10.21 also show the projections of the velocity vector on the cross-sections a, b, c, d, e, which are presented in Fig.10.6. Now there is the increase in the velocity shift at the inlet, i.e. $\alpha = 0.75$, $\beta = 0.5$.

Along with the increase in the velocity shift, the character of the flow does not vary essentially. However, the intensity of the secondary flow increase considerably.
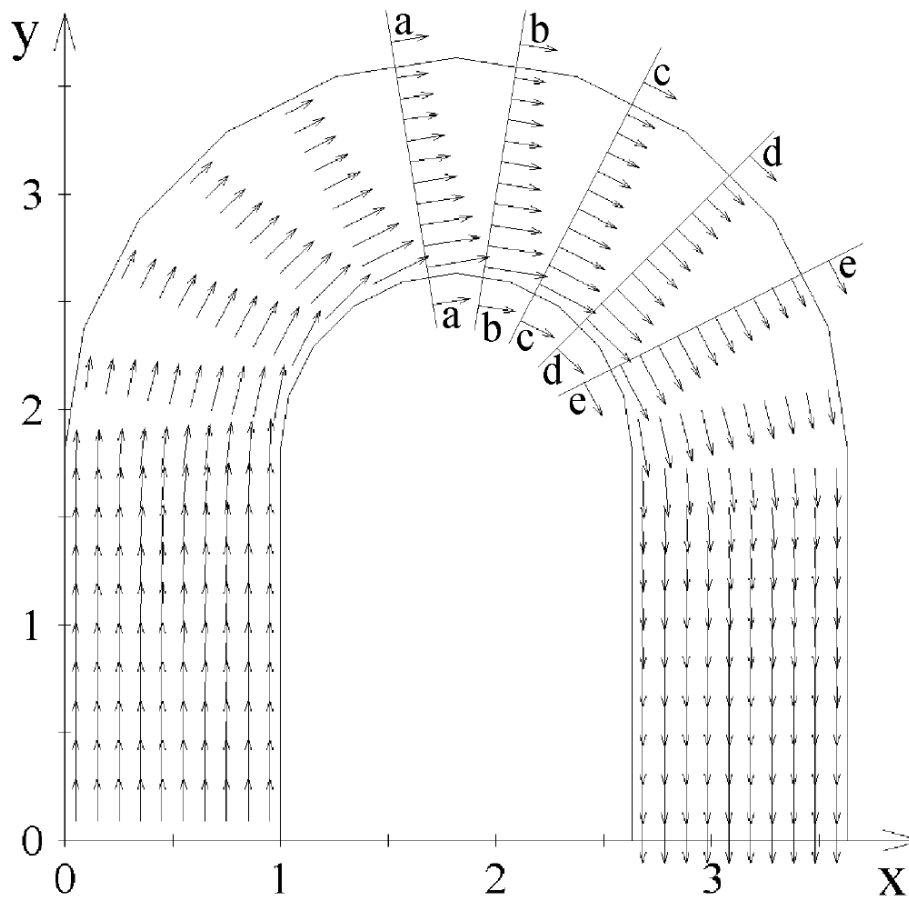
Figure 10.6: The velocity vector field of three-dimensional flow at $\alpha = 1$, $\beta = 0$ in the cut in z-direction

Figure 10.7: The projection of velocity vector on the cross-section $j_2 = 11$ of the duct at $\alpha = 1$, $\beta = 0$

Figure 10.8: The projection of velocity vector on the cross-section $j_2 = 12$ of the duct at $\alpha = 1$, $\beta = 0$

Figure 10.9: The projection of velocity vector on the cross-section $j_2 = 15$ of the duct at $\alpha = 1$, $\beta = 0$

113

Figure 10.10: The projection of velocity vector on the cross-section $j_2 = 19$ of the duct at $\alpha = 1$, $\beta = 0$

Figure 10.11: The projection of velocity vector on the cross-section $j_2 = 20$ of the duct at $\alpha = 1$, $\beta = 0$

114

Figure 10.12: The projection of velocity vector on the cross-section $j_2 = 15$ of the duct at $\alpha = 0.9$, $\beta = 0.2$

Figure 10.13: The projection of velocity vector on the cross-section $j_2 = 16$ of the duct at $\alpha = 0.9$, $\beta = 0.2$

Figure 10.14: The projection of velocity vector on the cross-section $j_2 = 17$ of the duct at $\alpha = 0.9$, $\beta = 0.2$

Figure 10.15: The projection of velocity vector on the cross-section $j_2 = 18$ of the duct at $\alpha = 0.9$, $\beta = 0.2$

116

Figure 10.16: The projection of velocity vector on the cross-section $j_2 = 19$ of the duct at $\alpha = 0.9$, $\beta = 0.2$
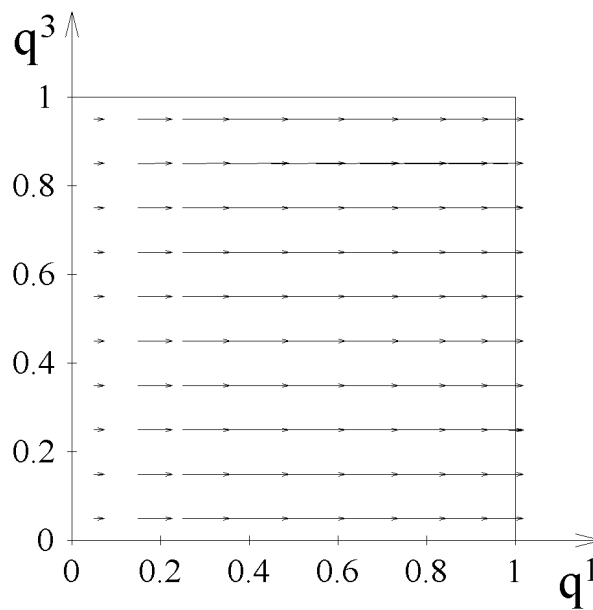

Figure 10.17: The projection of velocity vector on the cross-section $j_2 = 15$ of the duct at $\alpha = 0.75$, $\beta = 0.5$
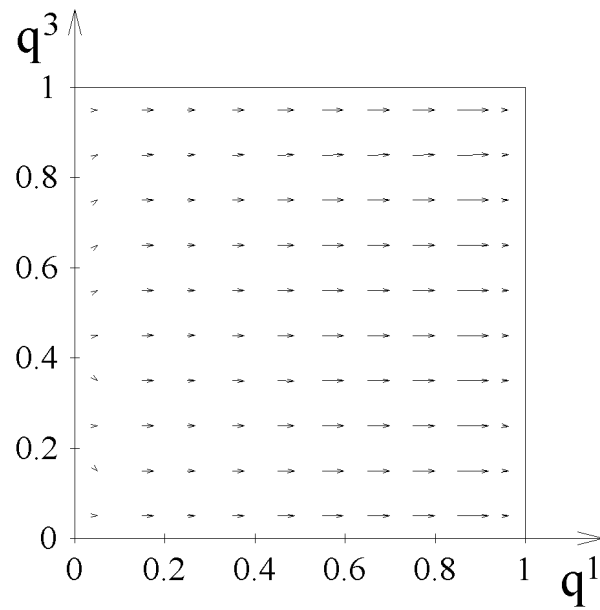
Figure 10.18:   The projection of velocity vector on the cross-section $j_2 = 16$ of the duct at $\alpha = 0.75$, $\beta = 0.5$
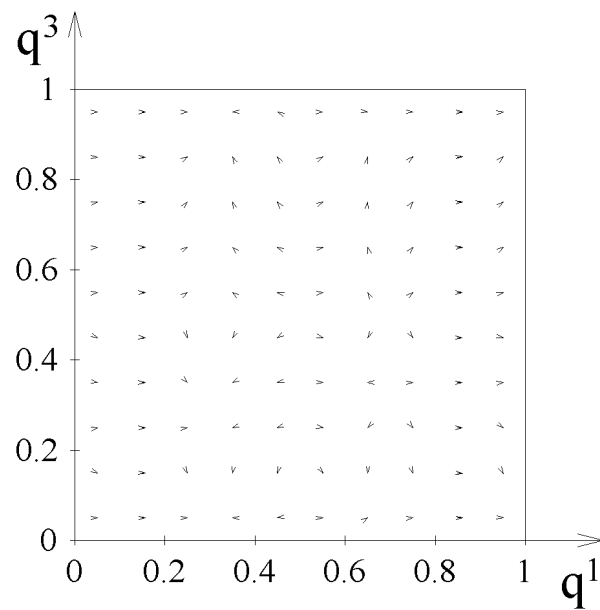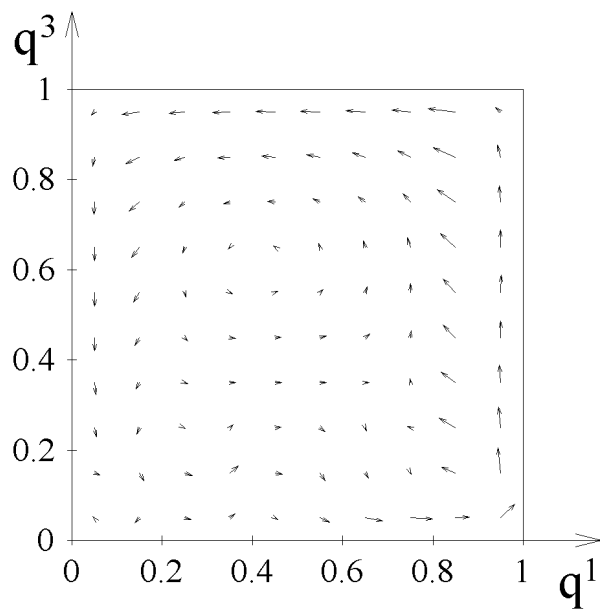

Figure 10.19:   The projection of velocity vector on the cross-section $j_2 = 17$ of the duct at $\alpha = 0.75$, $\beta = 0.5$
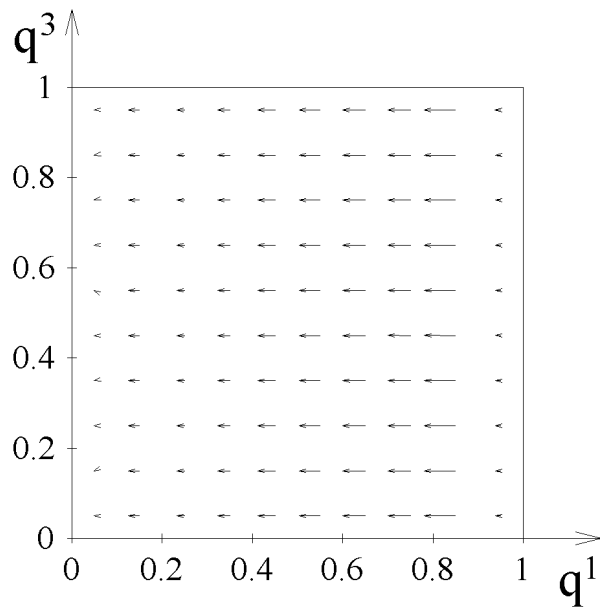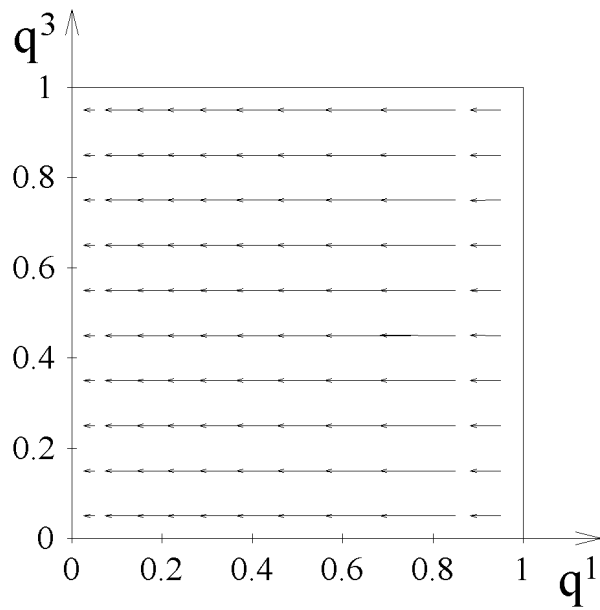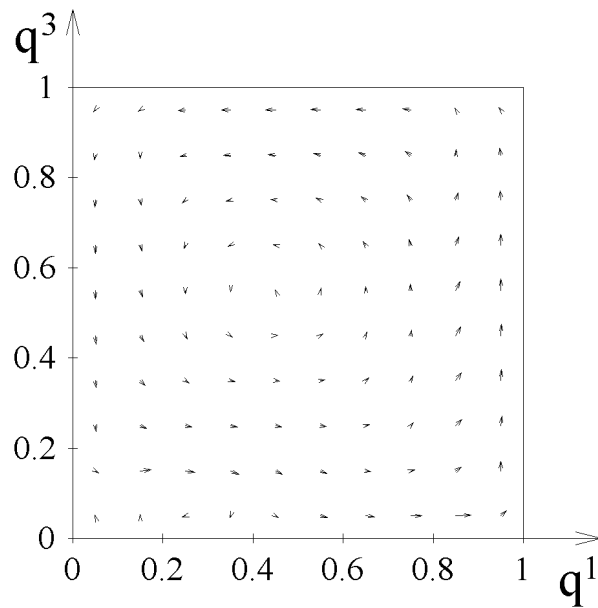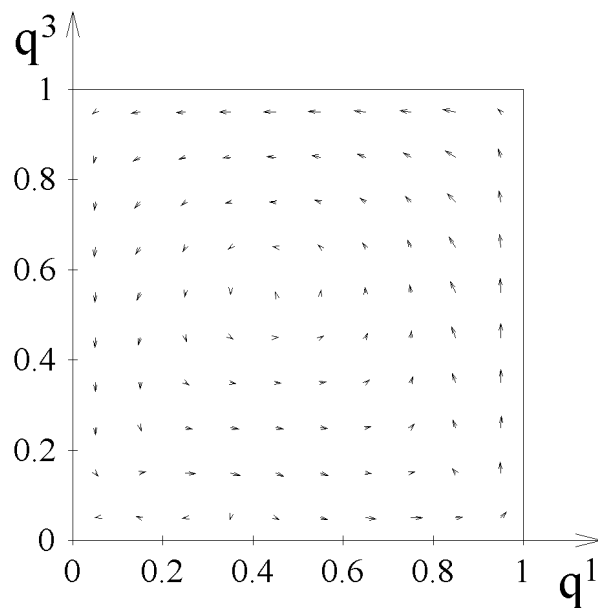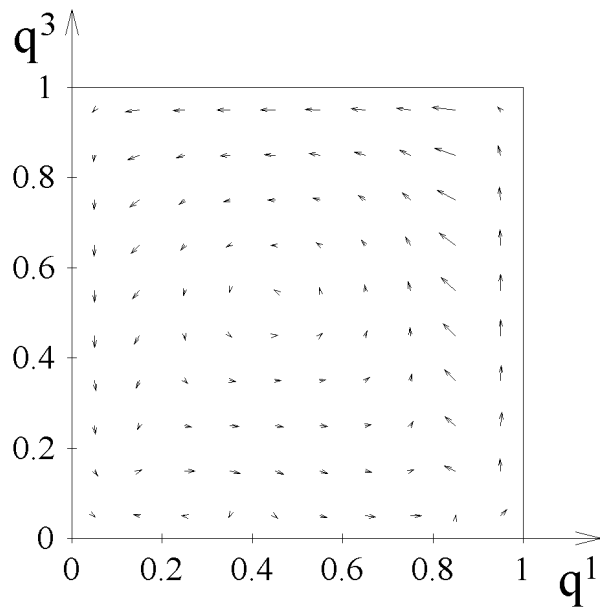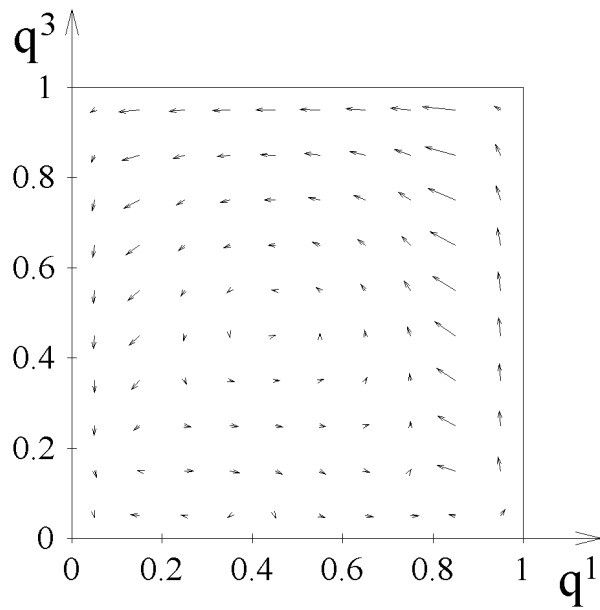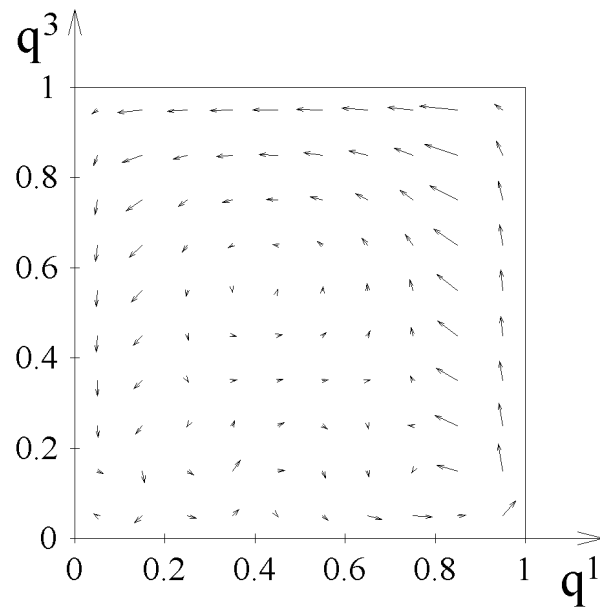
Figure 10.20: The projection of velocity vector on the cross-section $j_2 = 18$ of the duct at $\alpha = 0.75$, $\beta = 0.5$
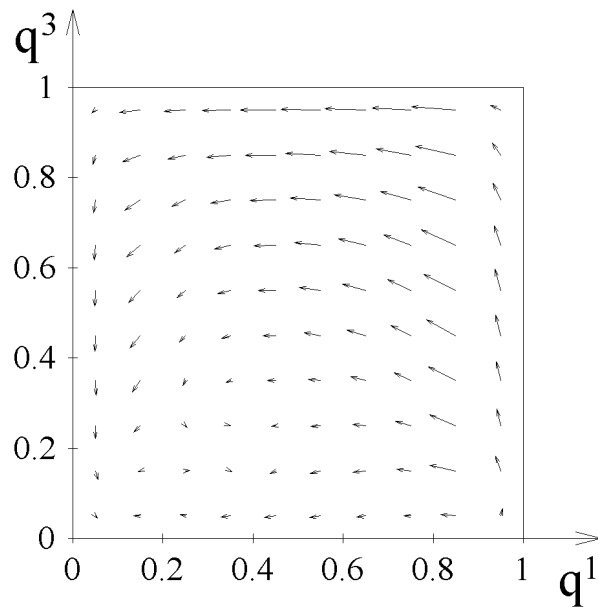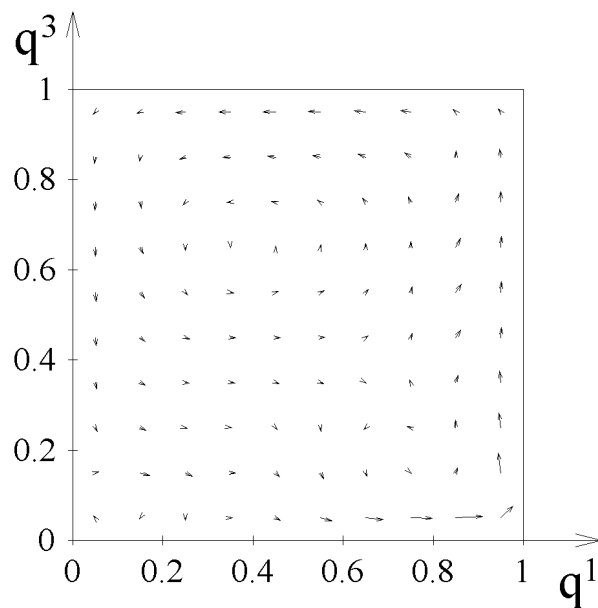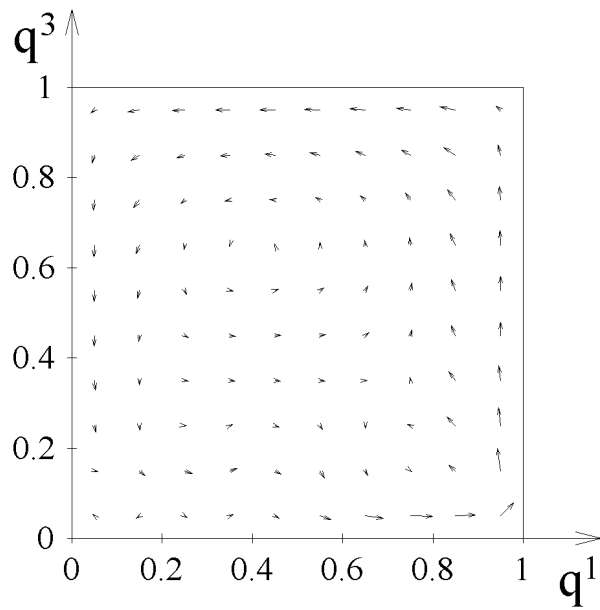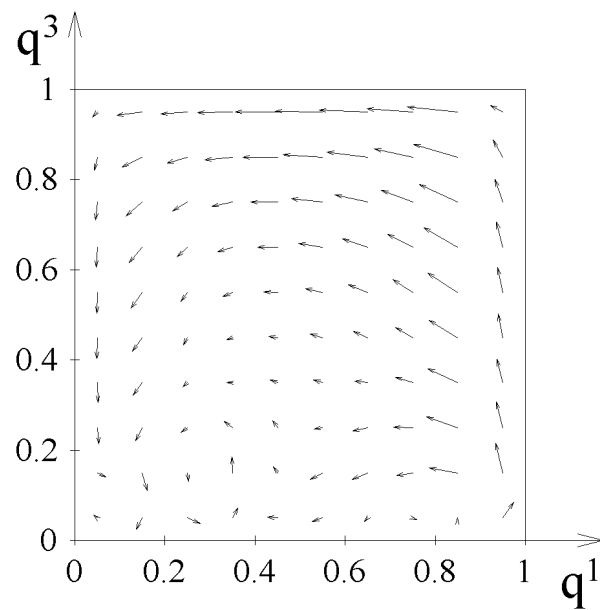

Figure 10.21: The projections of velocity vector on the cross-section $j_2 = 19$ of the duct at $\alpha = 0.75$, $\beta = 0.5$

Chapter 11

Iterative method for calculating plane steady fluid flows in the rivers within the framework of the shallow water model

11.1   Mathematical model in Cartesian coordinates

Let Ω be a simply connected domain in the plane of Cartesian coordinates $x^1 O x^2$. The mathematical statement of the problem on steady fluid flow with the surface gravitational waves through the domain Ω consists in obtaining the velocity vector $\mathbf{u}$ and the elevation $\eta(x)$ of the fluid surface above the unperturbed level, satisfying the continuity equation and the motion equation in Ω:

$$\nabla \cdot H\mathbf{u} = 0, \quad \mathbf{x} = (x^1, x^2) \in \Omega, \tag{11.1}$$

$$(H\mathbf{u} \cdot \nabla)\mathbf{u} + g\nabla\frac{H^2}{2} = gH\nabla h - kH[\mathbf{e}_3 \times \mathbf{u}] - \frac{g}{C^2}\mathbf{u}u, \tag{11.2}$$

and the boundary conditions on the boundary $\Gamma = \partial\Omega$:

$$H\mathbf{u}\Big|_{\mathbf{x}\in\Gamma_1} = \vec{\nu}_1(\mathbf{x}), \quad \mathbf{u} \cdot \mathbf{n}\Big|_{\mathbf{x}\in\Gamma_0} = 0, \quad H\mathbf{u} \cdot \mathbf{n}\Big|_{\mathbf{x}\in\Gamma_2} = \nu_2(\mathbf{x}), \tag{11.3}$$

where $\mathbf{u} = (u_1, u_2)$, u_α $(\alpha = 1, 2)$ are the components of the velocity vector along the axes Ox^α. $\nabla = \left(\frac{\partial}{\partial x^1}, \frac{\partial}{\partial x^2}\right)$, $\mathbf{n}$ is the external normal to Γ. $\Gamma = \Gamma_1 \cup \Gamma_0 \cup \Gamma_2$, Γ_1 is the inlet to Ω $(\vec{\nu}_1 \cdot \mathbf{n} < 0)$, Γ_0 is the impermeable part of the boundary, Γ_2 is the outlet from Ω $(\nu_2 > 0)$, $\Gamma_1 \cap \Gamma_2 = \emptyset$. H is the total depth, $H = \eta + h$, $z = -h(\mathbf{x})$ is the function which describes the bottom. g is the free fall acceleration, $\mathbf{e}_3 = (0, 0, 1)$ is the basis vector which is directed along the vertical axis Oz perpendicularly to the plane $x^1 O x^2$. $V = |\mathbf{u}|$, C is the Chezy coefficient, k is the Coriolis parameter. The density of the fluid is assumed to be equal to 1.

The system of equations (11.1)–(11.2) have the following form in the dimensionless variables:

$$\frac{\partial \mathbf{F}^1}{\partial x^1} + \frac{\partial \mathbf{F}^2}{\partial x^2} = \mathbf{G}, \tag{11.4}$$

where

$$\mathbf{F}^1 = \begin{pmatrix} Hu_1 \\ Hu_1^2 + H^2/2 \\ Hu_1u_2 \end{pmatrix}, \quad \mathbf{F}^2 = \begin{pmatrix} Hu_2 \\ Hu_1u_2 \\ Hu_2^2 + H^2/2 \end{pmatrix},$$

$$\mathbf{G} = \begin{pmatrix} 0 \\ Hh_{x^1} + f_{Cor}u_2H - u_1V/f_{Ch}^2 \\ Hh_{x^2} - f_{Cor}u_1H - u_2V/f_{Ch}^2 \end{pmatrix}.$$

The transformation to the dimensionless variables is carried out using the following formulas:

$$\tilde{x}^\alpha = x^\alpha h_0, \quad \tilde{\eta} = \eta h_0, \quad \tilde{H} = H h_0,$$

$$\tilde{h} = h h_0, \quad \tilde{u}_\alpha = u_\alpha \sqrt{g h_0}, \tag{11.5}$$

where h_0 is the characteristic depth. The dimensional values are denoted by the symbol "~". f_{Cor} and f_{Ch} denote the dimensionless values of the Coriolis parameter and the Chezy coefficient:

$$f_{Cor} = k\sqrt{h_0/g}, \qquad f_{Ch} = C/\sqrt{g}.$$

The boundary conditions for the dimensionless variables look like (11.3). $\vec{\nu}_1$ and ν_2 are equal to the ratio of the appropriate values from (11.3) to $h_0\sqrt{gh_0}$.

In addition to the boundary conditions (11.3) it is assumed that the total depth is known at the certain point $M_0 \in \bar{\Omega}$:

$$H(M_0) = H_0. \tag{11.6}$$

For the numerical solution of the problem new dependent variables, i.e. the stream function ψ and the vorticity function ω, are introduced:

$$Hu_1 = \frac{\partial \psi}{\partial x^2}, \quad Hu_2 = -\frac{\partial \psi}{\partial x^1}, \quad \omega = \mathrm{rot}\,\mathbf{u} \equiv -\frac{\partial u_1}{\partial x^2} + \frac{\partial u_2}{\partial x^1}. \tag{11.7}$$

Then for ψ and ω we obtain the following equations:

$$\sum_{i=1}^2 \frac{\partial}{\partial x^i}\left(\frac{1}{H}\frac{\partial \psi}{\partial x^i}\right) = -\omega, \tag{11.8}$$

$$\nabla \cdot H\mathbf{u}\omega = \mathrm{rot}\left(H\nabla(h - \frac{V^2}{2})\right) - \frac{1}{f_{Ch}^2}\mathrm{rot}\,(\mathbf{u}V). \tag{11.9}$$

Here the boundary values for ψ are uniquely determined from the conditions (11.3).

11.2 Mathematical model in curvilinear coordinates

Let

$$x^\alpha = x^\alpha(q^1, q^2), \quad \alpha = 1, 2, \tag{11.10}$$

be a one-to-one non-degenerate mapping of the square Q in the plane of coordinates $q^1 O q^2$ onto the domain Ω. For the simplicity, let us assume that the inlet and the outlet are the connected parts of the boundary. Γ_1 is the image under the mapping (11.10) of the left side γ_1 of the square Q, Γ_2 is the image under the mapping of the right side γ_2. The impermeable part Γ_0 consists of two intervals Γ_0' and Γ_0'' which are the images of the lower side γ_0' and the upper side γ_0'' of Q respectively.

The equations (11.8) and (11.9) have the following form in new independent variables q^α:

$$\frac{\partial}{\partial q^1}\left(k_{11}\frac{\partial\psi}{\partial q^1} + k_{12}\frac{\partial\psi}{\partial q^2}\right) + \frac{\partial}{\partial q^2}\left(k_{21}\frac{\partial\psi}{\partial q^1} + k_{22}\frac{\partial\psi}{\partial q^2}\right) = -J\omega, \tag{11.11}$$

$$\frac{\partial}{\partial q^1}(HJv^1\omega) + \frac{\partial}{\partial q^2}(HJv^2\omega) = -\frac{\partial f_1}{\partial q^2} + \frac{\partial f_2}{\partial q^1}, \tag{11.12}$$

where

$$k_{11} = \frac{g_{22}}{HJ}, \quad k_{12} = k_{21} = -\frac{g_{12}}{HJ}, \quad k_{22} = \frac{g_{11}}{HJ},$$

$g_{\alpha\beta}$ are the covariant components of the metric tensor, $\alpha, \beta = 1, 2$,

$$g_{11} = x_{q^1}^2 + y_{q^1}^2, \quad g_{12} = x_{q^1}x_{q^2} + y_{q^1}y_{q^2}, \quad g_{22} = x_{q^2}^2 + y_{q^2}^2,$$

$x = x^1$, $y = x^2$, J stands for the Jacobian of the mapping (11.10), $J = x_{q^1}y_{q^2} - x_{q^2}y_{q^1}$, v^α are the contravariant velocity components connected with ψ by the following relations:

$$v^1 = \frac{1}{HJ}\frac{\partial\psi}{\partial q^2}, \quad v^2 = -\frac{1}{HJ}\frac{\partial\psi}{\partial q^1}. \tag{11.13}$$

In the equation for the vorticity:

$$f_\alpha = H\frac{\partial}{\partial q^\alpha}\left(h - \frac{V^2}{2}\right) - \frac{1}{f_{Ch}^2}v_\alpha V, \quad \alpha = 1, 2, \tag{11.14}$$

v_α are the contravariant velocity components:

$$v_1 = g_{11}v^1 + g_{12}v^2, \quad v_2 = g_{12}v^1 + g_{22}v^2.$$

In calculating the total depth the motion equations in the Gromeka-Lamb form written in curvilinear coordinates are used:

$$-HJv^2\omega + \frac{\partial p}{\partial q^1} = f_1 + f_{Cor}HJv^2,$$

$$HJv^1\omega + \frac{\partial p}{\partial q^2} = f_2 - f_{Cor}HJv^1, \tag{11.15}$$

where $p = H^2/2$.
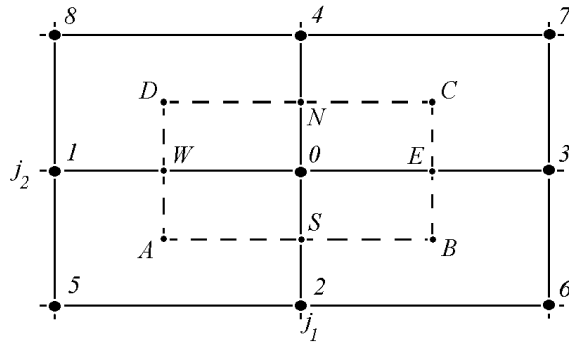
Figure 11.1: The pattern of the difference equation for ψ
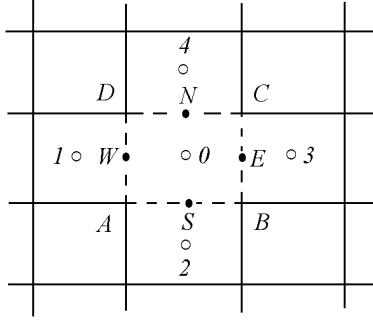
Figure 11.2: The pattern of the difference equations for ω and H

11.3   Difference equations

The difference equation for the grid function ψ is obtained using the integro-interpolational method by approximating the integrated relation:

$$\oint_{\mathcal{C}} \left(k_{11} \frac{\partial \psi}{\partial q^1} + k_{12} \frac{\partial \psi}{\partial q^2} \right) dq^2 - \left(k_{21} \frac{\partial \psi}{\partial q^1} + k_{22} \frac{\partial \psi}{\partial q^2} \right) dq^1 = - \int\int_{D_{\mathcal{C}}} J \omega dq^1 dq^2, \qquad (11.16)$$

where $D_{\mathcal{C}}$ is the rectangle with the contour $\mathcal{C}$ denoted by a dashed line in Fig.11.1.

The approximation of the relation (11.16) is the same as for ideal gas. The obtained difference equation for ψ is nine-point. The functions ψ, H, J, $g_{\alpha\beta}$ are defined in the integer nodes of the grid. The grid function ω is calculated at the mesh centres of the grid which covers the computational domain Q.

The equation for the vorticity (11.12) is approximated by the scheme with central differences:

$$\Lambda \omega_0 = (f)_0, \qquad (11.17)$$

where

$$\Lambda = \Lambda_1 + \Lambda_2,$$

$$\Lambda_1 \omega_0 = \frac{1}{2h_1} \left[\frac{\psi_C - \psi_B}{h_2} \omega_3 - \frac{\psi_D - \psi_A}{h_2} \omega_1 \right],$$

124

$$\Lambda_2 \omega_0 = \frac{1}{2h_2}\left[-\frac{\psi_C - \psi_D}{h_1}\omega_4 + \frac{\psi_B - \psi_A}{h_1}\omega_2\right],$$

$$(f)_0 = -\frac{(f_1)_N - (f_1)_S}{h_2} + \frac{(f_2)_E - (f_2)_W}{h_1}.$$

The pattern is shown in Fig.11.2.

For solving the equation (11.17) the implicit method of establishing the steady state is used:

$$(J\mathcal{E} + \tau\Lambda)\frac{\omega^{n+1} - \omega^n}{\tau} + \Lambda\omega^n = f, \tag{11.18}$$

where τ is the iterative parameter, n is the number of the iteration, $\mathcal{E}$ is the identical operator. After the approximate factorization [95] of the operator $J\mathcal{E} + \tau\Lambda$:

$$J\mathcal{E} + \tau\Lambda \approx \left(\sqrt{J}\mathcal{E} + \frac{\tau}{\sqrt{J}}\Lambda_1\right)\left(\sqrt{J}\mathcal{E} + \frac{\tau}{\sqrt{J}}\Lambda_2\right)$$

the equation (11.18) has the following form:

$$\left(\sqrt{J}\mathcal{E} + \frac{\tau}{\sqrt{J}}\Lambda_1\right)\left(\sqrt{J}\mathcal{E} + \frac{\tau}{\sqrt{J}}\Lambda_2\right)\frac{\omega^{n+1} - \omega^n}{\tau} = -\Lambda\omega^n + f. \tag{11.19}$$

If we denote

$$\omega^{n+1/2} = (\sqrt{J}\mathcal{E} + \frac{\tau}{\sqrt{J}}\Lambda_2)\frac{\omega^{n+1} - \omega^n}{\tau},$$

and introduce the new variable $\xi = (\omega^{n+1} - \omega^n)/\tau$, then the difference equations for the vorticity function have the following form:

$$(\sqrt{J}\mathcal{E} + \frac{\tau}{\sqrt{J}}\Lambda_1)\omega^{n+1/2} = -\Lambda\omega^n + f, \tag{11.20}$$

$$(\sqrt{J}\mathcal{E} + \frac{\tau}{\sqrt{J}}\Lambda_2)\xi = \omega^{n+1/2}, \tag{11.21}$$

$$\omega^{n+1} = \omega^n + \tau\xi. \tag{11.22}$$

The difference equations (11.20) and (11.21) are 3-point formulas, therefore it is possible to use the sweep method for solution. Applying this method to the equation (11.20) we find the values of $\omega^{n+1/2}$. Substituting these values into (11.21) we find the values of ξ and then ω^{n+1} is calculated by the formula (11.22). In this case the sweep method is stable under some restriction on the iterative parameter τ.

The boundary conditions for the vorticity are necessary for the realisation of the sweep method. For the horizontal sweep on the left boundary the boundary values of the vorticity are calculated using the boundary conditions (11.3). The description of the procedure of calculating is given below. The values of the vorticity on the right boundary are defined with the help of the extrapolation. The boundary values for the vorticity are

not required for realizing the vertical sweep, because the impermeability conditions are fulfilled on Γ_0, and $\psi\big|_{\Gamma_0} = \text{const}$.

The function p is defined on the basis of the following expression which is obtained from the equations (11.15):

$$p(q_j) = p_0 + \int_{\gamma(q_0,q_j)} \left(f_1 + HJv^2(\omega + f_{Cor})\right) dq^1 + \left(f_2 - HJv^1(\omega + f_{Cor})\right) dq^2,$$

$$\tag{11.23}$$

where $p_0 = H_0^2/2$, q_0 is the pre-image of the point M_0 from (11.6). We take a polygonal line whose links are parallel to the axes Oq^α and pass along the sides of the meshes as a curve γ, connecting the point $\mathbf{q}_j$, where it is required to define the pressure, with the point $\mathbf{q}_0$, where the pressure is given initially.

Let us show the independence of calculating $p(q_j)$ of the integration path. We consider an arbitrary mesh of the computational domain Q (see Fig.11.2). Let us show that the calculation of p at the point C using different contours ABC and ADC leads to the equal values if we apply the following approximation of the integrals from (11.23):

$$p_{ABC}(C) = p_A + h_1(f_1)_S - (\psi_B - \psi_A)f_{Cor} - (\psi_B - \psi_A)\frac{\omega_0 + \omega_2}{2} + \tag{11.24}$$

$$+ h_2(f_2)_E - (\psi_C - \psi_B)f_{Cor} - (\psi_C - \psi_B)\frac{\omega_0 + \omega_3}{2},$$

$$p_{ADC}(C) = p_A + h_2(f_2)_W - (\psi_D - \psi_A)f_{Cor} - (\psi_D - \psi_A)\frac{\omega_0 + \omega_1}{2} + \tag{11.25}$$

$$+ h_1(f_1)_N - (\psi_C - \psi_D)f_{Cor} - (\psi_C - \psi_D)\frac{\omega_0 + \omega_4}{2}.$$

If we subtract (11.25) from (11.24), then the following relation is obtained:

$$p_{ABC}(C) - p_{ADC}(C) = -h_1 h_2 \left[\frac{1}{2h_1}\left(\frac{\psi_C - \psi_B}{h_2}\omega_3 - \frac{\psi_D - \psi_A}{h_2}\omega_1\right) - \right.$$

$$\left. - \frac{1}{2h_2}\left(\frac{\psi_C - \psi_D}{h_1}\omega_4 - \frac{\psi_B - \psi_A}{h_1}\omega_2\right) + \frac{(f_1)_N - (f_1)_S}{h_2} - \frac{(f_2)_E - (f_2)_W}{h_1} \right] = \tag{11.26}$$

$$= -h_1 h_2 \left[\Lambda_1 \omega_0 + \Lambda_2 \omega_0 - (f)_0\right].$$

If the iterative process (11.20)–(11.22) has been converged, then the stationary difference equation (11.17) for the vorticity is fulfilled. Therefore, we obtain that the right-hand side of the equality (11.26) is equal to zero. Thus, the value of p does not depend on the integration contour, and the method of coordinated approximation is used for calculating p. For the case of the rectangular grids this method is considered in [76]. For viscous incompressible fluid flows it is known as the marching method for calculating the pressure [115].

After the calculation of p the total depth is obtained from the following formula:

$$H = \sqrt{2p}. \tag{11.27}$$

11.4　Iterative process

The problem on steady fluid flow with the surface waves is solved in three stages.

I. The problem on the potential flow "under the cover" is solved. It is assumed that $\eta(x) \equiv 0$, $H(x) = h(x)$, $\omega(x) \equiv 0$. The difference equation for ψ is solved by the method of successive over relaxation.

II. The problem on the vortical flow "under the cover" is solved. The obtained solution of the problem on the potential flow "under the cover" is used as the initial approximation. It is assumed that $H(x) = h(x)$, and the iterative process is organized. On the $(n+1)$-th step of the process the following calculations are made.

1. The system of the difference equations for ψ_j^{n+1} is solved.

2. The boundary values of the vorticity are calculated at the inlet Γ_1. For this purpose, the following expression for the vorticity in curvilinear coordinates is used:

$$\omega = \frac{1}{J}\left(-\frac{\partial v_1}{\partial q^2} + \frac{\partial v_2}{\partial q^1}\right). \tag{11.28}$$

The covariant components of the velocity are calculated using the condition (11.3) at the inlet. In calculating the tangential derivative $\partial v_1/\partial q^2$ the components of the vector $\vec{v}_1$ and the value of the total depth H at Γ_1 are used. In calculating the derivative $\partial v_2/\partial q^1$ the value of v_2 which is defined by the values of ψ_j^{n+1} at the centre of the mesh adjacent to the boundary is used. The difference analogue of the formula (11.28) is applied to defining the preliminary value of $\bar{\omega}$. The final values of the vorticity at the inlet are obtained by the relaxation of the values of $\bar{\omega}$ and the boundary values of the vorticity from the previous iteration:

$$\omega^{n+1}\Big|_{\Gamma_1} = \delta_\omega \bar{\omega} + (1 - \delta_\omega)\omega^n\Big|_{\Gamma_1}, \tag{11.29}$$

where $0 < \delta_\omega$ is the relaxation parameter [146], $\delta_\omega = O(h_1)$.

3. The system of equations for the vorticity $\omega_{j+1/2}^{n+1}$ in the internal nodes is solved by the method of stabilizing corrections.

The iterations $\psi - \omega$ are carried out as long as ω^{n+1} and ω^n differ in the norm of the space C by the value which is larger than the given value $\varepsilon_\omega > 0$.

III. The problem on the vortical flow with the free surface is solved. The solution of the problem on the vortical flow "under the cover" is taken as the initial approximation. In the iterative process, in addition to the calculation of ψ_j^{n+1}, $\omega^{n+1}\big|_{\Gamma_1}$ and $\omega_{j+\frac{1}{2}}^{n+1}$, the total depth H_j^{n+1} is obtained. The preliminary values of $\bar{H}_j$ are obtained on the basis of formulas (11.27), and the values interpolated on $\bar{H}$ and H^n are taken as the final values:

$$H_j^{n+1} = \delta_H \bar{H}_j + (1 - \delta_H)H_j^n, \tag{11.30}$$

where the parameter $\delta_H > 0$ increases linearly from 0 up to 1 for the given number of steps. Thus, "the cover" is removed gradually. This procedure helps to be saved of the calculation instability which sometimes has a place at an instant release of the fluid from "the cover".

The iterations are carried out as long as H^{n+1} and H^n differ by the value which is larger than the given value $\varepsilon_H > 0$.

11.5 Description of the reservoir geometry

In the example of modelling of fluid flow with the surface waves on the specified segment of the river-bed which is described below the side boundaries are assumed to be vertical walls. The geometry S_b of the boundaries and the bottom surface is specified by the set of basic cross-sections and basic points.

Let Ω be the projection of S_b on the plane $z = 0$. Then the basic cross-section is the segment $A_j B_j$ of the straight line crossing the axis of the reservoir and two opposite parts Γ_0' and Γ_0'' of the boundary Γ of the domain Ω. Here j is the number of the cross-section, $j = 1, \ldots, N$, N is the total number of cross-sections. An arbitrary straight or curvy line which lies in the direction of the extension of the reservoir approximately "in the middle of" the domain Ω can be taken as the axis of the reservoir.

Let us assume that Ω is the plane curvilinear quadrangle with the sides Γ_1, Γ_2, Γ_0', Γ_0''. Γ_1 and Γ_2 are the rectilinear segments which coincide with the first $A_1 B_1$ and last $A_N B_N$ cross-sections respectively. The geometry of two other sides Γ_0' and Γ_0'' is defined by the location of the points A_j and B_j respectively.

Every cross-section $A_j B_j$ is connected with the following parameters:

– x_j^0, y_j^0 are the coordinates of the point $\mathbf{r}_j^0$ of the intersection of the basic cross-section with the reservoir axis;

– α_j is the angle between the vector $\overrightarrow{A_j B_j}$ and Ox-axis;

– $l_{j,k}$ is the distance between the k-th basic point of the j-th cross-section and the point $\mathbf{r}_j^0$. For the basic points which are placed on the segment $A_j B_j$ between $\mathbf{r}_j^0$ and B_j it is assumed that $l_{j,k} > 0$. For the basic points which are placed on the segment $A_j B_j$ between A_j and $\mathbf{r}_j^0$ it is assumed that $l_{j,k} < 0$. $k = 1, \ldots, N_{A_j B_j}$, $N_{A_j B_j}$ is the number of basic points in the cross-section $A_j B_j$;

– $d_{j,k}$ is the vertical marker of the bottom level in the k-th basic point. This mark is counted off the sea level.

Let us describe the restrictions for these data. The depthes in basic points $h_{j,k} = d_0 - d_{j,k}$ should differ from zero, $h_{j,k} > 0$. Here d_0 is the vertical marker of the level of non-perturbed surface of the fluid (it is the plane $z = 0$). The angle α_j is counted off the positive direction of Ox-axis, thus $-180^0 < \alpha_j \leq 180^0$. The points A_j and B_j necessarily enter into the total number of basic points. A_j and B_j have the numbers $k = 1$ and $k = N_{A_j B_j}$ respectively. The other basic points are numbered by their disposition from A_j to B_j. If the depth is constant at some cross-section $A_j B_j$, then entering the data for this cross-section it is enough to take $N_{A_j B_j} = 2$ and to set the distances $l_{j,1} < 0$ and $l_{j,2} > 0$ of the points A_j and B_j from r_j^0.

We use the piecewise parametrization for the surface S_b. For the part, which is projected on $A_j B_j B_{j+1} A_{j+1}$, its own parametrization by the parameters p, q, $0 \leq p$, $q \leq 1$, is used which is independent of the other quadrangles.

We use the bilinear interpolation for the coordinates $x^1 = x$, $x^2 = y$ of an arbitrary point from $A_j B_j B_{j+1} A_{j+1}$:

$$x^\alpha(p, q) = (1 - q - p + pq)x_{A_j}^\alpha + q(1 - p)x_{B_j}^\alpha + p(1 - q)x_{A_{j+1}}^\alpha + pq x_{B_{j+1}}^\alpha. \qquad (11.31)$$

The coordinates $x_{A_j}^\alpha$, $x_{B_j}^\alpha$ of the points A_j B_j are calculated with the help of the formulas for the coordinates of basic points:

$$x_{j,k} = l_{j,k} \cos \alpha_j + x_j^0, \quad y_{j,k} = l_{j,k} \sin \alpha_j + y_j^0, \quad k = 1, \ldots, N_{A_j B_j}. \qquad (11.32)$$
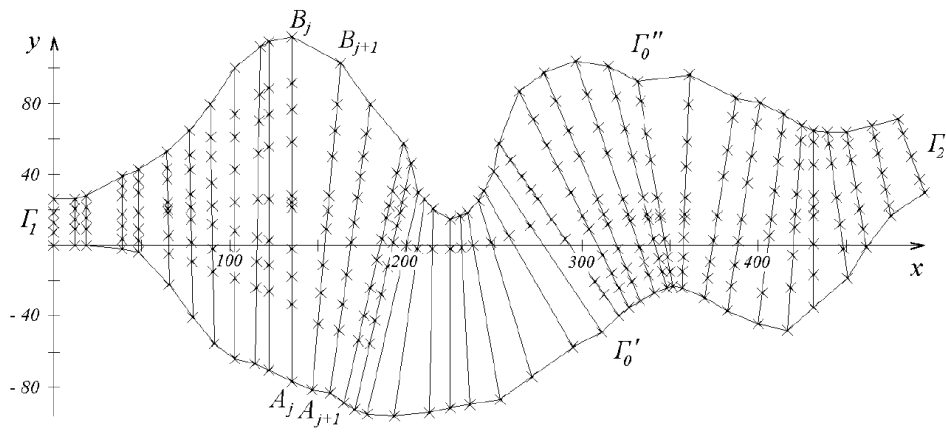
Figure 11.3: The geometry of the reservoir, the basic cross-sections, and the basic point

The following interpolation is used for the third coordinate:

$$z(p, q) = (1 - p)z_j(q) + pz_{j+1}(q), \tag{11.33}$$

where $z_j(q)$ is the piecewise linear function given on the intervals $q_{j,k} \leq q \leq q_{j,k+1}$ by the following formula:

$$z_j(q) = -h_{j,k} + \frac{q - q_{j,k}}{q_{j,k+1} - q_{j,k}}(-h_{j,k+1} + h_{j,k}), \quad k = 1, \ldots, N_{A_j B_j} - 1. \tag{11.34}$$

$q_{j,k}$ are the values of the parameter q which correspond to the basic points:

$$q_{j,k} = \frac{l_{j,k} - l_{j,1}}{l_{j,N_{A_j B_j}} - l_{j,1}}. \tag{11.35}$$

Thus, the part of the surface S_b which is projected on the quadrangle $A_j B_j B_{j+1} A_{j+1}$ of the plane $z = 0$ is one-to-one mapped on the quadrate $\bar{Q} = [0; 1] \times [0; 1]$. For the arbitrary parameters $(p, q) \in \bar{Q}$ the coordinates of the appropriate point $\mathbf{r}(p, q) \in S_b$ are calculated by the formulas (11.31), (11.33).

Fig.11.3 shows the geometry of the part of the river-bed, the basic cross-sections and the basic points (denoted by the markers). The example is taken from [15]. The characteristic depth h_0 is taken equal to three meters for the transformation to the dimensionless variables.

11.6   Construction of the curvilinear grid

The curvilinear grid is constructed before the iterative process, and it does not vary during the iterations. The node coordinates are calculated on the basis of two-dimensional analogue of the equidistribution method which is described in Chapter 4. For placing the nodes on the boundary of the domain one-dimensional equidistribution method with the same control function is used. The constructed grid is shown in Fig.4.11.

11.7　Calculation of the depth at the grid nodes

After the grid is constructed it is necessary to calculate the depth in all nodes. Let $P(x_*, y_*)$ be one of the grid nodes. As Ω is the union of the convex quadrangles, then, first of all, it is necessary to define which quadrangle contains P. The partition of the quadrangle $A_j B_j B_{j+1} A_{j+1}$ into two triangles is made for this purpose. The conditions for the point P to belong to each of these triangles are checked. For example, if three inequalities are fulfilled simultaneously:

$$L_{A_j B_j}(P) \cdot L_{A_j B_j}(A_{j+1}) \geq 0,$$

$$L_{B_j A_{j+1}}(P) \cdot L_{B_j A_{j+1}}(A_j) \geq 0, \tag{11.36}$$

$$L_{A_{j+1} A_j}(P) \cdot L_{A_{j+1} A_j}(B_j) \geq 0,$$

where L denotes the following expression:

$$L_{A_j B_j}(P) = -(y_* - y_{A_j})(x_{B_j} - x_{A_j}) + (x_* - x_{A_j})(y_{B_j} - y_{A_j}),$$

then the point P lies in the triangle $A_j B_j A_{j+1}$.

Let, for example, $P \in A_j B_j B_{j+1} A_{j+1}$. Then the unique pair of the parameters (p_*, q_*) corresponds to the point P. The values of these parameters are necessary for calculating z-coordinate z_* of the point P under the formula (11.33) and, therefore, they are necessary for calculating the depth. It is possible to define these parameters from the relations (11.31) where we should use the known values of x_*^{α} in the left-hand side. Excluding the parameter p from (11.31) we obtain the quadratic equation for defining q_*:

$$aq^2 + bq + c = 0, \tag{11.37}$$

where

$$a = [\overrightarrow{A_j B_j} \times \overrightarrow{A_{j+1} B_{j+1}}], \qquad b = [\overrightarrow{A_{j+1} P} \times \overrightarrow{A_j B_j}] - [\overrightarrow{A_j P} \times \overrightarrow{A_{j+1} B_{j+1}}],$$

$$c = [\overrightarrow{A_j P} \times \overrightarrow{A_{j+1} P}].$$

It is easy to show that if $P \in A_j B_j B_{j+1} A_{j+1}$, then the equation (11.37) has the unique radical q_* which satisfies the condition $0 \leq q_* \leq 1$.

Let $M_j \in A_j B_j$, $M_{j+1} \in A_{j+1} B_{j+1}$ be the points which correspond to the parameters $q = q_*$, $p = 0$, and $q = q_*$, $p = 1$ under the mapping (11.31). Then the parameter p_* which is defined by the following formula corresponds to the point P:

$$p_* = |\overrightarrow{PM_j}| \, / \, |\overrightarrow{M_{j+1} M_j}|.$$

Further on the basis of the obtained values of p_*, q_*, and with the help of the formula (11.33) the depth is calculated in the node P.

Fig.11.4 shows the isolines of the depth of the reservoir which is taken as the example.
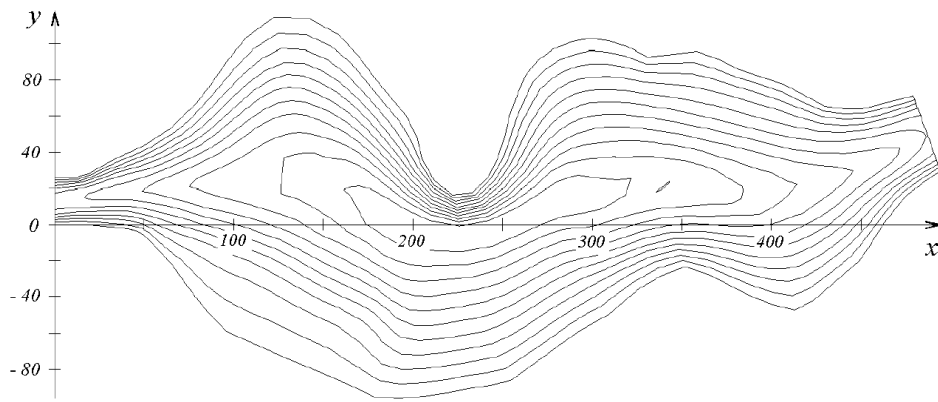
Figure 11.4: The isolines of the depth

11.8   Results of the calculations

Figures show some results of the calculations for the reservoir with the irregular bottom at the same values of the parameters as in the article [15]:

$$k = 1.19 \cdot 10^{-4}, \quad C = 45 \text{ m}^{1/2}\text{sec}^{-1}, \quad u_{in} = 0.5 \text{ m sec}^{-1}, \tag{11.38}$$

where u_{in} is the velocity of the fluid inflow through the inlet Γ_1. The vector of the mass inflow $\vec{\nu}_1$ and the expenditure ν_2 from (11.3) are given as follows:

$$\vec{\nu}_1(x)\Big|_{x \in \Gamma_1} = (h(x)u_{in};\ 0), \quad \nu_2(x)\Big|_{x \in \Gamma_2} = h(x)u_{out},$$

where the constant u_{out} is defined from the equality of the fluid inflow through Γ_1 and its expenditure through Γ_2:

$$\int_{\Gamma_1} (\vec{\nu}_1 \cdot \mathbf{n})d\Gamma + \int_{\Gamma_2} \nu_2 d\Gamma = 0.$$

The point of the intersection of the inlet Γ_1 and the wall Γ_0' is taken as the point M_0 where the total depth is given by the formula (11.6). At this point it is assumed that $H_0 = h(M_0)$. The depth of bottom near the side walls Γ_0' and Γ_0'' is equal to 0.5 m. The depth is about 3 m in the average part of the reservoir.

From Fig.11.6 it is clear that the fluid velocity is high in the places where the stream narrows, in particular, near the inlet and outlet. In other parts of the reservoir the stream is decelerated, and the stagnation zones appear near the left bank.

Opposite to [15] the closed streamlines do not appear in our calculations by the ideal fluid model. The variation of the parameters (11.38) in a rather wide range does not lead to the qualitative modifications in the behaviour of streamlines. In particular, when there is no bottom friction the character of streamlines remains the same as shown in Fig.11.5.

On the other hand, the change in the function which describes the bottom geometry significantly changes the flow. The series of calculations with the different bottom geometry is been done.

Fig.11.7 and Fig.11.8 show two modifications of the original river: the river with the shoal near the outlet, and the river with two shoals near the inlet.

131
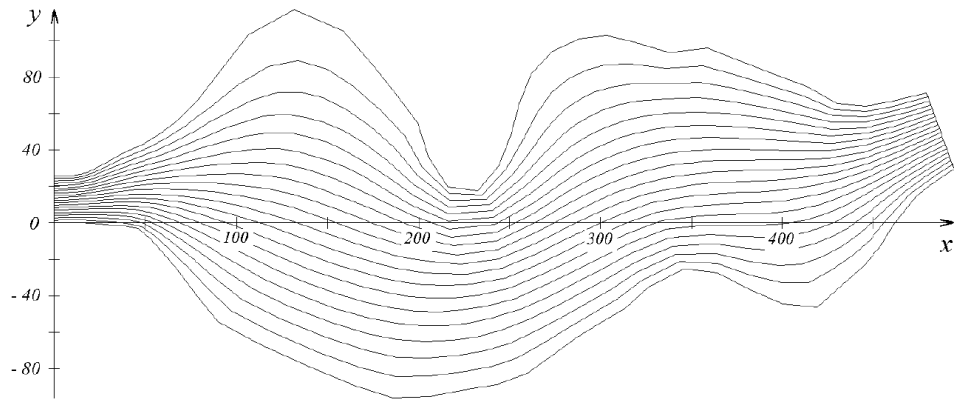
Figure 11.5: The streamlines of the steady flow
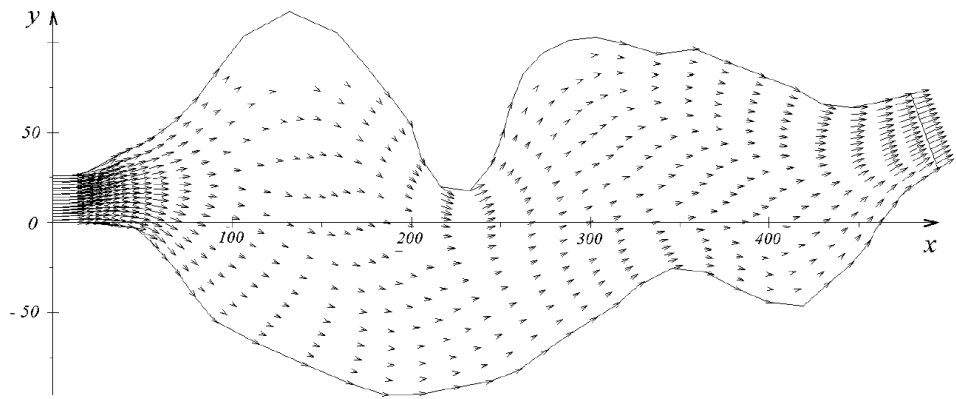
Figure 11.6: The velocity vector field of the steady flow
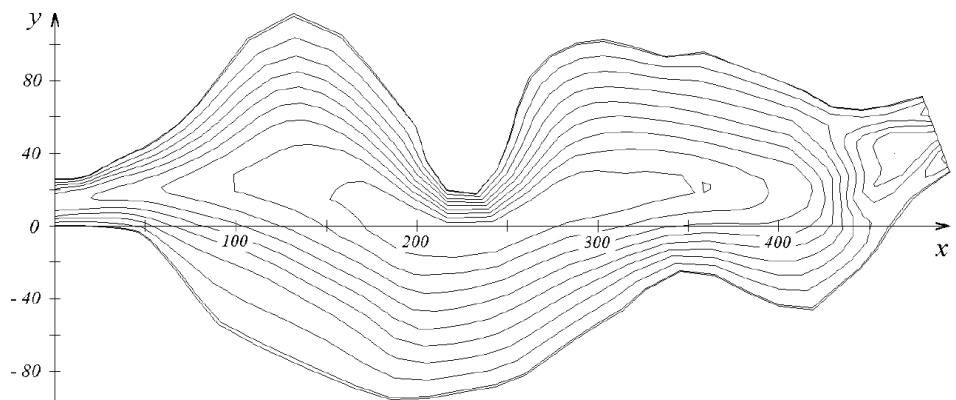
Figure 11.7: The river with the shoal near the outlet
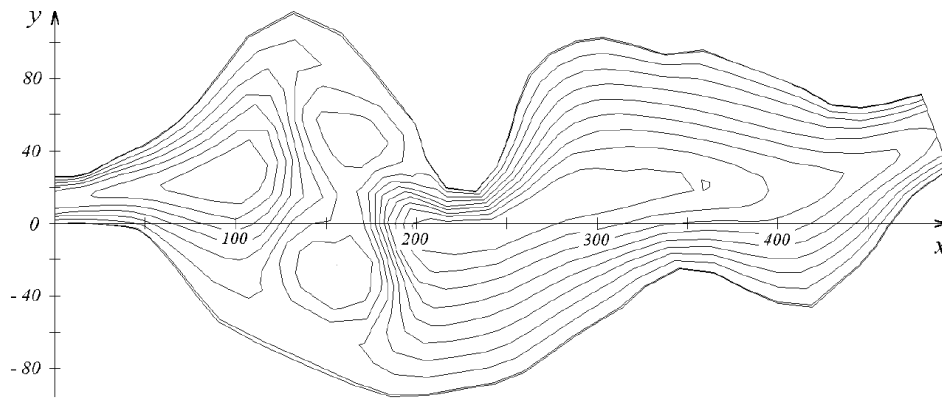
Figure 11.8:   The river with two shoals near the inlet
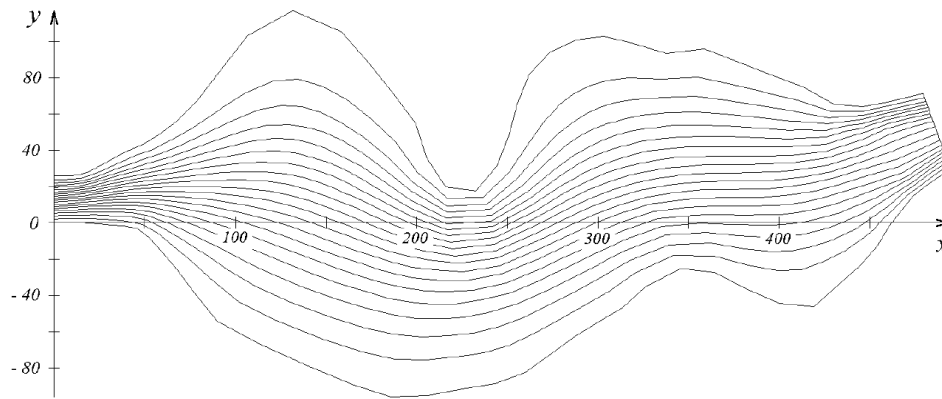
Figure 11.9:   The river with the shoal near the outlet. The streamlines

Fig.11.9 and Fig.11.10 show the streamlines for these examples. The streamlines reflect the changes in the bottom geometry. In the first case the streamlines diverge above the shoal. In the second case the streamlines diverge over the shoals and converge between them.

Fig.11.11 and Fig.11.12 show the velocity vector fields.

If there is the shoal near the outlet, then the flow velocity is increased at the outlet. If there are two shoals, then the velocity is increased between them, and the stagnation zone decreases near the left bank.

The calculations for various velocities of the flow at the inlet are performed. Fig.11.13 shows the velocity vector field using the example of the river with two shoals near the inlet when the fluid velocity is equal to 1 m/sec at the inlet. It is clear that the increased fluid velocity significantly reduces the stagnation zone near the left bank and increases the flow velocity over the entire domain.

133
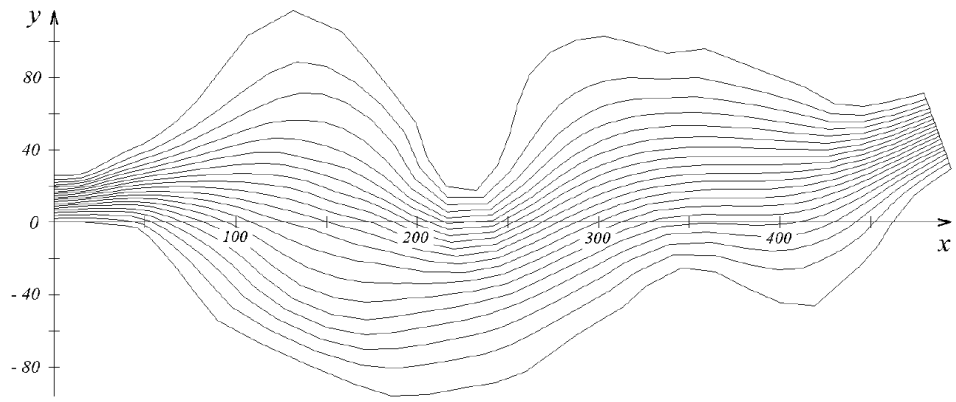
Figure 11.10:   The river with two shoals near the inlet. The streamlines
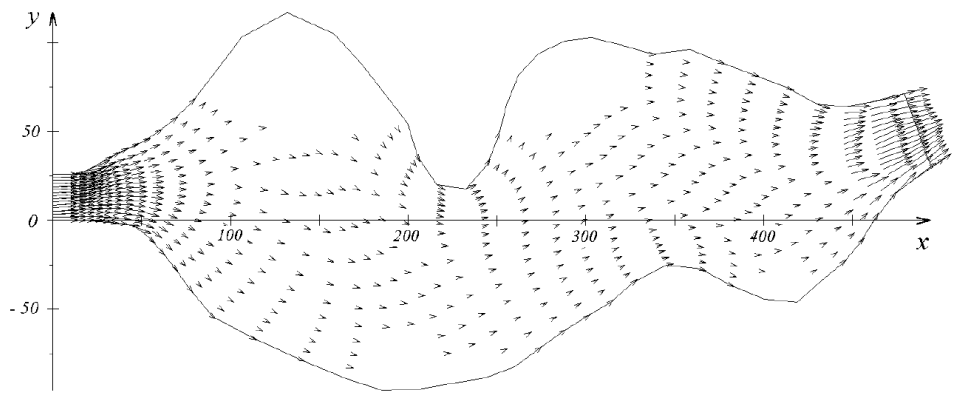
Figure 11.11:   The river with the shoal near the outlet. The velocity vector field
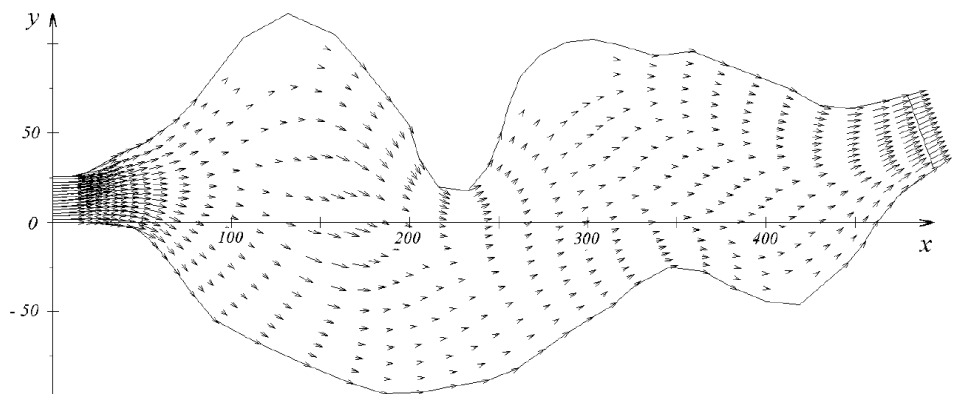
Figure 11.12:   The river with two shoals near the inlet. The velocity vector field

134
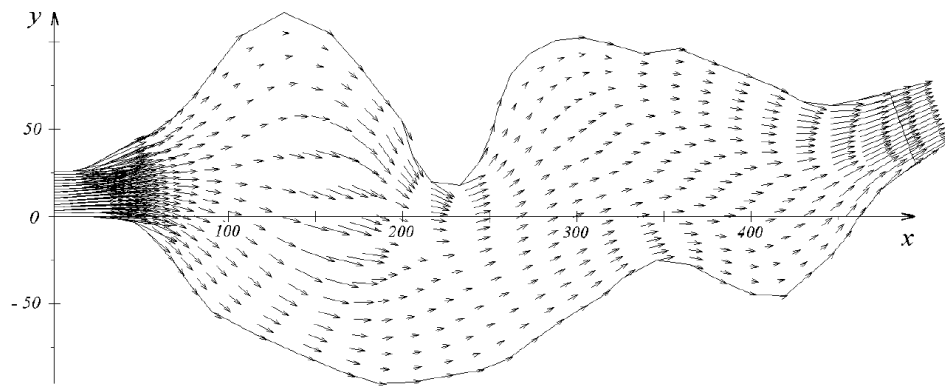
Figure 11.13:   The fluid velocity is equal to 1 m/sec at the inlet

Chapter 12

Calculation of steady flows around the island in the river on the basis of the plane shallow water model

12.1 Statement of the problem

Let us consider the algorithm of calculating steady flows in the river-beds with the islands. As in Chapter 11, we use the shallow water model of the first approximation for ideal incompressible fluid with the free surface for describing the flow. The equations of this model are the same as (11.4), but the domain Ω is multiply connected because there are islands in the river-bed. Further, without limiting the generality, we assume that there is only one island. Therefore, the domain Ω is doubly connected. The exterior boundary of the domain is still denoted by $\Gamma = \Gamma_1 \cup \Gamma_0 \cup \Gamma_2$, and the contour of the island which lies inside Γ is denoted by Γ_0^{is}. Assuming that the boundary of the island is the vertical impermeable wall we come to the conclusion that together with the conditions (11.3) it is necessary to set the additional condition on the boundary of the island:

$$\mathbf{u} \cdot \mathbf{n} \Big|_{x \in \Gamma_0^{is}} = 0. \tag{12.1}$$

This condition leads to the following boundary condition for the stream function on the contour of the island:

$$\psi \Big|_{x \in \Gamma_0^{is}} = \psi^{is} \equiv \text{const}, \tag{12.2}$$

which is obtained on the basis of the expression for the tangential derivative:

$$\frac{\partial \psi}{\partial \tau} \Big|_{x \in \Gamma_0^{is}} = H \mathbf{u} \cdot \mathbf{n} \Big|_{x \in \Gamma_0^{is}}. \tag{12.3}$$

Using the stream function for solving the problems in simply connected domains the values of the stream function on the impermeable walls are constant. They are defined from the given conditions at the inlets and the outlets of the boundary. In the case of doubly connected domain Ω the constant values of ψ on Γ_0 are also defined uniquely. The value of ψ^{is} is not given on the part Γ_0^{is} and it can not be defined before solving the problem. This constant is obtained during the process of solving the problem together with the solution inside the domain.
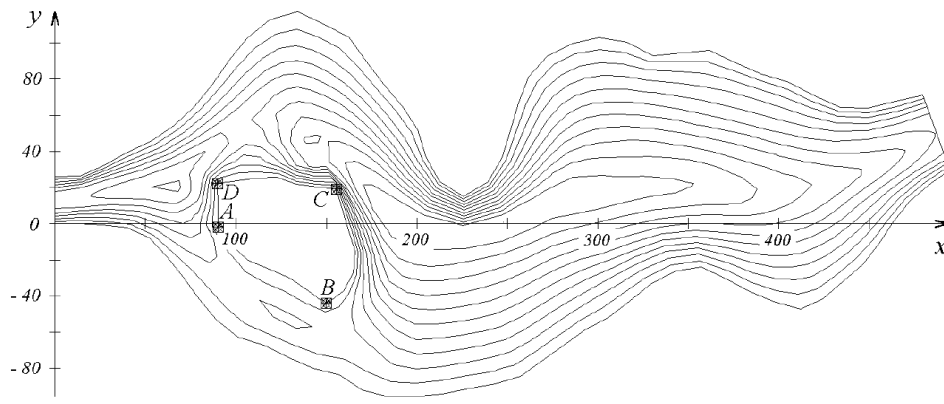
Figure 12.1: The flow domain, the boundary of the island, and the isolines of the depth
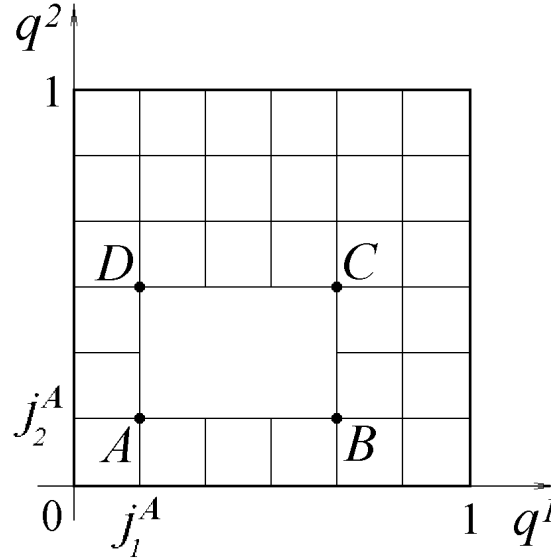
Figure 12.2: The computational domain

12.2 Construction of the curvilinear grid

Fig.12.1 shows the flow domain Ω. The grid for doubly connected domain is constructed on the basis of the variant of two-dimensional equidistribution method for multiply connected domains.

Let us describe the modifications of ED2-method which was used earlier only for simply connected domains. Assuming the boundary of the island Γ_0^{is} is the curvilinear quadrangle we consider that it is the image under the mapping (11.10) of the contour γ_0^{is} of the rectangle which lies inside the unit quadrate in the plane q^1Oq^2. The sides of this rectangle which are the pre-images of the arcs AB, DC, AD, BC are parallel to the axes Oq^1 and Oq^2 respectively (see Fig.12.2).

Thus, in the considered case the computational domain Q is the unit quadrate with the rectangle which is cut out from the quadrate. This rectangle has the contour γ_0^{is}. The domain Q is covered by the rectangular uniform grid $\bar{Q}_h$. The sides of the rectangle γ_0^{is} pass along some lines of this grid. Therefore, the position of the rectangle on the grid and the lengths of its sides are defined by the number of the nodes N_1^{is} on the sides AB
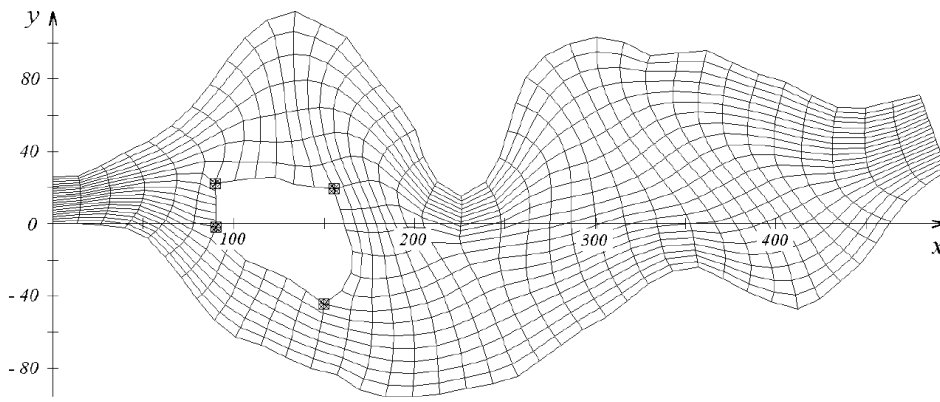
Figure 12.3: The curvilinear grid at $\alpha = 1$
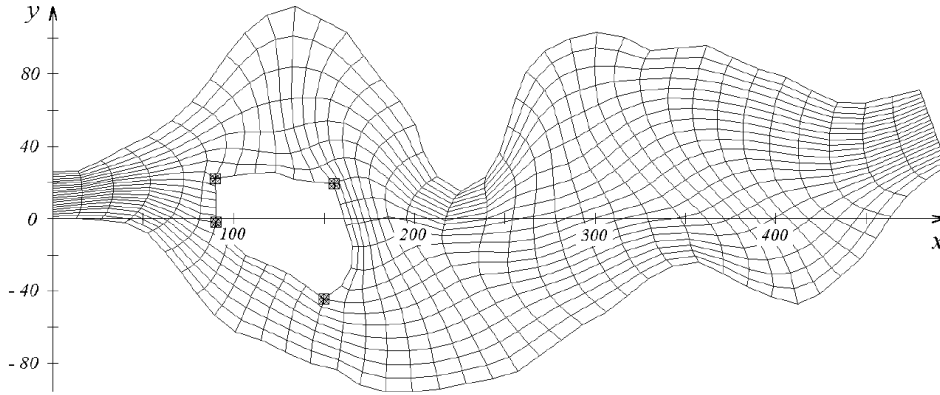
Figure 12.4: The curvilinear grid at $\alpha = 100$

and DC, the number of the nodes N_2^{is} on the sides AD and BC (these numbers are given initially), and with the help of the indication of the node $\mathbf{q}_j^A$ which is the pre-image of the angular point A.

In comparison with simply connected domains it is necessary to place the nodes not only on the exterior boundary Γ, but also on the contour of the island Γ_0^{is}. On each of four sides of this contour either N_1^{is} or N_2^{is} nodes are placed with the help of EDC2-method for plane curves, which is described above. Further the initial approximation is constructed on the basis of the algebraic method, and the iterative process is organized for solving the equations of ED2-method for the definition of the coordinates of the interior nodes of the grid. In the case of multiply connected domain it is more convenient to use the method of successive over relaxation instead of the iterative method of longitudinal-transversal sweeps which was used earlier.

The examples of constructed grids which are shown in Figures 12.3 and 12.4 are obtained for the following control function:

$$w(x^1, x^2) = 1 + \frac{\alpha}{\rho(x^1, x^2)}, \tag{12.4}$$

where ρ is the distance from the point (x^1, x^2) to the centre of the island. It is clear that the grid is condensing in the neighbourhood of the island with the increase in the parameter α.

139
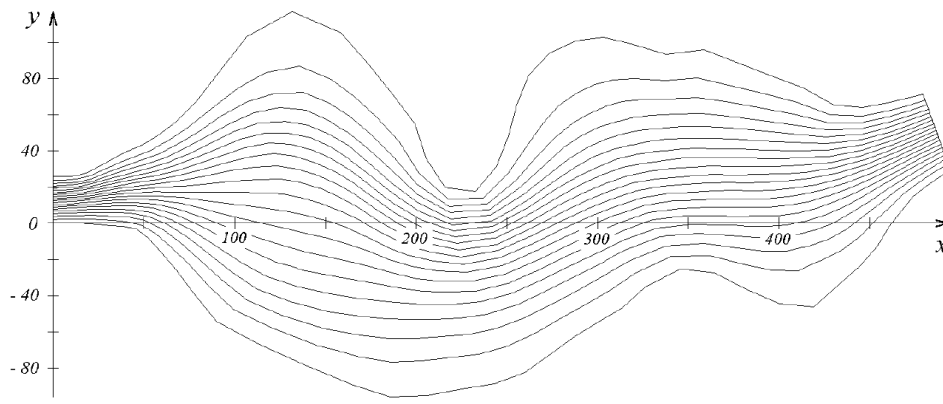
Figure 12.5: The river with the shoal on the depth 0.5 m

Table 12.1: The dependence of the average value ψ_{aver} of the stream function above the shoal on the depth of the shoal.

Depth	0.5	0.25	0.125	0.0625	0.0313	0.0157
ψ_{aver}	1.444	1.433	1.423	1.419	1.417	1.415

12.3 Algorithm

Let us describe the differences between the algorithm for calculating steady flows in simply connected domains and the algorithm for multiply connected domains.

The iterative process, as well as in simply connected domain, consists of the following three stages: the calculation of the potential flow, the calculation of the vortical flow "under the cover", and the calculation of the vortical flow with the free surface.

Beginning with the calculation of the potential flow for realisation of the first iteration it is necessary to know the value of ψ^{is} on the contour of the island Γ_0^{is}. For the definition of this value we proceed as follows.

Instead of the island we consider the shoal with the constant depth of the bottom. The shoal is placed in that place where the island should be. In this case we can perform the calculation of flow in simply connected domain with the shoal.

The streamlines diverge above the shoal, and the stream function has an almost constant value above the shoal. By carrying out some calculations with the decreasing depth it is possible to define the limiting value of the stream function when the depth of the shoal close to zero. This approximate value of ψ is taken on the first iteration as the value of ψ^{is}.

The calculations in simply connected domain are carried out for the shoals with various depths. Figures 12.5-12.7 show the streamlines. The streamlines diverge above the shoal as the water depth decreases.

Table 12.1 shows the dependence of the average value ψ_{aver} of the stream function above the shoal on the depth of the shoal. The results of the calculations show that with the decrease in the depth the average value of ψ has the limiting value ψ^{is}.

During the next iterations the value of ψ^{is} is defined uniformly either for the potential flow "under the cover" or for the vortical flow. Therefore, we shall explain the algorithm
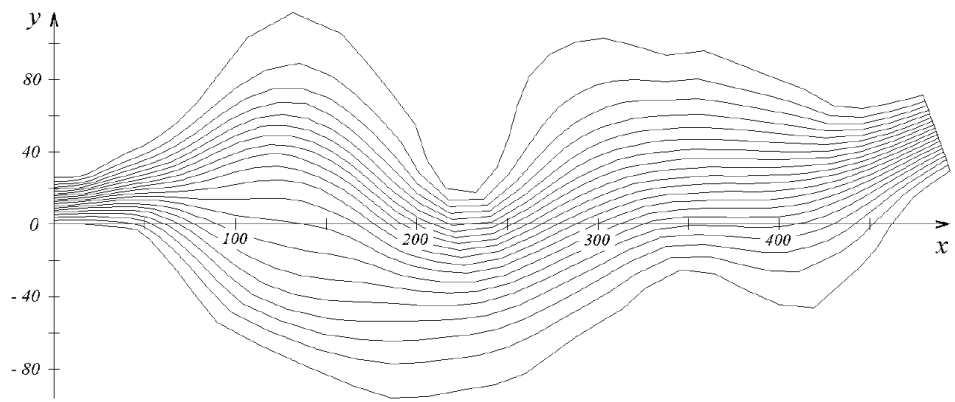
Figure 12.6: The river with the shoal on the depth 0.125 m
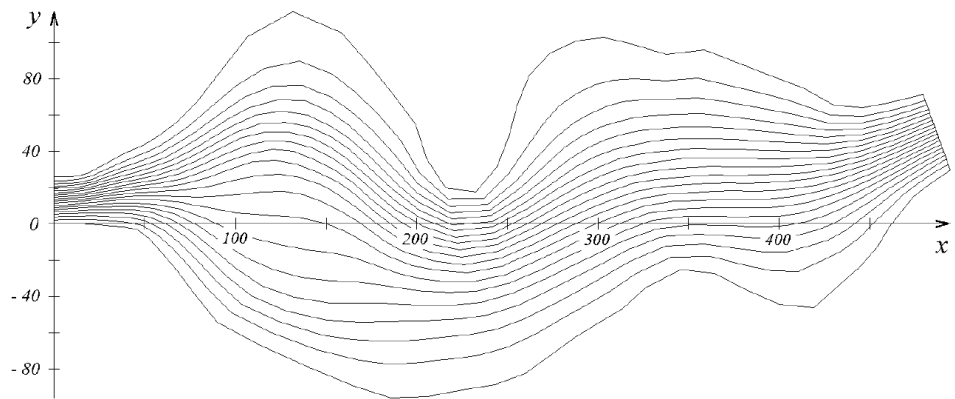
Figure 12.7: The river with the shoal on the depth 0.0313 m

141

of calculating ψ^{is} for the last case. The expression (11.28) for the vorticity is written in the following form:

$$J\omega = -\frac{\partial v_1}{\partial q^2} + \frac{\partial v_2}{\partial q^1}. \tag{12.5}$$

It is integrated over the domain Q:

$$\int\limits_Q \int J\omega dq^1 dq^2 = \oint\limits_\gamma \left(v_1 dq^1 + v_2 dq^2\right) + \oint\limits_{\gamma_0^{is}} \left(v_1 dq^1 + v_2 dq^2\right). \tag{12.6}$$

This expression is used for calculating the constant ψ^{is} on the $(n+1)$-th iteration. It is supposed that all values are already known on the n-th iteration. Therefore, the integral in the left-hand side and the first integral in the right-hand side can be defined numerically using, for example, the quadrature formula of rectangles. Here the Jacobian and the vorticity are defined at the mesh centres. The component v_1 is calculated at the centres of the horizontal sides of the meshes which are adjacent to the appropriate parts of the boundary. The component v_2 is calculated at the centres of the vertical sides of the meshes near the boundary. The connection between the covariant and contravariant components of the velocity vector is used for calculating these components. The contravariant components of the velocity vector are calculated by the stream function under the formulas (7.29). The values of ψ are known on the exterior boundary γ from the boundary conditions. The normal derivative of ψ is known at the inlet.

On calculating the second integral in (12.6) it is necessary to substitute the unknown value of ψ^{is} into the approximating formula instead of the values of ψ on γ_0^{is}. This value is constant, therefore there are no derivatives of ψ in the tangential direction to γ_0^{is} in the resulting formula.

Thus, we obtain the following equation for calculating ψ^{is}:

$$L = R_1 + \psi^{is} \cdot a + b, \tag{12.7}$$

where L is the approximation of the integral in the left-hand side of (12.6), R_1 is the approximation of the first integral in the right-hand side of (12.6).

$$a = -\left[\frac{h_2}{h_1} \cdot \sum_{j_2=j_2^A}^{j_2^A+N_2^{is}-2} \left\{ \left(\frac{g_{22}}{HJ}\right)_{j_1^A,j_2+1/2} + \left(\frac{g_{22}}{HJ}\right)_{j_1^B,j_2+1/2} \right\} + \right.$$

$$\left. + \frac{h_1}{h_2} \cdot \sum_{j_1=j_1^A}^{j_1^A+N_1^{is}-2} \left\{ \left(\frac{g_{11}}{HJ}\right)_{j_1+1/2,j_2^A} + \left(\frac{g_{11}}{HJ}\right)_{j_1+1/2,j_2^D} \right\} \right],$$

$$b = \frac{h_2}{2h_1} \cdot \sum_{j_2=j_2^A}^{j_2^A+N_2^{is}-2} \left\{ \left(\frac{g_{22}}{HJ}\right)_{j_1^A,j_2+1/2} \cdot \left(\psi_{j_1^A-1,j_2+1} + \psi_{j_1^A-1,j_2}\right) + \right.$$

$$\left. + \left(\frac{g_{22}}{HJ}\right)_{j_1^B,j_2+1/2} \cdot \left(\psi_{j_1^B+1,j_2+1} + \psi_{j_1^B+1,j_2}\right) \right\} +$$

142

$$+ \frac{h_1}{2h_2} \cdot \sum_{j_1 = j_1^A}^{j_1^A + N_1^{is} - 2} \left\{ \left(\frac{g_{11}}{HJ} \right)_{j_1 + 1/2, j_2^A} \cdot \left(\psi_{j_1 + 1, j_2^A - 1} + \psi_{j_1, j_2^A - 1} \right) + \right.$$

$$\left. + \left(\frac{g_{11}}{HJ} \right)_{j_1 + 1/2, j_2^D} \cdot \left(\psi_{j_1 + 1, j_2^D + 1} + \psi_{j_1, j_2^D + 1} \right) \right\},$$

j_1^A, j_2^A, j_1^B, j_2^D are the indices of the vertexes of the rectangle $ABCD$ (see Fig.12.1). It is easy to see that $a < 0$.

Let us describe the algorithm for calculating ψ^{is} in the iterative process of calculating the fluid flow with the free surface. This process works after the iterative process of calculating the flow "under the cover" has converged. As it was described in Chapter 11, it is necessary to calculate the complete depth H at this stage. In the case of simply connected domain H is calculated with the help of the integrated relation (11.23). Therefore, the value of p does not depend on the contour of the integration $\gamma(q_0, q_j)$. For the value of p the condition of the independence of the integration contour is also necessary in doubly connected domain, and the value ψ^{is} is defined from this condition.

Let γ^1 and γ^2 be the curves from the formula (11.23). They connect the point q_j where it is required to define p with the point q_0 where p_0 is given. In addition, let D be the domain which is limited by these curves and is not containing γ_0^{is} in itself. Therefore, D is simply connected domain. The boundary of the domain D is denoted by L. Then for the value of p the condition of independence of the curves γ^1 and γ^2 is written as the following equality:

$$\oint_L \left(f_1 + HJv^2(\omega + f_{Cor}) \right) dq^1 + \left(f_2 - HJv^1(\omega + f_{Cor}) \right) dq^2 = 0. \tag{12.8}$$

The domain D is simply connected, therefore, it is possible to apply the Green's formula to the left-hand side of this relation. Thus, we obtain the condition of independence as follows:

$$\int_D \int \left[\frac{\partial}{\partial q^1} \left(HJv^1(\omega + f_{Cor}) \right) + \frac{\partial}{\partial q^2} \left(HJv^2(\omega + f_{Cor}) \right) \right] dq^1 dq^2 =$$

$$= \int_D \int \left[-\frac{\partial f_1}{\partial q_2} + \frac{\partial f_2}{\partial q_1} \right] dq^1 dq^2. \tag{12.9}$$

In view of the continuity equation which has the following form in curvilinear coordinates:

$$\frac{\partial}{\partial q^1} \left(HJv^1 \right) + \frac{\partial}{\partial q^2} \left(HJv^2 \right) = 0, \tag{12.10}$$

we come to the conclusion that the equality (12.9) is fulfilled by virtue of the realisation of the vorticity equation (11.12).

Thus, if the curve L does not contain in itself the contour of the island γ_0^{is}, then the value of p does not depend on the curves γ^1 and γ^2. At the difference level the given statement is proved, as in Chapter 11, with the help of the formulas (11.24)–(11.26).

Now we shall consider the case when the curves γ^1 and γ^2 make the closed curve L which envelopes the boundary of the island γ_0^{is}. Therefore, the domain D is doubly connected. Thus [43], the curvilinear integral along the curve L is equal to the curvilinear integral along the boundary of the island γ_0^{is}. The condition (12.8) for p to be independent of the curve L has the following form:

$$\oint_{\gamma_0^{is}} \left(f_1 + HJv^2(\omega + f_{Cor}) \right) dq^1 + \left(f_2 - HJv^1(\omega + f_{Cor}) \right) dq^2 = 0. \tag{12.11}$$

Using the impermeability condition (12.1), which look as follows in the curvilinear coordinates (see Fig.12.1):

$$v^1 \Big|_{AD} = v^1 \Big|_{BC} = 0, \quad v^2 \Big|_{AB} = v^2 \Big|_{DC} = 0, \tag{12.12}$$

the condition (12.11) can be written:

$$\oint_{\gamma_0^{is}} \left[H \frac{\partial}{\partial q^1} \left(h - \frac{V^2}{2} \right) - \frac{1}{f_{Ch}^2} v_1 V \right] dq^1 + \left[H \frac{\partial}{\partial q^2} \left(h - \frac{V^2}{2} \right) - \frac{1}{f_{Ch}^2} v_2 V \right] dq^2 = 0.$$

$$\tag{12.13}$$

As well as for the banks of the river in Chapter 11, here we assume that the depth of the bottom h near the banks of the island is the constant value. In addtition, by virtue of the conditions (12.12) we obtain the following:

$$v_1 \Big|_{AB} = v_1 \Big|_{DC} = g_{11} v^1, \quad v_2 \Big|_{AD} = v_2 \Big|_{BC} = g_{22} v^2, \tag{12.14}$$

$$u^2 \Big|_{AB} = u^2 \Big|_{DC} = g_{11} \left(v^1 \right)^2, \quad u^2 \Big|_{AD} = u^2 \Big|_{BC} = g_{22} \left(v^2 \right)^2.$$

Taking into account the constancy of the depth h near the banks of the island, and the expression (12.14), the condition for p to be independent of the integration curve has the following form:

$$\oint_{\gamma_0^{is}} \left[-\frac{1}{2} H \frac{\partial}{\partial q^1} \left(g_{11} \left(v^1 \right)^2 \right) - \frac{1}{f_{Ch}^2} g_{11} v^1 \sqrt{g_{11}} |v^1| \right] dq^1 +$$

$$+ \left[-\frac{1}{2} H \frac{\partial}{\partial q^1} \left(g_{22} \left(v^2 \right)^2 \right) - \frac{1}{f_{Ch}^2} g_{22} v^2 \sqrt{g_{22}} |v^2| \right] dq^2 = 0. \tag{12.15}$$

Expressing the contravariant components of the velocity vector v^α through ψ by the formulas (7.29) and approximating them by one-sided differences we obtain the equation for calculating ψ^{is}.

Let us make some notes about the singularities of the iterative process for calculating the flow in the river channel with the island in comparison with the algorithm which is described in Chapter 11. The stream function ψ is also calculated with the help of the method of successive over relaxation only in the interior nodes of the grid which covers
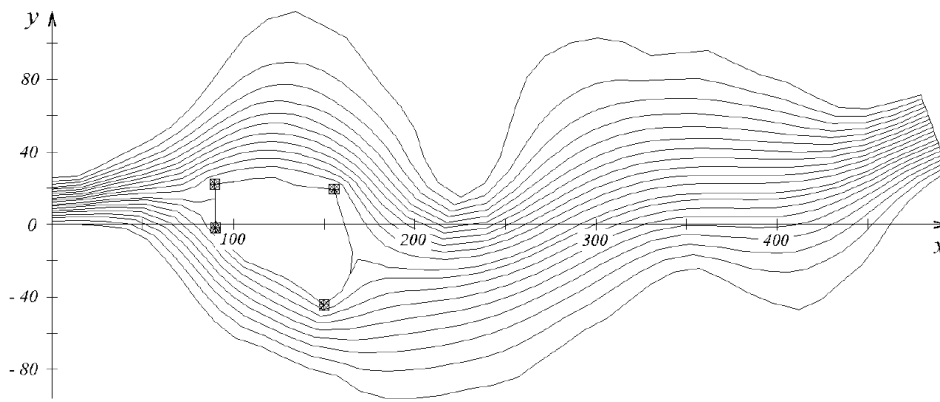
Figure 12.8: The streamlines of the steady vortical flow

the domain Q. Thus, the iterations are not carried out in the nodes of the grid which covers the island.

For calculating the vorticity function ω the method of stabilizing corrections is also applied. It is realized with the help the horizontal and vertical sweeps. But in the case of the island the horizontal sweeps on the lines intersecting with the island are carried out separately for the parts of the lines which lie further to the left of the island and for the parts of the lines which lie further to the right of the island. The same procedure is performed for the vertical sweeps: if the coordinate line intersects with the island, then it is divided in two parts, and the sweep is carried out separately for the lower and upper parts of the line.

In addition, the boundary values of ω on the contour of the island are not required either for the horizontal sweeps or for the vertical sweeps by virtue of the realisation of the impermeability conditions on the boundary of the island.

12.4   Calculation results

In this section some results of the calculations for the reservoir with the irregular bottom are presented for the same values of the parameters (11.37) as in Chapter 11, but in the presence of the island.

Fig.12.8 shows the streamlines of the steady vortical fluid flow with the free surface.

Fig.12.9 shows the velocity vector field of the steady vortical flow.

Fig.12.10 shows the velocity vector field of the vortical flow around the island in the enlarged form. The part of the domain is "cut off" along the lines of the grid.

The calculations for various velocities of the flow at the inlet are carried out. Fig.12.11 and Fig.12.12 show the velocity vector field at $u_{in} = 1$ m/sec.

On comparing the velocity vector fields over the entire domain in Fig.12.9 and Fig.12.11 it is clear that the increase in the fluid velocity at the inlet leads to the increase in the fluid velocity over the entire domain, and to the increase in the stagnation zones behind the island and near the boundaries of the river-bed. On comparing Fig.12.10 and Fig.12.12 it is clear that the fluid velocity is increased when the fluid approaches the island, and when the fluid goes around the island. At $u_{in} = 1$ m/sec the flow behind the island is decelerated in the greater degree than at $u_{in} = 0.5$ m/sec.

145

Figure 12.9: The velocity vector field of the steady vortical flow
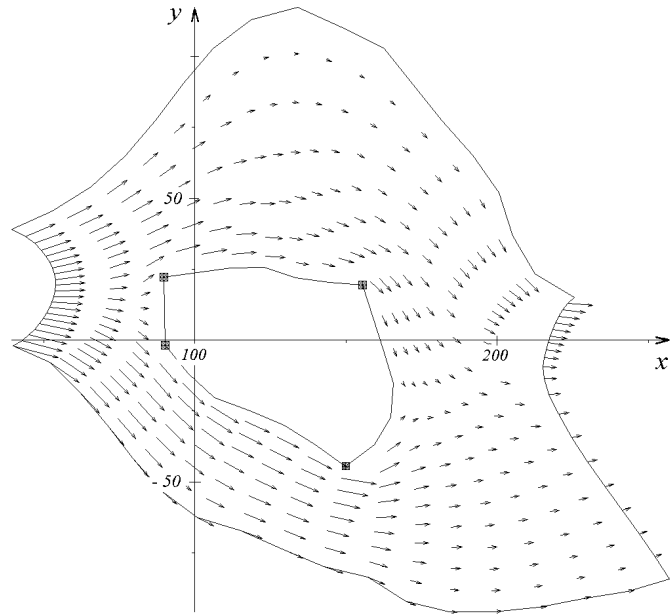
Figure 12.10: The velocity vector field of the steady vortical flow around the island
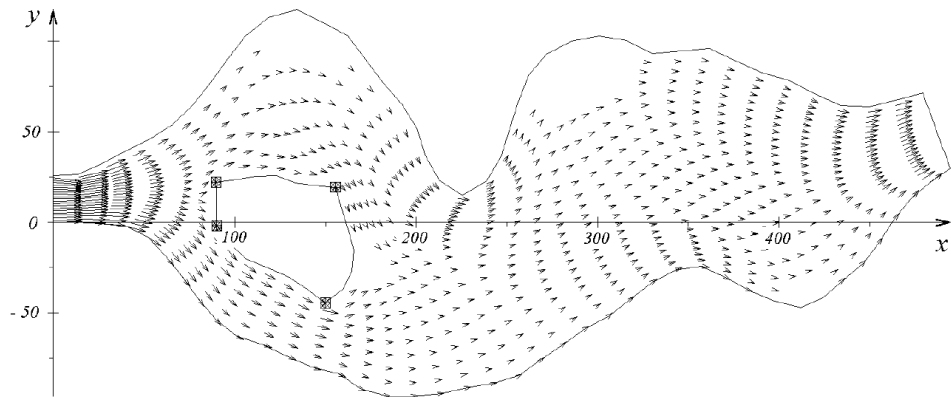
Figure 12.11: The velocity vector field at $u_{in} = 1$ m/sec

146
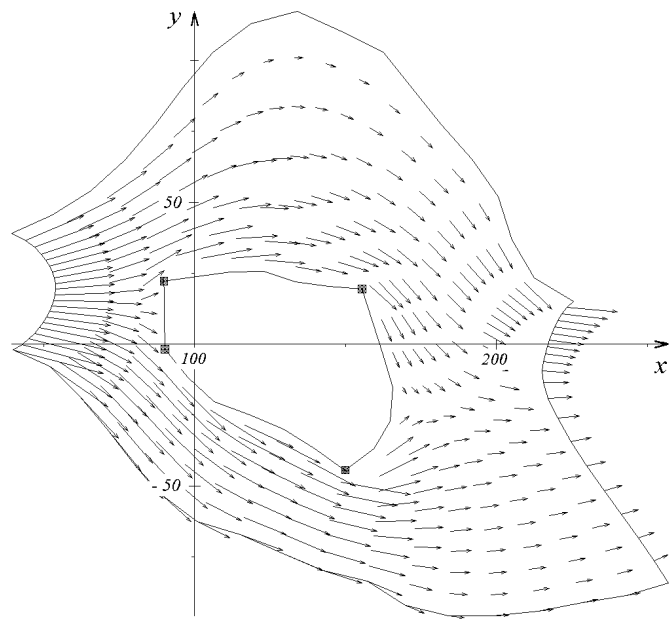
Figure 12.12:   The velocity vector field around the island at $u_{in} = 1$ m/sec

147

Chapter 13

Conclusion

In the present thesis the iterative finite difference methods are developed for the numerical solution of steady ideal compressible and incompressible fluid flows in the domains of complicated geometry. The following basic results are obtained.
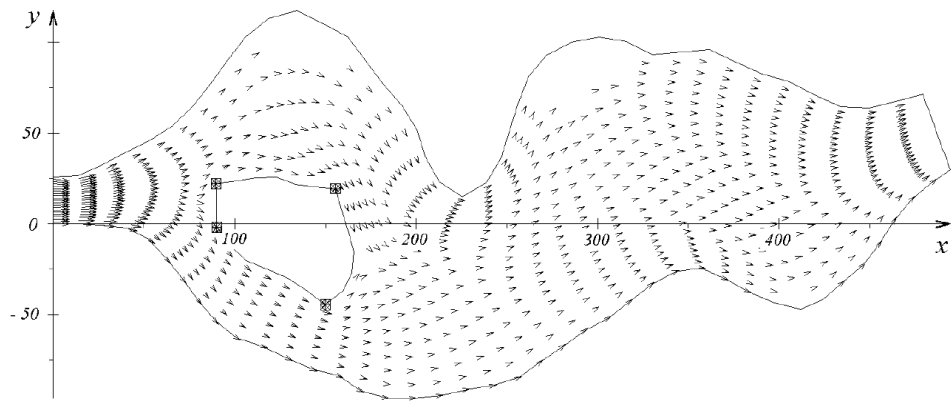
1. On the basis of the equidistribution principle the equations for constructing two-dimensional adaptive grids are obtained. The equivalence of the principle and the differential equations of the equidistribution method is proved. It is shown that the coordinates of any quasi-orthogonal adaptive grid satisfy the difference equations of the equidistribution method.

2. The iterative finite difference method for the numerical solution on adaptive grids of two-dimensional stationary problems on ideal fluid flows through the channels of complicated geometry is developed using new dependent variables: the stream function and the vorticity function. It is proved that the iterative process has the property of the preservation of the constant flow on an arbitrary curvilinear grid.

3. The original nine-point approximation of the equation for the stream function is obtained. In curvilinear coordinates the equation has variable coefficients and terms with the mixed derivatives. The appropriate difference operator is proved to be self-adjoint and positively definite. It is shown that for the grid functions, which assign the correspondence between the nodes of the physical domain and the nodes of the computational domain, the obtained difference equation is satisfied identically at the zero right part.

4. The approximations of the equations for the vorticity function and the total energy are constructed with the upstream differences on the curvilinear grids using the variable pattern. It is shown that if there are no closed streamlines and stationary points of the gas, then it is possible to calculate the values of the vorticity function and the total energy in any node through the values of these functions at the inlet of the domain with the help of the non-iterative method of running calculation.

5. It is shown that the coordinated approximation for the equations for the vorticity function and the finite-difference relations which are obtained approximating the equations of motion in the Gromeka-Lamb form is necessary for the values of the pressure to be independent of the integration path using the marching method on curvilinear grids.

6. The mathematical statement of three-dimensional problem on ideal incompressible fluid flows through the given domain of complicated form in the curvilinear system of coordinates using new dependent variables, i.e. the vector potential and the vorticity vector, is formulated.

7. The equidistribution principle is formulated and the equations of the equidistribu-

tion method for constructing three-dimensional adaptive grids are obtained. The equivalence of the principle and the differential equations of the equidistribution method is proved. The conditions are formulated under which the grid on the boundary of three-dimensional domain can be constructed by the equidistribution method using the same control function as inside the domain. The differential equations of the equidistribution method for the space surfaces and curves are obtained. The iterative algorithms for solving the difference equations for constructing adaptive grids are developed.

8. The finite difference approximations on curvilinear grids of the equations and the boundary conditions for the covariant components of the vector potential are obtained. The vector potential is not assumed to be solenoidal. The marching implicit method of calculating the contravariant components of the vorticity vector is developed. It is shown that making use of the staggered curvilinear grids for the approximation of the contravariant components of the velocity vector the difference continuity equation is fulfilled on each step of the iterative process.

9. The developed algorithms for calculating ideal gas flows are applied to solving the numerical problems on fluid flows with the surface gravitational waves in the river beds of complicated configuration within the framework of the plane shallow water model of the first approximation. The iterative process for solving the difference problem on steady fluid flows is developed which is used for calculations of potential and vortical flows with the surface waves in the river beds with the possible presence of the islands.

10. The developed algorithms are realized as the complexes of computer codes for the numerical solution of the problems on ideal gas and fluid flows through the channels of complicated configuration.

Chapter 14

Appendix

Lemma 3.1. *The contravariant components of the velocity satisfy the following relations on the boundary* $\gamma = \partial Q$:

$$v^1 \Big|_{\gamma_1} > 0, \quad v^1 \Big|_{\gamma_2} > 0, \quad v^2 \Big|_{\gamma_0' \cup \gamma_0''} = 0. \tag{3.11}$$

Proof. First of all, it should be mentioned that the contravariant components of the velocity can be expressed using Cartesian components as follows:

$$v^1 = \frac{y_{q^2}}{J} u_1 - \frac{x_{q^2}}{J} u_2,$$

$$v^2 = -\frac{y_{q^1}}{J} u_1 + \frac{x_{q^1}}{J} u_2. \tag{5.A1}$$

Let us prove that $v^1 \Big|_{\gamma_1} > 0$. The vector $\vec{\tau}$ tangential to the boundary Γ_1 has the coordinates $\vec{\tau} = (x_{q^2}, y_{q^2})$. The vector perpendicular to it has the following coordinates: $\mathbf{m} = (-y_{q^2}, x_{q^2})$, $|\mathbf{m}| = \sqrt{x_{q^2}^2 + y_{q^2}^2} = \sqrt{g_{22}}$. Therefore, the vector normal to Γ_1 is the following:

$$\mathbf{n} = \frac{\mathbf{m}}{|\mathbf{m}|} = \left(-\frac{y_{q^2}}{\sqrt{g_{22}}}, \frac{x_{q^2}}{\sqrt{g_{22}}}\right).$$

Γ_1 is the inlet of Ω, therefore, $\mathbf{u} \cdot \mathbf{n} < 0$ at Γ_1:

$$\mathbf{u} \cdot \mathbf{n} = -\frac{y_{q^2}}{\sqrt{g_{22}}} u_1 + \frac{x_{q^2}}{\sqrt{g_{22}}} u_2 = \left(-\frac{y_{q^2}}{J} u_1 + \frac{x_{q^2}}{J} u_2\right) \frac{J}{\sqrt{g_{22}}} < 0.$$

Using (5.A1) we obtain that $v^1 \Big|_{\gamma_1} > 0$.

Now we shall prove that $v^1 \Big|_{\gamma_2} > 0$. Similarly the vector $\vec{\tau}$ tangential to Γ_2 is considered. And the vector $\mathbf{m}$ which is perpendicular to Γ_2 and external to Q is considered. The coordinates of the vectors are the following: $\vec{\tau} = (x_{q^2}, y_{q^2})$, $\mathbf{m} = (y_{q^2}, -x_{q^2})$.

Therefore, the vector normal to Γ_2: $\mathbf{n} = \left(\frac{y_{q^2}}{\sqrt{g_{22}}}, -\frac{x_{q^2}}{\sqrt{g_{22}}}\right)$. Γ_2 is the outlet of Ω, therefore, $\mathbf{u} \cdot \mathbf{n} > 0$. Thus,

$$\mathbf{u} \cdot \mathbf{n} = \frac{y_{q^2}}{\sqrt{g_{22}}} u_1 - \frac{x_{q^2}}{\sqrt{g_{22}}} u_2 = \left(\frac{y_{q^2}}{J} u_1 - \frac{x_{q^2}}{J} u_2\right) \frac{J}{\sqrt{g_{22}}} > 0.$$

Using (5.A1) we obtain that $v^1 \Big|_{\gamma_2} > 0$.

Now we shall show that $v^2\big|_{\gamma_0'\cup\gamma_0''} = 0$. Let us consider, for example, Γ_0''. The tangential vector $\vec{\tau}$, and the vector $\mathbf{m}$ which is perpendicular to $\vec{\tau}$ have the following coordinates: $\vec{\tau} = (x_{q^1}, y_{q^1})$, $\quad \mathbf{m} = (-y_{q^1}, x_{q^1})$.

The normal vector is $\mathbf{n} = (-\frac{y_{q^1}}{\sqrt{g_{11}}}, \frac{x_{q^1}}{\sqrt{g_{11}}})$. $\mathbf{u}\cdot\mathbf{n}\big|_{\mathbf{x}\in\Gamma_0''} = 0$. Therefore,

$$\mathbf{u}\cdot\mathbf{n}\Big|_{\mathbf{x}\in\Gamma_0''} = -\frac{y_{q^1}}{\sqrt{g_{11}}}u_1 + \frac{x_{q^1}}{\sqrt{g_{11}}}u_2 = \left(-\frac{y_{q^1}}{J}u_1 + \frac{x_{q^1}}{J}u_2\right)\frac{J}{\sqrt{g_{11}}} = 0.$$

From here it follows that $v^2\big|_{\gamma_0''} = 0$. The proof for γ_0' is similar. Thus, the lemma is proved completely.

Lemma 4.1. *If the mapping (4.23) assigned by the solutions of the equations (4.27) is non-degenerate and orthogonal, then the equidistribution principle (4.26) is fulfilled for it.*

Proof. Using the equation $g_{12} = 0$ from the statement of the lemma and the following identity:

$$g_{\beta\beta}\frac{\partial x^\alpha}{\partial q^{3-\beta}} - g_{12}\frac{\partial x^\alpha}{\partial q^\beta} = (-1)^{\alpha+\beta-1}J\frac{\partial x^{3-\alpha}}{\partial q^\beta}, \qquad \alpha, \beta = 1, 2,$$

where the summation on the repeating indices α and β is not made, we obtain the relations:

$$g_{22}\frac{\partial x^\alpha}{\partial q^1} = (-1)^{\alpha+1}J\frac{\partial x^{3-\alpha}}{\partial q^2}, \quad g_{11}\frac{\partial x^\alpha}{\partial q^2} = (-1)^\alpha J\frac{\partial x^{3-\alpha}}{\partial q^1}, \quad \alpha = 1, 2.$$

Substituting them into the equations (4.27) we obtain the homogeneous system of two equations:

$$\frac{\partial wJ}{\partial q^1}\frac{\partial x^\alpha}{\partial q^2} - \frac{\partial wJ}{\partial q^2}\frac{\partial x^\alpha}{\partial q^1} = 0, \qquad \alpha = 1, 2,$$

with respect to the derivatives $\partial wJ/\partial q^\alpha$. The determinant of this system is equal to the Jacobian J. According to the assumption $J \neq 0$ the system has only the trivial solution $\partial wJ/\partial q^\alpha = 0$, $\alpha = 1, 2$. Thus, $wJ = \text{const}$.

Lemma 4.2. *The coordinates of the nodes of any quasiorthogonal adaptive grid with convex meshes satisfy the equations (4.38).*

Proof. Using the operators (4.30)–(4.31) we obtain the following formulas for the grid functions x_j^α:

$$\left(g_{\beta\beta}D_{q^{3-\beta}}x^\alpha - g_{12}D_{q^\beta}x^\alpha\right)_{j+1/2} = (-1)^{\alpha+\beta-1}\left(JD_{q^\beta}x^{3-\alpha}\right)_{j+1/2}, \tag{5.A2}$$

$\alpha, \beta = 1, 2$, the summation on the indices α and β is not made. Therefore, taking into account the quasiorthogonality condition (4.41) the left-hand side of the equation (4.38) can be written in the following form:

$$\frac{1}{2}\left\{\left((D_{q^1}wJ)D_{q^2}x^\alpha\right)_{j_1, j_2+1/2} + \left((D_{q^1}wJ)D_{q^2}x^\alpha\right)_{j_1, j_2-1/2} - \right.$$

$$- \left((D_{q^2}wJ)D_{q^1}x^\alpha\right)_{j_1+1/2,j_2} - \left((D_{q^2}wJ)D_{q^1}x^\alpha\right)_{j_1-1/2,j_2} \Big\}.$$

If the grid is adaptive, then each item in the identity (5.A2) becomes equal to zero. Therefore, the coordinates of the grid satisfy the equation (4.38). Thus, the lemma is proved.

Lemma 5.1. *The difference operator A is self-adjoint.*

Proof. It is necessary to prove that for the abitrary functions $\overset{\circ}{\varphi}, \overset{\circ}{\psi} \in \mathcal{H}$ the equality is fulfilled:

$$(A \overset{\circ}{\psi}, \overset{\circ}{\varphi}) = (\overset{\circ}{\psi}, A \overset{\circ}{\varphi}).$$

We have the following relations:

$$(A \overset{\circ}{\psi}, \overset{\circ}{\varphi}) = - \sum_{j_1=2}^{N_1-1} \sum_{j_2=2}^{N_2-1} (\Lambda\psi \, \overset{\circ}{\varphi})_{j_1,j_2} h_1 h_2 =$$

$$= - \sum_{j_1=2}^{N_1-1} \sum_{j_2=2}^{N_2-1} (D_{q^1}(k_{11}D_{q^1}\psi + k_{12}D_{q^2}\psi)+$$

$$+ D_{q^2}(k_{12}D_{q^1}\psi + k_{22}D_{q^2}\psi))_{j_1,j_2} \, \overset{\circ}{\varphi}_{j_1,j_2} \, h_1 h_2 =$$

$$= -\frac{1}{2} \sum_{j_1=2}^{N_1-1} \sum_{j_2=2}^{N_2-1} \left[(D_{q^1}F^1)_{j_1,j_2+\frac{1}{2}} \, \overset{\circ}{\varphi}_{j_1,j_2} + (D_{q^1}F^1)_{j_1,j_2-\frac{1}{2}} \, \overset{\circ}{\varphi}_{j_1,j_2} \right] h_1 h_2 -$$

$$-\frac{1}{2} \sum_{j_1=2}^{N_1-1} \sum_{j_2=2}^{N_2-1} \left[(D_{q^2}F^2)_{j_1+\frac{1}{2},j_2} \, \overset{\circ}{\varphi}_{j_1,j_2} + (D_{q^2}F^2)_{j_1-\frac{1}{2},j_2} \, \overset{\circ}{\varphi}_{j_1,j_2} \right] h_1 h_2.$$

$\varphi = 0$ in the boundary nodes, therefore, we can change the limits of the integration in the last expression:

$$(A \overset{\circ}{\psi}, \overset{\circ}{\varphi}) =$$

$$= -\frac{1}{2} \sum_{j_1=2}^{N_1-1} \sum_{j_2=1}^{N_2-1} \left[(D_{q^1}F^1)_{j_1,j_2+\frac{1}{2}}\varphi_{j_1,j_2} + (D_{q^1}F^1)_{j_1,j_2+\frac{1}{2}}\varphi_{j_1,j_2+1} \right] h_1 h_2 -$$

$$-\frac{1}{2} \sum_{j_1=1}^{N_1-1} \sum_{j_2=2}^{N_2-1} \left[(D_{q^2}F^2)_{j_1+\frac{1}{2},j_2}\varphi_{j_1,j_2} + (D_{q^2}F^2)_{j_1+\frac{1}{2},j_2}\varphi_{j_1+1,j_2} \right] h_1 h_2 =$$

$$= -\frac{1}{2} \sum_{j_1=2}^{N_1-1} \sum_{j_2=1}^{N_2-1} \left[\frac{F^1_{j_1+\frac{1}{2},j_2+\frac{1}{2}} - F^1_{j_1-\frac{1}{2},j_2+\frac{1}{2}}}{h_1} \varphi_{j_1,j_2} + \right.$$

$$+\frac{F^1_{j_1+\frac{1}{2},j_2+\frac{1}{2}} - F^1_{j_1-\frac{1}{2},j_2+\frac{1}{2}}}{h_1}\varphi_{j_1,j_2+1}\Bigg] h_1 h_2 -$$

$$-\frac{1}{2}\sum_{j_1=1}^{N_1-1}\sum_{j_2=2}^{N_2-1}\Bigg[\frac{F^2_{j_1+\frac{1}{2},j_2+\frac{1}{2}} - F^2_{j_1+\frac{1}{2},j_2-\frac{1}{2}}}{h_2}\varphi_{j_1,j_2}+$$

$$+\frac{F^2_{j_1+\frac{1}{2},j_2+\frac{1}{2}} - F^2_{j_1+\frac{1}{2},j_2-\frac{1}{2}}}{h_2}\varphi_{j_1+1,j_2}\Bigg] h_1 h_2 =$$

$$= -\frac{1}{2h_1}\sum_{j_2=1}^{N_2-1}\Bigg[\sum_{j_1=2}^{N_1-1}\left(F^1_{j_1+\frac{1}{2},j_2+\frac{1}{2}}\varphi_{j_1,j_2} + F^1_{j_1+\frac{1}{2},j_2+\frac{1}{2}}\varphi_{j_1,j_2+1}\right) -$$

$$-\sum_{j_1=1}^{N_1-2}\left(F^1_{j_1+\frac{1}{2},j_2+\frac{1}{2}}\varphi_{j_1+1,j_2} + F^1_{j_1+\frac{1}{2},j_2+\frac{1}{2}}\varphi_{j_1+1,j_2+1}\right)\Bigg] h_1 h_2 -$$

$$-\frac{1}{2h_2}\sum_{j_1=1}^{N_1-1}\Bigg[\sum_{j_2=2}^{N_2-1}\left(F^2_{j_1+\frac{1}{2},j_2+\frac{1}{2}}\varphi_{j_1,j_2} + F^2_{j_1+\frac{1}{2},j_2+\frac{1}{2}}\varphi_{j_1+1,j_2}\right) -$$

$$-\sum_{j_2=1}^{N_2-2}\left(F^2_{j_1+\frac{1}{2},j_2+\frac{1}{2}}\varphi_{j_1,j_2+1} + F^2_{j_1+\frac{1}{2},j_2+\frac{1}{2}}\varphi_{j_1+1,j_2+1}\right)\Bigg] h_1 h_2 =$$

$$= \frac{1}{2}\sum_{j_2=1}^{N_2-1}\Bigg[\sum_{j_1=1}^{N_1-1}F^1_{j_1+\frac{1}{2},j_2+\frac{1}{2}}(D_{q^1}\varphi)_{j_1+\frac{1}{2},j_2} + \sum_{j_1=1}^{N_1-1}F^1_{j_1+\frac{1}{2},j_2+\frac{1}{2}}(D_{q^1}\varphi)_{j_1+\frac{1}{2},j_2+1}\Bigg] h_1 h_2 +$$

$$+\frac{1}{2}\sum_{j_1=1}^{N_1-1}\Bigg[\sum_{j_2=1}^{N_2-1}F^2_{j_1+\frac{1}{2},j_2+\frac{1}{2}}(D_{q^2}\varphi)_{j_1,j_2+\frac{1}{2}} + \sum_{j_2=1}^{N_2-1}F^2_{j_1+\frac{1}{2},j_2+\frac{1}{2}}(D_{q^2}\varphi)_{j_1+1,j_2+\frac{1}{2}}\Bigg] h_1 h_2 =$$

$$= \sum_{j_1=1}^{N_1-1}\sum_{j_2=1}^{N_2-1}F^1_{j_1+\frac{1}{2},j_2+\frac{1}{2}}(D_{q^1}\varphi)_{j_1+\frac{1}{2},j_2+\frac{1}{2}}h_1 h_2 +$$

$$+\sum_{j_1=1}^{N_1-1}\sum_{j_2=1}^{N_2-1}F^2_{j_1+\frac{1}{2},j_2+\frac{1}{2}}(D_{q^2}\varphi)_{j_1+\frac{1}{2},j_2+\frac{1}{2}}h_1 h_2.$$

Thus,

$$(A\,\mathring{\psi},\mathring{\varphi}) = \sum_{j_1=1}^{N_1-1}\sum_{j_2=1}^{N_2-1}h_1 h_2\left(\sum_{\alpha,\beta=1}^{2}k_{\alpha\beta}D_{q^\alpha}\psi D_{q^\beta}\varphi\right)_{j_1+\frac{1}{2},j_2+\frac{1}{2}}. \qquad (5.A3)$$

$(\mathring{\psi}, A\,\mathring{\varphi}) = (A\,\mathring{\varphi}, \mathring{\psi})$, therefore, the expression for $(\mathring{\psi}, A\,\mathring{\varphi})$ is obtained from (5.A3) by replacing ψ by φ. This expression coincides with (5.A3) up to the permutation of the factors because of the equality: $g_{12} = g_{21}$. Thus, A is the self-adjoint operator.

Lemma 5.2. *The difference operator A is positively definite in the Hilbert space $\mathcal{H}$, and the following estimation is fulfilled:*

$$(A\,\mathring{\varphi}, \mathring{\varphi}) \geq C(\mathring{\varphi}, \mathring{\varphi}),$$

where

$$C = c_1 \frac{\pi^2}{(\max\{h_1, h_2\})^2}[h_1^2 + h_2^2 - 2\pi^2 h_1^2 h_2^2].$$

Proof. According to the formula (5.A3) we have the following relation:

$$(A\,\mathring{\varphi}, \mathring{\varphi}) = \sum_{j_1=1}^{N_1-1}\sum_{j_2=1}^{N_2-1} h_1 h_2 \left(\sum_{\alpha,\beta=1}^{2} k_{\alpha\beta} D_{q^\alpha}\varphi D_{q^\beta}\varphi\right)_{j_1+\frac{1}{2}, j_2+\frac{1}{2}}.$$

Using the condition of the uniform ellipticity (5.17) we obtain:

$$(A\,\mathring{\varphi}, \mathring{\varphi}) \geq c_1 \sum_{j_1=1}^{N_1-1}\sum_{j_2=1}^{N_2-1} \left((D_{q^1}\varphi)^2 + (D_{q^2}\varphi)^2\right) h_1 h_2.$$

The following Dirichlet problem in the domain Q with the boundary $\gamma = \partial Q$ is considered:

$$\Delta\varphi = 0, \quad \varphi\Big|_\gamma = 0.$$

We approximate this problem on the rectangular grid with the step sizes h_1, h_2. We apply the finite-difference scheme Δ_h which is obtained from the scheme Λ by replacing the coefficients by the constants: $k_{11} = k_{22} = 1$, $k_{12} = 0$. Let us consider the operator $B = -\Delta_h$. It is clear that

$$(B\,\mathring{\varphi}, \mathring{\varphi}) = h_1 h_2 \sum_{j_1=1}^{N_1-1}\sum_{j_2=1}^{N_2-1} \left((D_{q^1}\varphi)^2 + (D_{q^2}\varphi)^2\right)(q_{j_1+1/2, j_2+1/2}).$$

Therefore,

$$(A\,\mathring{\varphi}, \mathring{\varphi}) \geq c_1(B\,\mathring{\varphi}, \mathring{\varphi}).$$

The eigenvalues of the operator B have the following form:

$$\lambda_{k_1,k_2} = \frac{4}{h_1^2}\sin^2\left[\frac{\pi}{2}(k_1-1)h_1\right]\cos^2\left[\frac{\pi}{2}(k_2-1)h_2\right] +$$

$$+ \frac{4}{h_2^2}\sin^2\left[\frac{\pi}{2}(k_2-1)h_2\right]\cos^2\left[\frac{\pi}{2}(k_1-1)h_1\right],$$

155

$$k_\alpha = 2, \ldots N_\alpha - 1,$$

where

$$\lambda_{min} = \frac{4}{h_1^2} \sin^2\left[\frac{\pi h_1}{2}\right]\left(1 - \sin^2\left[\frac{\pi h_2}{2}\right]\right) + \frac{4}{h_2^2} \sin^2\left[\frac{\pi h_2}{2}\right]\left(1 - \sin^2\left[\frac{\pi h_1}{2}\right]\right) \geq$$

$$\geq \frac{\pi^2}{(\max\{h_1, h_2\})^2}[h_1^2 + h_2^2 - 2\pi^2 h_1^2 h_2^2] = c_2.$$

For sufficiently small step sizes h_α we obtain $c_2 > 0$. Thus,

$$(A\,\mathring{\varphi}, \mathring{\varphi}) \geq c_1(B\,\mathring{\varphi}, \mathring{\varphi}) \geq c_1 \lambda_{min}(\mathring{\varphi}, \mathring{\varphi}) \geq c_1 c_2(\mathring{\varphi}, \mathring{\varphi}).$$

If we introduce $C = c_1 c_2$, then the lemma is proved.

Lemma 5.3. *The coefficients of the difference equation (5.18) satisfy the following relations:*

$$\beta_k \leq 0, \quad k = 1, 2, 3, 4; \quad \beta_0 \geq 0; \quad \sum_{k=0}^{4} \beta_k = 0. \tag{5.20}$$

Proof. Let us prove the first part of the statement for the coefficient β_1. If $v^1(W) > 0$, then $\beta_1 = -h_2 J v^1(W) < 0$. If $v^1(W) \leq 0$, then $\beta_1 = 0$. Therefore, $\beta_1 \leq 0$. The proof for the coefficients $\beta_2, \beta_3, \beta_4$ is similar.

Now let us show that $\sum_{k=0}^{4} \beta_k = 0$. The equation (5.18) can be written in the following way:

$$h_2\left[\frac{\rho J v^1(E) + |\rho J v^1(E)|}{2}\omega_0 + \frac{\rho J v^1(E) - |\rho J v^1(E)|}{2}\omega_3\right] -$$

$$-h_2\left[\frac{\rho J v^1(W) + |\rho J v^1(W)|}{2}\omega_1 + \frac{\rho J v^1(W) - |\rho J v^1(W)|}{2}\omega_0\right] +$$

$$+h_1\left[\frac{\rho J v^2(N) + |\rho J v^2(N)|}{2}\omega_0 + \frac{\rho J v^2(N) - |\rho J v^2(N)|}{2}\omega_4\right] - \tag{5.A4}$$

$$-h_1\left[\frac{\rho J v^2(S) + |\rho J v^2(S)|}{2}\omega_2 + \frac{\rho J v^2(S) - |\rho J v^2(S)|}{2}\omega_0\right] = d_0.$$

Therefore,

$$\beta_0 + \sum_{k=1}^{4} \beta_k = h_2\frac{\rho J v^1(E) + |\rho J v^1(E)|}{2} - h_2\frac{\rho J v^1(W) - |\rho J v^1(W)|}{2} +$$

$$+h_1\frac{\rho J v^2(N) + |\rho J v^2(N)|}{2} - h_1\frac{\rho J v^2(S) - |\rho J v^2(S)|}{2} -$$

$$-h_2\frac{\rho J v^1(W) + |\rho J v^1(W)|}{2} - h_1\frac{\rho J v^2(S) + |\rho J v^2(S)|}{2} +$$

$$+h_2\frac{\rho J v^1(E) - |\rho J v^1(E)|}{2} + h_1\frac{\rho J v^2(N) - |\rho J v^2(N)|}{2} =$$

$$= -h_2\rho J v^1(W) - h_1\rho J v^2(S) + h_2\rho J v^1(E) + h_1\rho J v^2(N).$$

Using the following relations:

$$\rho J v^1(W) = \frac{\psi_{j_1,j_2+1} - \psi_{j_1,j_2}}{h_2}, \quad \rho J v^1(E) = \frac{\psi_{j_1+1,j_2+1} - \psi_{j_1+1,j_2}}{h_2},$$

$$\rho J v^2(S) = -\frac{\psi_{j_1+1,j_2} - \psi_{j_1,j_2}}{h_1}, \quad \rho J v^1(N) = -\frac{\psi_{j_1+1,j_2+1} - \psi_{j_1,j_2+1}}{h_1}, \quad (5.A5)$$

we obtain that

$$\beta_0 + \sum_{k=1}^{4} \beta_k = -\psi_{j_1,j_2+1} + \psi_{j_1,j_2} + \psi_{j_1+1,j_2} - \psi_{j_1,j_2}+$$

$$+\psi_{j_1+1,j_2+1} - \psi_{j_1+1,j_2} - \psi_{j_1+1,j_2+1} + \psi_{j_1,j_2+1} = 0.$$

Thus, the third part of the statement is proved.

The first and third parts of the statement are used for proving the second part. $\beta_k \leq 0, k = 1, 2, 3, 4$ and $\sum_{k=0}^{4} \beta_k = 0$, therefore $\beta_0 \geq 0$. Thus, the lemma is proved.

Lemma 5.4. Let $\mathbf{q}_{j+1/2} \in Q_h^0$. Then the following statements for the coefficients of the equation (5.18) are equivalent (the notations of Fig. 5.3 are used):
1. $\beta_0 = 0$;
2. $\beta_1 = \beta_2 = \beta_3 = \beta_4 = 0$;
3. $v^1(W) = v^1(E) = v^2(N) = v^2(S) = 0$;
4. $\psi(A) = \psi(B) = \psi(C) = \psi(D)$.

Proof. Let us show that the statement 1 leads to the statement 2. We assume that $\beta_0 = 0$. According to Lemma 5.3 the following relation is fulfilled: $\sum_{k=0}^{4} \beta_k = 0$. Therefore, $\sum_{k=1}^{4} \beta_k = 0$. $\beta_k \leq 0$, $k = 1, 2, 3, 4$, thus, the relations $\beta_k = 0$, $k = 1, 2, 3, 4$ are obtained.

Now let us obtain the statement 4 from the statement 2. Let $\beta_k = 0$, $k = 1, 2, 3, 4$. From the definition of these coefficients (5.19) it follows that:

$$\beta_1 = 0 \rightarrow Jv^1(W) \leq 0, \quad \beta_2 = 0 \rightarrow Jv^2(S) \leq 0,$$

$$\beta_3 = 0 \rightarrow Jv^1(E) \geq 0, \quad \beta_4 = 0 \rightarrow Jv^1(N) \geq 0.$$

The difference relations (5.A5) lead to the following inequalities:

$$\psi(D) - \psi(A) \leq 0, \quad \psi(B) - \psi(A) \geq 0,$$

$$\psi(C) - \psi(B) \geq 0, \quad \psi(C) - \psi(D) \leq 0.$$

Thus, the following sequence of inequalities is obtained:

$$\psi(D) \leq \psi(A) \leq \psi(B) \leq \psi(C) \leq \psi(D).$$

These inequalities are fulfilled if the following equality is true:

$$\psi(A) = \psi(B) = \psi(C) = \psi(D).$$

The statement 3 follows from the statement 4 by virtue of the approximating formulas (5.A5) for the contravariant components of the velocity.

From the form (5.A4) of the difference equation for the vorticity, it is obvious that if the statement 3 is fulfilled, then the coefficient β_0 at ω_0 is equal to zero. Thus, the proof of the lemma is completed.

Theorem 5.1. *If $Q \in K_1(P)$, then $P \notin K_1(Q)$. If $Q_2 \in K(Q_1)$, $Q_3 \in K(Q_2)$, then $Q_3 \in K(Q_1)$.*

Proof. Let us prove the first statement of the theorem. Let $Q \in K_1(P)$. Therefore, the coefficient at $\omega(Q)$ in the equation (5.18) is not equal to zero: $\beta_Q \neq 0$. Let, for example, $\beta_Q = \beta_2$. Therefore, from the definition of the coefficient β_2 it follows, that $v^2(S) > 0$.

Let us assume the opposite: $P \in K_1(Q)$, i.e. $\beta_P \neq 0$. $\beta_P = \beta_4 \neq 0$ in the pattern $\Sigma(Q)$. It means that $v^2(N) < 0$ because of the definition of the coefficient β_4. The node N in $\Sigma(Q)$ is the point S in $\Sigma(P)$, therefore, it is the same point of the grid. Thus, we have $v^2(N) > 0$ and $v^2(N) < 0$ simultaneously at this point. The obtained inconsistency proves that $P \notin K_1(Q)$.

Now, we shall prove the second statement of the theorem. Firstly, we shall prove two auxiliary lemmas.

Lemma 5.A1. *If $Q_2 \in K(Q_1)$, $Q_3 \in K_1(Q_2)$, then $Q_3 \in K(Q_1)$.*
Proof.

$$Q_2 \in K(Q_1) = \bigcup_{i=1}^{n_0} K_i(Q_1),$$

therefore, some n' exists such that $Q_2 \in K_{n'}(Q_1)$. From here it follows that

$$K_{n'+1}(Q_1) = \bigcup_{Q_k \in K_{n'}(Q_1)} K_1(Q_k) \supset K_1(Q_2) \ni Q_3.$$

Thus, $Q_3 \in K_{n'+1}(Q_1) \subset \bigcup_{i=1}^{n_0} K_i(Q_1) = K(Q_1)$.

Lemma 5.A2. *If $Q_2 \in K(Q_1)$, $Q_3 \in K_n(Q_2)$, then $Q_3 \in K(Q_1)$.*
Proof. According to the statement of the lemma

$$Q_3 \in K_n(Q_2) = \bigcup_{Q_k \in K_{n-1}(Q_2)} K_1(Q_k),$$

therefore, some k_0 exists such that $Q_3 \in K_1(Q_{k_0})$, $Q_{k_0} \in K_{n-1}(Q_2)$.
Now let us consider the node Q_{k_0}:

$$Q_{k_0} \in K_{n-1}(Q_2) = \bigcup_{Q_k \in K_{n-2}(Q_2)} K_1(Q_k),$$

therefore, some k_1 exists such that $Q_{k_0} \in K_1(Q_{k_1})$, $Q_{k_1} \in K_{n-2}(Q_2)$.

n is finite, thus, we reach the node $Q_{k_{n-3}}$:

$$Q_{k_{n-3}} \in K_2(Q_2) = \bigcup_{Q_k \in K_1(Q_2)} K_1(Q_k),$$

therefore, some k_{n-2} exists such that $Q_{k_{n-3}} \in K_1(Q_{k_{n-2}})$, $Q_{k_{n-2}} \in K_1(Q_2)$.

Thus, $Q_2 \in K(Q_1)$, $Q_{k_{n-2}} \in K_1(Q_2)$. According to Lemma 5.A1 $Q_{k_{n-2}} \in K(Q_1)$.

Further, $Q_{k_{n-2}} \in K(Q_1)$, $Q_{k_{n-3}} \in K_1(Q_{k_{n-2}})$, therefore, according to Lemma 5.A1 $Q_{k_{n-3}} \in K(Q_1)$.

Thus, the node Q_{k_0} is reached. $Q_{k_1} \in K(Q_1)$, $Q_{k_0} \in K_1(Q_{k_0})$, therefore, according to Lemma 5.A1 $Q_{k_0} \in K(Q_1)$.

Finally $Q_{k_0} \in K(Q_1)$, $Q_3 \in K_1(Q_{k_0})$, therefore, according to Lemma 5.A1 $Q_3 \in K(Q_1)$. Thus, the proof is complete.

Now we shall prove the last statement of Theorem 5.1.

$$Q_3 \in K(Q_2) = \bigcup_{i=1}^{n_0} K_i(Q_2),$$

therefore, some n_0 exists such that $Q_3 \in K_{n_0}(Q_2)$. Thus, $Q_2 \in K(Q_1)$, $Q_3 \in K_{n_0}(Q_2)$. According to Lemma 5.A2 $Q_3 \in K(Q_1)$.

Theorem 5.2. *For the realisation of the condition*

$$P \notin K(P) \tag{5.22}$$

in the arbitrary node $P \in Q_h^0$ it is necessary and sufficient that some neighbourhood of the node P should be completely located at the inlet (in other words, some number n_0 should exist such that $K_{n_0} \subseteq \gamma_{1,h}^0$).

Proof. Let us prove the necessity. Let $P \notin K(P)$ be fulfilled for any node $P \in Q_h^0$. It is necessary to prove that n_0 exists: $K_{n_0} \subseteq \gamma_{1,h}^0$. If $K_{n_0} \subseteq \gamma_{1,h}^0$, then $K_{n_0+1} = \emptyset$. Thus, it is necessary to prove that certain n_0 for the selected node P exists: $K_{n_0} = \emptyset$.

Let us assume the opposite. Let there be the node $P_0 \in Q_h^0$ for which the neighbourhood $K_i(P_0)$ is not empty at every i. Therefore, because of the finiteness of the set of the nodes Q_h^0, there will be an infinite sequence of the coinciding neighbourhoods:
$K_{i_1}(P_0) = K_{i_2}(P_0) = \ldots, \quad i_1 < i_2 < \ldots$.

Let P_k $(k = 1, 2, \ldots, m)$ denote all nodes of one neighbourhood and, thus, also all nodes of each of the neighbourhoods mentioned above. Let us show that $P_k \in K(Q_j)$, where Q_j $(j = 1, 2, \ldots, t)$ are also the nodes of these neighbourhoods, $t < m$. Let us take, for example, the node P_1. $P_1 \in K_{i_2}(P_0) = K_{i_1}(P_0)$.

$$K_{i_2}(P_0) = \bigcup_{Q_k \in K_{i_2-1}(P_0)} K_1(Q_k).$$

Therefore, the node $Q \in K_{i_2-1}(P_0)$ exists such that $P_1 \in K_1(Q)$. Thus,

$$K_{i_2-1}(P_0) = \bigcup_{Q_k \in K_{i_2-2}(P_0)} K_1(Q_k).$$

From here it follows that the node $Q' \in K_{i_2-2}(P_0)$ exists such that $Q \in K_1(Q')$. We proceed further in the same way: $i_1 < i_2 < \ldots$, therefore we reach some $\overline{Q} \in K_1(Q_0)$, $Q_0 \in K_{i_1}(P_0)$.

$P_1 \in K_1(Q)$, $Q \in K_1(Q')$, ..., $\overline{Q} \in K_1(Q_0)$, thus, $P_1 \in K(Q_0)$. Because of the arbitrariness of P_1, we obtain that any of the nodes $P_k(k = 1, 2, \ldots, m)$ is located at least in one of the neighbourhoods $K(Q_j)$.

Now we consider only the nodes Q_j. These nodes are some of the nodes P_k. Therefore, as it is shown above, we obtain that $Q_j \in K(Q_r)$, $j, r = 1, 2, \ldots, t$. According to the statement of the theorem (5.22), $j \neq r$, from here we obtain that $Q_j \in K(Q_r)$, $j \neq r$, $j, r = 1, 2, \ldots, t$. Using the second statement of Theorem 5.1 we obtain that $Q_j \in K(Q_j)$. It contradicts the statement of Theorem 5.2. (Let us explain this contradiction using the simple example of two nodes. For instance, if $Q_{j_1} \in K(Q_{j_2})$, $Q_{j_2} \in K(Q_{j_1})$, then, according to the second statement of Theorem 5.1 we obtain that $Q_{j_1} \in K(Q_{j_1})$. It is the contradiction to the statement of Theorem 5.2.) Thus, there is no node $P_0 \in Q_h^0$, for which $K_i(P_0) \neq \emptyset$ at every i. From here the statement of the theorem follows.

Now we shall prove the sufficiency. Let us assume that for the arbitrary node $P \in Q_h^0$ some n_0 exists such that $K_{n_0}(P) \subseteq \gamma_{1,h}^0$. Let us prove that $P \notin K(P)$. $K_{n_0} \subseteq \gamma_{1,h}^0$, thus, $K_{n_0+1} = \emptyset$. Let us assume the contrary: $P \in K(P)$. According to the definition $K(P) = \overset{n_0}{\underset{i=1}{\cup}} K_i(P)$. Therefore, some n' exists such that $P \in K_{n'}(P)$, $n' < n_0$.

Let us consider $K_{n'+1}(P)$. We shall prove that $K_{n'+1}(P) \supseteq K_1(P)$.

$$K_{n'+1}(P) = \underset{Q_k \in K_{n'}(P)}{\cup} K_1(Q_k) \supseteq K_1(P).$$

Now let us prove that $K_{n'+2}(P) \supseteq K_2(P)$.

$$K_{n'+2}(P) = \underset{Q_k \in K_{n'+1}(P)}{\cup} K_1(Q_k) \supseteq \underset{Q_k \in K_1(P)}{\cup} K_1(Q_k) = K_2(P).$$

Let us assume that the following is proved already: $K_{n'+l}(P) \supseteq K_l(P)$. Now we shall show that $K_{n'+l+1}(P) \supseteq K_{l+1}(P)$:

$$K_{n'+l+1}(P) = \underset{Q_k \in K_{n'+l}(P)}{\cup} K_1(Q_k) \supseteq \underset{Q_k \in K_l(P)}{\cup} K_1(Q_k) = K_{l+1}(P).$$

Hence we obtain the following:

$$K_{n'+n'}(P) = K_{2n'}(P) \supseteq K_{n'}(P) \ni P.$$

Therefore, $P \in K_{2n'}(P)$. Similarly, we obtain that $P \in K_{3n'}(P)$ and so on. Thus, $K_{mn'}(P) \neq \emptyset$ for any $m \in N$, but $K_i(P) = \emptyset$ beginning from $i = n_0 + 1$. Therefore, the contradiction is obtained which shows that any node $P \in Q_h^0$ does not belong to its area of dependence: $P \notin K(P)$. Thus, the theorem is proved completely.

Lemma 5.5. *For $\omega \equiv 0$ the functions $x = x(q^1, q^2)$, $y = y(q^1, q^2)$ satisfy the difference equation (5.4).*

Proof. Let us consider the result of applying the operator Λ from (5.4) to the function $y = y(q^1, q^2)$ (the notations of Fig. 5.1 are used):

$$\Lambda y_{j_1,j_2} = \frac{1}{2}\left[D_{q^1}\left(\frac{g_{22}}{J}D_{q^1}y - \frac{g_{12}}{J}D_{q^2}y\right)(N) + D_{q^1}\left(\frac{g_{22}}{J}D_{q^1}y - \frac{g_{12}}{J}D_{q^2}y\right)(S)\right] +$$

$$+ \frac{1}{2}\left[D_{q^2}\left(-\frac{g_{12}}{J}D_{q^1}y + \frac{g_{11}}{J}D_{q^2}y\right)(E) + D_{q^2}\left(-\frac{g_{12}}{J}D_{q^1}y + \frac{g_{11}}{J}D_{q^2}y\right)(W)\right] =$$

$$= \frac{1}{2} \left[\frac{\left(\frac{g_{22}}{J} D_{q^1} y - \frac{g_{12}}{J} D_{q^2} y \right) (C) - \left(\frac{g_{22}}{J} D_{q^1} y - \frac{g_{12}}{J} D_{q^2} y \right) (D)}{h_1} + \right.$$

$$\left. + \frac{\left(\frac{g_{22}}{J} D_{q^1} y - \frac{g_{12}}{J} D_{q^2} y \right) (B) - \left(\frac{g_{22}}{J} D_{q^1} y - \frac{g_{12}}{J} D_{q^2} y \right) (A)}{h_1} \right] +$$

$$+ \frac{1}{2} \left[\frac{\left(-\frac{g_{12}}{J} D_{q^1} y + \frac{g_{11}}{J} D_{q^2} y \right) (D) - \left(-\frac{g_{12}}{J} D_{q^1} y + \frac{g_{11}}{J} D_{q^2} y \right) (A)}{h_2} + \right.$$

$$\left. + \frac{\left(-\frac{g_{12}}{J} D_{q^1} y + \frac{g_{11}}{J} D_{q^2} y \right) (C) - \left(-\frac{g_{12}}{J} D_{q^1} y + \frac{g_{11}}{J} D_{q^2} y \right) (B)}{h_2} \right].$$

Let us consider, for example, the items defined at the point C, and let us transform them:

$$\frac{1}{2h_1} \left(\frac{g_{22}}{J} D_{q^1} y - \frac{g_{12}}{J} D_{q^2} y \right) + \frac{1}{2h_2} \left(\frac{-g_{12}}{J} D_{q^1} y + \frac{g_{11}}{J} D_{q^2} y \right) =$$

$$= \frac{1}{2h_1} \frac{1}{J} \left(D_{q^2} x D_{q^2} x D_{q^1} y + D_{q^2} y D_{q^2} y D_{q^1} y - D_{q^1} x D_{q^2} x D_{q^2} y - D_{q^1} y D_{q^2} y D_{q^2} y \right) +$$

$$+ \frac{1}{2h_2} \frac{1}{J} \left(-D_{q^1} x D_{q^2} x D_{q^1} y - D_{q^1} y D_{q^2} y D_{q^1} y + D_{q^1} x D_{q^1} x D_{q^2} y + D_{q^1} y D_{q^1} y D_{q^2} y \right) =$$

$$= -\frac{1}{2h_1} D_{q^2} x + \frac{1}{2h_2} D_{q^1} x.$$

Similarly, by transforming the items at the points A, B and D we obtain the following:

$$\Lambda y_{j_1, j_2} = \frac{1}{2} \left[\left(-\frac{1}{h_1} D_{q^2} x + \frac{1}{h_2} D_{q^1} x \right) (C) + \left(\frac{1}{h_1} D_{q^2} x - \frac{1}{h_2} D_{q^1} x \right) (A) - \right.$$

$$\left. - \left(\frac{1}{h_1} D_{q^2} x - \frac{1}{h_2} D_{q^1} x \right) (B) + \left(\frac{1}{h_1} D_{q^2} x + \frac{1}{h_2} D_{q^1} x \right) (D) \right] =$$

$$= \frac{1}{2h_1 h_2} \left[x(3) - x(4) + x(1) - x(2) + x(2) - x(3) + x(4) - x(1) \right] = 0.$$

Thus, the function $y = y(q^1, q^2)$ satisfies the homogeneous equation (5.4). For the function $x = x(q^1, q^2)$ the proof is similar.

Lemma 8.1. *If the mapping (8.1) given by the solutions of the equations (8.6) is non-degenerate and orthogonal, then it is also adaptive in the sense of the realisation of the equality (8.5).*

Proof. From the statement of the lemma it follows that $g_{\alpha\beta} = 0$ for $\alpha \neq \beta$. Thus, the functions $\varphi = x^\alpha$ satisfy the following equation:

$$\frac{\partial}{\partial q^\gamma}\left(Jg^{\gamma\beta}\frac{\partial x^\alpha}{\partial q^\beta}Jw\right) = 0, \qquad \alpha, \beta, \gamma = 1, 2, 3.$$

On differentiating this equation and taking into account the identity (8.2) we obtain the system of equations with respect to the values $\partial(Jw)/\partial q^\gamma$:

$$g^{\gamma\beta}\frac{\partial x^\alpha}{\partial q^\beta}\frac{\partial Jw}{\partial q^\gamma} = 0, \qquad \alpha, \beta, \gamma = 1, 2, 3.$$

The determinant of this system is equal to J^3. By virtue of the nondegeneracy of the mapping it follows from here that the system has only the trivial solution $\partial(Jw)/\partial q^\gamma = 0$, $\gamma = 1, 2, 3$. Thus, the equality (8.5) is fulfilled.

Lemma 8.A1. *Let the mapping (8.1) satisfy the conditions (8.25)–(8.27). Then*

$$\left.\frac{\partial g_{3\alpha}}{\partial q^3}\right|_{q^3=0} = 0, \qquad \alpha = 1, 2. \tag{8.A1}$$

Proof. From the equality

$$\frac{\partial \mathbf{r}_3}{\partial q^3} = \Gamma_{33}^\gamma \mathbf{r}_\gamma$$

using (8.27) it follows that

$$\Gamma_{33}^1 = 0, \qquad \Gamma_{33}^2 = 0.$$

Here $\Gamma_{\alpha\beta}^\gamma$ are the Christoffel's symbols.

By virtue of the orthogonality (8.25) of the coordinate system we obtain:

$$\Gamma_{33}^\alpha = g^{\alpha\alpha}\Gamma_{33,\alpha} = \frac{1}{g_{\alpha\alpha}} \cdot \frac{1}{2}\left(\frac{\partial g_{3\alpha}}{\partial q^3} + \frac{\partial g_{3\alpha}}{\partial q^3} - \frac{\partial g_{33}}{\partial q^\alpha}\right), \qquad \alpha = 1, 2.$$

Using the condition (8.27) the equality (8.A1) is obtained.

Lemma 8.2. *If the conditions (8.25)–(8.27) are satisfied and the equation (8.6) is fulfilled in Ω up to the boundary Γ_{bot}, then*

$$wJ(q^1, q^2, 0) = \text{const}, \qquad 0 < q^\alpha < 1, \quad \alpha = 1, 2. \tag{8.28}$$

Proof. By virtue of (8.25) and the obtained equality (8.A1) the equation (8.6) can be written in the following form on Γ_{bot}:

$$\frac{\partial}{\partial q^\beta}\left(wJ^2g^{\beta\gamma}\frac{\partial x^\alpha}{\partial q^\gamma}\right) = 0, \quad \alpha = 1, 2, 3. \tag{8.A2}$$

We have the following equality for any $\beta = 1, 2, 3$:

$$g^{\beta\gamma}\frac{\partial x^\alpha}{\partial q^\gamma} = \delta^{mm}\frac{\partial q^\beta}{\partial x^m}\frac{\partial q^\gamma}{\partial x^m}\frac{\partial x^\alpha}{\partial q^\gamma} = \delta^{mm}\frac{\partial q^\beta}{\partial x^m}\delta_m^\alpha = \frac{\partial q^\beta}{\partial x^\alpha}.$$

Therefore, the equation (8.A2) can be written as follows:

$$J\frac{\partial q^\beta}{\partial x^\alpha}\frac{\partial}{\partial q^\beta}(wJ) + wJ\frac{\partial}{\partial q^\beta}\left(J\frac{\partial q^\beta}{\partial x^\alpha}\right) = 0, \quad \alpha = 1, 2, 3. \tag{8.A3}$$

Here $\delta^{\alpha\beta} = \delta^\alpha_\beta = \delta_{\alpha\beta}$ are the Kronecker's symbols.

Taking into account the identity:

$$\frac{1}{J}\frac{\partial}{\partial q^\beta}\left(J\frac{\partial q^\beta}{\partial x^\alpha}\right) = 0,$$

we obtain that the values $\partial(wJ)/\partial q^\beta$ are the solution of the homogeneous system (8.A3). The determinant of this system is not equal to zero. Thus, the equality (8.28) is fulfilled.

Lemma 8.3. *If the conditions (8.39)–(8.41) are satisfied and the equation (8.6) is fulfilled in Ω up to the boundary edge L, then the equality (8.38) is satisfied on L.*

Proof. By virtue of the orthogonality condition (8.39) and the assumption (8.40) we have the following equality:

$$0 = \Gamma^\beta_{\alpha\alpha} = g^{\beta\beta}\Gamma_{\alpha\alpha,\beta} = \frac{g^{\beta\beta}}{2}\left(2\frac{\partial g_{\alpha\beta}}{\partial q^\alpha} - \frac{\partial g_{\alpha\alpha}}{\partial q^\beta}\right). \tag{8.A4}$$

The indices α and β have the values which are indicated in the condition (8.41). Taking into account this condition in (8.A4) we obtain the equalities:

$$\frac{\partial g_{\alpha\beta}}{\partial q^\alpha} = 0, \quad \alpha = 2, 3, \quad \beta = 1, 2, 3, \quad \beta \neq \alpha,$$

which are fulfilled at each point of the curve L.

By virtue of the orthogonality condition (8.39) the obtained equalities lead to the following relations on the curve L:

$$g^{\alpha\beta} = 0, \quad \frac{\partial g^{\alpha\beta}}{\partial q^\alpha} = 0, \quad \alpha = 2, 3, \quad \beta = 1, 2, 3, \quad \beta \neq \alpha.$$

Thus, the equation (8.6) can be written on L in the form of (8.A2) or (8.A3). Taking into account that the componenets g_{22} and g_{33} are constant on L we obtain the relation (8.38).

Bibliography

[1] Abdallah S., Hamed A. Inviscid solution for the secondary flow in curved ducts // AIAA J. - 1981. - Vol. 19. - P. 993-999.

[2] Alekseev G.V. About the vanishing viscosity in two-dimensional stationary problems of incompressible fluid hydrodynamics // Dynamics of continuous medium. - Novosibirsk, IHD SB AS USSR, 1972. - N. 10. - P. 5-27. (in Russian)

[3] Alekseev G.V. About uniqueness and smoothness of plane vortical ideal fluid flows // Dynamics of continuous medium. - Novosibirsk, IHD SB AS USSR, 1973. - N. 15. - P. 7-17. (in Russian)

[4] Alekseev G.V. About the stabilization of solutions of two-dimensional equations of ideal fluid dynamics // Journal of applied mechanics and technical physics. - 1977. - N. 2. - P. 85-92. (in Russian)

[5] Anderson D., Tannehill J., Pletcher R. Computational hydromechanics and heat exchange. Vol. 1-2. - Moscow: Mir, 1990. - 728 p. (in Russian)

[6] Andreev V.K., Kaptsov O.V., Pukhnachyov V.V., Rodionov A.A. Application of group methods theory in hydrodynamics. - Novosibirsk: Science, 1994. - 320 p. (in Russian)

[7] Antontsev S.N., Kazhikhov A.V., Monakhov V.N. Boundary value problems of inhomogeneous fluid mechanics. - Novosibirsk: Science, 1983. - 319 p. (in Russian)

[8] Aregbesola Y.A.S., Burley D.M. The vector and scalar potential method for the numerical solution of two- and three-dimensional Navier-Stokes equations // J. Comput. Phys. - 1977. - Vol. 24. - P. 398-415.

[9] Aziz K., Hellums J.D. Numerical solution of the three-dimensional equations of motion for laminar natural convection // Phys. Fluids. - 1967. - Vol. 10. - No. 2. - P. 314-324.

[10] Batchelor G. An introduction to fluid dynamics. - Moscow: Mir, 1973. - 758 p. (in Russian)

[11] Belolipetskii V.M., Kostyuk V.Yu., Shokin Yu.I. Mathematical modelling of stratified fluid flows. - Novosibirsk: Science, 1991. - 176 p. (in Russian)

[12] Belotserkovskii O.M. Numerical modelling in mechanics of continuous media. - Moscow: Science, 1984. - 520 p. (in Russian)

[13] Boor C. Good approximation by splines with variable knots. II // Lecture Notes in Mathematics. - 1974. - Vol. 363. - P. 12-20.

[14] Borisov V.M. Development of software packages of computational type. - Moscow: MSU, 1990. - 126 p. (in Russian)

[15] Borthwick A. G. L., Barber R. W. River and reservoir flow modelling using the transformed shallow water equations // Int. J. Numer. Methods Fluids. - 1992. - Vol. 14. - P. 1193-1217.

[16] Briley W.R. Numerical method for predicting three-dimensional steady viscous flow in ducts // J. Comput. Phys. - 1974. - Vol. 14. - P. 8-28.

[17] Chang P.Y., Shyy W. Adaptive grid computation of three-dimensional natural convection in horizontal high-pressure mercury lamps // Int. J. Numer. Methods Fluids. - 1991. - Vol. 12. - P. 143-160.

[18] Chang S.-C., Adamczyk J. A new approach for solving the three-dimensional steady Euler equations. I. General Theory // J. Comput. Phys. - 1985. - Vol. 60. - P. 23-40.

[19] Chang S.-C., Adamczyk J. A new approach for solving the three-dimensional steady Euler equations. II. Application to secondary flows in a turning channel // J. Comput. Phys. - 1985. - Vol. 60. - P. 41-61.

[20] Cheng S.I. Accuracy of difference formulation of Navier-Stokes equations // Phys. Fluids. - 1969. - Vol. 12. - P. 11-34.

[21] Cherny S., Gryazin Yu., Sharov S., Shashkin P. An efficient LU-TVD finite volume method for 3D inviscid and viscous incompressible flow problems // Proceedings of the third ECCOMAS computational fluid dynamics conference. - J. Wiley - Sons. - 1996. - P. 90-96.

[22] Christov C.I. Orthogonal coordinate meshes with managable jacobian // Numerical Grid Generation; Applied Mathematics and Computation. - 1982. - Vol. 10/11. - P. 885-894.

[23] Comini G., Giudice S., Strada M. Finite element analysis of laminar flow in the entrance region of ducts // Int. J. Numer. Methods Eng. - 1980. - Vol. 15. - P. 507-517.

[24] Connor G., Brebbia C. Finite element method in mechanics of fluid. - Leningrad: Shipbuilding, 1979. - 204 p. (in Russian)

[25] Daikovskii A.G., Polezhaev V.I., Fedoseev A.I. About calculation of boundary conditions for the non-stationary Navier-Stokes equations in variables "vorticity, stream function" // Numerical methods of mechanics of continuous medium. - Novosibirsk, 1979. - Vol. 10. - N. 2. - P. 49-58. (in Russian)

[26] Danilov Yu.M. Numerical solution of the stationary equations of hydrodinamics in the subsonic flow region // Notes of high education institutions. Aviation technics. - 1980. - N. 3. - P. 42-45. (in Russian)

[27] Danilov Yu.M., Kondratiev V.V. Calculation of the mixed up subsonic and supersonic gas flows in the channels of complicated form with the partialy penetratable wall // Notes of high education institutions. Aviation technics. - 1980. - N. 1. - P. 33 - 36. (in Russian)

[28] Daripa P. Iterative schemes and algorithms for adaptive grid generation in one dimension // J. Comput. Physics. - 1992. - Vol.100. - P. 284-293.

[29] Darmaev T.G., Liseikin V.D. Method of constructing many-dimensional adaptive difference grid // Modelling in mechanics. - Novosibirsk, 1987. - Vol. 1(18). - N. 1. - P. 49-58. (in Russian)

[30] Degtyaryov L.M., Ivanova T.S. Method of adaptive grids in one-dimensional non-stationary problems of convection - diffusion // Differential equations. - 1993. - Vol. 29. - N. 7. - P. 1179-1192. (in Russian)

[31] Dennis S.C.R., Ingham D.B., Cook R.N. Finite-difference methods for calculating steady incompressible flows in three dimensions // J. Comput. Phys. - 1979. - Vol. 33. - P.325-339.

[32] Deshpande M.D., Giddens D.P. Turbulence measurements in a constricted tube // J. Fluid Mech. - 1980. - Vol. 97. - Part 1. - P. 65-89.

[33] Dorodnitsyn .., Meller N.. About some approaches to solution of the stationary Navier-Stokes equations // Journal of computational mathematics and mathematical physics. - 1968. - Vol. 8. - N. 2. - P. 393-402. (in Russian)

[34] Dwyer H.A., Kee R.J., Sanders B.R. An adaptive grid method for problems in fluid mechanics and heat transfer // AIAA J. - 1980. - Vol. 18. - No. 10. - P. 1205-1212.

[35] Dwyer H.A. Grid adaption for problems in fluid dynamics // AIAA J. - 1984. - Vol. 22. - No. 12. - P. 1705-1712.

[36] E W., Liu J. Vorticity boundary condition and related issues for finite difference schemes // J. Comput. Phys. - 1996. - Vol. 124. - P. 368-382.

[37] Eisemann P.R. Alternating direction adaptive grid generation. AIAA Paper 83-1937. - 1983.

[38] Essers J.A. Quasi-natural numerical methods for the computation of inviscid potential or rotational transonic flows // Applied Mathematical Modelling. - 1979. - Vol. 3. - No. 1. - P. 55-66.

[39] Essers J.A. New fast super-dashpot time-dependent techniques for the numerical simulation of steady flows. I. Numerical formulation // Comput. Fluids. - 1980. - Vol. 8. - No. 3. - P. 351-368.

[40] Farouk B., Fusagi T. A coupled solution of the vorticity-velocity formulation of the incompressible Navier-Stokes equations // Int. J. Numer. Methods Fluids. - 1985. - Vol. 5. - P. 1017-1034.

[41] Feistauer M. Some cases of numerical solution of differential equations describing the vortex-flow through three-dimensional axially symmetric channels // Aplikace Matematiky. - 1971. - Vol. 16. - P. 265-288.

[42] Feistauer M. On two-dimensional and three dimensional axially-symmetric rotational flows of an ideal incompressible fluid // Aplikace Matematiky. - 1977. - Vol. 22. - P. 199-213.

[43] Fikhtengolts G.. Course of differential and integrated calculation. Vol. 3. - Moscow: Science, 1963. (in Russian)

[44] Fletcher C. Computational techniques for fluid dynamics. Vol. 2. - Moscow: Mir, 1991. - 552 p. (in Russian)

[45] Gatski T.B., Grosch C.E., Rose M.E. The numerical solution of the Navier-Stokes equations for 3-dimensional, unsteady, incompressible flows by compact schemes // J. Comput. Phys. - 1989. - Vol. 82. - P. 298-329.

[46] Giudice S. Step-by-step analysis of flow development in ducts // Numer. Heat Transfer. - 1979. - Vol. 2. - P. 291-302.

[47] Giudice S., Strada M., Comini G. Three-dimensional laminar flow in ducts // Numer. Heat Transfer. - 1981. - Vol. 4. - P. 215-228.

[48] Godunov S.K. and others. Numerical solution of many-dimensional problems of gas dynamics. - Moscow: Science, 1976. - 400 p. (in Russian)

[49] Goldshtik M.A. Vortical streams. - Novosibirsk: Science, 1981. (in Russian)

[50] Gorbunov-Posadov .., Koryagin D.., Martynyuk V.V. System security of applied software packages. - Moscow: Science, 1990. - 206 p. (in Russian)

[51] Gryazin Yu.A., Chyorny S.G., Sharov S.V. Numerical modelling of incompressible fluid flows on the basis of the method of artificial compressibility // Computational technologies. - 1995. - Vol. 4. - N. 13. - P. 180-203. (in Russian)

[52] Gurov B.G. Existence and uniqueness of steady unpotential fluid flows in flat channels // Numerical methods of mechanics of continuous medium. - Novosibirsk, 1970. - Vol. 1. - N. 3. - P. 43-55. (in Russian)

[53] Gurov B.G., Yanenko N.N., Yaushev I.K. Numerical calculation of unpotential ideal fluid flows in flat channels // Numerical methods of mechanics of continuous medium. - Novosibirsk, 1971. - Vol. 2. - N. 1. - P. 3-16. (in Russian)

[54] Hille P., Vehrenkamp P., Schulz-DuBois E.O. The development and structure of primary and secondary flow in a curved square duct // J. Fluid Mech. - 1985. - Vol. 151. - P. 219-241.

[55] Hirasaki G.J., Hellums J.D. A general formulation of the boundary conditions on the vector potential in three-dimensional hydrodynamics // Quart. Appl. Math. - 1968. - Vol. 26. - No. 3. - P. 331-342.

[56] Hirasaki G.J., Hellums J.D. Boundary conditions on the vector and scalar potentials in viscous three-dimensional hydrodynamics // Quart. Appl. Math. - 1970. - Vol. 28. - No. 2. - P. 293-296.

[57] Hou T.Y., Wetton B.T.R. Convergence of a finite difference scheme for the Navier-Stokes equations using vorticity boundary conditions // SIAM J. Numer. Anal. - 1992. - Vol. 29. - No. 3. - P. 615-639.

[58] Huang H., Seymour B.R. A finite difference method for flow in a constricted channel // Comput. Fluids. - 1995. - Vol. 24. - P. 153-160.

[59] Huang H., Seymour B.R. The no-slip boundary condition in finite difference approximations // Int. J. Numer. Methods Fluids. - 1996. - Vol. 22. - P. 713-729.

[60] Huang W., Sloan D.M. A simple adaptive grid method in two dimensions // SIAM J. Sci. Comput. - 1994. - Vol. 15. - No. 4. - P. 776-797.

[61] Humphrey J.A.C., Taylor A.M.K., Whitelaw J.H. Laminar flow in a square duct of strong curvature // J. Fluid Mech. - 1977. - Vol. 83. - P. 509-527.

[62] Karpov V.Ya., Koryagin D.A. Development and usage of the applied software packages // Computer science and scientific-technical progress. - Moscow: Science, 1987. - P. 104-120. (in Russian)

[63] Karpov V.Ya., Koryagin D.A., Samarskii .. Principles of developing applied software packages for the problems of mathematical physics // Journal of computational mathematics and mathematical physics. - 1978. - Vol. 18. - N. 2. - P. 458-467. (in Russian)

[64] Kato T. On classical solutions of the two-dimensional non-stationary Euler equations // Archive Rational Mech. Anal. - 1967. - Vol. 25. - No. 3. - P. 188-200.

[65] Kazhihov .V. Correctness of non-stationary problem on ideal fluid flow through the given domain // Dynamics of continuous medium. - 1980. - N. 47. - P. 37-56. (in Russian)

[66] Kazhihov .V., Ragulin V.V. Non-stationary problems on ideal fluid flow through the limited domain // Reports of AS USSR. - 1980. - Vol. 250. - N. 6. - P. 1344 - 1347. (in Russian)

[67] Khairullina .B. Calculation of stationary subsonic vortical ideal gas streams in axially symmetric channels of complicated geometries // Problems of atomic science and technics. Mathematical modelling of physical processes. - 1990. - N. 3. - P. 32-39. (in Russian)

[68] Khairullina .B. Construction of block-regular optimum grids // Problems of atomic science and technics. Mathematical modelling of physical processes. - 1994. - N. 1. - P. 19-25. (in Russian)

[69] Khakimzyanov G.S. About two-dimensional ideal fluid flows with inflow of mass // Numerical methods of mechanics of continuous medium. - Novosibirsk, 1978. - Vol. 9. - N. 4. - P. 119-130. (in Russian)

[70] Khakimzyanov G.S., Shokina N.Yu. About equidistribution method for constructing two-dimensional adaptive grids // Computational technologies. - 1995. - Vol. 4. - N. 13. - P. 271-282. (in Russian)

[71] Khakimzyanov G.S., Shokina N.Yu. Numerical modelling of the steady fluid flows in the framework of a shallow-water model // Russian Journal of Numerical Analysis and Mathematical Modelling. - 1997. - Vol. 12. - No. 4. - P. 335-348.

[72] Khakimzyanov G.S., Shokina N.Yu. Numerical modeling of two-dimensional river flows // Final program of the 16th International Conference on Numerical Methods in Fluid Dynamics. - Arcachon, 1998. - P. 335-348.

[73] Khakimzyanov G.S., Shokina N.Yu. Numerical simulation of fluid flows using 3D adaptive grids // Advances in hydro-science and -engineering. Volume III. The electronic proceedings of papers of the 3rd international conference on hydro-science and -engineering. - Cottbus, 1998.

[74] Khakimzyanov G.S., Shokina N.Yu. Equidistribution method for the construction of adaptive grids // Russian Journal of Numerical Analysis and Mathematical Modelling. - 1999. - Vol. 14. - No. 4. - P. 339-358.

[75] Khakimzyanov G.S., Yaushev I.K. About numerical calculation of the subsonic steady axially symmetric flows of ideal compressible fluid in channels of complicated form // Notes of SB AS USSR. Technical sciences. - 1981. - N.13, Issue 3. - P. 50-57. (in Russian)

[76] Khakimzyanov G.S., Yaushev I.K. About calculation of pressure in two-dimensional stationary problems of ideal fluid dynamics // Journal of computational mathematics and mathematical physics. - 1984. - Vol. 24. - N. 10. - P. 1557-1564. (in Russian)

[77] Khakimzyanov G.S., Yaushev I.K. Iterative method of calculation of subsonic steady interior flows of ideal compressible fluid. - Novosibirsk, 1987. - 30 p. - (Pre-print N. 4-87, ITAM SB AS USSR) (in Russian)

[78] Kim H.J., ThompsonJ.F. Three-dimensional adaptive grid generation on a composite-block grid // AIAA Journal. - 1990. - Vol. 28. - No. 3. - P. 948.

[79] Knupp P., Steinberg S. Fundamentals of grid generation. - CRC Press, 1994. - 286 p.

[80] Kochergin V.P. Theory and methods of calculation of oceanic flows. - Moscow: Science, 1978. - 127 p. (in Russian)

[81] Konovalov .N., Yanenko N.N. Modular principle of constructing the programs as the basis of developing the applied software package for solving problems of mechanics of continuous medium // Complexes of the programs of mathematical physics. - Novosibirsk, CC SB AS USSR, 1972. - P. 48-54. (in Russian)

[82] Kovenya V.., Tarnavskii G.., Chyorny S.G. Application of splitting method in problems of aerodynamics. - Novosibirsk: Science, 1990. - 246 p. (in Russian)

[83] Kovenya V.., Yanenko N.N. Splitting method in problems of gas dynamics. - Novosibirsk: Science, 1981. - 304 p. (in Russian)

[84] Kozlov N.I. Organization of computational procedures. - Moscow: Science, 1981. - 240 p. (in Russian)

[85] Kuskova .V., Chudov L.. About the approximate boundary conditions for vorticity at calculation of viscous incompressible fluid flows // Computational methods and programming. - Moscow.: CC MSU, 1968. - N. 11. - P. 27-31. (in Russian)

[86] Kuznetsov B.G., Sirocenko V.P. About statement of hydrodynamics problems in multiply connected domains // Computational technologies. - 1995. - Vol. 4. - N. 12. - P. 209-218. (in Russian)

[87] Li M., Tang T., Fornberg B. A compact fourth order finite difference scheme for the steady incompressible Navier-Stokes equations // Int. J. Numer. Methods Fluids. - 1995. - Vol. 20. - P. 1137-1151.

[88] Liseikin V.D. Process of constructing three-dimensional grids for problems of aero gas dynamics // Problems of atomic science and technics. Mathematical modelling of physical processes. - 1991. - N. 3. - P. 31-45. (in Russian)

[89] Liseikin V.D. Survey of grid generation technology // Advanced Mathematics: Computations and Applications. Proceedings of AMCA-95. (Eds. A.S.Alexeev, N.S.Bakhvalov). - Novosibirsk, 1995. - P. 511-517.

[90] Liseikin V.D. Review on methods of constructing structural adaptive grids // Journal of computational mathematics and mathematical physics. - 1996. - Vol. 36. - N. 1. - P. 3-41. (in Russian)

[91] Liseikin V.D. Method of algebraic adaptation // Journal of computational mathematics and mathematical physics. - 1998. - Vol. 38. - N. 10. - P. 1692-1709. (in Russian)

[92] Liseikin V.D. Grid generation methods. - Springer-Verlag: Berlin, Heidelberg, New York. - 1999. - 362 p.

[93] Maliska C.R., Raithby G.D. A method for computing three dimensional flows using non-orthogonal boundary-fitted coordinates // Int. J. Numer. Methods Fluids. - 1984. - Vol. 4. - P. 519-537.

[94] Mallinson G.D., Davis G. Three-dimensional natural convection in a box: a numerical study // J. Fluid Mech. - 1977. - Vol. 83. - No. 1. - P. 1-31.

[95] Marchuk G.I. Methods of comupational mathematics. - Moscow: Science, 1980. - 535 p. (in Russian)

[96] Marchuk G.I. Splitting methods. - Moscow: Science, 1988. - 264 p. (in Russian)

[97] Melaanen M.C. Analysis of fluid flow in constricted tubes and ducts using body-fitted non-staggered grids // Int. J. Numer. Methods Fluids. - 1991. - Vol. 15. - P. 895-923.

[98] Methods of calculation of flow around the elements of flying vehicles at trans-sonic velocities. Part II. Methods of grid generation. - Moscow: ONTI TsAGI, 1989. - 119 p. (in Russian)

[99] Miyata H.N., Nishimura S. Finite-difference simulation of nonlinear ship waves // J. Fluid Mech. - 1985. - Vol. 157. - P. 327-357.

[100] Moiseenko B.D., Rozhdestvenskii B.L. Numerical solution of the stationary equations of hydrodynamics at presence of the tangential ruptures // Journal of computational mathematics and mathematical physics. - 1970. - Vol. 10. - N. 2. - P. 499-505. (in Russian)

[101] Morgulis .B. Solvability of three-dimensional stationary flow problem // Siberian mathematical journal. - 1999. - Vol. 40. - N. 1. - P. 142-158. (in Russian)

[102] Nakahashi K., Deiwert G.S. Three-dimensional adaptive grid method // AIAA Journal. - 1986. - Vol. 24. - P. 948.

[103] Napolitano M. Efficient solution of two-dimensional steady separated flows // Comput. Fluids. - 1991. - Vol. 20. - P. 213-222.

[104] Oleinik .., Radkevich .B. Second-order equations with non-negative characteristic form. Mathematical analysis, 1969 (Totals of the science). - Moscow: VINITI, 1971. - 252 p. (in Russian)

[105] Orlandi P. Vorticity-velocity formulation for high Re flows // Comput. Fluids. - 1987. - Vol. 15. - No. 2. - P.137-149.

[106] Osipov I.L., Paschenko V.P., Shipilin A.V. Calculation of inviscid gas flows in channels with strongly varying geometry // Journal of computational mathematics and mathematical physics. - 1978. - Vol. 18. - N. 4. - P. 964-973. (in Russian)

[107] Ovsyannikov L.V. Lectures on the basics of gas dynamics. - Moscow: Science, 1981. - 368 p. (in Russian)

[108] Ozoe H., Yamamoto K., Churchill S.W., Sayama H. Three-dimensional numerical analysis of laminar natural convection in a confined fluid heated from bellow // Trans. ASME, J. Heat Transfer. - 1976. - Vol. 98. - P. 202-207.

[109] Paskonov V.., Polezhaev V.I., Chudov L.. Numerical modelling of processes of warmth and mass exchange. - Moscow: Science, 1984. (in Russian)

[110] Peyret R., Tailor T.D. Computational methods in problems of fluid mechanics. - Leningrad: Gidrometeoizdat, 1986. - 352 p. (in Russian)

[111] Polezhaev V.I., Gryaznov V.L. Method of calculation of boundary conditions for the Navier-Stokes equations in variables "vorticity, stream function" // Reports of AS USSR. - 1974. - Vol. 219. - N. 2. - P. 301-304. (in Russian)

[112] Popov Yu.P., Samarskii .. Computational experiment // Computers, models, computational experiment. - Moscow: Science, 1988. - P. 16-78. (in Russian)

[113] Ragulin V.V. About one statement of the problem on ideal fluid flow // Dynamics of continuous medium. - Novosibirsk, IHD SB AS USSR, 1978. - N. 33. - P. 76-83. (in Russian)

[114] Raul R., Bernard P.S., Buckley F.T. An application of the vorticity - vector potential method to laminar cube flow // Int. J. Numer. Methods Fluids. - 1990. - Vol. 10. - P. 875-888.

[115] Richards C.W., Crane C.M. Pressure marching schemes that work // Int. J. Numer. Methods Eng. - 1980. - Vol. 15. - P. 599-610.

[116] Richardson S.M., Gornish A.R.H. Solution of three-dimensional incompressible flow problems // J. Fluid Mech. - 1977. - Vol. 82. - No. 2. - P. 309-319.

[117] Roache P. Computational hydrodynamics. - Moscow: Mir, 1980. - 616 p. (in Russian)

[118] Rozhdestvenskii B.L., Yanenko N.N. Systems of quasilinear equations and their applications to gas dynamics. - Moscow: Science, 1978. - 688 p. (in Russian)

[119] Samarskii A.A. Theory of difference scemes. - Moscow: Science, 1977. - 656 p. (in Russian)

[120] Samarskii A.A., Andreev V.B. Difference methods for elliptical equations. - Moscow: Science, 1976. - 352 p. (in Russian)

[121] Samarskii A.A., Nikolaev .S. Methods of solution of grid equations. - Moscow: Science, 1978. - 592 p. (in Russian)

[122] Sarmin E.N. Modification of splitting method of boundary conditions for solution of biharmonic equation // Journal of computational mathematics and mathematical physics. - 1973. - Vol. 13. - N. 5. - P. 1341-1347. (in Russian)

[123] Sedov L.I. Mechanics of continuous medium. Vol. 1. - Moscow: Science, 1973. - 536 p. (in Russian)

[124] Sidorov A.F., Ushakova .V. About one method for constructing the optimum difference grids for multi-dimensional domains // Numerical methods of mechanics of continuous medium. - Novosibirsk, 1981. - Vol. 12. - N. 5. - P. 106-123. (in Russian)

[125] Sidorov A.F., Ushakova .V. About one algorithm for constructing the optimum adaptive grids and its applications // Numerical methods of mechanics of continuous medium. - Novosibirsk, 1985. - Vol. 16. - N. 5. - P. 101-115. (in Russian)

[126] Shi D. Numerical methods in problems of heat exchange. - Moscow: Mir, 1988. - 544 p. (in Russian)

[127] Shokin Yu.I., Khakimzyanov G.S. Numerical calculation of stationary subsonic gas dynamic problems // Proceedings of the eighth GAMM-conference on numerical methods in fluid mechanics. Notes on Numerical Fluid Mechanics. - Veiweg, Braunschweig, 1990. - Vol. 29. - P. 513-521.

[128] Shokina N.Yu. Numerical simulation of plane ideal incompressible fluid using adaptive grids // International workshop on current directions in numerical software and high performance computing. - Kyoto, 1995. - P. 36.

[129] Shokina N.Yu. Numerical simulation of two-dimensional steady fluid and gas flows using adaptive grids // Mathematical models and numerical methods of mechanics of continuous media. Thesises of international conference. - Novosibirsk, 1996. - P. 523-524. (in Russian)

[130] Shokina N.Yu. About equidistribution method for generation of two-dimensional adaptive grids // Mathematical modelling of scientific-technological and ecological problems in oil- and gas-extracting industry. Proceedings of Kazakhstanian-Russian scientific-practical conference. - Almaty, 1997. - P. 128. (in Russian)

[131] Shokina N.Yu. Numerical modelling of two-dimensional steady fluid and gas flows using adaptive grids // Computational Technologies, 1998. - Vol. 3. - N. 3. - P. 85-93. (in Russian)

[132] Shokina N.Yu. Numerical modelling of 3D fluid flows using adaptive grids // Proceedings of the sixth Japan-Russian joint symposium on computational fluid dynamics. - Nagoya, 1998. - P. 156-160.

[133] Shokina N.Yu. About one method of constructing adaptive grids in three-dimensional domains // Problems of numerical mathematics and informational technologies. Proceedings of international scientific-practical conference. - Almaty, 1999. - P. 387. (in Russian)

[134] Shokina N.Yu. One method of constructing grids in three-dimensional domains // Computational mechanics and modern applied program systems. Thesises of the X anniversary international conference. - Pereslavl-Zalesskii, 1999. - P. 97. (in Russian)

[135] Shokina N.Yu. About one method of numerical modeling of ideal fluid flows in ducts // Modern methods of mathematical modelling of natural and antropogeneous catastrophes. Abstracts of the V scientific conference, devoted to the 275-th anniversary of Russian Academy of Sciences. - Krasnoyarsk: ICM SB RAS, 1999. - P. 104. (in Russian)

[136] Shokina N.Yu. About numerical calculation of three-dimensional flows using vector potential and vorticity vector // Mathematical models and methods of their investigation (problems of continuous medium mechanics, ecology, technical processes, economics). Abstracts of international conference. - Krasnoyarsk: Krasnoyarsk state university, 1999. - P. 214. (in Russian)

[137] Shokina Nina Yu., Khakimzyanov Gayaz S., Roesner Karl.G. Numerical simulation of 3D fluid flows in the vorticity-vector potential formulation on adaptive grids // Electronic proceedings of the 8th international symposium on computational fluid dynamics. - Bremen, 1999.

[138] Shyy W. Computation of complex fluid flows using an adaptive grid method // Int. J. Numer. Methods Fluids. - 1988. - Vol. 8. - P. 475-489.

[139] Sotiropoulos F., Abdallah S. The discrete continuity equation in primitive variable solutions of incompressible flow // J. Comput. Phys. - 1991. - Vol. 95. - No. 1. - P. 212-227.

[140] Sotiropoulos F., Kim W.J., Patel V.C. A computational comparision of two incompressible Navier-Stokes solvers in three-dimensional flows // Comput. Fluids. - 1994. - Vol. 23. - No. 4. - P. 627-646.

[141] Stricwerda J.C., Nagel Y.M. A numerical method for the incompressible Navier-Stokes equations in three-dimensional cylindrical geometry // J. Comput. Phys. - 1988. - Vol. 78. - No. 1. - P. 64-78.

[142] Sud E. Numerical solution of the Navier-Stokes equations in doubly connected domains for incompressible fluid flow // Rocket engineering and cosmonautics. - 1974. - Vol. 12. - N. 5. - P. 76-82. (in Russian)

[143] Takagi T., Miki K., Chen B.C.J., Sha W.T. Numerical generation of boundary-fitted curvilinear coordinate systems for arbitrarily curved surfaces // J. Comput. Phys. - 1985. - Vol. 58. - P. 67-79.

[144] Tarunin E.L. Optimization of implicit schemes for the Navier-Stokes equations in variables: stream function and vorticity of velocity // Proceedings of V All-Union seminar on numerical methods of viscous fluid mechanics: - Novosibirsk, CC SB AS USSR, 1975. - P. 3-26. (in Russian)

[145] Tarunin E.L. Analysis of approximating formulas for vorticity of velocity on rigid boundary // Scientific notes of PGPI. - 1976. - N. 152. - Issue 9. - P. 167-178. (in Russian)

[146] Tarunin E.L. About the choice of approximating formula for vorticity of velocity on rigid boundary in solving of problems on viscous fluid dynamics // Numerical methods of mechanics of continuous medium. - Novosibirsk, 1978. - Vol. 9. - N. 7. - P. 97-111. (in Russian)

[147] Taylor A.M.K., Whitelaw J.H., Yanneskis M. Curved ducts with strong secondary motion: velocity measurements of developing laminar and turbulent flow // J. Fluids Engng. - 1982. - Vol.104. - P. 350-359.

[148] Thom ., Aplte C. Field computations in engineering and physics. - London: D. Van Nosrand Company, 1961. - 165 p.

[149] Thompson J.F. A survey of dynamically adaptive grids in the numerical solution of partial differential equations // Applied Numerical Mathematics. - 1985. - Vol. 1. - P. 3-28.

[150] Thompson J.F., Warsi Z.U.A., Mastin C.W. Numerical grid generation, foundations and applications. - Amsterdam: North-Holland, 1985. - 483 p.

[151] Tolstukha A.S. Transposition of vorticity: the variational approach // Mathematical structures and modelling. - 1998. - N. 2. - P. 116-123. (in Russian)

[152] Troshkin .V. Admissibility of the set of boundary values in one stationary hydrodynamic problem // Reports of AS USSR. - 1983. - Vol. 272. - N. 5. - P. 1086-1090. (in Russian)

[153] Tutty O.R. On vector potential - vorticity methods for incompressible flow problems // J. Comput. Phys. - 1986. - Vol. 64. - P. 368-379.

[154] Vabischevich P.N. Realisation of boundary conditions for solution of the Navier-Stokes equations in "stream function, vorticity of velocity" variables // Reports of AS USSR. - 1983. - Vol. 273. - N. 1. - P. 22-26. (in Russian)

[155] Vabischevich P.N. Implicit difference schemes for the non-stationary Navier-Stokes equations in "stream function - vorticity" variables // Differential equations. - 1984. - Vol. 20 - N. 7. - P. 1135-1144. (in Russian)

[156] Vaganova N.A., Kovrizhnykh O.O., Khairullina O.B. Modelling of gas dinamics processes in combustion cameras using multiprocessor copmuter // Computational technologies. - 1996. - Vol. 1. - N. 2. - P. 57-64. (in Russian)

[157] Voevodin A.F. Stability and realisation of the Thom conditions for the difference boundary value Stokes problem // Numerical methods of mechanics of continuous medium. - Novosibirsk, 1992. - Vol. 6(23). - N. 1. - P. 37-47. (in Russian)

[158] Voevodin A.F., Goncharova O.N., Leontiev N.A. Calculation of free convection in annular domain at the reduced gravitation // Numerical methods of viscous fluid dynamics: Proceedings of IX All-Union school-seminar. - Novosibirsk, 1983. - P. 85-89. (in Russian)

[159] Voevodin A.F., Ovcharova A.C. About calculation of vorticity function on the boundary of closed circular domain // Numerical methods of mechanics of continuous medium. - Novosibirsk, 1991. - Vol. 5(22). - N. 1. - P. 113-120. (in Russian)

[160] Wong A.K., Reizes J.A. An effective vorticity - vector potential formulation for the numerical solution of three-dimensional duct flow problem // J. Comput. Phys. - 1984. - Vol. 55. - P. 98-114.

[161] Wong A.K., Reizes J.A. The vector potential in the numerical solution of three-dimensional fluid dynamics problems in multiply connected regions // J. Comput. Phys. - 1986. - Vol. 62. - P. 124-142.

[162] Yanenko N.N., Karnachuk V.I., Konovalov .N. Problems of mathematical technology // Numerical methods of mechanics of continuous medium. - Novosibirsk, 1977. - Vol. 8. - N. 3. - P. 129-157. (in Russian)

[163] Yang H., Camarero R. An improved vorticity - potential method for three-dimensional duct flow simulations // Int. J. Numer. Methods Fluids. - 1986. - Vol. 6. - P. 35-45.

[164] Yaushev I.K. Numerical calculation of two-dimensional potential and vortical ideal fluid flows // Numerical methods of mechanics of continuous medium. - Novosibirsk, 1973. - Vol. 4. - N. 5. - P. 147-155. (in Russian)

[165] Yaushev I.K., Khakimzyanov G.S. About numerical calculation of stationary plane-parallel ideal fluid and gas flows in channels of complicated configuration // Notes of SB AS USSR. Technical sciences. - 1977. - N.13, Issue 3. - P. 37-45. (in Russian)

[166] Young D.F., Tsai F.Y. Flow characteristics in models of arterial stenoses - I. Steady flow // J. Biomech. - 1973. - Vol. 6. - P. 395-410.

[167] Yudovich V.I. Non-stationary ideal incompressible fluid flows // Journal of computational mathematics and mathematical physics. - 1963. - Vol. 3. - N. 6. - P. 1032-1066. (in Russian)

[168] Zakharenkov .N. Approximation of the boundary condition for vorticity on the surface of rigid body at solution of the Navier-Stokes equations in variables: stream function and vorticity // Numerical methods of mechanics of continuous medium. - Novosibirsk, 1980. - Vol. 11. - N. 7. - P. 56-74. (in Russian)

[169] Zakharenkov .N. About approximation of boundary condition for vorticity // Numerical methods of mechanics of continuous medium. - Novosibirsk, 1982. - Vol. 13. - N. 2. - P. 64-81. (in Russian)

[170] Zorich V.A. Mathematical analysis. Part 2. - Moscow: Science, 1984. - 640 p. (in Russian)

<div align="center">

Curriculum Vitae

of

Nina Yurievna Shokina

</div>

22.05.1974	born in Novosibirsk, Russia
1981-1983	Elementary school education in Novosibirsk, Russia
1983-1991	High school education in Krasnoyarsk, Russia
1991-1997	Studies in Mechanics and Applied Mathematics at Novosibirsk State University, Novosibirsk, Russia
1995	Bachelor's degree in Mechanics and Applied Mathematics
1997	Master's degree in Mathematics
from 1995	Member of research group of Institute of Computational Technologies of Siberian Branch of Russian Academy of Sciences
from 1998	Post-graduate student of Mechanical Engineering Department of Technical University of Darmstadt Supervisors: Prof. Dr.rer.nat. M. Schäfer, Prof. Dr.rer.nat. K. G. Roesner

I declare that the present Ph.D. thesis was written by myself, and all the references and additional tools necessary to perform the numerical simulation were cited.

Besides, I declare that up to this date I have not tried to pass an examination for getting Ph.D. by this material.

Novosibirsk, Akademgorodok, 20.05.2000.